

University of Nottingham
UK | CHINA | MALAYSIA

Faculty of Engineering – Department of Civil Engineering

Permanent Deformation Resistance of Fibre Reinforced Asphalt Mixture

By

Monketh Sadeq Mohammed

Thesis submitted to the University of Nottingham for the degree of

Doctor of Philosophy

June 2019

Abstract

The loss of strength in road pavements due to high traffic loads, increasing number of road users, severe climate conditions and moisture is a recurring problem, creating distress such as ravelling, fatigue and permanent deformation. It is, therefore, important to find a way to improve or at least delay the loss of strength in asphalt mixtures. Such an improvement would lead to longer service life and a more comfortable drive for road users.

This research develops a fundamental understanding of the effect of fibre on binder and asphalt mortar, leading to an evaluation of fibre reinforced dense asphalt mixtures. It determines which fibre type provides the best, most cost-effective performance improvement in terms of rutting and cracking resistance. The study also gives an understanding of the factors that affect the behaviour of fibres in the mix, such as fibre surface texture, distribution and fibre length.

The dynamic shear rheological test results of complex modulus and phase angle master curves indicate that the modification mechanism of fibre reinforcement consists of three dimensional networks within the mastic or the mortar as shown in scanning electronic microscope images. These three dimensional networks increase the stiffness and elastic properties of the modified mastic or mortar, mainly at high temperatures (45-70)℃. Under these circumstances, the viscosity of mastic and/or mortar is low enough to allow the fibre entanglement to control the rheological properties of fibre reinforced materials. The modification mechanisms of cellulose fibre also consist of a possible chemical change by absorption/adsorption of bitumen fractions that increases the stiffness and elasticity of the binder, mainly at high temperatures (45-70)℃. This study assesses the potential modification of the binder due to the presence of fibres, by means of work of cohesion and work of adhesion calculations, based on surface energy parameters. The study also evaluates the influence of different filler to bitumen

ratios and fibre percentages on pull-off tensile strength. The test results indicate that the fibres enhance the pull-off tensile strength of the mortar, in addition to changing the failure mode from cohesive to hybrid, implying an improvement in the cohesive strength of the mortar.

This thesis examines the relative performance of the asphalt mixture modified with different fibre types and contents in terms of the main distress types related to flexible pavement. Also, fibre distribution and orientation in the asphalt mixture was explored in this study. The results show that fibre has a significant influence on the performance; the irrecoverable strain and peak strain in the multiple stress creep recovery test both decrease; the stiffness increases; the recovery percentage increases; and, the accumulated strain decreases. The repeated load axial test and immersed Hamburg wheel tracking test indicate a significant improvement in permanent deformation resistance of fibre modified mixtures compared to the unmodified case. Also, the test results show that fibres have a notable impact on the stiffness modulus and fracture toughness of asphalt mixtures at the 20℃ test temperature. Moreover, fibres give slightly improved fatigue life of asphalt mixtures, mainly at low strain values. However, results indicate that there is no clear influence of fibres on the indirect tensile strength and moisture damage of asphalt mixture at the 20℃ test temperature.

A comparison of the pavement analysis and design results of control and fibre reinforced asphalt mixtures reveal that adding fibre to the asphalt mixture results in an increase in pavement life mainly for cellulose and steel fibres.

Dedication

To my Mother and Father souls

Acknowledgements

My gratitude and thanks to God '**Allah**' who gave me the courage, the health and the knowledge to accomplish this study.

I would like to express my sincere gratitude to **Dr Tony Parry** and **Dr Nick Thom,** my research supervisors, for their valuable and constructive suggestions during this research work. Their guidance helped me in all the time of research and writing of this thesis. I would also like to thank my third supervisor **Dr James Grenfell** for his advice and assistance were important and very supporting in this study. Besides my supervisors, I would like to thank my internal examiner **Professor Gordon Airey** for his valuable suggestion and help during this research.

Big thanks to all technicians in the laboratory, Lawrence, Martyn, Richard, Jonathan, Antony, Matthew, Peter, and Laura for their support and help. Without their precious support, it would not be possible to conduct this research.

A very special word of thanks to every researcher, academic and staff at NTEC with whom I shared many enjoyable moments and experience. My sincere thanks are due to the Higher Committee for Education Development in Iraq (HCED) for awarding me a scholarship to study in the UK, and their financial support is highly appreciated.

And finally, last but by no means least, warm-hearted thanks go to my wonderful family, brother, sister and dear Uncles Dr Ali and Salem for their encouragement, love and support that have got me where I am.

Monketh Mohammed

June 2019

Declaration

The research described in this thesis was conducted at the University of Nottingham, Department of Civil Engineering, Nottingham Transportation Engineering Centre (NTEC), between July 2015 and June 2019.

I declare that the work is my own and has not been submitted for a degree of another university.

Monketh Sadeq Mohammed

The University of Nottingham

June 2019

Contents

Chapter 1 Introduction 1

1.1 Introduction 1

1.2 Background 2

1.3 Problem statement 3

1.4 Aims and Objectives 4

1.5 Thesis structure and outline 5

1.6 Publications list 7

Chapter 2 Literature review 9

2.1 Introduction 9

2.2 General information about fibre reinforcement 10

2.3 Types of fibres 11

2.3.1 Glass fibres 12

2.3.2 Cellulose fibres 12

2.3.3 Polypropylene fibres 12

2.3.4 Polyester fibres 13

2.3.5 Carpet fibres 13

2.3.6 Carbon fibres 14

2.3.7 Steel fibres 14

2.4 Fibre influence on the properties of asphalt binder mastic and mortar.. 15

2.5 Fibres influence on mix design criteria 17

2.6 Effect of fibres on mechanical properties of asphalt mixture 22

2.7 Evaluation of reinforcing effects of fibres in the field 28

2.8 Most common distress types in flexible pavement 31

2.8.1 Permanent deformation in flexible pavement 31

2.8.2 Fatigue phenomenon in asphalt pavements 34

2.8.3 Fatigue testing of asphalt mixtures 35

2.8.4 Semi-Circular Bending test (SCB) 39

2.9 Discussion of performance of fibre-reinforced bitumen mastics, mortars and mixtures 42

Chapter 3 Methodology and Materials 46

3.1 Introduction 46

3.2 Methodology 48

3.2.1 Stage 1 48

3.2.2 Stage 2 49

3.2.3 Stage 3 50

3.3 Materials 53

3.3.1 Fibre types 53

3.3.2 Fibre characteristics 54

3.3.3 Bitumen 56

3.3.4 Limestone filler 57

3.3.5 Aggregate 57

3.4 Preparation of bitumen-fibre mastic and mortar 57

3.5 Asphalt mixtures 59

3.5.1 Aggregate gradation 59

3.5.2 Mixing and compaction 60

3.5.3 Specimens coring and cutting 61

3.5.4 Volumetric characteristics of DBM mixtures 63

Chapter 4 Mastic properties 64

4.1 Introduction 64

4.2 Characterisation 65

4.2.1 Scanning electron microscope (SEM) 66

4.2.2 Penetration test 66

4.2.3 Softening point (ring and ball) test 67

4.2.4 Viscosity test 67

4.2.5 Dynamic shear rheometer (DSR) 68

4.2.6 Double edge notch tension test (DENT) 71

4.3 Results and Discussions 71

4.3.1 Scanning electronic microscope 71

4.3.2 Penetration 72

4.3.3 Softening point (Ring and Ball) 73

4.3.4 Viscosity 74

4.4 Master Curves 77

4.4.1 Complex Modulus Master Curves 77

4.4.2 Phase Angle Master Curves 80

4.5 Rutting parameters 84

4.6 Double edge notched tension (DENT) test 86

4.7 Summary and conclusions 90

Chapter 5 Mortar properties 92

5.1 Introduction 92

5.2 The microstructure of fibre modified asphalt mortar 93

5.3 Results and analysis 94

5.3.1 Penetration test results 94

5.3.2 Viscosity test results 97

5.3.3 Complex modulus master curve of base and modified mortar 101

5.3.4 Phase angle isochronal plots 107

5.3.5 Phase angle master curve 111

5.3.6 Rutting parameter 117

5.3.7 Double edge notch tension (DENT) test 122

5.4 Summary and conclusions 125

Chapter 6 Bond Strength 127

6.1 Introduction 127

6.2 Characterisation 129

6.2.1 Binder drainage test basket method 129

6.2.2 Determination of asphaltene content 129

6.2.3 Complex modulus test 130

6.2.4 Pneumatic adhesion tensile testing instrument (PATTI) test 130

6.2.5 Surface energy measurement 131

6.3 Surface energy 132

6.3.1 Work of cohesion 133

6.3.2 Work of adhesion 133

6.4 Results and Discussions 135

6.4.1 Binder drainage test results 135

6.4.2 Asphaltene test results 136

6.4.3 Complex modulus and phase angle master curves of base and drained binder 137

6.4.4 Pneumatic adhesion tensile testing instrument (PATTI) 139

6.4.5 Surface energy 147

6.4.6 Work of cohesion and adhesion 148

6.5 Summary and conclusions 151

Chapter 7 Permanent deformation 153

7.1 Introduction 153

7.2 Characterisation 154

7.2.1 Multiple stress creep recovery (MSCR) test 154

7.2.2 Immersed Hamburg wheel tracking test 156

7.2.3 Repeated load axial test (RLAT) 157

7.3 Results and analysis 158

7.3.1 Multiple stress creep recovery (MSCR) results 158

7.3.2 Immersed Hamburg wheel tracking test results 165

7.3.3 Repeated Load axial test (RLAT) 168

7.4 Discussion 172

7.5 Summary and conclusions 173

Chapter 8 Other Mechanical properties 175

8.1 Introduction 175

8.2 Experimental programme 176

8.3 X-ray computed tomography imaging 176

8.3.1 General procedure for X-ray CT imaging 178

8.3.2 Results and Discussion 179

8.4 Indirect tensile stiffness modulus (ITSM) test 182

8.4.1 Experimental setup 182

8.4.2 Sample preparation 183

8.4.3 Results and Discussion 184

8.5 Indirect tensile fatigue test (ITFT) 186

8.5.1 Experimental setup 186

8.5.2 Sample preparation 189

8.5.3 Results and Discussion 190

8.6 Indirect tensile strength test (ITS) 197

8.6.1 Experimental setup 197

8.6.2 Sample preparation 198

8.6.3 Results and Discussion 199

8.7 Moisture damage test 200

8.7.1 Results and Discussion 201

8.7.2 Results and discussion of moisture damage for RLAT specimens . 204

8.8 Semi-circular bending test (SCB) 206

8.8.1 Experimental setup 207

8.8.2 Sample preparation 208

8.8.3 Results and Discussion 209

8.9 Summary and conclusions 216

Chapter 9 Pavement design 218

9.1 Introduction 218

9.2 Pavement structure 219

9.3 Pavement structure and material properties 221

9.4 Design principle and analysis 223

9.5 Results and Discussions 225

9.5.1 Strain distribution in pavement layers 225

9.5.2 Design of FRAM binder course for fatigue life 228

9.6 Summary and conclusions 229

Chapter 10 Conclusions 231

10.1 Introduction 231

10.2 Conclusions and implications 232

10.2.1 Conclusions are drawn from the literature review: 232

10.2.2 Characteristics of fibre reinforced asphalt mastics and mortars 232

10.2.3 Microstructure, permanent deformation and mechanical properties of fibre reinforced asphalt mixture 235

10.3 Recommendations for future research 237

References 241

List of Figures

Figure 2-1 Relations between asphalt content and air voids of fibre reinforced asphalt cement (FRAC) (Chen et al., 2009) 19

Figure 2-2 Bulk specific gravity (Gmb) of mixtures (Note: asphalt content of 4.49% is the optimum asphalt content of ordinary mixture), (Chen et al., 2009) 20

Figure 2-3 Voids filled with asphalt (VFA) of mixtures with different fibre types (Chen et al., 2009) 21

Figure 2-4 Lengths and contents of waste polyester fibre additives and indirect tensile strengths of the mixtures (Anurag et al., 2009) 23

Figure 2-5 Result of analysis of fatigue test (Vale et al., 2013) 27

Figure 2-6 Definition of downward and total rutting (John C. Glennon, 2015).... 34

Figure 2-7 Fatigue cracks in asphalt pavements (Seattlie WA Paving, 2019) 35

Figure 2-8 Schematic diagram of commonly used fatigue test 36

Figure 3-1 Strategy for developing the multifunctional high performance asphalt mixture 47

Figure 3-2 Thesis roadmap 52

Figure 3-3 Images of fibre types 55

Figure 3-4 Scanning Electron Microscope (SEM) images of glass fibre 55

Figure 3-5 Scanning Electron Microscope (SEM) images of cellulose fibre with different scale 56

Figure 3-6 Optical microscope images of steel fibre with different diameter 56

Figure 3-7 Bitumen-fibre mastic blending facilities 58

Figure 3-8 Gradation curve of 0/20 mm binder course DBM 60

Figure 3-9 (a) Mechanical asphalt mixer, and (b) square steel mould 61

Figure 3-10 Steel roller compactor and asphalt mixture after compaction 61

Figure 3-11 Specimens after coring and cutting 62

Figure 4-1 Bohlin Gemini 200 DSR 70

Figure 4-2 Dynamic shear rheometer working principle (Airey, 1997) 70

Figure 4-3 (a and b) SEM images of fibre reinforced mastics 72

Figure 4-4 Penetration values of base and fibre reinforced binders 73

Figure 4-5 Softening point of base and fibre reinforced binders 74

Figure 4-6 (a and b) Viscosity of base and fibre reinforced binders 76

Figure 4-7 (a, b and c) Complex modulus master curves for unaged base bitumen and bitumen-fibre mastics 80

Figure 4-8 (a, b and c) Phase angle master curves for unaged base bitumen and bitumen-fibre mastics 83

Figure 4-9 (a, b and c) Rutting parameter for unaged base bitumen and bitumen-fibre mastics 85

Figure 4-10 Specific total work of fracture 88

Figure 4-11 DENT samples of fibre reinforced mastic after the test 89

Figure 4-12 Essential and plastic works of fracture 89

Figure 5-1 (a, b and c) SEM images of fibre modified asphalt mortars 94

Figure 5-2 Penetration of asphalt mortar mixing with four fibre types and three filler bitumen ratios 96

Figure 5-3 (a, b and c) Viscosity for base mortar and 0.5% mortar-fibre 99

Figure 5-4 (a, b and c) Viscosity for base mortar and 1.0% mortar-fibre 100

Figure 5-5 Complex modulus master curves for base mortar and 0.5% fibre modified mortar 103

Figure 5-6 Complex modulus master curves for base mortar and 1.0% fibre modified mortar 105

Figure 5-7 Complex modulus master curves for base mortar and 2.0% fibre modified mortar 106

Figure 5-8 (a, b and c) Isochronal plots of phase angle at 1.58 Hz for the base and 0.5% fibre modified mortars 108

Figure 5-9 (a, b and c) Isochronal plots of phase angle at 1.58 Hz for the base and 1.0% fibre modified mortars 109

Figure 5-10 (a, b and c) Isochronal plots of phase angle at 1.58 Hz for the base and 2.0% fibre modified mortars 110

Figure 5-11 (a, b and c) Phase angle master curves for base mortar and 0.5% fibre modified mortar 114

Figure 5-12 (a, b and c) Phase angle master curves for base mortar and 1.0% fibre modified mortar 115

Figure 5-13 (a, b and c) Phase angle master curves for base mortar and 2.0% fibre modified mortar 117

Figure 5-14 Rutting parameter for base mortar and fibre modified mortar 119

Figure 5-15 Rutting parameter for base mortar and fibre modified mortar 120

Figure 5-16 Rutting parameter for base mortar and fibre modified mortar 121

Figure 5-17 (a, b and c) Essential and plastic works of fracture at 15℃ 125

Figure 6-1 General representation of PATTI test 131

Figure 6-2 Complex modulus master curves for drained binders (2.0% fibre by volume) 138

Figure 6-3 Phase angle master curves for drained binders (2.0% fibre by volume) 139

Figure 6-4 Pull-off tensile strength of the base and modified mortars 145

Figure 6-5 Failure surfaces of 0.8 filler to bitumen ratio asphalt mortar with limestone aggregate with different fibre types: (a) Cellulose, (b) Glass-s, (c) Glass-l, (d) Steel and (e) base mortar. 146

Figure 6-6 Failure surfaces of 1.2 filler to bitumen ratio asphalt mortar with limestone aggregate with different fibre types: (a) Cellulose, (b) Glass-s, (c) Glass-l, (d) Steel and (e) base mortar. 146

Figure 6-7 Comparison between work of cohesion of drained binders and pull-off tensile strength of 0.8 filler to bitumen ratio and 0.5% fibre mortars (specimens undergoing cohesive failure) 151

Figure 7-1 Malvern instruments CVO model dynamic shear rheometer (DSR).. 156

Figure 7-2 Immersed Hamburg wheel tracking test configuration 157

Figure 7-3 RLAT test configuration 158

Figure 7-4 a, b and c Deformation recovery for the base and fibre modified asphalt mastic at 50℃..... 159

Figure 7-5 a, b and c Deformation recovery for the base and fibre modified asphalt mastic at 50℃..... 160

Figure 7-6 Relationship of stress with %R at different fibre types and contents at 50℃ 163

Figure 7-7 Non-recoverable creep compliance (%Jnr) obtained from MSCR tests at 50℃ 164

Figure 7-8 Immersed Hamburg wheel tracking results at 50℃ for control and 2.0% fibre reinforced asphalt mixture 166

Figure 7-9 Dynamic stability of control and 2.0% fibre reinforced asphalt mixtures 167

Figure 7-10 (a, b, c and d) Accumulate axial strain versus load cycle for control and fibre reinforced asphalt mixture 169

Figure 7-11 Ultimate strain of control and fibre reinforced asphalt mixtures.... 171

Figure 7-12 Strain rate of control and fibre reinforced asphalt mixtures 171

Figure 8-1 Simple configuration for the components of the X-ray system 179

Figure 8-2 Three dimensional distribution of steel fibres inside asphalt mixture180

Figure 8-3 Total areas of fibres along with the specimen depth 181

Figure 8-4 Aspect ratio of steel fibres 181

Figure 8-5 ITSM test configuration 183

Figure 8-6 Stiffness values of control and fibre reinforced asphalt mixtures 185

Figure 8-7 ITFT test configuration 189

Figure 8-8 Roller compacted slabs and core specimens 190

Figure 8-9 Fatigue life of 0.5% fibre reinforced asphalt mixtures versus strain 193

Figure 8-10 Fatigue life of 1.0% fibre reinforced asphalt mixtures versus strain 193

Figure 8-11 Fatigue life of 2.0% fibre reinforced asphalt mixtures versus strain 194

Figure 8-12 Fatigue life of 0.5% fibre reinforced asphalt mixtures versus stress 196

Figure 8-13 Fatigue life of 1.0% fibre reinforced asphalt mixtures versus stress 196

Figure 8-14 Fatigue life of 2.0% fibre reinforced asphalt mixtures versus stress 197

Figure 8-15 Experimental setups of ITS 198

Figure 8-16 Indirect tensile strength of control and fibre reinforced asphalt mixtures 199

Figure 8-17 (a) Steel, (b) glass fibre reinforced asphalt mixtures 200

Figure 8-18 Moisture damage results of control and 0.5% fibre reinforced asphalt mixtures 202

Figure 8-19 Moisture damage results of control and 1.0% fibre reinforced asphalt mixtures 203

Figure 8-20 Moisture damage results of control and 2.0% fibre reinforced asphalt mixtures 203

Figure 8-21 Asphalt mixture samples after ITS test 204

Figure 8-22 Moisture damage results of control and 0.5% fibre reinforced asphalt mixtures after RLAT test 205

Figure 8-23 Moisture damage results of control and 1.0% fibre reinforced asphalt mixtures after RLAT test 205

Figure 8-24 Moisture damage results of control and 2.0% fibre reinforced asphalt mixtures after RLAT test 206

Figure 8-25 SCB test configuration 208

Figure 8-26 Fracture toughness of control and fibre reinforced asphalt mixtures at 20℃ 209

Figure 8-27 Fracture toughness of control and fibre reinforced asphalt mixtures at 0℃ 210

Figure 8-28 Long glass fibre into the notch area of asphalt mixture 211

Figure 8-29 Fracture face at 0℃ test temperature 213

Figure 8-30 Maximum stress of control and fibre reinforced asphalt mixtures at 20℃ 214

Figure 8-31 Maximum stress of control and fibre reinforced asphalt mixtures at 0℃ 214

Figure 8-32 Peak load of control and fibre reinforced asphalt mixtures at 20℃ 215

Figure 8-33 Peak load of control and fibre reinforced asphalt mixtures at 0℃.. 215

Figure 9-1 Structure of flexible pavement..... 220

Figure 9-2 Pavement structure considered for the analysis 223

Figure 9-3 Major principal strain distribution through the pavement structure . 226

Figure 9-4 Minor principal strain distribution through the pavement structure . 227

Figure 9-5 Number of passes to failure for control and fibre reinforced asphalt mixtures 229

List of Tables

Table 3-1 Fibre percentages and types 53

Table 3-2 Basic properties of fibres 54

Table 3-3 Properties of 40/60 bitumen used in this study 57

Table 3-4 0/20 mm size DBM specification 59

Table 4-1 Experimental programme 66

Table 6-1 Results of binder drainage test (basket method) 135

Table 6-2 Asphaltene content test results 137

Table 6-3 Failure mode in fibre modified asphalt mortar 140

Table 6-4 Pull-off tensile strength t-test results 144

Table 6-5 Contact angle measurement of the bitumen binder 148

Table 6-6 Surface energy components of the drained binder 148

Table 6-7 Surface energy components of limestone aggregate 148

Table 6-8 Work of cohesion ($2\gamma^{total}$) and pull-off tensile strength values (0.8 filler to bitumen ratios and 0.5% fibre) 150

Table 6-9 Work of adhesion results 150

Table 8-1 Experimental programme 176

Table 8-2 T-test for stiffness of control and fibre reinforced asphalt mixtures .. 185

Table 8-3 Summary data for all the asphalt mixtures tested during this study using the ITFT 192

Table 8-4 Summary data for all the asphalt mixtures tested during this study using the ITFT 195

Table 8-5 T-test for fracture toughness of control and fibre reinforced asphalt mixtures 212

Table 9-1 Control and fibre reinforced asphalt mixtures used in pavement analysis and design** 222

List of abbreviations

AC	Asphalt cement
ACWC	Conventional wearing course
APA	Asphalt pavement analyser
ASTM	American society for testing and materials
BBR	Bending beam rheometer
BS	British standards
CT	Computed tomography
DBM	Dense bitumen macadam
DCA	Dynamic contact angle
DENT	Double edge notch tension
DS	Dynamic stability
DSR	Dynamic shear rheometer
DVS	Dynamic vapour sorption
F/B	Filler bitumen ratio
FRAC	Fibre reinforced asphalt cement
FRAM	Fibre reinforced asphalt mixture
Glass-l	Glass long
Glass-s	Glass short

G_{mb}	Bulk specific gravity
HMA	Hot mix asphalt
ITFT	Indirect tensile fatigue test
ITS	Indirect tensile strength
ITSM	Indirect tensile stiffness modulus
K_i	Fracture toughness
LVDTs	Linear variable differential transformers
MSCR	Multiple stress creep recovery
NAT	Nottingham asphalt tester
N_f	Number of cycles
NMAS	Nominal maximum aggregate size
OCA	Optimum asphalt contents
PATTI	Pneumatic adhesion tensile testing instrument
PE	Polyethylene
PG	Performance grade
RLAT	Repeated load axial test
SARA	Saturates, aromatic, resin and asphaltene
SBR	Styrene butadiene rubber
SBS	Styrene butadiene styrene

SCB	Semi-circular bending
SEM	Scanning electronic microscope
SMA	Stone mastic asphalt
TTSP	Time temperature superposition principle
TSR	Tensile strength ratio
VMA	Voids mineral aggregate
VFA	Voids filled with asphalt
W_a	Work of adhesion
W_c	Work of cohesion
G*	Complex modulus
δ	Phase angle

Chapter 1 Introduction

1.1 Introduction

There has been an increasing interest in modifying asphalt mixtures in order to improve their performance and the service life of pavements. Asphalt pavement performance is influenced mainly by three factors, axle loads, environmental temperature (since it is a viscoelastic material) and moisture (Kim and Koh, 2012, Perez-Jimenez et al., 2013). Many researchers have utilised different modifiers to improve asphalt mixture service quality (Cheng et al., 2015, Oda et al., 2012). Among these modifiers, different types of fibre such as steel, basalt, natural, polypropylene and thermoplastic have been used to improve asphalt mixture performance (Qin et al., 2016, Kim and Park, 2013, Herraiz et al., 2016, Yoo and Kim, 2014). The influence of fibres on asphalt mixtures is different from that of polymers including Styrene-Butadiene Rubber (SBR), Styrene-Butadiene-Styrene (SBS) and Polyethylene (PE). Fibres not only modify asphalt binder to prevent drain down in asphalt mixtures, but also enhance the mechanical properties of asphalt mixtures such as viscoelasticity, rutting resistance, dynamic modulus, and reflective cracking (Wu et al., 2007, Lee et al., 2005, Putman and Amirkhanian, 2004). This study includes a comprehensive investigation of the potential benefit of using fibres in both asphalt mastics and mixtures.

1.2 Background

The idea of adding fibre to improve the performance of materials is an old suggestion (Hongu and Philips, 1990). The first use of fibres in construction belongs to a 4000-year-old arch in China built with clay earth mixed with fibres, or the Great Wall built 2000 years ago. One of the earliest studies on fibres in asphalt examined the effect of wire mesh in an attempt to prevent reflection cracking in asphalt mixture overlay (Zube, 1956). The study concluded that the formation of reflective cracks was prevented or highly delayed by using wire reinforcement. Therefore, the author recommended that the use of wire mesh would lead to reducing the thickness of asphalt overlays and maintaining the required performance as well.

In the early 1960s, the modern developments of using new fibre type reinforcement were started, including non-synthetic fibres (cotton and asbestos) in asphalt mixtures (Busching and Antrim, 1968). But these types of fibre degrade over time, therefore were not adequate for long term reinforcement. More recently, the effect of adding various types of fibres (rock wool, asbestos, glass wool and cellulose) into asphalt mixtures were investigated by Serfass and Samanos (1996). The authors included different tests (low-temperature direct tension, resilient modulus, fatigue resistance and rutting resistance) in their study. Since then, different types of fibres have been introduced into asphalt mixtures and in different countries. Fibres were reportedly added to improve the following properties of the resulting composite (Busching et al., 1970, Peltonen, 1991):

- Fibres resist the propagation of cracking.
- Adding fibres increased resistance to cracking by increasing tensile strength of the resulting composite.
- Increased fatigue life.
- Durability will improve as a result of higher bitumen contents.

Furthermore, early uses of fibres were in dense asphalt mixtures. First use of fibres in stone mastic asphalt (SMA) mixtures came afterwards and started in Europe and exhibited successful use. In 1991, after more than 30 years of effective use in Europe the first SMA mixtures were placed in the United States (Cooley Jr and Brown, 2001). The main reason for designing these mixes in Europe was to resist studded tyre wear but was discovered to be effective in improving permanent deformation resistance at the same time. Using SMA mixtures with fibres increased rapidly in the United States. In 1997 more than 140 SMA projects over the United States were investigated by the National Centre for Asphalt Technology (NCAT) (Cooley Jr and Brown, 2001). Cellulose or mineral fibres are the types of fibres that were most used in these mixes, in order to prevent drain down of the binder in these gap-graded mixtures. Fibres are also added to open-graded mixes to prevent drain down.

In conclusion, there are three main reasons for adding fibres: (1) to prevent drain down in gap and open-graded mixtures, (2) to improve asphalt mixture mechanical properties to resist cracking and (3) to enhance the mechanical, thermal induction heating and healing properties of asphalt mixtures. These uses, in addition to other possible advantages and applications of the use of fibres, are explored in this study.

1.3 Problem statement

The traffic increases, severe climate conditions, the high loaded vehicles, also the increases in the number of electric and hybrid electric vehicles, which are heavier than diesel and petrol engine vehicles (Faria et al., 2012); all these reasons will cause the early deterioration of asphalt pavement. Therefore, it is become essential to enhance material properties by means of modifying the base binder or the asphalt mixture using different modifiers. Fibres are considered one of these modifiers and have been reported in the literature very often, especially with stone mastic asphalt (SMA) and gap graded asphalt mixtures. Very few studies examined

this effect on dense bitumen macadam asphalt mixture because their focus was only on the drain down problem in SMA and gap-graded mixtures.

However, there is still a number of unsolved or unclear issues and knowledge gaps associated with the use of fibre in the asphalt mixtures.

1.4 Aims and Objectives

This study aims are to explore and develop a fundamental understanding of the effect of fibre on the binder and compare the binder test results with the test results of asphalt mortars and mixtures. In addition, the study aims to determine which fibre type will provide the best, most cost-effective performance improvement in terms of rutting and cracking resistance. Also, to understand the factors that affect the behaviour of fibres in the mix, such as fibre surface texture, distribution and fibre length.

To achieve the aims, it is necessary to conduct a laboratory test program to examine the utility of adding fibres into the bitumen and dense bitumen macadam asphalt mix (DBM) for paving purposes. Therefore, the main objectives of this project can be summarised as:

- Evaluate the basic and more fundamental rheological properties of base bitumen and bitumen modified by different percentages and types of fibres.
- Examine the influence of fibres on asphalt mortar with different filler to bitumen ratios.
- Understand the asphalt mixture behaviour in the laboratory, with regard to permanent deformation, fatigue, moisture damage, fracture toughness and stiffness by carrying out laboratory tests.
- Understand the microstructure of the asphalt mixture.
- Proper approach for the design of pavements of fibre reinforced mixture.

1.5 Thesis structure and outline

This thesis consists of ten chapters and the roadmap for each chapter is briefly explained below:

- **Chapter 1: Introduction**. This chapter covers a general introduction and the background of the research topic. Identification of the research problem, aims and objectives are also included in this chapter.
- **Chapter 2: Literature Review**. Comprehensive literature of the main topics related to the background of this thesis is offered. Previous studies on the effect of fibre on asphalt mastic, mortar and mixture performance are discussed. In addition, this chapter reviews the literature on the use of fibre in the field.
- **Chapter 3: Methodology and materials**. This chapter summarises the roadmap followed to achieve the aims and objectives of this thesis. Also, material types and properties used in this study are described. Especial attention is paid to the fibre types and characteristics since fibre is the main focus of this study. Also, three-dimensional images of different types of fibres are illustrated in this chapter.
- **Chapter 4: Mastic properties**. In an effort to understand the influence of different fibre types and contents, the basic and more fundamental rheological properties of base and modified bitumen are investigated in this chapter at different testing temperatures and loading rates. Also, fibre distribution and orientation in the asphalt mastic is explored using the scanning electronic microscope (SEM).
- **Chapter 5: Mortar properties**. The influence of different filler to bitumen ratios and fibre types on the conventional and rheological properties of asphalt mortar are examined. Different testing temperatures and loading rates are used in this investigation. Fracture toughness of base and modified asphalt mortars are evaluated. The study also explores the microstructure,

fibre distribution and orientation into the asphalt mortar using scanning electronic microscope (SEM).

- **Chapter 6: Mortar bond strength**. Three key issues are discussed in this chapter. Firstly, the bond strength of asphalt mortars with different filler to bitumen ratios and fibre types is examined using the pull-off tensile strength test. Secondly, the influence of fibre on bitumen properties by absorption/adsorption of bitumen fractions is explored using drainage basket method. Thirdly, the work of cohesion and work of adhesion of drained binder, before and after mixing with fibres are estimated from surface energy parameters.
- **Chapter 7: Mastic and mixture permanent deformation**. The reinforcing effects of glass, steel and cellulose fibre additives for asphalt mastic are examined through multiple stress creep recovery test (MSCR) at different stress levels and 50℃ test temperature. Also, the permanent deformation resistance of fibre reinforced asphalt mixtures is evaluated using immersed Hamburg wheel tracking test at 50℃ and repeated load axial test (RLAT) at 30℃.
- **Chapter 8: Other mixture mechanical properties**. Provides the results of performance characterisation of control and fibre reinforced asphalt mixtures. This characterisation is carried out in terms of mechanical tests such as stiffness, fatigue, moisture damage and fracture test. In addition, steel fibres distribution and orientation in the asphalt mixture are investigated based on the X-ray computed tomography test and image J program.
- **Chapter 9: Pavement analysis and design**. The mechanical-empirical pavement design approach is used to examine the influence of different fibre types and amounts on the pavement thickness. The procedure used in this study is limited since it is based only on the stiffness and fatigue criterion.

- **Chapter 10: Summary, applications and recommendations**. This chapter provides a summary of the main conclusions and contributions can be drawn from this thesis. Also, recommendations and suggestions for future work are presented.

1.6 Publications list

The main findings of this thesis have been published or are under review, as shown below:

❖ Journal papers:

- **MOHAMMED, M.**, PARRY, T. & GRENFELL, J. 2018. Influence of fibres on rheological properties and toughness of bituminous binder. ***Construction and Building Materials***, 163, 901-911. (**Published**)
- **MOHAMMED, M.**, T. PARRY, N. THOM, and J. GRENFELL. Investigation into the bond strength of bitumen-fibre mastic. ***Construction and Building Materials***, Vol. 190, 2018, pp. 382-391. (**Published**)
- **MOHAMMED, M.**, T. PARRY, N. THOM, and J. GRENFELL. Microstructure and mechanical properties of fibre reinforced asphalt mixtures. ***Construction and Building Materials***. (**Submitted**)

❖ Conference papers:

- **MOHAMMED, M.**, PARRY, T. & GRENFELL, J. 2017. Fibre behaviour and influence on the properties of asphalt mortar. ***Bearing Capacity of Roads, Railways and Airfields***, Greece. (**Published and presented as a poster**)
- **MOHAMMED, M.,** T. PARRY, N. THOM, and J. GRENFELL. 2019. Permanent deformation resistance of cellulose fibre reinforced asphalt mastic and

mixture. ***Transportation Research Board Annual Meeting,*** United States. (**Published and presented as a poster**).

Chapter 2 Literature review

2.1 Introduction

Bitumen (or asphalt binder as it is referred to in North America) is a sticky, black and highly viscous liquid or semi-solid form of oil. Seventy percent of bitumen use is in building roads, where it is used to glue aggregate particles together to form asphalt mixture as one composite material (Sorensen and Wichert, 2009). Bituminous binders are a viscoelastic material, and the unique behaviour of viscoelastic materials is the dependency of their mechanical response on time of loading and temperature. At any combination of time and temperature, viscoelastic behaviour, within the linear range, must be characterised by at least two properties: the total resistance to deformation and the relative distribution of that resistance between an elastic part and a viscous part. Asphalt mixture consists of bitumen and aggregates. Consequently, it is considered a sensitive material to temperature and loading time compared to other construction materials (Castro and Sanchez, 2008).

However, asphalt seems to be widely accepted as the choice of highway pavement material around the world. With the traffic increase, the high loaded vehicles will cause the early deterioration of asphalt pavement, including low-temperature cracks, high-temperature rutting, reflective cracks, subsidence and potholes (Qiu et al., 2013). Therefore, many methods have been used to find solutions to these problems and improve the performance of asphalt mixtures. Among them adding fibre is considered one of the technologies of modified asphalt (Chen et al., 2008, Abtahi et al., 2013).

Some researchers have examined the effect of fibre on bitumen binder and mortar. The rheological properties of bitumen-fibre mastic and mortar need to be assessed by the use of various binder mechanical tests such as double edge notched tension test (DENT) and dynamic shear rheometer (DSR). Several researchers have studied the effects of fibre on asphalt mixture properties. But there is no study that evaluates the effect of fibre on binder, mortar and mixture in a successive process. In addition, very few of them have investigated the effect of fibre on pavement and design thickness.

This chapter is a review of the considerable work which has been conducted to measure empirical and fundamental properties of bitumen-fibre mastics and fibre reinforced mixtures. The rheological properties of fibre modified binders and fibre reinforced mixture design are also included in this chapter.

2.2 General information about fibre reinforcement

Fibre reinforcement generally has been used to improve the properties of a material by incorporating other materials that have some desired properties. The reinforcing element purpose is to stop the formation and spread of cracks as well as to bear the tensile loads. Fibre has been used as a crack barrier in addition to provide increasing tensile strength of the resulting composite (Maurer and Malasheskie, 1989). Fine fibres behave like filler materials because they have a high surface area per unit weight. The high surface area and absorption of fibres mean that fibre reinforced mixtures need a slight increase in the optimum binder content compared to normal mixtures (Peltonen, 1991).

It has been indicated that because of the lack of understanding of the reinforcing mechanisms and the methods of evaluating fibre characteristics (fibre length, surface texture and diameter), performance improvement of reinforced mixtures

by all fibres was found to be marginal. The performance of the asphalt mixture after adding fibres can be quite varied depending on the properties of the fibres. Therefore, several attempts have led to modelling of fibre reinforced binder materials such as Slippage Theory. Slippage Theory has been used and derived from composite science to predict the performance of different fibres. Thus, based on the essential features of each fibre. An index λ represents the value of fibre contribution in the bearing of tensile stresses applied into the composite and can be found as shown in the following equation:

$$\lambda = (d_f . E_f . \varepsilon_f)/(2 . \zeta . L_f) \quad \text{Equation 2-1}$$

Where: d_f. E_f. ε_f are fibre diameter, Young's Modulus and strain at failure of fibre, respectively. ζ is interfacial shear stress between the fibre and matrix of asphalt mixture (Abtahi et al., 2010).

Adding fibres to enhance the performance of materials is not new. In the 1960s one of the earlier attempts in the developments of fibre reinforcement started. Many types of fibres were presented and are still presented in the market with different features such as glass fibre, polyester fibre, asbestos fibre, tyre rubber fibre, polypropylene fibre, carbon fibre, cellulose fibre, etc. (Serfass and Samanos, 1996).

2.3 Types of fibres

There are several types and forms of fibres that have been used in asphalt mixtures, either experimentally or routinely. The most common fibres are mineral, cellulose and polymer fibres. The following section summarises the most commonly used types of fibres.

2.3.1 Glass fibres

E-glass is the most popular type used as a reinforcement material in the engineering project and industrial structures. It is produced from lime-alumina-borosilicate which can be simply obtained from raw materials such as sand (Mathews and Rawlings, 1994). Glass fibres using have not been reported often in the literature but appear to have desirable properties, including low thermal expansion coefficient, high tensile modulus (~60 GPa), high elastic recovery (100%), and high softening point (815℃). However, due to these features for glass fibre, it is expected that fracture strength for glass fibre reinforced mixture will be greater than that for normal asphalt mixture. Consequently, adding glass fibre into bitumen mixture may lead to enhance the stability and the deformability of the bitumen mixture without increasing bitumen content in the mixture and this will have a good effect on the rutting resistance and bleeding especially in high temperature regions (Najd et al., 2005).

2.3.2 Cellulose fibres

They are plant-based fibres produced through dissolving wood pulp into liquid and then treating by chemicals. Cellulose fibre is highly absorbent and due to this feature, cellulose fibres hold on to high binder contents in mixtures (NCHRP, 2015). The effects of loose cellulose fibres, pelletized cellulose fibre and two polymer fibres were investigated by Stuart and Malmquist (1994) on binder drain down. Test results showed that control and polymer modified mixtures drained much more than those with fibre.

2.3.3 Polypropylene fibres

Polypropylene fibres are widely used to strengthen asphalt concrete, and this is because of two reasons, firstly they are low cost and secondly the high compatibility between polypropylene and asphalt mixture. Reflective cracking and crack

intensities of the fibre reinforced overlay sections can be reduced by using polypropylene fibres. In addition, using polypropylene fibres in asphalt mixtures showed increases in the Marshall Stability values, whereas flow values decreased noticeably for asphalt cement specimens (Abtahi et al., 2013). But, the main problem with using polypropylene fibres is the low melting point (about 160℃). Therefore, using polypropylene fibres needs tight control of mixing temperature (Maurer and Malasheskie, 1989, Abtahi et al., 2010).

2.3.4 Polyester fibres

Polyester is a kind of polymeric fibre made from crude oil and has a smooth surface when observed using a microscope (Park, 2012). Polyester fibre is the most common choice for reinforcing asphalt concrete (Kim et al., 1999, Wu et al., 2006, Ling et al., 2008, Ye et al., 2009, Zhou et al., 2009, Yu and Sun, 2010). The high-temperature stability of the asphalt mixtures is improved by using polyester fibres, due to their stabilising and multi-directional reinforcing function (Haoran et al., 2007).

2.3.5 Carpet fibres

A large amount, about 4-6 million tons per year of waste carpet is generated worldwide and accumulated in landfills representing an abundant resource. This waste carpet could be incorporated into different beneficial products (Wang, 1999). A carpet normally consists of two layers of backing (usually polypropylene) filled styrene-butadiene latex rubber (SBR). Adding carpet fibre improved drain down the resistance of SMA mixture and did not weaken the mixture when exposed to moisture (Putman and Amirkhanian, 2004).

2.3.6 Carbon fibres

There are two types of carbon fibre; when the percentage of carbon is 99% it is generally known as graphite fibre, but when this percentage drops to 92% it is called carbon fibre (Reddy, 2014). Carbon fibre is considered a new and sophisticated material that has found many uses due to the high tensile strength, low densities, good electrical and thermal conductivities and excellent creep resistance. In the absence of oxidizing agents, carbon fibre has high thermal and chemical stabilities (Huang, 2009). In addition, carbon fibre showed consistency in results when added to the asphalt mixture (Jahromi and Khodaii, 2008). Also, it is interesting to note that they found the high electrical conductivity of carbon fibres will lead to improving the electrical conductivity of the pavement and its performance better than graphite. This gives the possibility of removing snow and ice on highways in winter by using thermo-electrical techniques (Abtahi et al., 2010).

2.3.7 Steel fibres

Steel fibres are an electrically conductive material. Therefore, it provides the multifunctional application in asphalt concrete pavement like self-healing, removal of snow and ice on the road surface and structural health self-monitoring. In addition, steel fibre has a high modulus of elasticity and tensile strength (Huang et al., 2009). On the other hand, adding steel fibre to the surface layer of flexible pavement may cause problems like discomfort for drivers and minimises safety on the road, which may be caused by a tyre puncture. Consequently, it is recommended to use steel fibres in any layer under the surface layer (Al-Ridha et al., 2014). However, very few studies have evaluated the potential effect of steel fibre on the performance of hot asphalt mixture.

2.4 Fibre influence on the properties of asphalt binder mastic and mortar

Serfass and Samanos (1996) recommended that tests of mastics (bitumen + fibres) and mortars (bitumen + fibre + fine aggregates) can help researchers understand the behaviour of fibre reinforced asphalt mixture. The service life-span and the performance of asphalt pavement are dependent on asphalt binder, which is considered one of the key factors. Recently, more attention is given to evaluate and improve asphalt binder performance, and researchers developed many methods to enhance the performance of flexible pavement such as stone matrix asphalt (SMA), the technology of modified asphalt. One of these technologies is adding fibre to asphalt pavement (Wu et al., 2006).

Many types of fibres, such as organic, cellulose, polyester and mineral fibres are added to asphalt, and this composite is known as bitumen-fibre mastic. The main mastic purpose is to work as the material that bonds the coarse and fine aggregate together, therefore, bitumen-fibre mastics are an important part of hot asphalt mix. Fibre should stabilise the mastic and prohibit the loss of binder through draining out, especially when the mix is hot. In addition, fibre will strengthen the bitumen phase, but studies find that different types and amounts of fibres are added, so they show different degrees of mechanisms to strengthen the modified asphalt and resist crack propagation (Chen et al., 2008). Consequently, fibre use should be further investigated. Wu et al. (2006) found that the optimum amounts of cellulose and polyester fibre were 6 percent and 4 percent by binder mass, respectively. Also, the experimental results show that mixing fibre with a binder can enhance the high temperature performance of binder significantly.

Moreover, they found the strengthening effect of polyester fibre higher than cellulose fibre, but cellulose fibres improve the stability of asphalt binder more than polyester fibre. Chen et al. (2008) came to the same conclusions when they evaluated the effect of three types of fibre on asphalt binder high temperature

performance, including polyester, polyacrylonitrile and cellulose. They found the optimum content 6%, 4% and 8% by bitumen mass for polyester, polyacrylonitrile and cellulose, respectively. Chen and Lin (2005) found that mixing fibres with binder will strengthen the bitumen and they suggested that the increase in stiffening value of ten times more than bitumen's viscosity seems to be suitable for the strength reinforcement using fibres.

Furthermore, the appropriate content of fibres was selected as 0.3, 0.3, 0.4 and 0.4% by total mix mass for organic, long polyester, short polyester and mineral fibres respectively (Chen and Lin, 2005). Qian et al. (2014) evaluated the influence of fibres in reinforcing asphalt binder at low temperature. They found that the failure tensile strain greatly improves when a sufficient amount of polyester fibre is added in addition to enhance other tensile properties of the fibre reinforced bitumen. However, when the temperature drops the bitumen becomes more brittle, but fibre reinforced bitumen maintains its tensile ductility when temperature drops (Qian et al., 2014). The stabilising and reinforcing effects for mastics modified by five types of fibres were investigated by Xu et al. (2010), and they reported that lignin and asbestos fibres have a better stabilising effect whereas polyester and polyacrylonitrile fibres are better for reinforcing. It is important to note that when fibres are added to bitumen, they increase binder stiffness. But, the binder stiffness may increase significantly and cause brittleness in the modified mixture. The high brittleness of the resulting composite will make the pavement disintegrate and fracture under the effect of traffic loading and climate conditions (Chen and Lin, 2005). In addition, adding fibres more than the optimum content will increase the cost. As a result, it is crucial to investigate the effect of fibre content in reinforcing asphalt binder and understand how the behaviour of binder fibre-mastics assists better control of the performance of asphalt mixtures and flexible pavement. However, there are few studies on the effect of fibre types and amount on the rheological properties of bitumen (Zou et al., 2001).

Until now there is infrequent research on the influence of fibre on bitumen mortar, and fibre modified bitumen mortar is poorly characterised scientifically. Wu et al. (2014) studied the reinforcement effect of three fibre types (carbon, mineral and lignin) on asphalt mortar and this is the only documented study for asphalt modified mortar. They found that the viscosity increased with the increase of filler to bitumen ratio. This increase in viscosity mainly comes from fibres because adding more fibre leads to a significant increase in viscosity. However, in terms of viscoelastic behaviour for fibre modified asphalt mortar, they found that the toughness of modified mortar increased when the percentage of lignin fibre increased and decreased with rising temperature. This behaviour shows that adding lignin fibre enhanced the cracking possibility of the modified mortars, therefore, had a detrimental influence on the cracking resistance of modified mortars.

Moreover, the creep rate slightly decreases with increasing lignin fibre content and significantly increased with a rise of temperature. Therefore, the increasing temperature would improve the cracking resistance of lignin modified asphalt mortar, and this was consistent with the result of low temperature creep stiffness analysis. According to these results, they suggested that 0.3 percent by mixture weight was the desirable content for lignin or mineral fibre, whereas the desirable content of carbon fibre was 4 percent.

2.5 Fibres influence on mix design criteria

Little appears in the previous studies in terms of mix design procedures with fibres. In general, the design procedures of asphalt mixtures with fibres are the same procedures used in conventional mixtures. But asphalt mixtures with fibres need the presence of a mechanism to introduce fibres into the asphalt mix plant (McDaniel, 2015). There is not a specific method showing how to introduce fibre into the mixture stated and matched by BS or ASTM (Abtahi et al., 2010).

However, there are two ways to introduce fibres into the bitumen mix, firstly wet-mixing; in this way, fibres can be added to the liquid binder before adding the binder into the mixture. The second way, dry-mixing; in this way fibres are mixed with the aggregate before adding binder (Abiola et al., 2014). Sometimes fibre type specifies the mixing method. For instance, if the fibre's melting point is lower than 160℃, it is better to use dry-mixing. On the other hand, if the fibres are brittle, using the dry method will lead to broken fibre and reduce fibre length (McDaniel, 2015). Generally, the dry method is better than wet-mixing due to a number of reasons. Firstly, dry-mixing helps to reduce the major problem of clumping or balling of fibres in the mixture (Labib and Maher, 1999).

Moreover, most of the previous field work on fibre reinforced asphalt mixtures have preferred to use dry mixing (Echols, 1989, Munn, 1989, Hejazi, 2007). Also, dry mixing is considered an easy way, and through this method, fibres have a good distribution in the mixture (Abtahi et al., 2010). But, Abtahi et al. (2008) examined the effect of two mixing methods on Marshall properties (Stability and Flow) when the Nylon 6.6 fibres of 12 mm length were added into the asphalt mixtures, they found the same results for wet and dry procedures.

Regardless of the method used to introduce fibres into the mix, adding a high percentage of fibre more than optimum content may make compaction more difficult, leading to higher air voids in the mixture (Serin et al., 2012, Crispino et al., 2013). Through the literature, the suitable fibre percentage to use in a given mixture type may become standard for certain fibre types. For example, 0.3 percent of cellulose fibre by weight of the mixture is a very common addition percentage in SMA (McDaniel, 2015). Chen et al. (2009) found that Marshall stability of control mixtures is slightly higher than fibre modified specimens when the same amount of bitumen is used, but when the bitumen content increased in modified specimens Marshal stability of modified mixtures became higher. Hence fibre reinforced asphalt cement (FRAC) mixture requires higher binder content than

a normal mixture. The large surface area of aggregates and fibres could be responsible for this increase in binder content; this large surface area needs to be wetted by the binder filling which would lead to an increase in the percentage of voids in the asphalt mixture (Huang and White, 1996, Kim et al., 1999, Tapkin et al., 2009). Therefore, as shown in Figure 2-1, the air voids of fibre reinforced asphalt cement (FRAC) mixture will increase when the same amount of binder is used. This is due to the insufficient binder, leading to strength reduction (Chen et al., 2009).

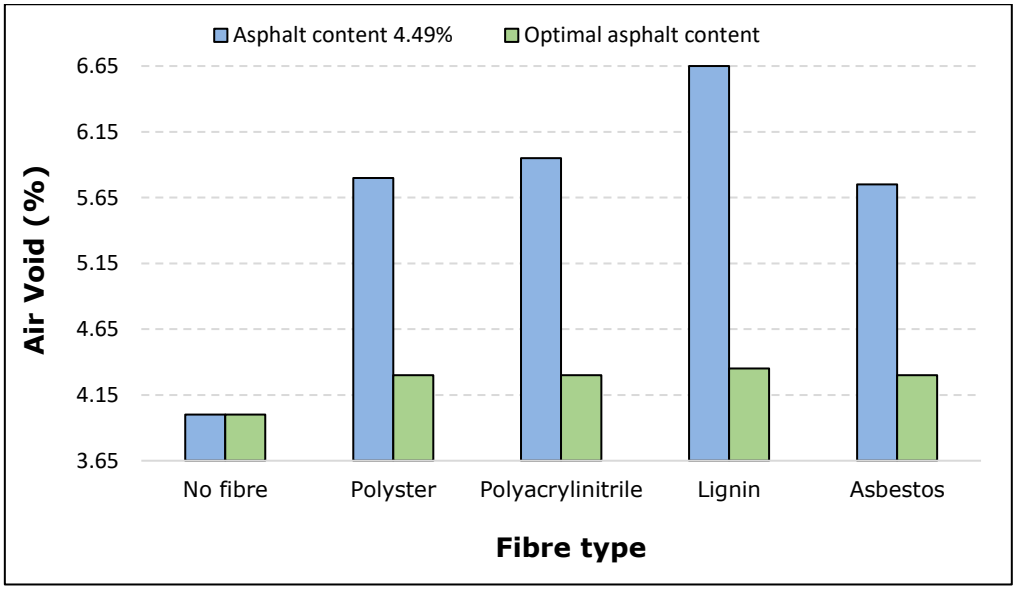


Figure 2-1 Relations between asphalt content and air voids of fibre reinforced asphalt cement (FRAC) (Chen et al., 2009)

Specific gravity correlates to air voids and lower specific gravity is associated with the higher air voids in the asphalt mix. Adding fibre will lead to a slight decrease in bulk specific gravity (Gmb) of asphalt mixtures as shown in Figure 2-2. This may be because the specific gravity of fibre is lower than that of mineral aggregates. Conversely, voids mineral aggregate (VMA) increase after adding fibre into asphalt mixtures. The percentage of increase in VMA depends on fibres type. For instance, the lignin and asbestos fibres asphalt mixtures have greater VMA than other fibres mixtures. The reason for this may be due to their lower Gmb. Furthermore, voids

filled with asphalt (VFA) slightly increase after adding fibre, and again the percentage of increase depend on the fibre properties, especially on the absorption value and specific surface area. For example, lignin and asbestos fibres mixtures have higher VFA than other fibres mixtures as illustrated in Figure 2-3, which is due to their higher optimum asphalt content (Chen et al., 2009). Otherwise, the inverse will happen in VMA and VFA when a high percentage of fibre added into the asphalt mix. Consequently, a high amount of fibre is not recommended. The decrease of VFA will result in a decrease in effective asphalt film thickness between aggregates particles to form a stable interface adhesion, according to the 'interlock adhesion theory' (the porosity and surface roughness of the substrate with the degree of adhesion that can be obtained (Masson and Lacasse, 1999)), interfacial failure between the asphalt film and aggregate surface may occur as a result of this reduction (Mo et al., 2009). Therefore, adding optimum fibre and asphalt content into mixture would produce interface adhesion more than that of normal mixtures (Chen et al., 2009).

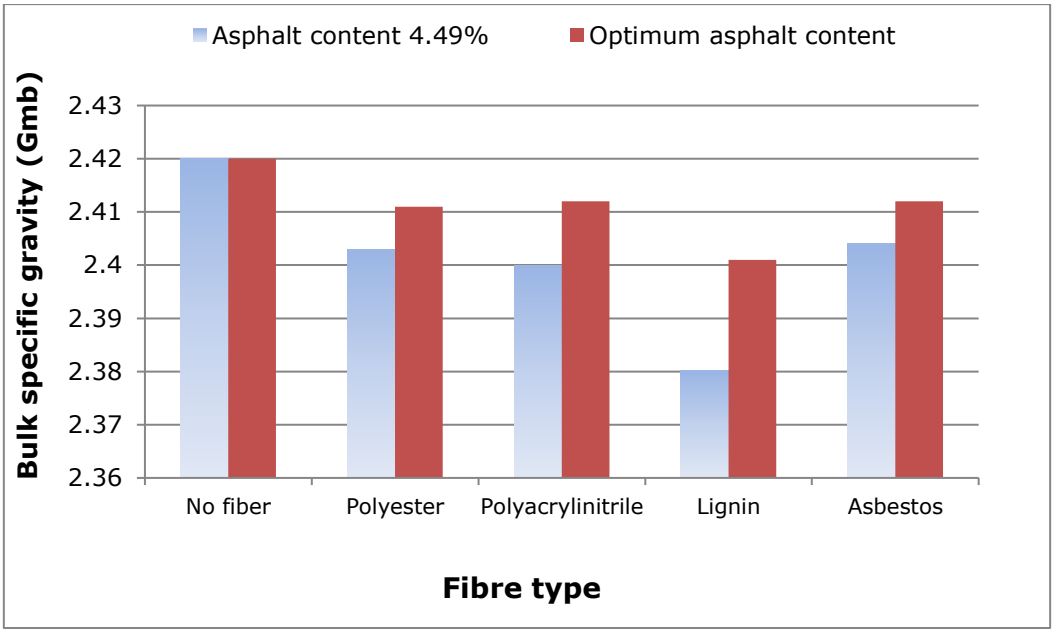


Figure 2-2 Bulk specific gravity (Gmb) of mixtures (Note: asphalt content of 4.49% is the optimum asphalt content of ordinary mixture), (Chen et al., 2009)

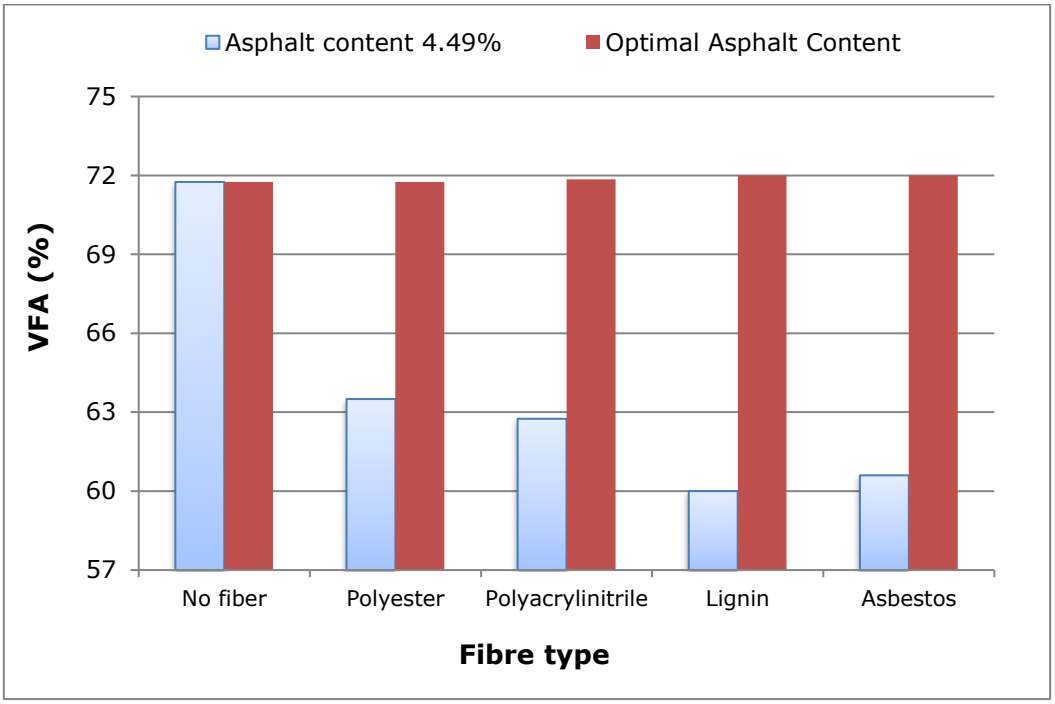


Figure 2-3 Voids filled with asphalt (VFA) of mixtures with different fibre types (Chen et al., 2009)

It is well known that optimum asphalt contents (OAC) will increase when fibres are added into asphalt mixture. This increase is due to two reasons. Firstly, fibre needs a high amount of bitumen to cover its surface. Secondly, most fibres absorb light components of bitumen, and this affects mixture stability (Serfass and Samanos, 1996, Mahrez et al., 2005, Chen et al., 2009). According to what has been mentioned before, the main difference between SMA and AC mixtures in using fibre is that SMA mixture is less sensitive to the variation of the binder content than the conventional AC mixture. This may be because the fibres kept the stability of the SMA mixture high when the binder content increases (Silva, 2008). In addition, the main reason for adding fibres into SMA mixture is to prevent drain-down of the binder when the mixture is hot (Mohamadzadeh et al., 2014).

2.6 Effect of fibres on mechanical properties of asphalt mixture

Fibres, in general, have high tensile strengths. Therefore, fibres are used in asphalt mixture as reinforcement in order to increase the tensile strength of the resulting materials. Furthermore, fibre can improve the value of the strain energy, which can be absorbed through the fatigue and fracture process (Mahrez et al., 2003). Both synthetic and natural fibres have been used in different hot mix asphalt applications. Synthetic fibres include polypropylene, polyester and aramid, whereas natural fibres include asbestos, cellulose and rock wool (Alrajhi, 2012). The possible benefit of adding fibres to reinforce asphalt mixtures include reducing fatigue, thermal and reflective cracking and increased service life. Consequently, many studies have been done to evaluate the influence of various fibres in asphalt mixtures (Mahrez et al., 2003, Mahrez and Karim, 2007, Alrajhi, 2012).

Haoran et al. (2007) found that the resistance to moisture damage and environmental disruption of the asphalt mixture will improve by adding polyester fibres. This is due to their ability to absorb the bitumen and thicken the bitumen film adhering to the aggregate. Also, according to Freeman et al. (1989), moisture susceptibility can be improved by adding polyester fibres. The results of the tests, which were conducted at room temperature, show that the tensile strength ratio (TSR), ratio of wet indirect tensile strength (ITS) to dry ITS, which represent moisture susceptibility of asphalt concrete, increases up to 15.0% when 0.5% of 12 mm polyester fibre is added to dense graded asphalt concrete mixture. Also, they suggested that using thicker, longer, and a larger amount of fibres are better for moisture damage resistance. Moreover, they examined toughness. They found that dry and wet toughness of fibre reinforced asphalt cement (FRAC) mixture were higher by up to 25.0% and 120.0%, respectively than that of the control mixture. On the other hand, Anurag et al. (2009) examined the influence of adding waste polyester fibres on the moisture susceptibility of dense graded asphalt mixture.

Figure 2-4 shows the relationship between dry and wet strengths and fibre contents. It is clear from the chart below that there is a slight decrease in dry strength and increase in wet strength with fibre addition.

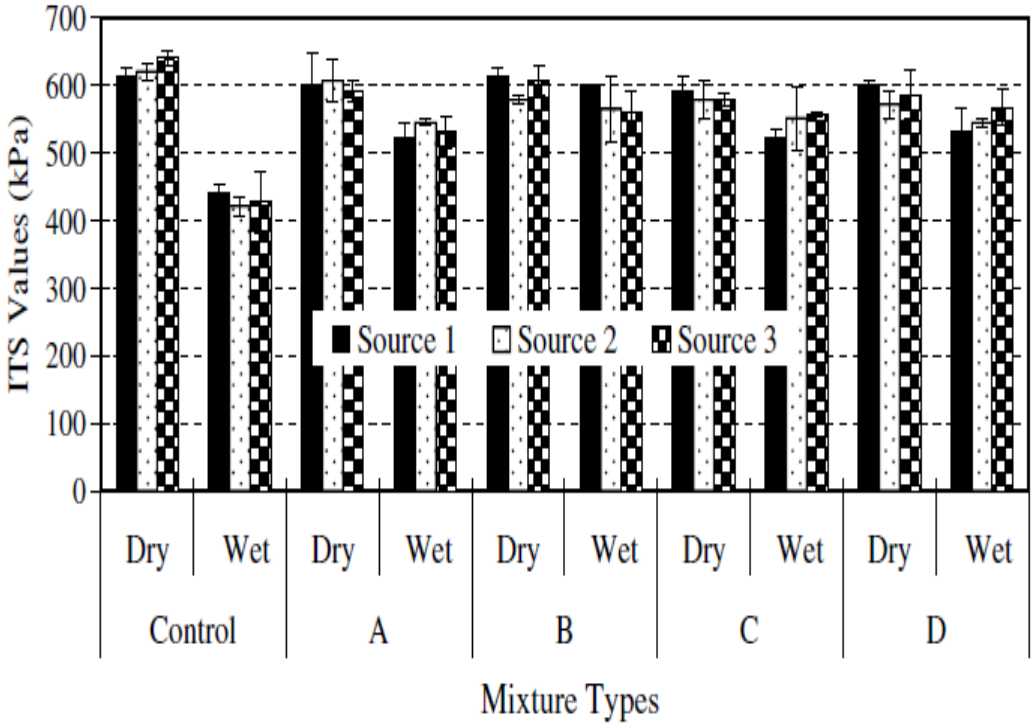


Figure 2-4 Lengths and contents of waste polyester fibre additives and indirect tensile strengths of the mixtures (Anurag et al., 2009)

Lee et al. (2005) discovered that the fracture energy increased when recycled carpet fibres were added to the asphalt mixture. This increase will lead to improved fatigue cracking resistance. The experimental result shows that the fracture energy of fibre reinforced asphalt mixture with 1% by mixture mass and a fibre length of 12 mm demonstrate 85% improvement in fatigue resistance compared to the normal asphalt mixture at the 20℃ test temperature.

Tapkin (2008) evaluated the effect of polypropylene fibre on the elastic and permanent deformation behaviour of asphalt mixture. He found that the pulse count has a big effect on the elastic deformation of fibre reinforced asphalt mixture and when pulse count increases the fibre influence will be very obvious leading to

a higher level of elastic deformation compared to the normal mixture. Moreover, the elastic deformation of the fibre reinforced samples drops below the elastic deformation of the control samples when the test approaches the breaking point. This indicates that reinforced samples showed a permanent deformation response. Also, the test results show that adding 1% of polypropylene fibres by mixture weight extended the fatigue life 27% more than that of control specimens.

Another notable laboratory test was reported by Lee (2004). He concluded that 1% of nylon fibres by asphalt mix mass with a fibre length of 12 mm could enhance fatigue cracking resistance by increasing the fracture energy. In addition, he noted up to 85.0% increase in the fracture energy as a result of adding fibres ((Lee, 2004), nylon fibres and (Lee et al., 2005), recycled carpet fibres). Furthermore, adding carbon fibres to asphalt mixtures would improve the resistance of the pavement to distress as different test results indicate that, such as repeated load indirect tensile test, creep test and indirect tensile test. As a result, pavement life would improve by increasing resistance to cracks or permanent deformation (Jahromi and Khodaii, 2008).

Meaningful information about the reinforcing effects of cellulose, polyester, and mineral fibres can be found in the study reported by Ye et al. (2009). Based on the dynamic modulus test and indirect tensile fatigue test, they found that fatigue resistance can be improved by adding fibres. Several studies came to the same conclusion: those are ((Ling et al., 2008), various fibres), ((Zhou et al., 2009), various fibres), ((Yu and Sun, 2010), polyester fibres), ((Alrajhi, 2012), aramid fibres) and ((Guan et al., 2014), brucite fibre).

Xu et al. (2010) examined fatigue and rutting properties of FRAC using polyester, polyacrylonitrile, lignin and asbestos fibres with different percentages (0.20, 0.35 and 0.50% by total weight of mixture). Results showed that adding fibres improved the mixtures' fatigue life at the stress ratio of 0.5. Polyacrylonitrile, polyester,

asbestos, and lignin fibre have improved fatigue life by 66.8%, 57.7%, 40.9%, and 22.5%, respectively. They explained the reason for this improvement might be attributed to fibre's absorption and adhesion of asphalt, entanglement function, bridging of cracking and reallocation of stresses.

In terms of rutting resistance, the laboratory results showed that polyester and polyacrylonitrile fibres had lowered rut depths by 19.57% and 32.56%, while lignin and asbestos fibres have reduced them by 8.43% and 11.40% at 2500 cycles respectively. This study recommended that the right amount of fibre for improving rutting resistance for these four fibres types were 0.35% by weight of the mixture. Furthermore, they believed that the increase in cracking resistance depended on fibre's geometry and physical properties. In general, as the fibre has a higher tensile strength that means this fibre will be more effective to resist cracking, and with the higher length/diameter ratio the formation of a networking system will be more effective for interweaving together. Therefore, polyacrylonitrile fibre has the highest effect on rutting resistance than other fibres used in Xu et al. (2010) study. Another study by Tapkin et al. (2009) indicated that rutting resistance at high service temperature (50℃) improved by adding polypropylene fibres.

Fibres have been widely used as a stabiliser for porous asphalt and SMA, but their use for improving mechanical performance was not investigated until recently. One of the earlier studies has been done by Selim et al. (1994). They studied the effect of cellulose fibre on two SMA mixtures, the first mixture with normal binder and fibres showed the highest indirect tensile strength and tensile strength ratio after conditioning. The second mixture was a polymer modified mixture containing fibres that exhibited the lowest resistance to moisture damage and tensile strength. Mohamadzadeh et al. (2014) examined the influence of adding four types of fibres (acrylic, polyester, cellulose and viscose) in SMA mixtures. All the mixtures have a tensile strength ratio (TSR) more than the minimum value of 80%. In addition, the analysis indicates that the mixture containing the acrylic fibres has 90% TSR which

is the highest value among all fibres and then polyester, cellulose and viscose fibres, respectively.

Another study by Liu et al. (2010) found that steel fibres content of 11.0% by bitumen volume improves the indirect tensile strength (ITS) of the plain porous asphalt mixtures and when the steel fibre content is more than 11.0%, the effect of steel fibre on the ITS is negative. This decrease may be due to high fibres content reducing the mastic film thickness, causing a bad adhesion between the asphalt components. Asphalt mixture that contains 0.1% and 0.2% steel fibres by volume of the total mix was found to have higher Marshall stability in comparison with the normal mixture without fibre (Al-Ridha et al., 2014).

Putman and Amirkhanian (2004) examined the performance of different fibre types (tyre, carpet, polyester and cellulose) in SMA mixtures. They concluded that the tensile strength ratios 100.9% and 101.8% for the mixes containing the tyre and carpet fibres, respectively. This shows that these fibres improved moisture susceptibility of the mixture. Moreover, the addition of tyre, carpet and polyester fibres increases the toughness of the SMA mixtures when compared to the cellulose fibres. In terms of permanent deformation, there was no significant difference between all fibres included in this study.

Behbahani et al. (2009) evaluated the effect of two types, cellulose fibres (made in Iran and Germany) and mineral fibres (rock wool) with different percentages, on the rutting performance of the SMA mixtures. The result showed that these fibres demonstrate higher rutting resistance and the optimum content seems to be 0.3% of cellulose fibre from Germany and mineral or cellulose fibre from Iran was 0.4% of the total weight of the mixture. According to Putman and Amirkhanian (2004), the permanent deformation performance of SMA mix containing carpet fibres and SMA mix containing cellulose or mineral fibre was found to be comparable.

Mahrez et al. (2005) published results that showed permanent deformation property of SMA could be improved by adding glass fibre. Mixes with 0.3% glass fibre by weight of mix had the best deformation behaviour. Additionally, it is observed that the mixes containing 0.1, 0.2 and 0.3% glass fibre by weight of mix demonstrated a significant effect on fatigue life and fatigue life improved by about 28.2, 37.2 and 44.4% at these contents, respectively. Mahrez and Karim (2010) demonstrated that glass fibre improves the fatigue life of the mix and this improvement is more considerable at higher stress levels as compared to lower stress levels. Consequently, this improvement is more important and useful when the heavily trafficked road is concerned. Whereas, Vale et al. (2013) found that adding 0.5% coconut fibres of total mixture did not improve fatigue life of SMA mixtures and surprisingly coconut fibre mixture performance was worse than both mixture with 0.3% cellulose fibre of total mixture and without fibre as shown in Figure 2-5, but they mention SMA mixtures without fibre had a noticeable drain down. They think the possible reason for this performance of coconut fibre might be the proportion of fibre in the mixture leading to stiffening of the mixture and asphalt absorption.

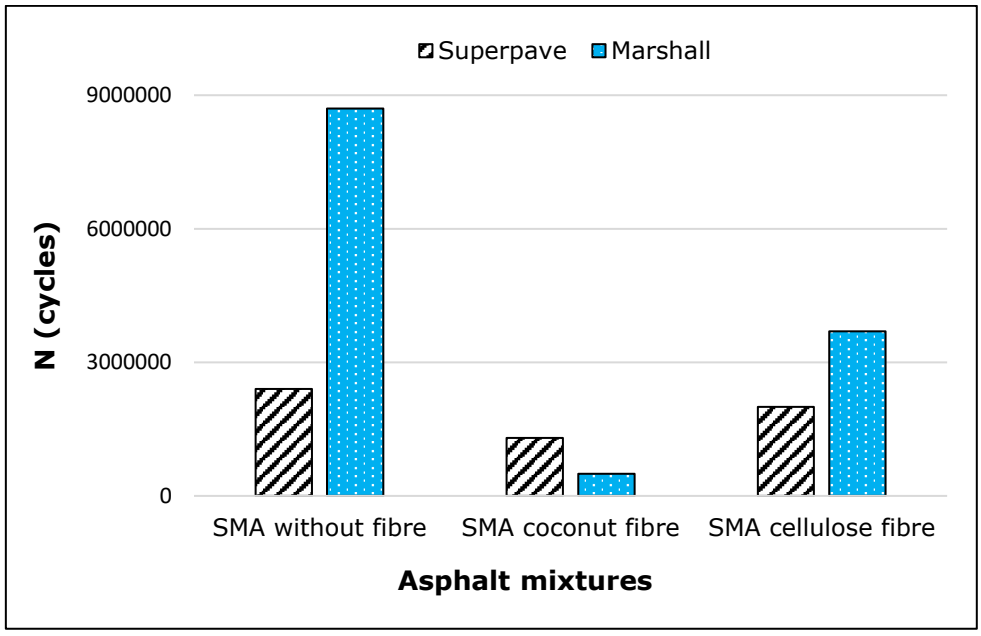


Figure 2-5 Result of analysis of fatigue test (Vale et al., 2013)

In conclusion, adding fibres to asphalt mixtures demonstrated noticeable improvement in mechanical properties. Only one study (Vale et al., 2013) found that adding (coconut) fibres had a detrimental effect on the fatigue life of SMA mixtures. However, just two studies examined the effect of fibre characteristics on mechanical properties. The first study recommended using thicker, longer, and a larger amount of fibres are better for moisture damage resistance. The second study recommended using fibres with high tensile strength would be more effective to resist cracking and with the higher length/diameter ratio, the formation of the entanglement system will be more effective for interweaving together. On the other hand, the majority of these studies agreed that adding too high a percentage of fibre has a negative influence on the asphalt mixture performance.

2.7 Evaluation of reinforcing effects of fibres in the field

The Indiana Department of Highways evaluated a test section of asphalt overlay containing polypropylene fibres by comparing this section with another section without fibres. An overlay with 50.8 mm thickness was placed over seriously deteriorated existing pavement. The fibre section length was about 167.6 m of the travel lane. The other part of this lane was without fibres and used as the control. (0.3%) of fibres by total mixture, weight was added to the batch plant (Galinsky, 1984). After 30 months, they observed the amount of cracking in the control section was more than twice that in the fibre section. In addition, the cracks were of much greater severity in the control section. The crack widths in the fibre section were less than 0.8 mm in width and had very little secondary cracking, while crack widths in the other section were about 6.35 mm, with some cracks almost 9.5 mm wide or more and had significant secondary cracking. Moreover, rut depths in the fibre section were less than 9.5 mm, whereas, in the control, section was 57.0 mm.

After this study, the Indiana Department of Highways began using polypropylene fibres in more situations.

Maurer and Malasheskie (1989) evaluated the difference in the field performance of four fabric interlayers, first one asphalt interlayer (stress-absorbing membrane interlayer, or SAMI) reinforced by fibre and the other asphalt overlay reinforced by fibre to a control lane without the reinforced overlay. 0.3% polyester fibres by total mixture weight were added to the asphalt mixture batch. In 1984 the test sections were constructed on a main arterial highway in Pennsylvania. After 44 months in service, they found that fibre reinforced overlay showed the best performance compared to all the other treatments with a reduction in reflective cracking of more than fifty percent relative to the control. The fibreised membrane had a reduction in reflective cracking of 46.4 percent compared with the control, but the life cycle cost could not be justified at that time.

Meaningful information about the reinforcing effects of fibres can be found in the field experiments reported by Oregon DOT; the performance of fibreised and polymer modified pavement sections constructed in 1985, after ten years this section withstood load application of more than 1.5 to 1.7 million equivalent single-axle loads. The modified dense-graded top course was placed over an unmodified base course over an existing section with severe fatigue and thermal cracks. There were two sections, one section included polyester fibres and another included polypropylene fibres. In addition, two unmodified sections and six sections with mixtures modified by various anti-strip and polymer additives. In terms of rutting and fatigue cracking, polypropylene and polyester fibre sections performed comparably to the controls. With regards to block cracking, both fibre sections performed better than the control section. Polypropylene fibres had no block cracking, and less than 10% of block cracking appeared in the polyester section of the travel line. The block cracking was between 30% and 50% of the travel lane in the control section (Edgar, 1998).

Another notable field experience was reported by Anderson et al. (1999). The test sections under investigation are an overlay constructed over an existing jointed concrete pavement. It included a control, polyester fibres, four different polymer-modified binders (ethylene vinyl acetate (EVA), polyethylene, styrene butadiene styrene (SBS), and styrene butadiene (SB)) and Gilsonite. Marshall mixture design method was used for designing all the mixes. The fibres were added into the batch plant at a rate of 0.28% by total mixture weight during the dry mixing period. Adding fibres required increasing in dry mixing time by 10–15 seconds compared to the normal mixture to ensure that fibres were uniformly distributed. According to this study, there were not construction problems recorded (Anderson et al., 1999). In terms of rutting, all sections performed well, but the control section had more rutting than the modified sections. After eight years, three of these sections but not fibre one showed a secondary cracking around the sawn and sealed joints. Moreover, the fibre reinforced section did not show top-down longitudinal cracking which were seen in the other three sections.

Huang and White (1996) measured actual fibre content and volumetric properties and conducted complex modulus and fatigue tests of a fibre reinforced asphalt overlay after five years. They found that there is a large difference in target fibre content (-44 ~ +22%). Therefore, this reflects the demand for improving fibre blending techniques. The reason for this is the relatively low melting point of the fibres used and the high aspect ratio. The result of the fatigue test showed that 0.22% fibre specimen had double the fatigue life. The rutting parameters were observed not to be greatly influenced by fibre content.

In conclusion, all field experience of using fibre reinforced asphalt overlay demonstrated that adding fibres lead to a significant decrease in reflective, longitudinal, secondary and block cracking in long term performance. Moreover, the long term performance of asphalt overlay in terms of rutting and fatigue

resistance is improved by adding fibres. However, none of these field experiences evaluated the effect of this improvement on the life cycle cost.

Generally, the reinforcing effects of fibres in the field and the laboratory test demonstrated a remarkable improvement in the asphalt mixture performance. Therefore, the laboratory test in evaluating the effect of fibre on bitumen and asphalt mixture is very important to predict the long term performance of the pavement. On the other hand, the field observation established the demand to find test methods to verify the presence and distribution of fibres in the asphalt mixture. At the same time, there is no specific laboratory test to verify the distribution of fibres in the asphalt mixture.

2.8 Most common distress types in flexible pavement

This section documents the current state of knowledge regarding the main distress types in flexible pavement. It outlines the different types of materials that have been used, their characteristics and mix design tested and laboratory performance of asphalt mixtures.

2.8.1 Permanent deformation in flexible pavement

Permanent deformation is the accumulation of residual strains under the wheel paths due to the repeated traffic loads. The residual strains are mainly due to the compaction of different pavement layers and shear strains. Shear strain is concerned with the stiffness and the load induced stresses, and when the pavement temperature is high, the probability of shear strains in asphalt concrete is higher. Rutting is a major concern for the integrity of road structure and traffic safety. Ruts are considered dangerous distress for traffic, especially when the pavement is wet (Laurinavicius and Oginskas, 2006). The extreme rutting leads to gather water or ice in the depression causing health hazard (aquaplaning) and longer braking

distance (Olsson et al., 2000). Rutting leads to premature damage to the pavement and requires expensive repair costs (Laurinavicius and Oginskas, 2006).

However, it is well known that asphalt concrete is a temperature, time and stress dependent material, showing elastic/ plastic/visco-elastic/ plastic response when it is subjected to repeated traffic. The plastic properties contribute to permanent deformation, which is the cumulative deformation effect of repeated load. There was a solution to minimise vertical stress on the surface of the road base by reinforcing the base, increasing its stiffness (Nagabhushana et al., 2013).

There are studies that have reported that rubber with conventional binders leads to improvement in permanent deformation resistance (Way, 2003, Sebaaly et al., 2003). Also, they point out that the crumb rubber size has an effect on the rutting resistance, but this effect depends on bitumen binder type. Navarro et al. (2004) found that 9%wt crumb tyre rubber to bitumen enhances the resistance to permanent deformation at high service temperatures. Xiao et al. (2007) believed that adding crumb rubber increase rutting resistance of asphalt mixtures. Also, they found that increasing rubber contents considerably leads to efficient improvement in rutting resistance of asphalt mixtures when measured by asphalt pavement analyser test (APA). But they did not give a minimum or maximum limit to this increase in rubber content.

Another way to improve pavement rutting resistance is by manipulating with aggregate shape. Topal and Sengoz (2005) evaluated the effect of fine aggregate angularity on rutting resistance of asphalt mixtures. The test results showed that rutting resistance of asphalt mixture prepared with gyratory crushed aggregate improved when higher fine aggregate angularity value used. The improvement in rutting resistance is mainly due to angular particles create more particle to particle interlock than less angular particles. But when aggregates shape is changed, this will affect other properties like workability, stability and bitumen content of the

asphalt mixture. For instance, the rough, angular aggregate has lower workability than the rounded aggregate. Another study by Kim et al. (2009) examined the effect of mix gradations on rutting potential, especially for low traffic volume roadways. The APA test results indicated that the finer-graded mixtures achieved better rut resistance than coarser-graded mixtures. However, the results of this study are based only on one laboratory test (APA). While according to Chiu and Lu (2007) the mixture with larger aggregate particle size had more resistance to permanent deformation.

The rutting resistance of SMA mixtures modified by different types of polymers has been investigated. Three types of elastomeric polymer modifiers, namely OL (very cohesive product), EL (reactive elastomeric terpolymer) and SB (styrene–butadiene–styrene block copolymer) are used with different percentages (Ozen et al., 2008). The results of repeated creep test exhibited that the rutting performance of the elastomer-modified asphalt mixture is better than the non-modified asphalt mixture. In addition OL and EL showed the best rutting resistance when test by French Rutting Tester (LCPC-wheel tracking test) at 60℃ (Ozen et al., 2008). Also, Casey et al. (2008) evaluated the rutting resistance of SMA mixtures containing two types of polymer. First one was a proprietary polymer (PMB) and the second one was developed recycled high density polyethylene (HDPE) modified binder (RP). The wheel tracking test results at 60℃ showed that the mixture with RP binder had a good resistant against rutting.

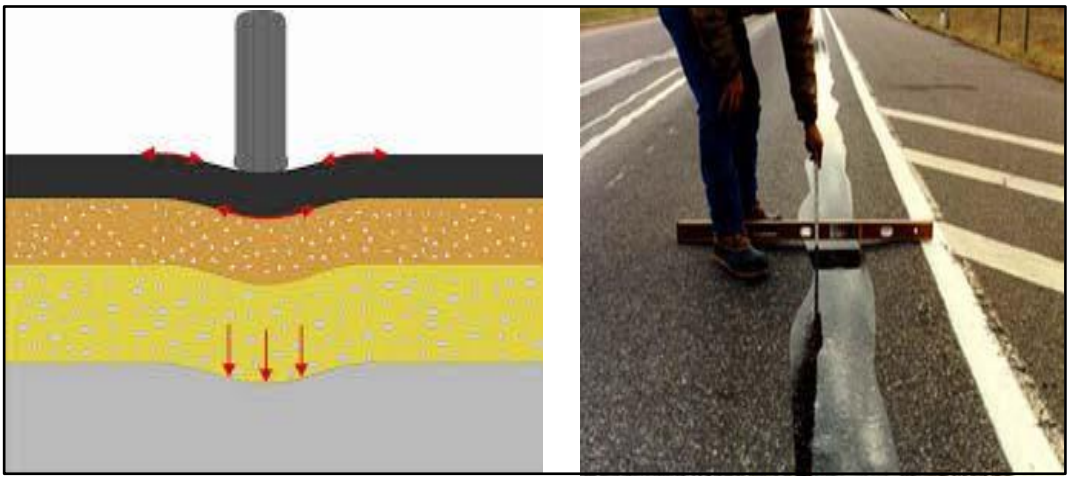


Figure 2-6 Definition of downward and total rutting (John C. Glennon, 2015)

2.8.2 Fatigue phenomenon in asphalt pavements

Fatigue failure caused by traffic is an important issue that influences pavement design life, and which the road designer seeks to avoid during the service life. The design life concept of the pavements is important as long as the pavements do not fail suddenly but gradually deteriorate over time. This is clearly a fatigue phenomenon, in that fatigue is fluctuating stress with a positive and negative phase results from both repetitive traffic loadings and value the road faces and causing failure (Brown, 1988). Data from several studies show that tensile stress is developed at the bottom of the pavement structure. The flaw is formed initially when the tensile stress is higher than the strength of the material. Consequently, the crack initiates at the bottom and starts gradually to propagate upward to the pavement surface. On the other hand, in the case of thick pavements, the highest tensile stress occurs at the top of the pavement structure initiating a crack at the top. This crack gradually propagates to the bottom of the asphalt layer. In general, fatigue cracking is interconnected cracks, called alligator cracks because of how it looks like, as shown in the following Figure 2-7 (Uhlmeyer et al., 2000).



Figure 2-7 Fatigue cracks in asphalt pavements (Seattlie WA Paving, 2019)

2.8.3 Fatigue testing of asphalt mixtures

Different methods have been proposed to classify the fatigue behaviour of asphalt mixtures. The accuracy of simulating the fatigue life of any of these methods is highly dependent on how this method implemented all the variable accurately, such as loading condition, rest period, environmental condition and support type. In addition, choosing any of these test methods is highly dependent on the availability of the equipment, cost and the duration of the test (Zeiada, 2012). There are different fatigue testing types available in the laboratory such as tension/compression test, indirect tensile fatigue test, two-point bending test and four-point bending test etc., as shown in Figure 2-8 However, still very difficult for these test methods to simulate accurately the fatigue life in the field. This is due to a number of reasons such as different loading conditions, different rest periods, healing effect and environmental conditions of the actual road face. Previous studies have shown that there is a clear difference between fatigue life obtained from laboratory test and field. Therefore, different values of shift factor have been used to correlate laboratory to field performance. These values are depending on many factors including layer thickness, temperature, repetitive traffic loading,

failure criteria, test and mixture types (Zeiada, 2012). The past study suggested a shift factor values from 10 to 100 (Harvey et al., 1997).

Asphalt mixture type and properties such as binder contents, air voids and aggregate gradations play a vital role in the fatigue life of the pavement (Wen, 2001). These characteristics will be discussed in detail in the following sections.

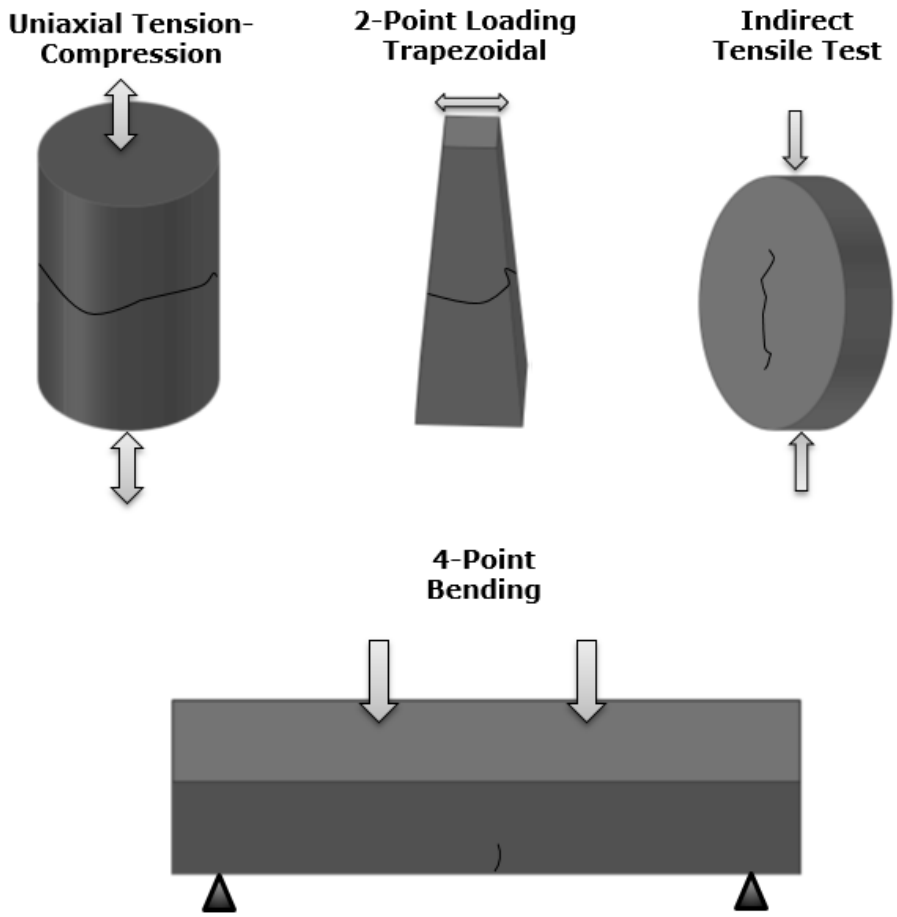


Figure 2-8 Schematic diagram of commonly used fatigue test

2.8.3.1 Influence of mixture type on fatigue life

Previous study examined fatigue life of three different asphalt mixture types, namely Gilsonite modified wearing course (GM-ACWC), stone mastic asphalt (SMA) and conventional asphalt wearing course (ACWC) (Suo and Wong, 2009). Indirect tensile fatigue test (ITFT) with two modes of loading controlled stress and the controlled strain was used in this study. The test results showed that GM-ACWC had the highest fatigue life, followed by SMA and then ACWC at strain level range between 80 and 200 micro-strain. Whereas at strain level around 1000 micro-strain, the three asphalt mixtures had similar fatigue lives (Suo and Wong, 2009). Another research investigated the fatigue lives of hot mix asphalt (HMA) and stone mastic asphalt (SMA) with similar nominal maximum aggregate size at specific test temperature, using indirect tensile fatigue test (ITFT). It was found that HMA has significantly higher stiffness value and generally higher fatigue life compared to SMA. They believed that HMA has a dense graded aggregate structure which may improve aggregate interlocked and adding more adherent effect compared to SMA with more stone on stone contact (Nejad et al., 2010).

2.8.3.2 Influence of bitumen type on fatigue life

There is a growing body of literature that recognises the influence of bitumen type on the fatigue life of asphalt mixture. Previous study examined the influence of two different bitumen grades on the fatigue life of asphalt mixture under a stress control mode of loading and at different testing temperatures. A 40-50 and 90-100 bitumen grades were used in this study. The test results indicated that the fatigue life was different in such a way that low bitumen grade showed higher fatigue resistance (Pell, 1967). One study by Myre (1990) examined the influence of different bitumen types and contents under stress controlled mode of loading. He points out that bitumen grade was the main factor affecting fatigue life of the asphalt mixture. The study suggested that at hot weather conditions using low bitumen grade is far more

effective, and therefore better adapted to the improving fatigue performance. Three different bitumen grades and both control stress and strain mode of loading were used to examine fatigue performance. The results showed that the asphalt mixture made with low bitumen grade exhibited higher fatigue life under controlled strain mode of loading compared to other mixtures (Myre, 1990).

2.8.3.3 Influence of bitumen content on fatigue life

Two previous studies evaluated the fatigue life of asphalt mixture under a controlled stress mode of loading. First study indicated that optimum asphalt content is the best for fatigue performance of asphalt mixture (Jimenez and Gallaway, 1962). The second study came to the same conclusion (Epps et al., 1969). Both studies used an experimental test in their investigation. On the other hand, another study examined the fatigue performance of different asphalt mixtures manufactured with different bitumen contents. It was indicated that there is not a clear effect of bitumen contents on fatigue life (Myre, 1990).

2.8.3.4 Influence of air voids on fatigue life

Evidence indicates that air void is among the factors affecting fatigue performance of asphalt mixture. Previous study found that fatigue performance of asphalt mixture highly influenced by air voids contents in the strain controlled mode of loading. As a result increasing air voids led to decrease in fatigue life (Santucci et al., 1969). Another study examined the influence of compaction level on fatigue life. The test results indicated that fatigue performance improved when air voids decreased (Raithby and Ramshaw, 1972). Research examined the influence of changing air void content by 5% and asphalt content by 1% on the fatigue performance of asphalt mixture. It was found that under controlled strain mode of loading the change in asphalt content had more influence on fatigue life than changing air void content. While, under controlled stress mode of loading, the theoretical analysis indicated that fatigue life was expected to be more sensitive to

the change in air void contents by 5% compared to 1% change in asphalt contents (Zeiada et al., 2013).

2.8.3.5 Influence of aggregate gradation and types on fatigue life

There seems to be some evidence to link aggregate surface textures and shapes to fatigue life based on the effect of these properties on the air void contents and shapes in the asphalt mixture. For instance, aggregate with high angularity, rough surface texture and open gradation is difficult to compact resulting in higher air void contents (Epps and Monismith, 1972). Another researcher claimed that asphalt mixture made with rounded aggregate exhibited higher fatigue life than asphalt mixture manufactured with crushed rock (Pell and Cooper, 1975) cited in (Na Chiangmai, 2010). Asphalt mixture made with quarry sand (high angularity, rough and a high percentage of aluminium oxide) showed higher fatigue life compared to asphalt mixture manufactured with mining sand. They believed that due to the good shape, strength and distribution of quarry sand particles in the asphalt mixture which result in better fatigue performance (Yasreen et al., 2011). However, other researcher has pointed out that it is difficult to examine the influence of aggregate gradations on fatigue life due to changing aggregate gradations lead to different bitumen contents and air voids (Epps and Monismith, 1972). Moreover, Pell and Taylor (1969) conclude that aggregate gradations and types do not significantly influence fatigue life.

2.8.4 Semi-Circular Bending test (SCB)

Tensile strength is a significant property of asphalt mixtures. It plays a significant role in pavement performance, as it is intimately related to many distress types in asphalt pavements such as low thermal cracking and fatigue cracking (Huang et al., 2003, Kim and Wen, 2002). The semi-circular bending test is a simply

supported three-point bending test of a semi-circular shaped specimen with an introduced notch. For many years, this test was frequently used to investigate the fracture strength of rock (Chong and Kuruppu, 1988, Lim et al., 1994). The SCB test gained more and more attention from pavement engineers and researchers to investigate the tensile strength since it was used in the United States by a number of researchers (van de Ven et al., 1997, Krans et al., 1996, Erkens et al., 2002, Molenaar et al., 2002).

Zegeye et al. (2012) examined the nature of the failure of asphalt mixtures in SCB fracture tests at a low temperature. In their study, the SCB specimens were manufactured with four diameter sizes: 76.4 mm, 101.0 mm, 147.0 mm and 296.0 mm. For each diameter size, samples were prepared to match notch length to specimen radius (a/r) ratios of notch less, 0.05, and 0.20. The testing temperature in this study was selected to be 24℃. It was found that in large samples without a notch cracks always initiated from the support far from the centre line where the measuring gauge was fitted. In addition, it was found that the nominal strength of samples increased as the size of the samples decreased.

Wu et al. (2005) investigated fracture resistance in several Superpave asphalt mixtures with four different compaction levels, four different binder types (AC-30, PAC-40, PG70-22M, and PG76-22M) and different nominal maximum aggregate sizes (NMAS) using the SCB test. Three replicates samples were prepared with three different notch lengths: 25.4 mm, 31.8 mm, and 38.0 mm. Samples were monotonically loaded at a load rate of 0.05 cm/min at a temperature of 25±1℃. The test results showed that at the notch length of 25.3 mm the peak load might be sensitive to the compaction level, binder type or the NMAS, but at the notch length of 31.8 peak load was only sensitive to NMAS. At notch length of 38.0 mm, it was not sensitive to any of the variables. Also, it was found that fracture resistance determined from the SCB tests was fairly sensitive to all mixture variables selected. Moreover, the results demonstrated that Superpave mixtures

with larger NMAS showed higher fracture resistance than those with smaller NMAS, due to larger stone-to-stone contact. According to Wu et al. (2005) after this study, it can be concluded that the SCB test can be considered as a valuable method in the evaluation of the fracture resistance of asphalt mixtures.

Li and Marasteanu (2010) examined low temperature fracture resistance on asphalt mixtures with different binder types: PG 58-28, PG 64-28, and a modified PG 64-28 SBS (Styrene Butadiene Styrene) and two aggregate types (granite and limestone). The test was conducted at three temperatures: -6, -18, and -30℃ on 25 mm thick specimens with three different initial notch length of (5, 15, 30 mm) and 2 mm width. The test was conducted at three different displacement rates (0.00015 mm/s, 0.0005 mm/s and 0.005 mm/s) with three replicates tested for each case. It was found that increasing the air voids, from 4% to 7%, reduced both the mixture peak load and fracture resistance. Laboratory test results showed that mixtures with limestone aggregate have lower peak load and fracture energy than mixtures with granite, all other factors being constant. It is interesting to note that the observation of fracture in a mixture made with limestone a significant portion of the fracture passed through the aggregate particles, while most of the fracture in mixtures containing granite passed through the mastic. With regard to binder type, the mixture with a modified binder (SBS) exhibited higher fracture energy than a mixture with a pure binder, especially at -18 and -30℃. In addition, mixtures with PG 58 binder showed higher fracture energy but lower peak load than mixtures with PG 64 binder, while other factors kept constant. The high peak load value for mixture with PG 64-28 is consistent with the fact that PG 58–28 binder is softer than the PG 64–28 binder. In general, the fracture energy decreases with the increase of loading rate, but this decrease varies with the test temperature. For instance, there is a significant decrease in fracture energy when loading rate increased at -6℃, while this decrease became very small at -18 and -30℃. In terms of notch length, the test results showed that fracture energy significantly differs

with notch length at -6℃, while at -18 and -30℃ exhibited no significant difference and mainly fracture energy decreased with the increases of notch length.

Molenaar et al. (2002) explained that the SCB specimen has an advantage over the ITS specimen in terms of failure mode. This is because the tension must be the failure mode even at higher temperatures. While a mixed mode of stress conditions was often observed at ITS test specimens. Moreover, the study found that there is a significant difference between the tensile strength values of the SCB test and ITS and the reason for this may be because the SCB geometry affected the tensile strength value. In addition, the cracking is the dominant failure mode in SCB test. Therefore, the SCB test showed relevant information on the tensile properties of the material tested.

2.9 Discussion of performance of fibre-reinforced bitumen mastics, mortars and mixtures

Recent studies comparing the influence of various fibres on the rheological properties of bitumen agree that fibres improve the stability and stiffness of bitumen. Correspondingly, significant increases in bitumen stiffness may cause brittleness in the asphalt mixture. This could lead to the development of pavement distress and fracture under the effect of climate and traffic loading. Just one study by Chen and Lin (2005) recommended that the increase in stiffening value of ten times more than bitumen's viscosity seems to be suitable for the strength reinforcement using fibres. None of the studies surveyed the influence of fibre length, distribution and geometry; topics that are considered in this study. Also, none of the studies investigated the influence of fibres on the toughness of bitumen mastic and mortar, topics that are explored in this work by using double edge notched tension test (DENT).

There is only one study that investigated the effect of fibre on bitumen mortar. Wu et al. (2014) evaluated the influence of three fibre types (carbon, mineral and lignin) on the viscoelastic behaviour of fibre modified asphalt mortar. They found that adding lignin fibres had a negative influence on the cracking resistance and creep rate of modified mortars at -18 and -12℃ but this effect completely changed when the temperature increased to -6 ℃. Consequently, increasing the cracking resistance of lignin modified asphalt mortar is enhanced.

In terms of mix design procedures with fibres, little appears in the literature, and the most common difference between FRA and normal mixture can be concluded on two issues. Firstly, adding fibre will increase air voids of asphalt mixtures and requires more binder content to coat the surface area of all mix components (aggregate and fibres). The slight increase in binder content was explored by various researchers (Serfass and Samanos, 1996, Mahrez et al., 2005, Chen et al., 2009). Secondly, there is no standard method of how to introduce fibre into the mixture stated by BS or ASTM. However, most of the previous works prefer to use dry mixing rather than wet mixing, and just one study Abtahi et al. (2008) explored the effect of two mixing methods on Marshall properties (Stability and Flow). They found the same results for wet and dry procedures.

There are some conflicting effects relating to the reinforcing effect of fibres. Some investigators (Freeman et al., 1989, Putman and Amirkhanian, 2004, Mohamadzadeh et al., 2014) found an increase in dry indirect tensile strength from FRAC samples, whereas Anurag et al. (2009) observed a slight decrease in dry indirect tensile strength. However, all these studies demonstrated substantial improvements in moisture susceptibility due to fibre additives. Moreover, Freeman et al. (1989) recommended that using thicker, longer, and a larger amount of fibres are better for moisture damage resistance (see section 3.2.1 and 4.2.6).

The strength improvements are not substantial when evaluated by Vale et al. (2013). They found that adding coconut fibres had a negative effect on fatigue life of SMA mixtures and coconut fibre mixture performance was worse than both mixtures with cellulose fibre and without fibre. On the other hand, more substantial improvements in cracking and rutting resistances were observed from fatigue and rutting tests by using other fibres (Lee et al., 2005, Kim et al., 1999, Tapkin, 2008, Mahrez and Karim, 2010) and field studies (Edgar, 1998, Anderson et al., 1999).

It seems to be from the literature survey the influence of adding fibre to bitumen mastic or asphalt mixtures has a good effect on the performance such as mastic stiffness and elasticity, in addition to moisture damage, rutting, fatigue and resistance to crack propagation of asphalt mixture. This was found consistent with the long term performance from the field experience observation of using fibre.

Previous studies on FRAC compared the influence of different fibre types. None of these studies examined the reinforcing mechanism effects of fibre on binders, mortars and mixtures in a consistent study as is attempted in this work.

As mentioned in the literature review reported here, a search of the literature revealed a number of gaps in the state of knowledge. There is little published data on the cost-effectiveness of using different types of fibres in road applications; exploring the effect of fibre on pavement thickness. No previous study investigated the best method for production and construction of modified mixtures by fibre; critical fibre characteristics to ensure quality. Much uncertainty still exists about the test procedures to verify the presence and distribution of fibres and the environmental effect with the use of different types of fibres. Also, the performance mechanisms of different types of fibres and the future recyclability of fibre mixes and effects on use with recycled material is still unclear.

The majority of the previous researches discussed in this chapter evaluated the effect of adding fibre on the rheological properties of the binder by using dynamic

shear rheometer and standard rotational viscometer (Brookfield). However, the compatibility and stability studies are important and, together with reliable fracture performance criteria, can contribute to better understanding. Consequently, the double edge notch tension test are used in this study. This test may help to gain a better understanding of the effect of fibre on low temperature properties of bitumen mastic.

Chapter 3 Methodology and Materials

3.1 Introduction

Two parts are discussed in this chapter. Firstly, the methodology used in this study is explained in detail, and secondly, the raw materials used in the present study are detailed. The methodology map details the steps to reach the aims and objectives of this research. Also, a flow chart is provided to give a clear and simple description of the research. The raw materials most important characteristics are provided in this chapter and special attention paid to fibre properties and morphology as it is a significant part of this study. Figure 3-1 explains the concept of developing a high performance asphalt mixture. It can be seen from this figure that different types of modifiers such as (polymer, crumb rubber, nano-material and chemical) can be added to asphalt mixture in order to improve the mechanical performance and durability. In this study, fibre will be used as a modifier to the dense bitumen asphalt mixture. Figure 3-2 illustrates the roadmap of the research, including the path towards future research efforts that result from the current research effort.

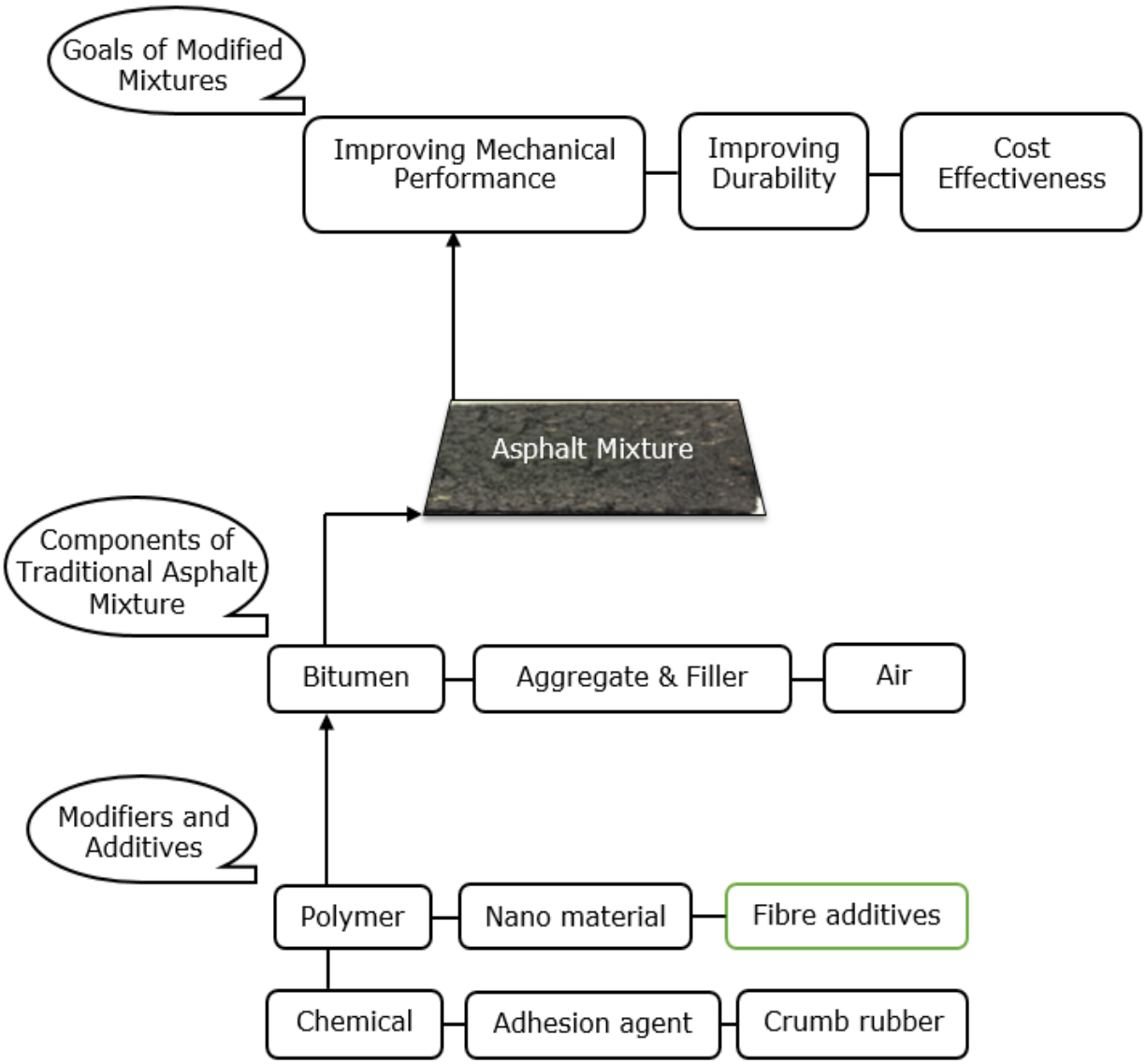


Figure 3-1 Strategy for developing the multifunctional high performance asphalt mixture

3.2 Methodology

In order to achieve the aims and objectives which are to gain a better understanding of the influence of different fibre types and amounts on the performance of binder, mortar and mixture, the methodology explained in this chapter will be followed. This methodology consists of the following stages and more details about the tests are included in following chapters:

3.2.1 Stage 1

The properties of the modified binder with three types of fibres (cellulose, glass and steel fibre recovered from tyres) will be investigated by using the following tests:

1- Penetration test

The penetration test was made to measure the hardness of the modified bitumen. Penetration is defined as the depth of penetration of a standard needle under a one hundred grams load after a five second loading time at a specified temperature and the penetration value expressed in units of 0.1 mm according to BS EN 1426 (2007).

2- Softening point (ring and ball)

The test was conducted under standardised test conditions to determine the temperature at which a phase change occurs in the bitumen or mastics according to BS EN 1427 (2015).

3- Rotational viscosity (RV) test

A standard rotational viscometer (Model LVDV-II+ PRD, Brookfield Engineering Inc.) was used to measure the viscosity of the binder (BS EN 13302, 2010). The viscosity in this test represents the resistance of the fluid against spindle rotation at a specific speed. The calibrated spindle is connected to dial to record the results.

4- Dynamic shear rheometer test (DSR)

A Bohlin Gemini 200 (DSR) was used in this study for measuring the rheological properties of base and fibre reinforced bitumen. It has a torque range between 0.5 (μN·m) and 200 (mN·m). There is a sensor attached to the shaft to detect the movement of the measuring system. A 1 and 2 mm gap and a 25 mm diameter plate were used.

5- Double-edge-notched tension test (DENT)

This test method covers the determination of bitumen's essential and plastic work of fracture (LS-299, 2001). A 45° notch angle was used to facilitate ease of handling during the removal of the specimens from the mould. The test was performed at a constant rate of displacement in a controlled testing temperature.

6- Binder drainage test basket method

This test method evaluates the ability of fibre to hold the bitumen at high temperature (160℃) for three hours (BS EN, 2004).

7- Dynamic contact angle (DCA)

This test is used to measure the surface energy components of each drained binder in order to evaluate the cohesive and adhesive strengths of the drained binder. Also, dynamic vapour sorption (DVS) approach was used to measure the surface energy component of limestone aggregate (Ahmad, 2011).

3.2.2 Stage 2

The structure composition and performance of fibre modified asphalt mortar were explored during this stage by using the dynamic shear rheometer (DSR), double-edge-notched tension test (DENT) and scanning electron microscope (used in this

study for direct observation of bitumen-fibre mortar). Pneumatic adhesion tensile testing instrument (PATTI) tests were used to measure the cohesive and adhesive properties of a bitumen-aggregate system by measuring pull-off tensile strength.

3.2.3 Stage 3

Mechanical properties of asphalt mixtures were assessed in this stage.

1. X-ray computed tomography (CT)

An X-ray computed tomography (CT) test is used in this study. This test is a non-destructive test used to explore fibre distribution, orientation and presence in asphalt mixture core specimens.

2. Immersed Hamburg wheel tracking test

The wheel tracking test is used to reflect the influence of traffic loading passes over the pavement and causing permanent deformation. This test is considered an important test due to the high correlation between the laboratory test results and field observations. Also, this test can be used to evaluate the moisture damage at the same time (BS EN 12697-22, 2003).

3. Repeated load axial test (RLAT)

Repeated load axial test is very common, economic and quick test used for assessing the rutting resistance of the asphalt mixtures. The machine applies a repetitive haversine load and measures the vertical deformation after each repeated load (BS EN 12697-25, 2016). Field or laboratory core specimen can be used for this test. The Nottingham Asphalt Tester (NAT) machine was used for this test.

4. Indirect tensile stiffness modulus (ITSM) test

This test method is used to evaluate the stiffness modulus of asphalt mixtures by using an indirect tensile test (BS EN 12697-26, 2012). The Nottingham Asphalt Tester (NAT) machine used for this test. Cylindrical specimens manufactured in the lab used for this test.

5. Indirect tensile fatigue test (ITFT)

The test was carried out using Nottingham Asphalt Tester (NAT) machine. The fatigue life obtained through indirect tensile fatigue test. The test is done in the stress control loading mode (the applied load is held constant during the test) (Draft BS, 2003).

6. Indirect tensile strength test (ITS)

An Instron testing machine used for evaluating the indirect tensile strength of asphalt mixtures (BS EN 12697-23, 2017). The test results will be interpreted to examine the moisture resistance of control and fibre reinforced asphalt mixtures.

7. Fracture test (Semi-circular bending test)

The test was carried out using the (NAT) machine. This test method measured the fracture energy (Gf) of asphalt mixtures by means of the semi-circular bend geometry (SCB). The method also includes procedures for calculating ultimate stress and total work of fracture (BS EN 12697-44, 2010).

8. Evaluate the effect of fibre on the pavement design thickness by using a software called KENLAYER.
9. General performance and cost-effectiveness

General performance and cost-effectiveness of fibre reinforced asphalt mixtures are examined in this stage.

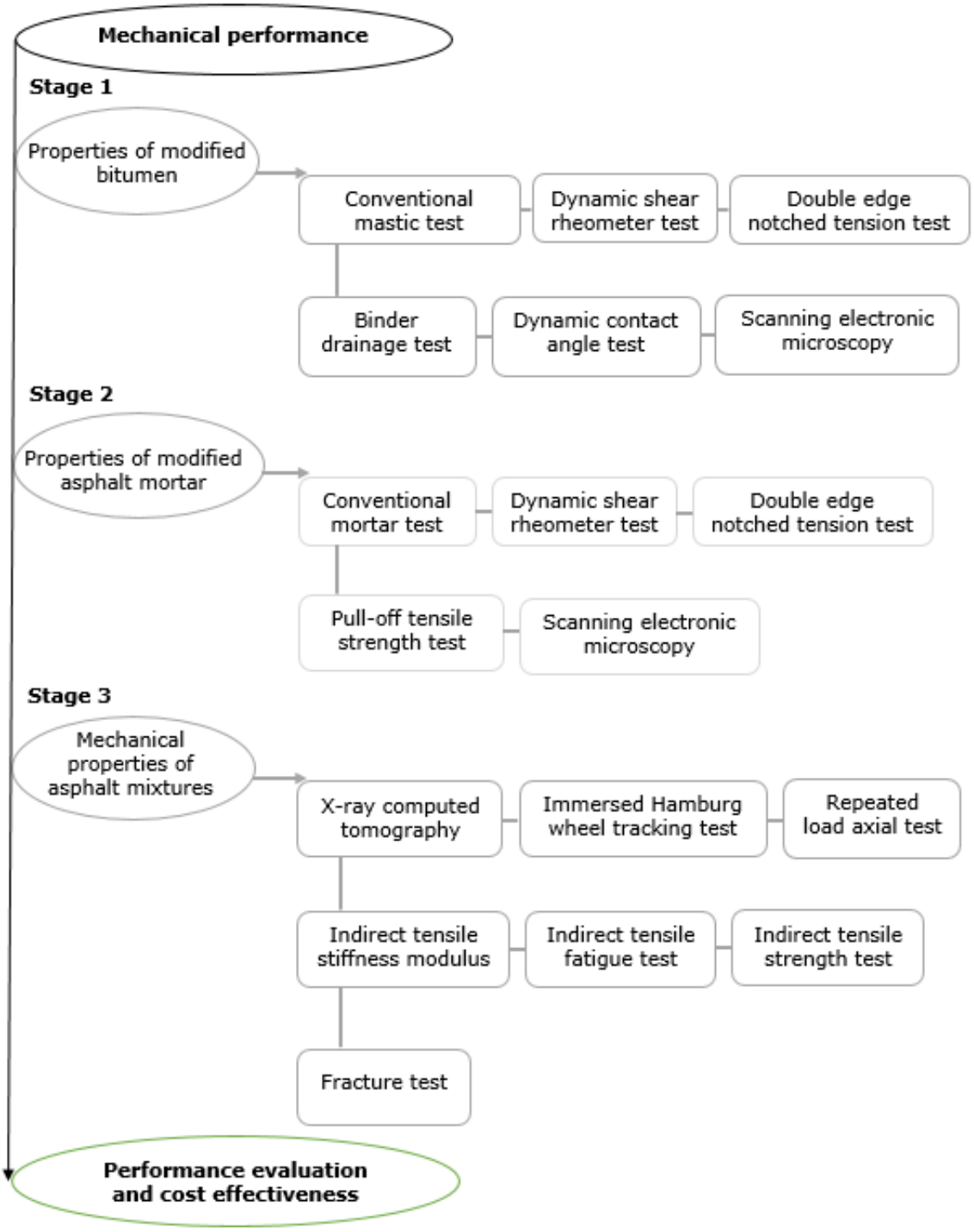


Figure 3-2 Thesis roadmap

3.3 Materials

3.3.1 Fibre types

The experimental work in this study focuses on the investigation of the influence of fibres on asphalt binder mastic, mortar and mixture. Among the various types of fibres, glass fibres with two different lengths, cellulose and steel fibres recovered from tyres are selected in this study. Although glass fibres have desirable properties, such as low thermal expansion coefficient, high tensile modulus, high elastic recovery and high softening point, a literature review showed that their use had not been reported very often (Abtahi et al., 2013). Cellulose fibres are natural fibres obtained most commonly from woody plants. Cellulose fibre is cheap and widely available. In terms of recyclability and cost-effectiveness this study decided to use steel fibre recovered from tyres.

Three fibre concentrations of 0.5%, 1.0% and 2.0% by bitumen volume was selected to assess the fibre effect on (1) mastic, mortar and mixture properties (2) investigate the reinforcing effects of various factors such as dimensions, shape, and content of fibres, and (3) provide fundamental information for the behaviour and optimisation of fibre reinforced bitumen. Table 3-1 showed fibre types and percentages used in this study.

Table 3-1 Fibre percentages and types

Fibre type	Percentage by bitumen volume (%)	Percentage by bitumen weight (%)
Glass long and short fibre	0.5	1.25
	1.0	2.5
	2.0	5.0
Cellulose fibre	0.5	0.72
	1.0	1.46
	2.0	2.91
Steel fibre	0.5	3.8
	1.0	7.6
	2.0	15.2

3.3.2 Fibre characteristics

Four fibres including two glass fibres, cellulose and steel fibres were used as an additive to mix with bitumen, mortar and mixture in the process of the experiment as shown in Figure 3-3. Table 3-2 lists the basic properties of these fibres. The glass fibres are made into two different lengths 13,000 and 6,000 μm, which are named by glass-l and glass-s respectively.

The micrographs of glass and cellulose fibres are given out in Figure 3-4 and Figure 3-5 respectively, using scanning electronic microscope (SEM) and steel fibre using optical microscope (Nikon Digital Sight DS-Ri1) as shown in Figure 3-6. In these figures, compared with glass and steel fibre, cellulose fibre is much rougher because the cellulose fibres are produced in uneven bundles, in which case the cellulose fibre diameter can even reach a micrometre level and has a rough surface texture with irregular sizes. At the same time, cellulose fibre shows irregularity in the surface shape with interweaved bundles and high surface area. In contrast, glass and steel fibres are manufactured. These fibres are regularly cylindrical shaped fibres with a smooth surface texture. Also, glass fibres are made up of bundles of individual fibres.

Table 3-2 Basic properties of fibres

Fibre types	Specific density (g/cm³)	Length (μm)	Width of individual fibres (μm)	Modulus of elasticity at 23℃ (GPa)	Specific surfaces area (m^2/g)
Glass-l	2.58	13,000	12 to 20	80.3	~0.019
Glass-s	2.58	6,000	12 to 20	80.3	~0.013
Cellulose	1.50	20 to 2,500	~25	-	~1.000
Steel	7.85	4,000 to~12,000	~110 to 350	210*	-

*Standard steel fibre modulus

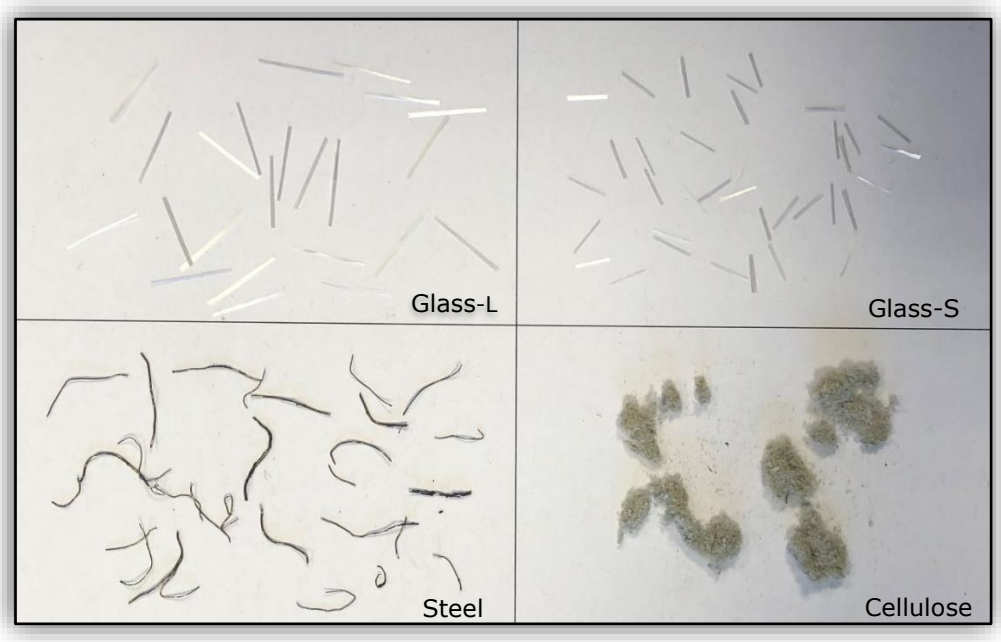
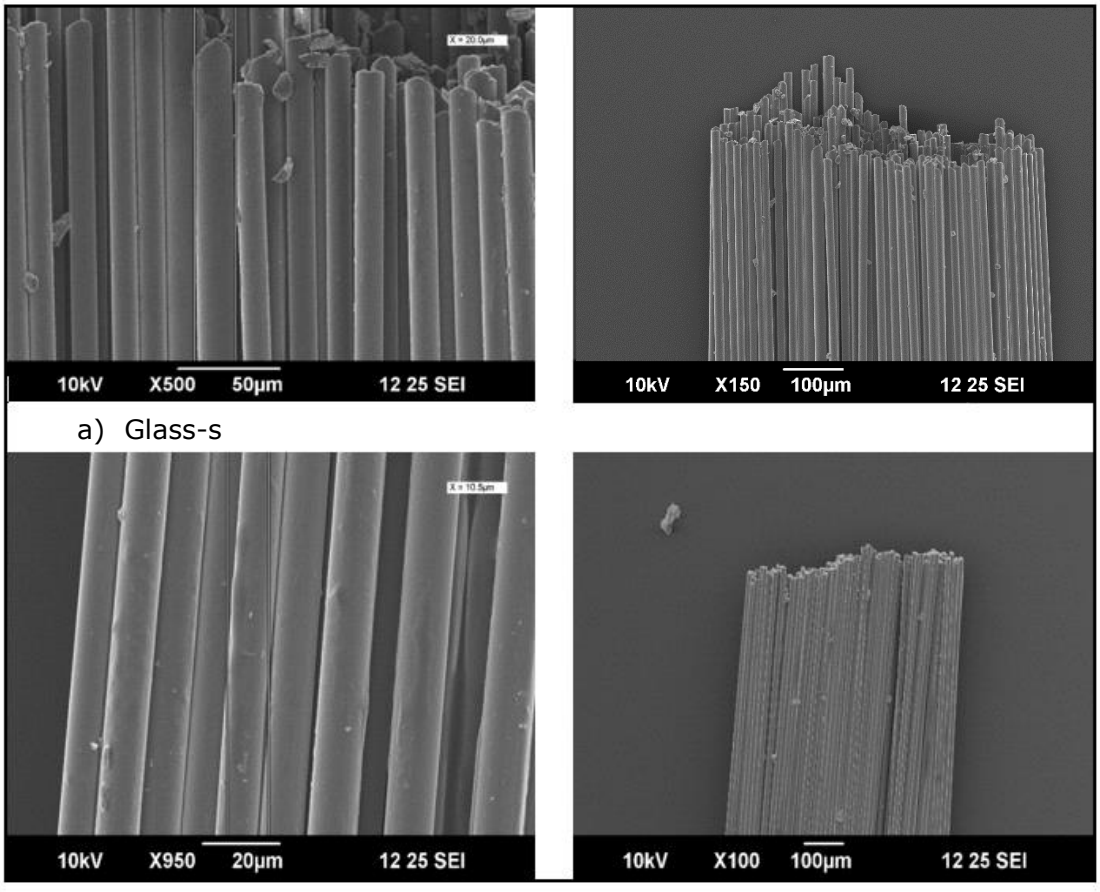


Figure 3-3 Images of fibre types



a) Glass-s

b) Glass-l

Figure 3-4 Scanning Electron Microscope (SEM) images of glass fibre

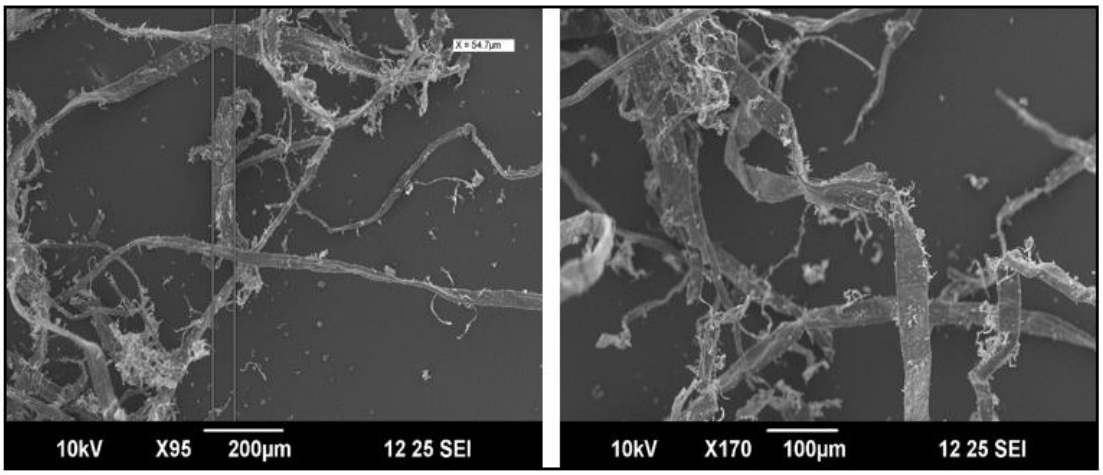


Figure 3-5 Scanning Electron Microscope (SEM) images of cellulose fibre with different scale

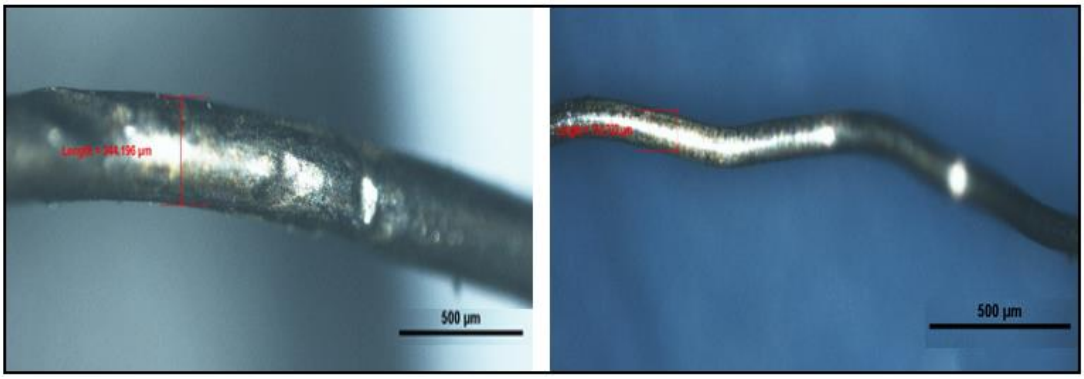


Figure 3-6 Optical microscope images of steel fibre with different diameter

3.3.3 Bitumen

The binder used in this study is characterised by penetration as 40/60 pen according to BS EN 1426 (2007). The properties of the bitumen used in this study are tabulated in Table 3-3.

Table 3-3 Properties of 40/60 bitumen used in this study

Property	Value	Standard
Specific gravity (g/cm^3)	1.03	BS 2000-549:2007
Penetration value at 25℃	54	BS EN 1426:2007
Softening Point (℃)	51	BS EN 1426:2015
Viscosity at 135℃ (mPa.s)	446.9	BS EN 13302:2010

3.3.4 Limestone filler

Limestone filler is a natural filler obtained from Tunsted quarry, Derbyshire, United Kingdom. Limestone filler with maximum size less than 0.063 mm was used. Practically, limestone filler is considered a very common option to be used in asphalt mixtures. The specific gravity for the limestone filler was 2.72 g/cm^3.

3.3.5 Aggregate

The aggregate fractions used in this research were crushed limestone aggregate obtained from Tunsted quarry, Derbyshire, United Kingdom. The maximum aggregate size of less than 31.5 mm was used. The specific gravity for the coarse aggregate was 2.71 g/cm^3.

3.4 Preparation of bitumen-fibre mastic and mortar

Bitumen was placed in an oven at 160℃ for more than one hour to make it fluid enough for mixing. A specific experimental procedure was used to obtain homogeneous bitumen-fibre mastics. A Stuart mixer with an SS10 stirrer was used to apply a specific mixing speed (500 rpm) which prevented air bubbles forming in the bitumen-fibre mastic. Thermocouple probes were used to monitor the temperature throughout mixing by placing the probe directly inside the composite

in the mixing vessel. Fibres were slowly added to the bitumen, while the mixing continued at a constant speed to prevent the fibres from agglomerating. Bitumen-fibre mastics were mixed for one hour at (160-170℃) to produce homogeneous composites. The influence of different fibre amounts on the bitumen properties were tested. These amounts were (0, 0.5, 1.0) percent by volume of the bitumen. Unmodified bitumen is represented by 0% and was used as the control.

This method used to prepare the sample for the following test (viscosity, penetration and double-edge-notched tension test) as shown in Figure 3-7.

The same procedure was used for asphalt mortar, but limestone filler was added first to the bitumen, and then fibre has been added, and the speed was 750 rpm.

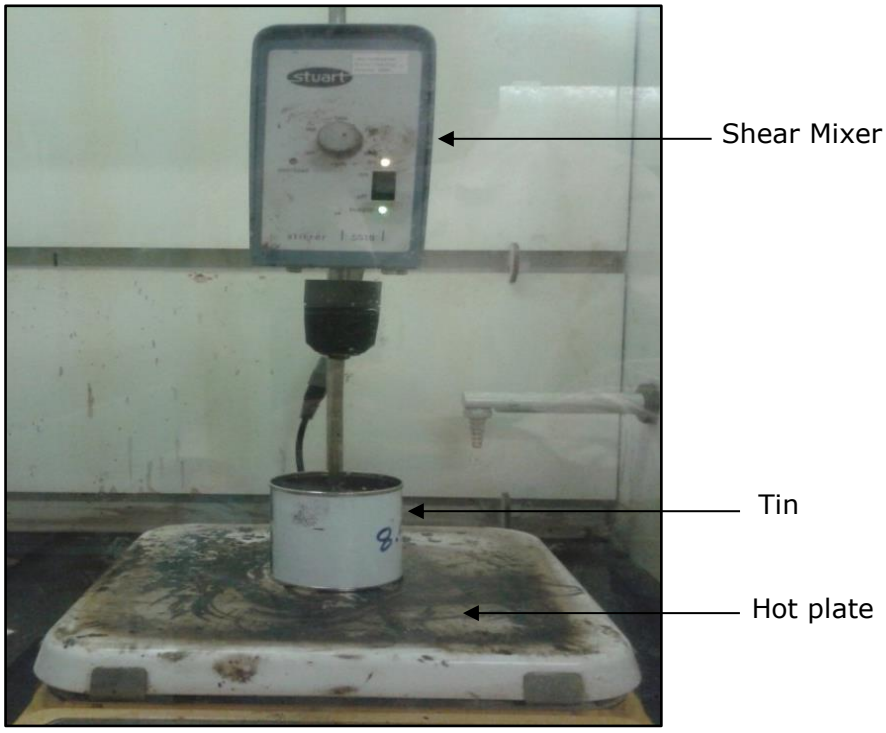


Figure 3-7 Bitumen-fibre mastic blending facilities

3.5 Asphalt mixtures

3.5.1 Aggregate gradation

A 0/20 mm size binder course Dense Bitumen Macadam (DBM) was used according to (BS 4987-1, 2005). The gradation for the 20 mm DBM is shown in Table 3-4, and Figure 3-8 shows the gradation design curve. This figure shows the upper, the lower limits, the mid curve from the British Standard and the aggregate gradation (BS 4987-1, 2005).

Table 3-4 0/20 mm size DBM specification

Test sieve aperture size (mm)	(%) Passing of Combined Aggregate
31.5	100
20.0	95-100
14.0	65-85
10.0	52-72
6.3	38-56
2.0	20-40
0.25	6-20
0.063	2-9

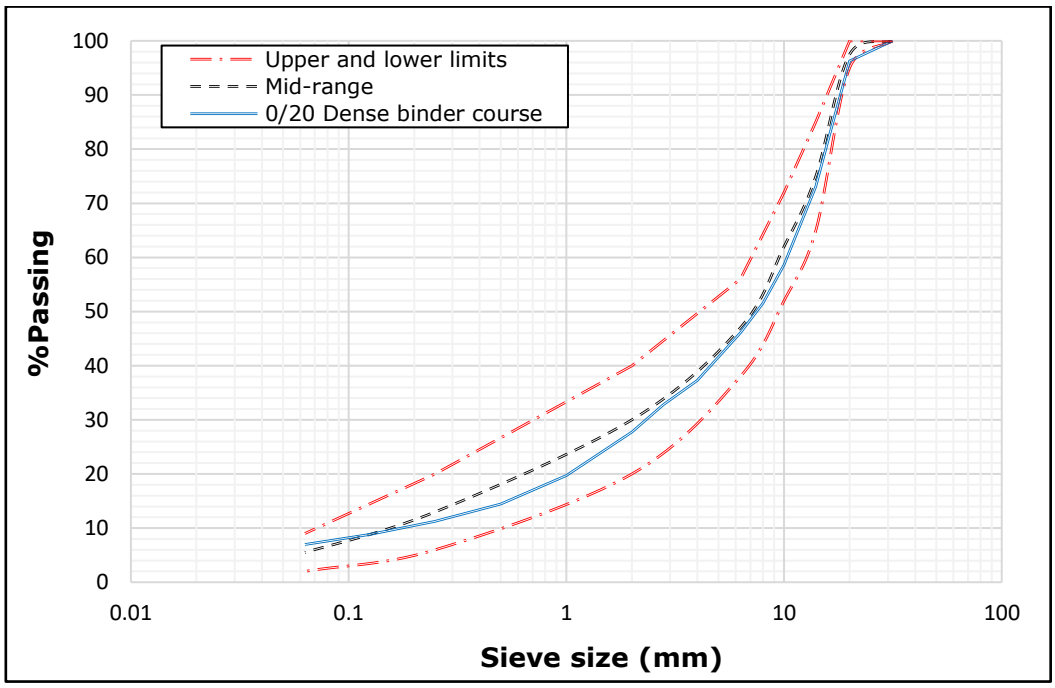


Figure 3-8 Gradation curve of 0/20 mm binder course DBM

3.5.2 Mixing and compaction

The required amounts of binder and aggregate for manufacturing asphalt mixtures were preheated at the required mixing temperature, three hours for the binder and eight hours for aggregate. First, the preheated aggregates were placed and mixed in a mechanical asphalt mixer for two minutes, as shown in Figure 3-9 a, at the required mixing temperature. Then fibre was added into the mixer and mixed manually for a few seconds after that the preheated binder was then added to the batch and the mixing procedure continued for another three minutes according to BS EN 12697-35 (2016). Once the mixing finished, calculated amount of asphalt batch was then poured in a preheated square mould (306 mm by 306 mm), as shown in Figure 3-9 b and then compacted by the roller compactor to the required thickness (65 mm) in attempt to reach the required air voids (7±1%) according to BS EN 12697-33 (2003), as shown in Figure 3-10.

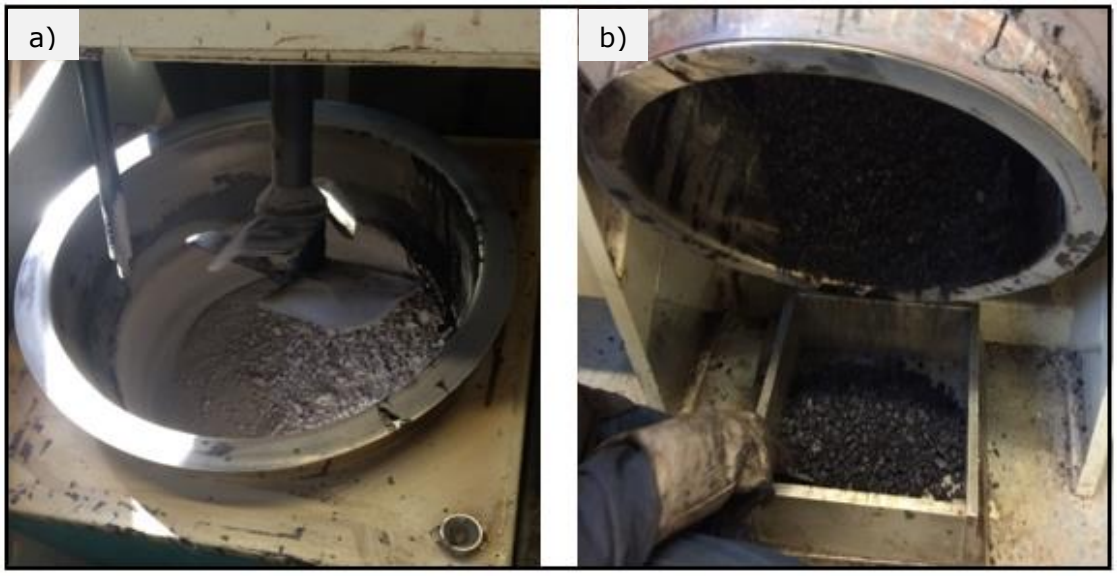


Figure 3-9 (a) Mechanical asphalt mixer, and (b) square steel mould

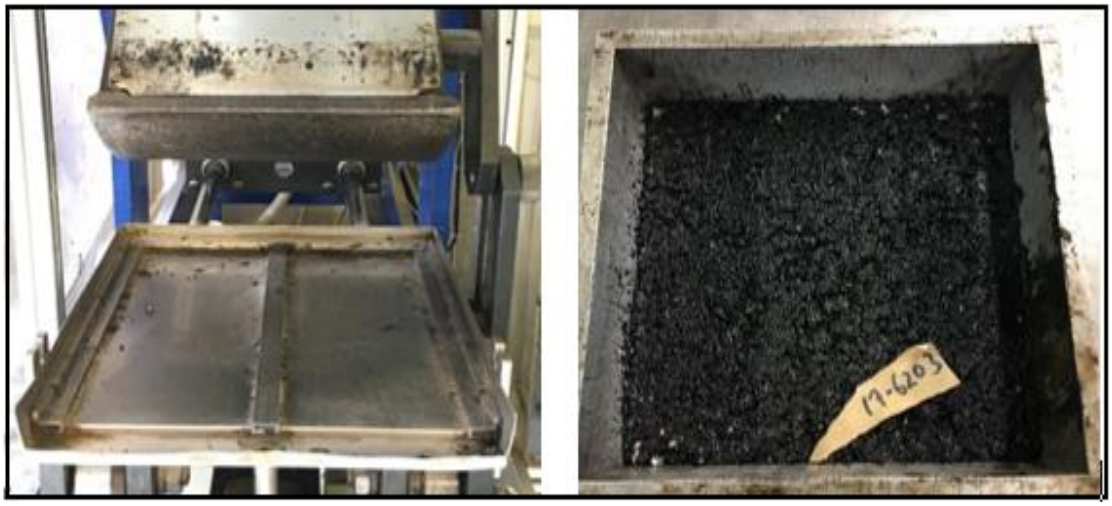


Figure 3-10 Steel roller compactor and asphalt mixture after compaction

3.5.3 Specimens coring and cutting

The compacted asphalt mixture slabs were fabricated into five cores (100 mm diameter and 65 mm thickness). The top and the bottom of each core are trimmed by using a masonry saw in order to get smooth and flat surface core with dimension (100 mm diameter and 45 mm thickness) as shown in Figure 3-11. Specimens with

a dimension of 100 mm diameter and 45 mm thickness were used in this study for ITSM, ITS, RLAT, ITFT and SCB tests.

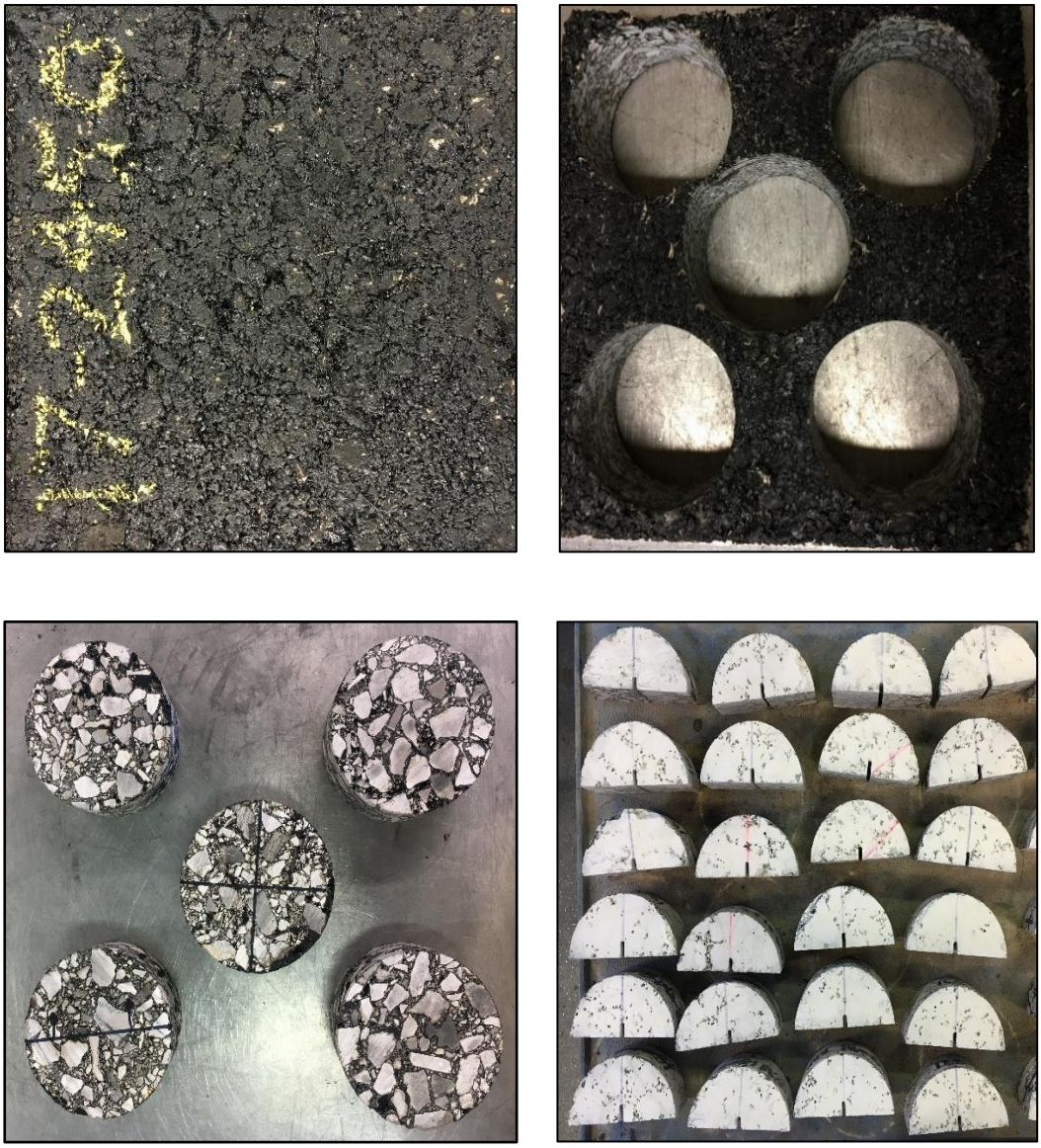


Figure 3-11 Specimens after coring and cutting

3.5.4 Volumetric characteristics of DBM mixtures

After coring and cutting process finished, the specimens are left for one day at room temperature to allow them to dry. Then the dimensions of each specimen are measured, and the maximum bulk densities of sealed specimens are measured as shown in the following equation according to BS EN 12697-6 (2012).

$$\rho_{base} = \frac{m_1}{(m_2-m_3)/\rho_w-(m_2-m_1)/\rho_{sm}} \quad \text{Equation 3-1}$$

where ρ_{base} is the maximum bulk density sealed, ρ_w is the density of the water at test temperature and ρ_{sm} the density of the sealed foil all in (Mg/m^3); m_1 is the mass of the dry specimen, m_2 is the mass of the sealed specimen dry and m_3 the mas of the sealed specimen in water all in (g).

The actual air voids of asphalt mixture samples calculated according to BS EN 12697-8 (2003), depending on the maximum theoretical densities of the asphalt mixture constituent materials (aggregate, filler, bitumen and fibre) according to BS EN 12697-5 (2009), and maximum bulk density of sealed specimen as shown in the following equation:

$$V_m = \frac{m-\rho_{base}}{m} \times 100\% \quad \text{Equation 3-2}$$

where V_m is the air void content of the asphalt mixture in percentage and m the maximum theoretical density of the asphalt mixture.

This procedure used in this study to check that the air voids of the manufactured samples are within the required limits.

Chapter 4 Mastic properties

Basic and rheological properties of fibre reinforced mastic

4.1 Introduction

This chapter examines the effect of the addition of fibres on conventional and more fundamental rheological properties of bituminous mastic. Seventy percent of bitumen is used in road construction as the binder mixed with aggregate and filler particles to form asphalt mixtures (Sorensen and Wichert, 2009). Bitumen is a viscoelastic material, and it is well known that the mechanical behaviour of viscoelastic materials depends on loading time and temperature. The behaviour of bitumen plays a significant role in the performance and service life of flexible pavements.

The binder composed of fibres and bitumen works as the material that bonds an asphalt mixture together and is, therefore, an important part of that mixture. The properties of fibres (length, adhesion, absorption, swelling) and how they affect bitumen is complex. Fibres are added to bitumen to enhance its viscoelastic properties, for instance, by improving the bitumen viscosity and stiffness (Brown et al., 1990, Chen et al., 2008). Fibres are mainly used in stone matrix asphalt and gap-graded mixtures to prevent the draining out of binder during mixing and compaction (Alvarez et al., 2008, Hassan and Al-Jabri, 2005, Putman and Amirkhanian, 2004). Additionally, fibres have the potential to increase moisture

resistance (Zhu et al., 2007), fatigue resistance (Guan et al., 2014, Alrajhi, 2012) and rutting resistance and creep compliance (Chen et al., 2004).

In this study, fibre modified binder mastics were prepared with different fibre types (cellulose, 6 mm glass, 13 mm glass and steel fibres). Cellulose fibres are natural fibres obtained most commonly from woody plants. Although glass fibres have desirable properties, such as low thermal expansion coefficient, high tensile modulus, high elastic recovery and high softening point, a literature review shows that their use has not been reported very often (Abtahi et al., 2013). In terms of recyclability and cost-effectiveness, this study utilised steel fibre recovered from tyres. Experiments were conducted to evaluate the viscoelastic characteristics of the base bitumen and modified mastic with various fibre additions. These tests included penetration, softening point, viscosity, dynamic shear rheometer (DSR) and the double edge notch tension (DENT) test.

4.2 Characterisation

Four fibre types including two types of glass fibre, cellulose and steel fibres, were used as the additive to bitumen. The basic properties of fibres used in this study are listed in Table 3-2 (see chapter three). Table 4-1 summarises the experimental programme. Micrographs of these fibre types and the fibre reinforced bitumen are given in Figure 4-3, using a scanning electron microscope (SEM). An SEM image of cellulose mastic is not included in this study because these fibres were difficult to identify and did not protrude from the faces of the mastic specimens in the same way as the glass and/or steel fibre.

Table 4-1 Experimental programme

Materials	Variables	Test methods	Test replicate
Bitumen 40/60	Fibre content 0.5% 1.0% 2.0%	Penetration test	3
		Softening point	2
		Brookfield viscosity	3
Fibre	Fibre type Glass-l Glass-s Cellulose Steel	Dynamic shear rheometer	2
		Double edge notch tension test	2
		Scanning electronic microscope	-

4.2.1 Scanning electron microscope (SEM)

Micrographs of these fibres and the fibre reinforced mastic were investigated by using a Cryo-scanning electron microscope (Quanta 200 3D (FEI)). Samples were coated with platinum (Pt) at -160℃ for 60 seconds at a current of 10 mA. Accelerating voltage used was 10 kV for glass and cellulose and 15 kV for steel fibre.

4.2.2 Penetration test

The penetration of the bitumen mixed with different fibres was measured with a STANHOPE-SETA penetrometer (BS EN 1426, 2007). The penetration test was used to evaluate the hardness of the fibre reinforced bitumen mastic. Penetration is defined as the depth of penetration of a standard needle under a one hundred grams load after a five second loading time at a specified temperature and the penetration value expressed in units of 0.1 mm. The fibre reinforced binder samples were left for one hour in the air and then placed in a water bath at 25℃ for one hour to equilibrate thermally before the penetration test.

4.2.3 Softening point (ring and ball) test

The test was conducted under standardised test conditions to determine the temperature at which a phase change occurs in the bitumen or mastics according to BS EN 1427 (2015).

4.2.4 Viscosity test

A standard rotational viscometer (Model LVDV-II+ PRD, Brookfield Engineering Inc.) was used to measure the viscosity of the base binder and fibre reinforced binder according to BS EN 13302 (2010). Viscosity is defined as the ability of a liquid to resist flow and also is known as the ratio of the applied shear stress to the rate of shear strain (Airey, 1997). Brookfield is well known and the most common test used for measuring bitumen viscosity since this test is able to cover a wider range of temperatures and bitumen grades than other tests (Zacharias and Emery, 1994).

A standard rotational viscometer consists of two cylinders. The first one is static and contains the bitumen sample. Second cylinder (spindle) is rotating coaxially inside the static cylinder. The bitumen sample between the two cylinders will resist the torque resulting from the movement of the cylinder or spindle at a specific testing temperature. The resistance of the bitumen sample to the spindle movement is recorded and then this value converted by using calibration factors to the viscosity of the bitumen.

The viscosity tests are used to evaluate the high temperature (>60℃) properties of the bitumen and/or mastic, while penetration and softening point are used to examine low to a moderated temperature usually lower than 60℃ for unmodified bitumen.

4.2.5 Dynamic shear rheometer (DSR)

A Bohlin Gemini 200 (DSR) was used in this study for measuring the rheological properties of base and fibre reinforced bitumen, as shown in Figure 4-1. It has a torque range between 0.5 (μN·m) and 200 (mN·m). There is a sensor attached to the shaft to detect the movement of the measuring system (Airey, 1997). Eleven testing frequencies ranging from 0.1 to 10.0 (Hz) were used in DSR tests with nine testing temperatures between 30 and 70℃ (at increments of 5℃).

The test can be done in either stress controlled or strain controlled. In this study, the controlled strain was applied. Strain controlled test mode is the most frequently used test condition used to determine the dynamic rheological properties of bitumen and/or mastic (Goodrich, 1988, Pink et al., 1980). In controlled strain, the condition is important to use low strain value to ensure that the test remains within the linear viscoelastic region.

In this test the bitumen sample sandwiched between two parallel plates is subjected to a sinusoidal strain with a specific frequency ω (rad/sec) as expressed in the following equation:

$$\gamma^* = \gamma_\circ \, e^{i\omega t} \qquad \text{Equation 4-1}$$

where γ^* is the dynamic oscillating shear strain, $\gamma_\circ$ is the maximum shear strain, ω is the angular frequency and $i = \sqrt{-1}$

The loading frequency ω is known as rotational, radian and/or angular frequency and can be defined as shown in the following equation (Van Poel, 1954):

$$\omega = 2\pi f \qquad \text{Equation 4-2}$$

where f is the frequency (Hz).

Stress is developed in the specimen as a result of the applied strain. The stress is sinusoidal and shifted by an amount δ out of the phase of the applied strain. The resulting stress can be expressed, as shown in the following equation:

$$\sigma^* = \sigma_\circ \sin(\omega t - \delta) \qquad \text{Equation 4-3}$$

where σ^* is the dynamic shear stress, $\sigma_\circ$ is the maximum stress both in Pa and δ is the phase or loss angle (degrees).

Phase or loss angle represents the difference between the stress and strain phase. Phase angle value determines whether the material is elastic or viscous. 0° is considered pure elastic and 90° is considered viscous. Consequently, the phase angle considers an important property of viscoelastic materials. The working principle of the strain, stress waveforms and the resulting dynamic shear test outputs are illustrated in Figure 4-2.

The complex shear modulus can be defined as the resulting stress divided by the applied strain, as shown in the following equation:

$$\mathrm{G}^*(\omega) = \frac{\sigma^*}{\gamma^*} = \frac{\sigma_\circ}{\gamma_\circ} e^{it} \qquad \text{Equation 4-4}$$

The ratio of the peak stress to the peak strain represents the absolute value of the complex shear modulus, as shown in the equations below:

$$\left| \mathrm{G}^*(\omega) \right| = \frac{\sigma_\circ}{\gamma_\circ} \qquad \text{Equation 4-5}$$

$$\mathrm{G}^*(\omega) = \left(\frac{\sigma_\circ}{\gamma_\circ}\right) cos\delta + i \left(\frac{\sigma_\circ}{\gamma_\circ}\right) sin\delta = G'(\omega) + i\, G''(\omega) \qquad \text{Equation 4-6}$$

where $\mathrm{G}^*(\omega)$ is the shear complex modulus, $\sigma_\circ$ is the peak stress both in Pa, $\gamma_\circ$ is the peak strain, $G'(\omega)$ is the storage modulus and $G''(\omega)$ is the loss modulus both in Pa.

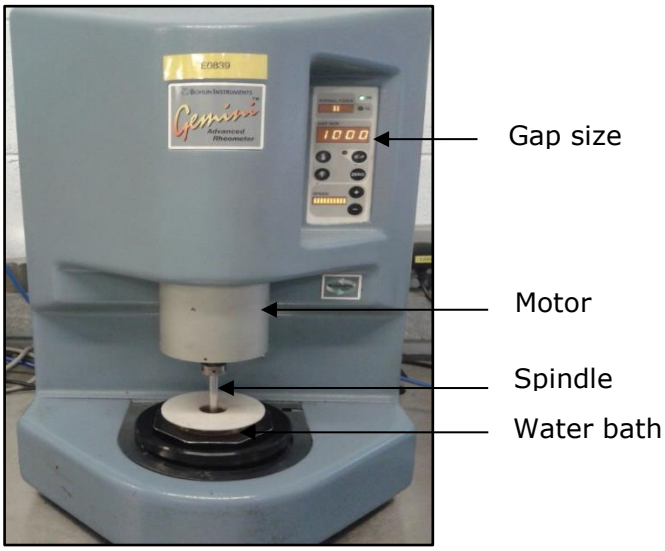
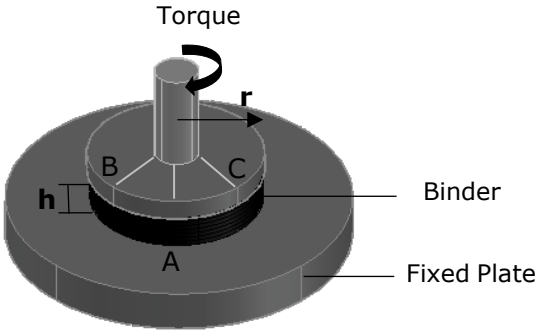


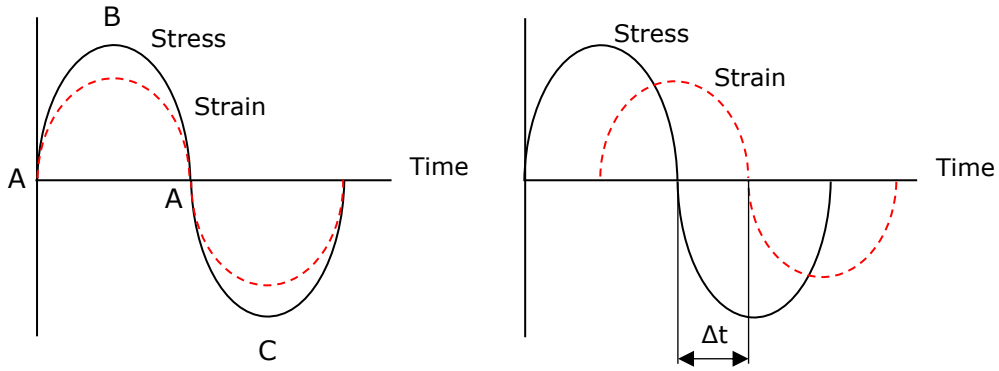
Figure 4-1 Bohlin Gemini 200 DSR



$$\tau = \frac{2T}{\pi r^3}$$

$$\gamma = \frac{\theta r}{h}$$

Elastic Viscous



Strain in phase δ=0° Strain out of phase δ=90°

Figure 4-2 Dynamic shear rheometer working principle (Airey, 1997)

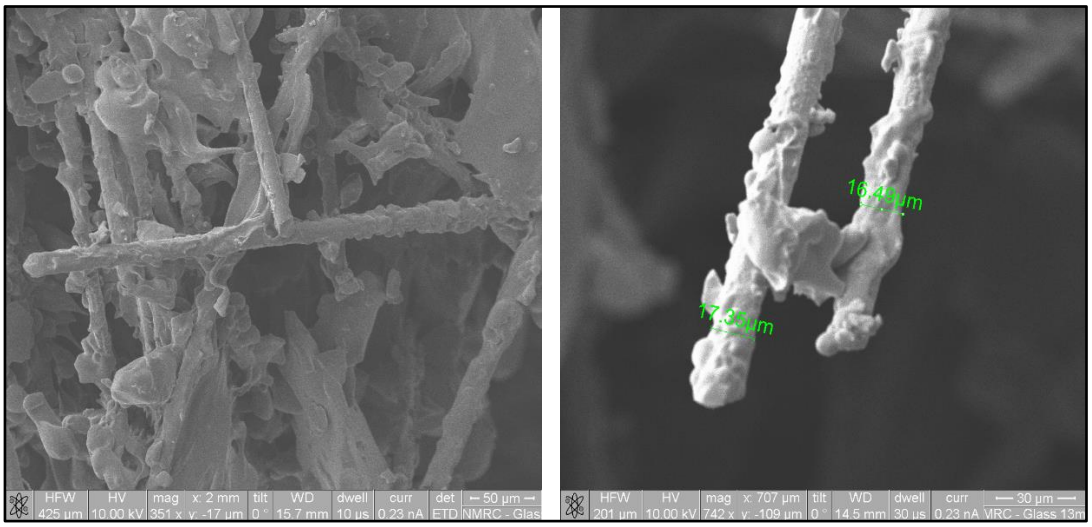
4.2.6 Double edge notch tension test (DENT)

The DENT test is used to measure the total essential and plastic work of fracture; samples were prepared by pouring the binder into moulds with inserts at both ends. A 45° notch angle was used to facilitate ease of handling during the removal of the specimens from the mould. The test speed was kept constant at 50 mm/min and the temperature at 15 (± 0.5℃). Six samples were prepared, two for each ligament length of 15, 10 and 5 mm (LS-299, 2001).

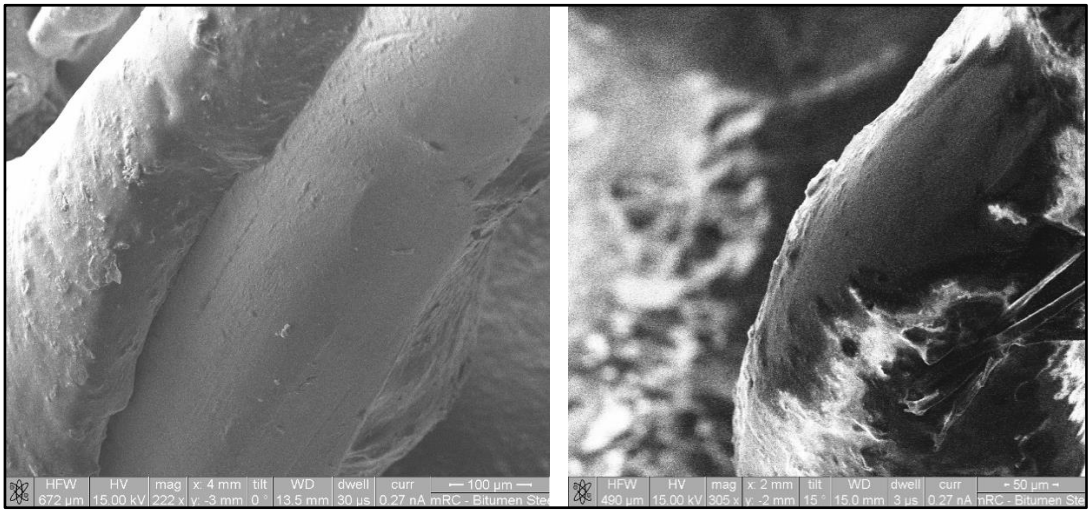
4.3 Results and Discussions

4.3.1 Scanning electronic microscope

Scanning electronic microscope (SEM) images of the fibre modified asphalt mastics are shown in Figure 4-3. These images were taken from the DENT test samples in the notch area. In the previous chapter, the microstructures of these fibres were observed. This analysis will try to explain how fibre microstructure affected the distribution and entanglement of fibres in the bitumen mastic. The microstructures of glass and steel fibres were different from that of cellulose fibre since the cross sections of glass and steel fibres were quite round, straight, with a smooth surface texture and also longer than cellulose fibre. The microstructure of continuous networks of fibre is shown in Figure 4-3. The formed network would resist crack propagation and aggregate sliding at the interface, spread stress, and reduce stress concentration, thereby improving the integral strength of asphalt matrix. With regard to steel fibres, the scanning electronic microscope could not show a lot of information about the entanglement of steel fibres through asphalt mastic as shown in Figure 4-3 (b) due to the large dimensions of the steel fibre compared to specimen size. However, steel fibres showed good interaction with the asphalt mastic reflects high adhesive strength between bitumen and steel fibre.



(a) Glass fibre reinforced mastic



(b) Steel fibre reinforced mastic

Figure 4-3 (a and b) SEM images of fibre reinforced mastics

4.3.2 Penetration

Penetration is a common test used to measure bitumen hardness. The penetration value was taken as the average of three readings. It was found that the penetration value decreases significantly with the addition of glass-l and glass-s fibres, and less so with the addition of cellulose and steel fibres, as illustrated in Figure 4-4 (error bars in the following Figures represent the standard deviation of original data

divided by the square root of the specimen numbers plus and minus standard error bar). The magnitude of the decrease in penetration is a function of glass fibre content, however, glass fibre length has a small effect, and there is little difference between glass-l and glass-s. Note that cellulose fibres are uneven and shorter than glass fibre and may, therefore, be less able to form a rigid network within the mastic. The high density of steel fibre maybe led the steel fibre to sink and reducing its influence on the bitumen penetration value.

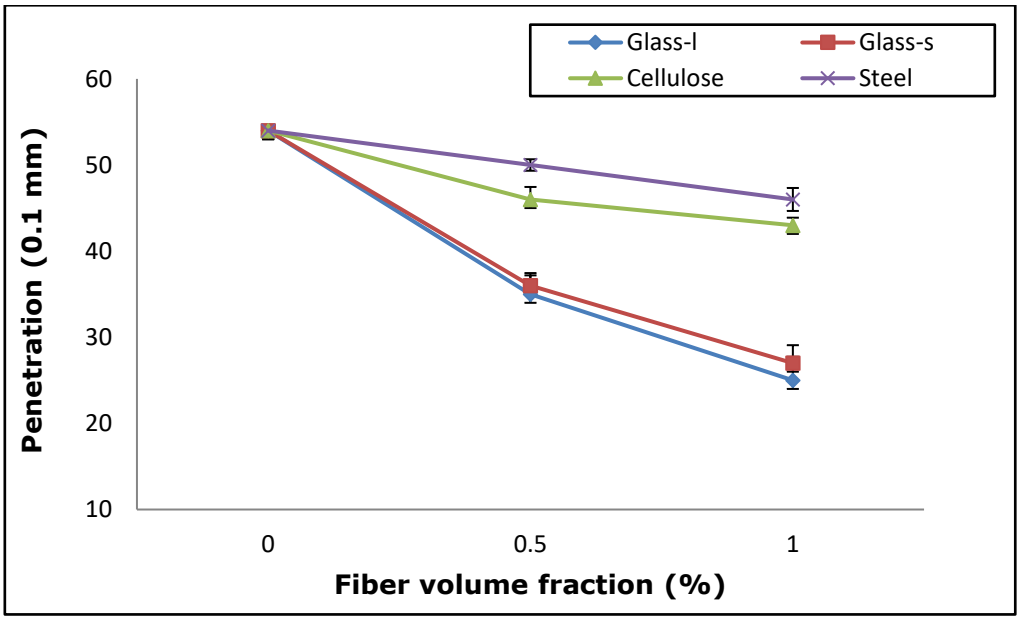


Figure 4-4 Penetration values of base and fibre reinforced binders

4.3.3 Softening point (Ring and Ball)

Softening point has been linked to the permanent deformation of asphalt mixtures. The softening point value increases significantly with the addition of fibres, as shown in Figure 4-5 (error bars represent plus and minus one standard error). The magnitude of the increase in softening point is a function of fibre content. Glass-l and steel fibres showed the highest increase in the softening point of the mastic.

This study was not able to measure the softening point for 2.0% of steel fibre due to the difficulty to pour the mastic into the small mould.

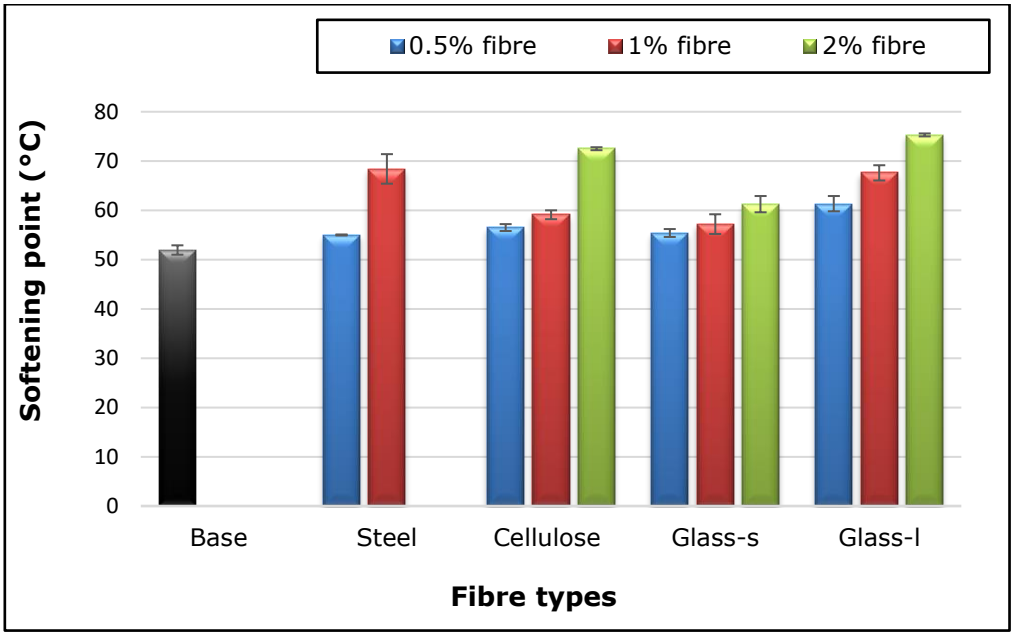


Figure 4-5 Softening point of base and fibre reinforced binders

4.3.4 Viscosity

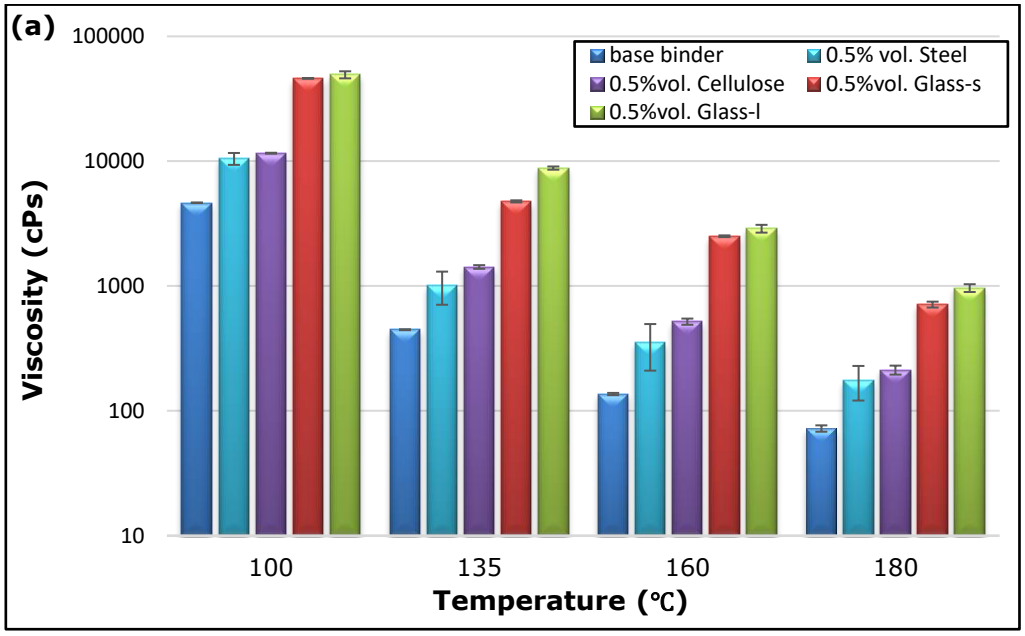
The addition of fibre increased the viscosity of the base bitumen, implying improved rutting resistance for asphalt mixtures using this binder (Chen and Lin, 2005), see also section 4.5. Figure 4-6 shows that viscosity increases with the addition of fibres and this became more evident at high temperatures. The figure shows the average of three values and error bars, which represent plus and minus one standard error. The addition of glass fibres led to a significant increase in viscosity. This effect could be due to the glass fibre surface texture and dimensions (length and width) which help to form a network of fibres, interacting to create a continuous network of fibres through the bitumen (see Figure 4-3). This network of fibres increased the resistance to deformation by reinforcing the bitumen. However, the addition of 0.5% cellulose fibre exhibited a more limited increase in viscosity, which may be due to cellulose fibres acting only as a dispersed material and not forming a continuous

network at the low fibre content. The mechanism of the test and the high density of steel fibre may have led the fibre to sink, and this minimised the possibility of forming a network, as the visual inspection showed that most of the steel fibres were at the bottom of the cylindrical test mould.

The viscosity ratio of fibre mastic to bitumen increases with increasing fibre content and temperature up to 160℃, which is important to asphalt mixture strength. This is because higher viscosity prevents drain-down and at the same time increases the resistance to deformation of an asphalt mixture (Chen and Lin, 2005).

Chen and Lin recommended that a stiffening effect (viscosity ratio) of ten times should be suitable to reinforce bitumen in terms of workability, as mentioned in the literature review chapter. They point out that using a high amount of fibre would lead to fibre-fibre interaction. Mixing more fibres than the optimum concentration is not good, because too much reinforcement could lead to brittle mastics. Therefore, special attention should be paid when high fibre contents are added, which may result in voids during the mixing process and lead to poor pavement performance (Chen and Lin, 2005). The stiffening effect is achieved for the glass fibres at the addition of 0.5% and 1.0% but the cellulose fibre only at the addition of 1.0%. The reinforcement effect is not the only factor that should be considered for the desirable content of fibres. It is important to note that other factors should be examined such as cost, workability of the resulting composite and that too much fibre could lead to brittleness. Adding a high fibre percentage to the bitumen may lead to the fibre properties dominating those of the bitumen, leading to a brittle material. Other research showed that increased fibre content led to decreased elongation at rupture (Chen and Lin, 2005). Note that long glass fibres showed a higher increase in viscosity than short ones. However, the effect of glass fibre length is clearer at low fibre content (0.5%).

Improving bitumen viscosity is important to improve asphalt performance, especially at high temperature. These mastics are not directly comparable with asphalt specifications, and further investigation should be made evaluating the influence of this increase on compaction by investigating the differences in the compaction effort between control and fibre reinforced asphalt mixture while using the same mixing time and temperature.



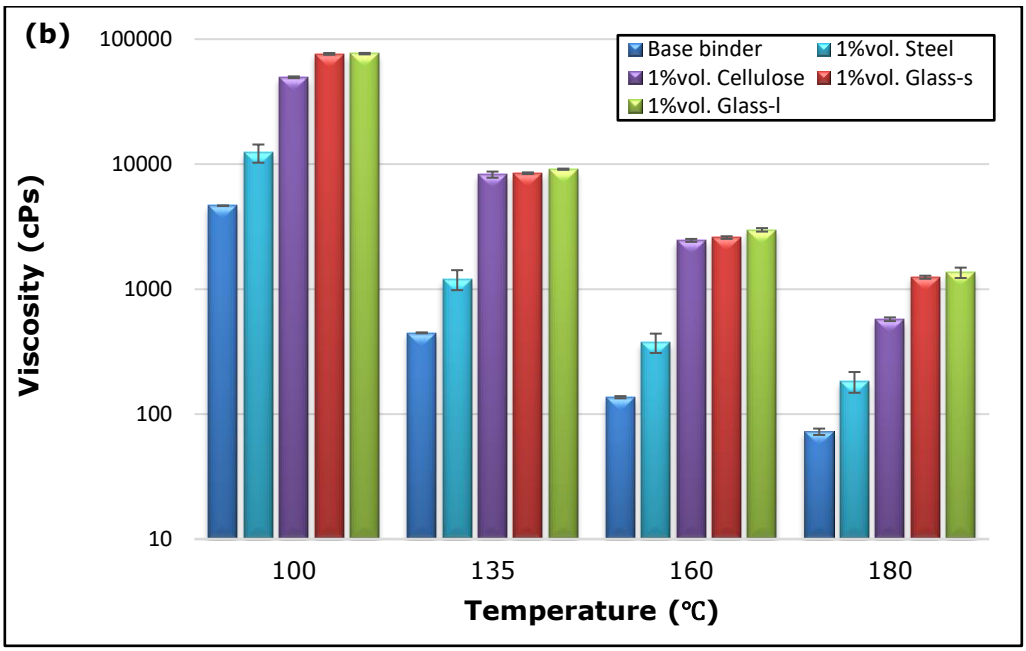


Figure 4-6 (a and b) Viscosity of base and fibre reinforced binders

4.4 Master Curves

4.4.1 Complex Modulus Master Curves

The rheological properties, complex modulus and phase angle master curves for fibre mastic can be constructed utilising the time-temperature superposition principle (TTSP) (Ferry, 1980). Figure 4-7 (a) depicts the complex modulus master curves for the base bitumen and binder containing different fibres at 0.5% by bitumen volume. The complex modulus for fibre mastics was slightly higher than that of base bitumen across all the range of frequencies and low temperatures (30 - 45℃).

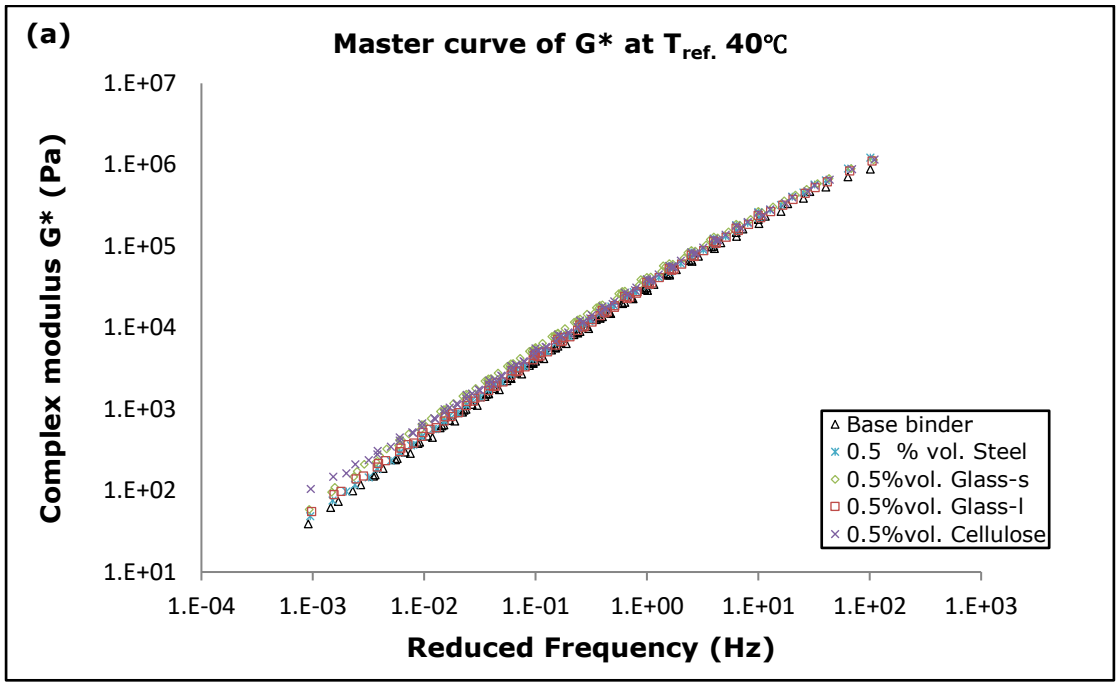
At low frequencies and high temperatures (50 - 70℃), the modulus value of the mastic containing cellulose, glass-l, glass-s and steel fibre was greater than the value for base bitumen, respectively. This indicates that the stiffening effects of fibre modifiers were of greater magnitude at low frequencies and high temperatures. The slight increase in complex modulus at low concentration may have been due to the fact that small amounts of fibre cannot interact with each other and act only as dispersed materials. It seems possible that these results are due to the viscosity of the base bitumen being low enough at high temperatures to permit the small amount of fibre to influence the stiffness. The conventional tests, such as penetration and high temperature viscosity, are able to demonstrate increases in hardness and viscosity, but they are unable to quantify the unique rheological characteristics of different fibre mastics. Constructing complex modulus (G*) master curves for fibre mastic allows (G*) to be predicted at frequencies and/or temperatures that would be difficult to determine in the laboratory and which represent all possible pavement climatic and loading conditions. DSR samples are small compared to penetration and viscosity test samples, and this may affected the degree of fibre entanglement in the DSR sample at low fibre content (0.5%).

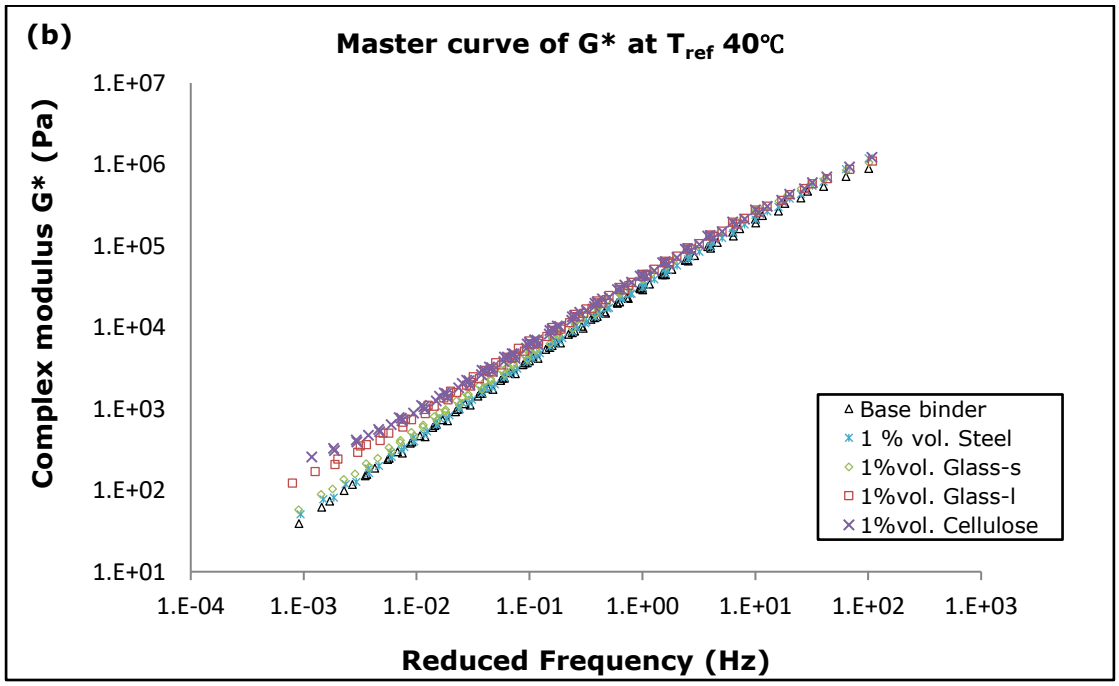
This might explain the different influence of fibres in the conventional tests (e.g. penetration) and properties of mastic measured using the DSR at low fibre content.

The master curves showed a marked influence of fibres on complex modulus for the 1.0% and 2.0% fibre mastics at low frequencies and high temperatures (50-70℃) as shown in Figure 4-7 (b and c). The complex modulus value of bitumen binder containing 1.0% cellulose fibre, glass-l, glass-s and steel fibre was about 7, 4, 2 and 1.2 times greater than the value of the base bitumen at low frequency and high temperatures, respectively. For 2.0% cellulose fibre, glass-l, glass-s and steel fibre, the values were about 18, 7, 3.5 and 1.4 times greater than the value of the original binder, respectively. This increase in complex modulus could be due to the fibres forming small networks, gradually interacting with each other to form extended networks in the bitumen. This three dimensional network acts as a supporting structure, strengthening the bitumen and reducing deformation (see Figure 4-3).

It should be noted that the effect of cellulose fibre on complex modulus was greater than that of glass and steel fibres. This result was considered to some extent surprising because the glass and steel fibres have a higher modulus of elasticity, tensile strength and are longer than the cellulose fibre. This may be due to the small size of the DSR sample, which affects the distribution and orientation of fibres and which could influence the strength and stiffness of the composites. This behaviour of glass fibre may have been due to unidirectional orientations providing poor properties, especially where the load was perpendicular to the fibres, leading to lower stiffness. This effect may not be so marked for the shorter cellulose fibres. In addition, short, randomly oriented fibres having a small aspect ratio are easily introduced into the matrix and give relatively isotropic behaviour in the composite (Bagherpour, 2012). In addition, the rough surface texture and absorption/adsorption properties of the cellulose fibre may have also affected the complex modulus result, (see drained down test results, chapter six). It is

important to note, however, that this possible effect of fibre length is not apparent for the shorter glass fibre compared to the longer, but both are much longer than the cellulose fibres.





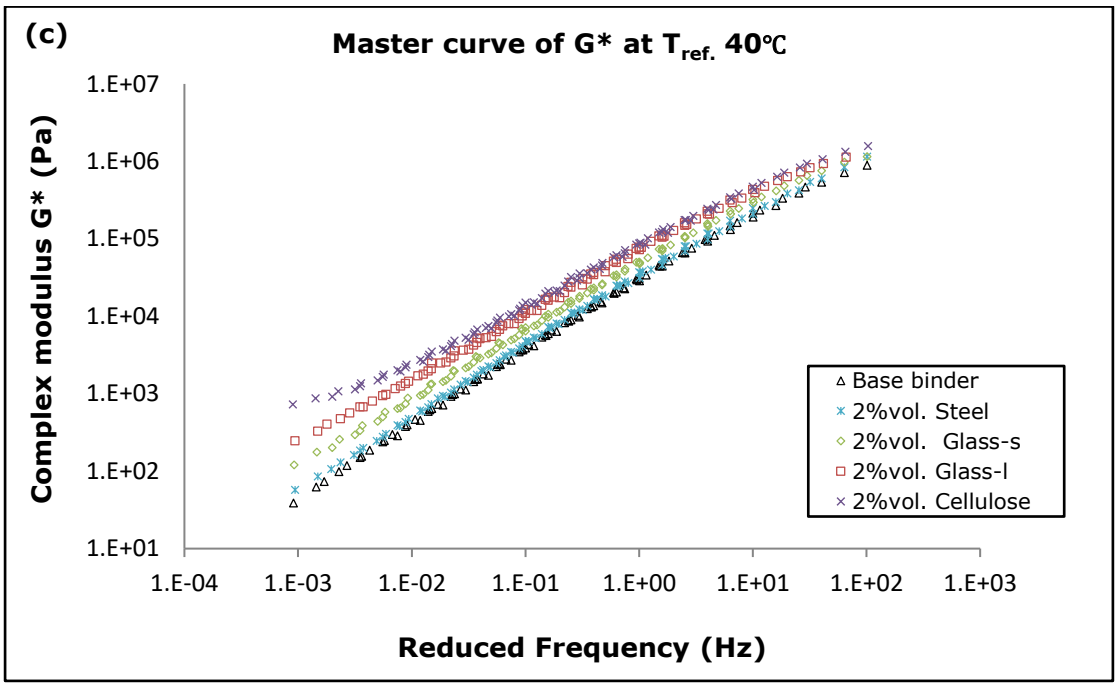


Figure 4-7 (a, b and c) Complex modulus master curves for unaged base bitumen and bitumen-fibre mastics

4.4.2 Phase Angle Master Curves

Phase angle is an indicator of the viscoelastic properties of bitumen binder. A 0° phase angle represents a purely elastic material, while 90° represents a purely viscous material (Mezger, 2011). Time temperature superposition may give an indication about the compatibility of the fibre mastic systems. This is characterised by smooth complex modulus master curves and the difference in the plots of phase angle master curves between fibre mastic and base binder. While the complex modulus master curves of all mastics followed a similar pattern, the phase angle master curves varied. The results can be seen in Figure 4-8.

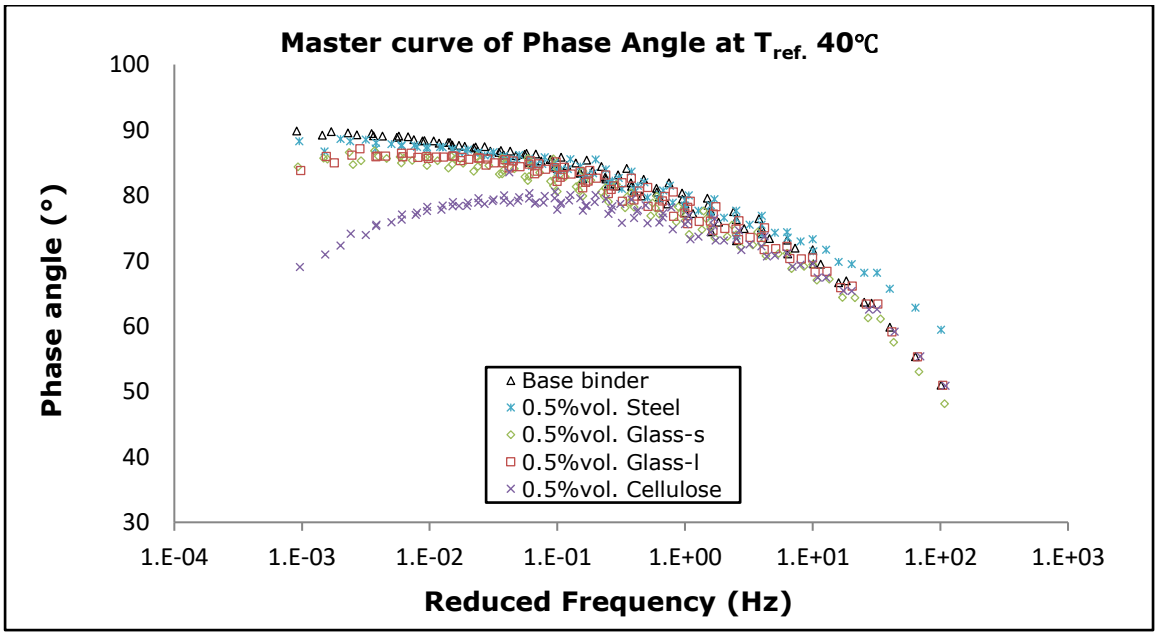
It is interesting to note that the phase angles decreased significantly when fibres were added, indicating that adding fibres led to improved elastic properties of asphalt binders, mainly at high temperatures and low frequency levels. The reduction of phase angle results in the improvement of the resistance to permanent

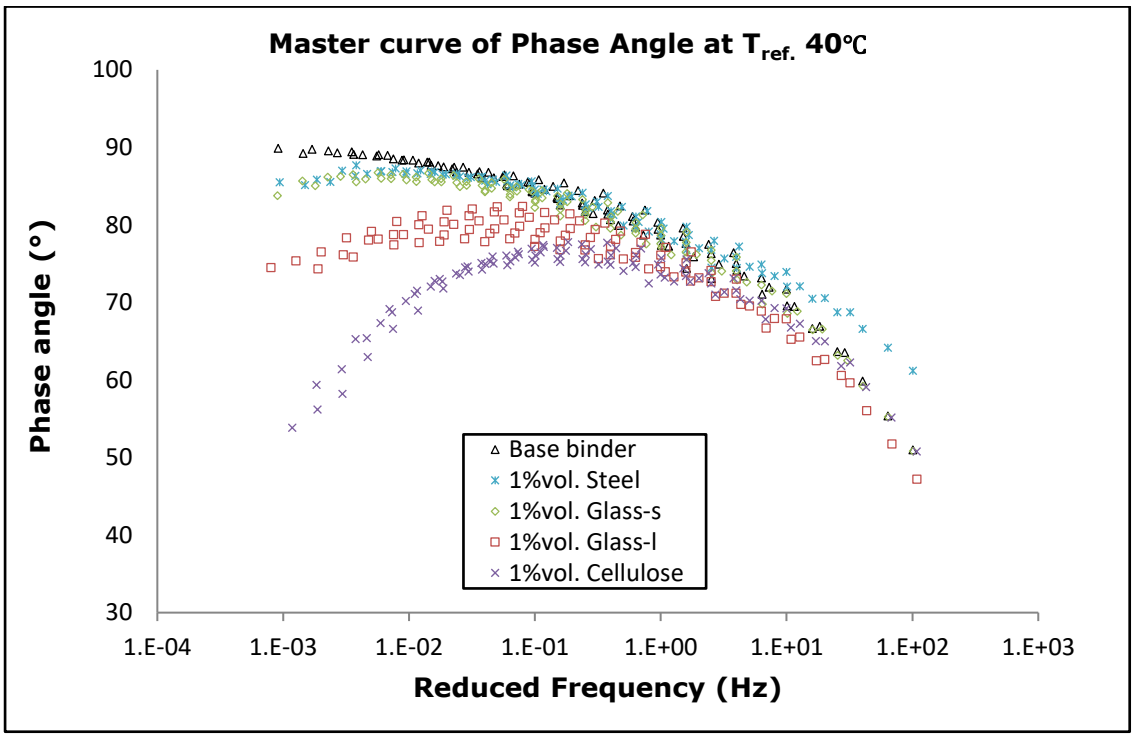
deformation for the bituminous binders because lower phase angle indicates more elastic behaviour than viscous behaviour (Wu et al., 2006, Ab-Wahab, 1993).

Three distinct patterns can be determined to identify their plateau zones. The phase angle of the base binder decreases with increase in frequency for all test temperatures. The phase angle master curve of the glass and steel fibre mastics showed an increase in phase angle with the increase of frequency at high temperatures (55-70℃) and high fibre content. The phase angle master curve of the cellulose fibre mastics showed a peak at intermediate temperatures, followed by a drop toward lower frequencies (high temperatures) and there was a noticeable decrease in phase angle at lower frequencies (high temperature range). Cellulose fibres led to a significant decrease in the phase angle compared to the base bitumen at low frequencies for all additions. This decrease in phase angle implies a significant improvement in bitumen elastic properties. The reason for the significant decrease in the phase angle may have been swelling of the cellulose fibres due to absorption/adsorption of bitumen and the interaction of the fibres to form a continuous network within a highly modified binder (2.0% addition) (Chen and Lin, 2005, Wu et al., 2006). This is consistent with the fact that cellulose fibre has high absorption value for water (although this has not been measured for bitumen) and swelling of the fibre due to absorption/adsorption of bitumen might increase as the temperature increases, within a highly modified binder. Cellulose fibres are usually used in the stone matrix and open graded asphalt mixtures to prevent drain down of the binder, which has been attributed in part to its higher absorption/adsorption of the bituminous light fraction compared with other fibres (Putman and Amirkhanian, 2004). This may also depend on the compatibility between the bitumen and the fibre used. For instance, polymers have good compatibility with a high aromatic content bitumen (Airey, 2003, Lu and Isacsson, 1997). Previous research has suggested that the occurrence of a plateau in the phase angle curves indicates a higher interaction level between the modifier and bitumen (Socal da

Silva et al., 2004). In this study, the cellulose fibre mastics showed a different behaviour to the glass and steel fibre mastics and base bitumen by forming such a plateau zone. This may indicate that cellulose fibre is more compatible with bitumen than other fibres. Moreover, the surface texture of cellulose fibres, as shown in the scanning electron microscope (SEM), consists of small bundles with a rough surface. This texture may help cellulose fibres to establish a greater network effect than the long and smooth surface texture of glass fibres inside the small DSR sample. Polymer modification of bitumen also leads to changes in phase angle master curves (Asgharzadeh et al., 2015) and this has been associated with the changes in the chemical composition of bitumen due to chemical reaction or absorption of bitumen fractions (Baumgardner et al., 2005, De Filippis et al., 1995). Absorption/Adsorption of some fraction of the bitumen by cellulose fibres may, therefore, also lead to changes in the master curves. However, further investigation is needed to explore the distribution and effect of fibre in the modified asphalt mortars and asphalt mixtures (see chapter 5 and 6).

Steel fibre showed the highest phase angle values in the range of low temperatures (30-40℃) and high frequencies.





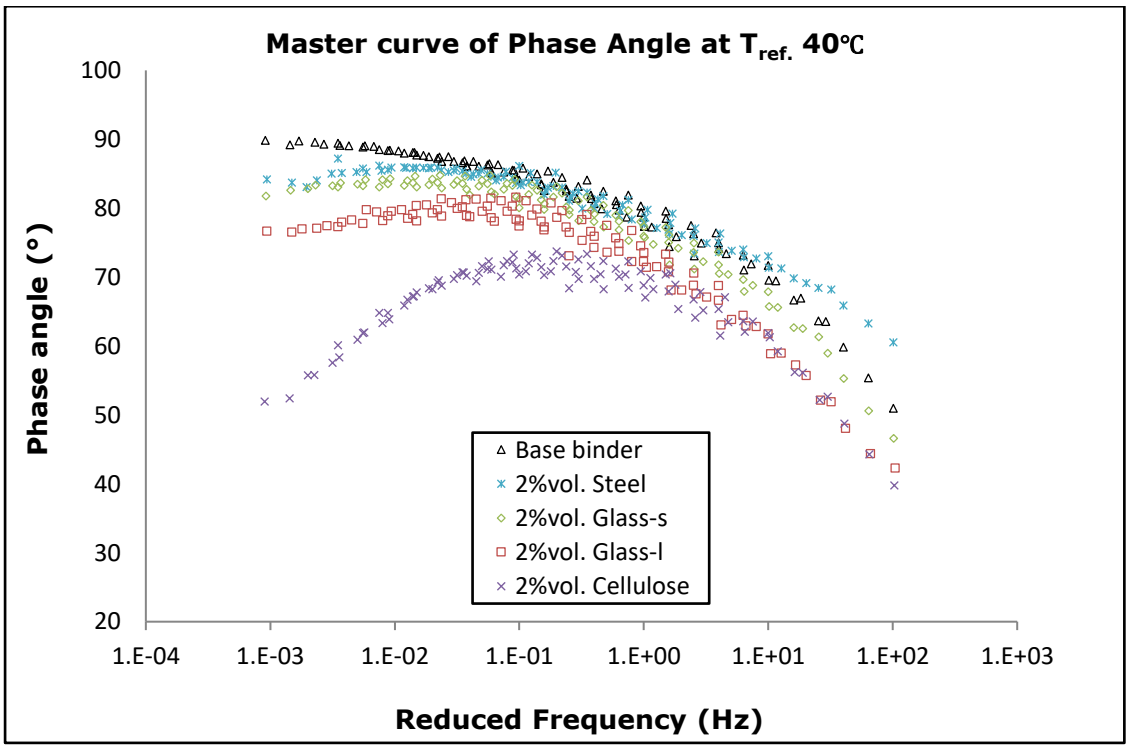
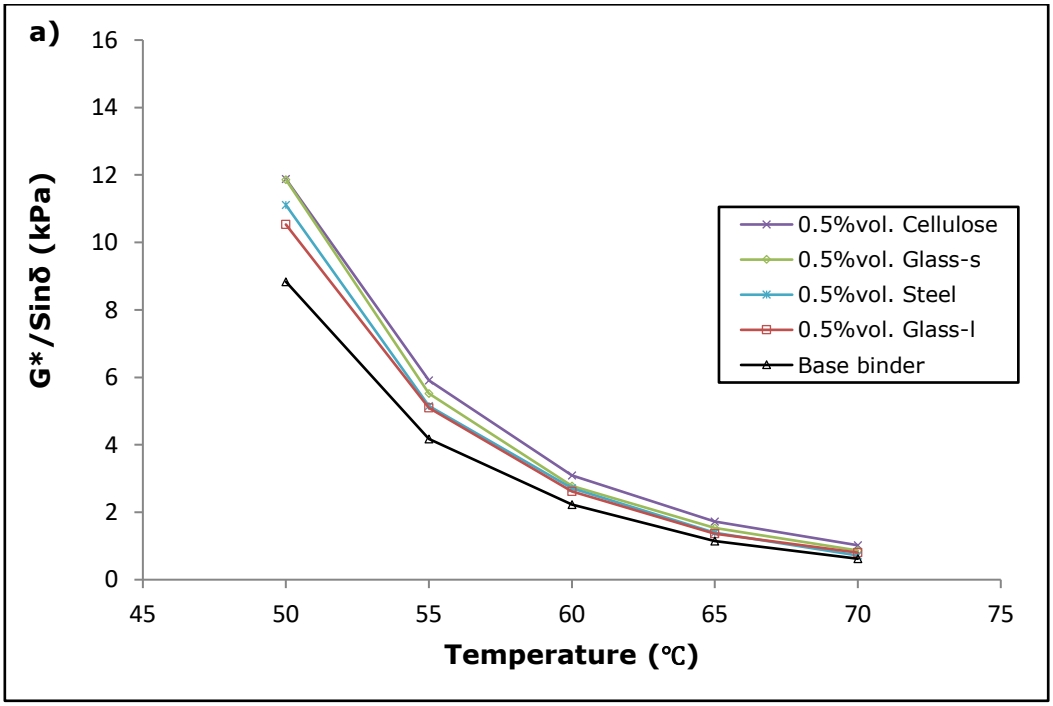
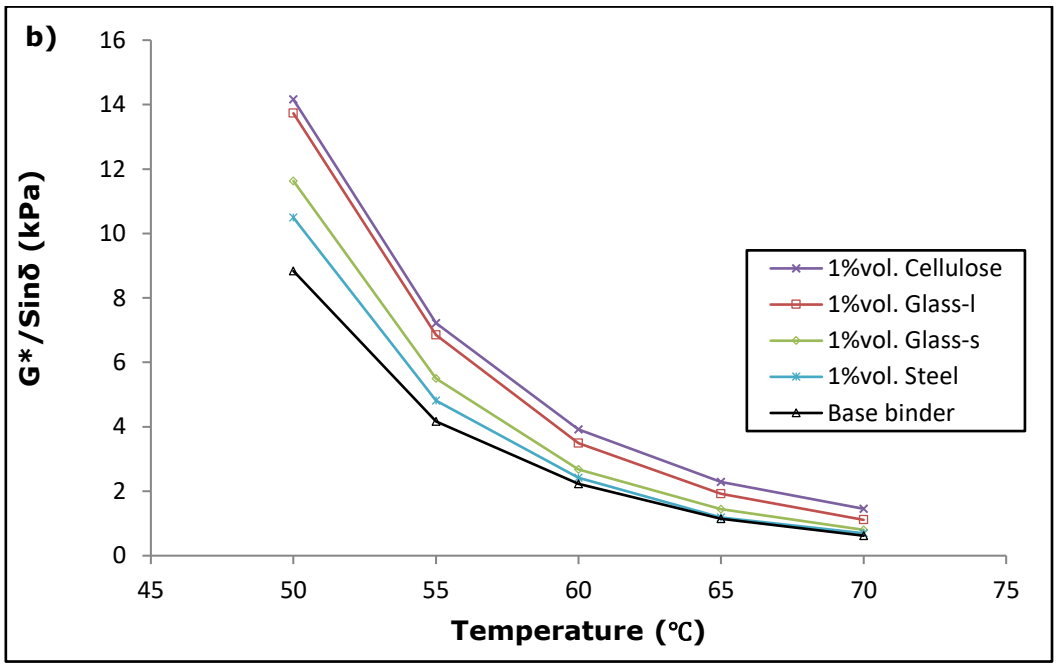


Figure 4-8 (a, b and c) Phase angle master curves for unaged base bitumen and bitumen-fibre mastics

4.5 Rutting parameters

The influence of frequency and temperature on the rutting parameter (G*/sinδ) is illustrated in Figure 4-9. The rutting parameter (G*/sinδ) is considered as an indicator for evaluating the resistance to permanent deformation of both pure and fibre modified binder (Wu et al., 2014, Wu et al., 2006, Al-Mansob et al., 2014). It was observed that the addition of fibre resulted in the improvement of bitumen binder's high temperature stability. The results indicate that the value of G*/sinδ using cellulose fibre was the highest followed by glass-l fibre then glass-s fibre and finally steel fibre for 1.0% and 2.0% addition of fibres. The value of rutting parameter increased with an increase in fibre percentage and decreased with an increase in test temperature. Therefore, the bituminous binder is characterised by obvious temperature sensitivity. This means fibres could improve permanent deformation resistance of asphalt mixtures, especially at high temperatures, where rutting is more likely to be a significant problem for asphalt mixture performance.





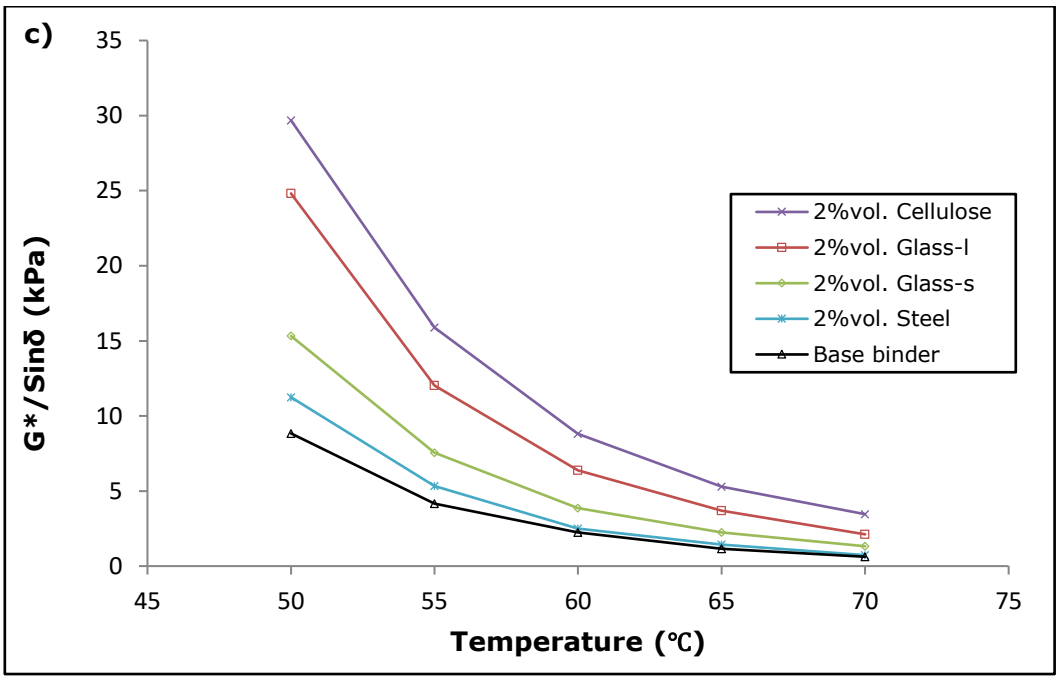


Figure 4-9 (a, b and c) Rutting parameter for unaged base bitumen and bitumen-fibre mastics

4.6 Double edge notched tension (DENT) test

The DSR results may indicate that the compatibility of fibre reinforced bitumen mastics is good. Compatibility is a complicated phenomenon due to the complex nature of bitumen. According to a past study, the degree to which a modifier enhances the bitumen's properties depends on the compatibility of the modifier and the bitumen. For instance, bitumen rheological and thermal properties will improve more with highly compatible polymers (Ragab et al., 2016). The formation of a plateau in the phase angle master curves shows a higher interaction level between the modifier and bitumen (Socal da Silva et al., 2004). Together with real fracture evaluation, this can give more detailed predictions of long-term performance. However, the linear viscoelastic region parameters are less likely to be correlated to high strain region parameters like a ductile failure and brittle fracture (Andriescu and Hesp, 2009). The following investigation provides more information about these potential failure mechanisms.

The total work of fracture was measured at 15℃, with a rate of displacement of 50 mm/min, to examine the binder performance under ductile failure conditions. The specific total work of fracture was obtained by dividing the total work of fracture by the cross-sectional area of each ligament, Figure 4-10.

The examination indicates that there was a slight increase in specific total work of fracture for a cellulose and steel fibres contents of 0.5%. At a cellulose fibre content of 1.0%, the specific total work of fracture increased markedly, which may have been due to the fibres beginning to tangle together to give more reinforcement effect (Wu et al., 2014). A 1.0% glass fibre content exhibits a more significant increase in specific total work of fracture, which is seven times higher than normal bitumen. This could be explained by the high tensile strength and length of glass fibre, and to the sample thickness being similar to the glass fibre length. This may cause the glass fibre to distribute into the DENT test sample in such a way that the

applied load was parallel to the fibre direction, thus the tensile strength approaches that of the fibres (Campbell, 2010). This is in agreement with the fact that composite anisotropic materials have different material properties in all directions at any point in the structure (Campbell, 2010). This may be the reason why 13 mm glass fibre had the highest specific total work. In addition, this study could not test at 0.5% vol. glass –l fibre with 15 mm ligament length and 1.0%vol. glass –l and steel fibre with 10 and 15 mm ligament length, because the failure occurred in the contact area between the mould edge and bitumen or in another place before the sample fractured in the notch area (see Figure 4-11). This could be explained by the existence of fibre in the notch area leading to a significant increase in the tensile force required to fracture the bitumen. The SEM images (see Figure 4-3) are taken from DENT specimens in the notch area. Consequently, the tensile fracture force may be higher than the adhesion force between the mould and binder, and the failure happens at the mould edge instead. Due to this issue, this study recommends design a new mould that is able to provide higher bond strength between mould edge and mastic sample.

The results showed that the glass-s fibre has the highest essential and plastic works of fracture, followed by cellulose fibre, as shown in Figure 4-12. Adding glass-s fibre leads to a significant increase in bitumen toughness, which should help minimise or prevent the occurrence of longitudinal and transverse cracking in flexible pavement. Andriescu and Hesp (2009) examined the ductile failure for different bitumens in a highway paving trial. The tested binders were original samples taken during the construction of the test road and had been stored for several months before testing. The results showed that the pavement section with the binder with the higher toughness showed no significant cracking, while that with the binder with lower essential and plastic work of fracture exhibited alligator and longitudinal cracks. This investigation was carried out over a period of less than four years, and the long-term performance may be different. However, binders with

very low plastic or essential works of fracture may not perform well when used in a pavement mixture (Andriescu et al., 2004).

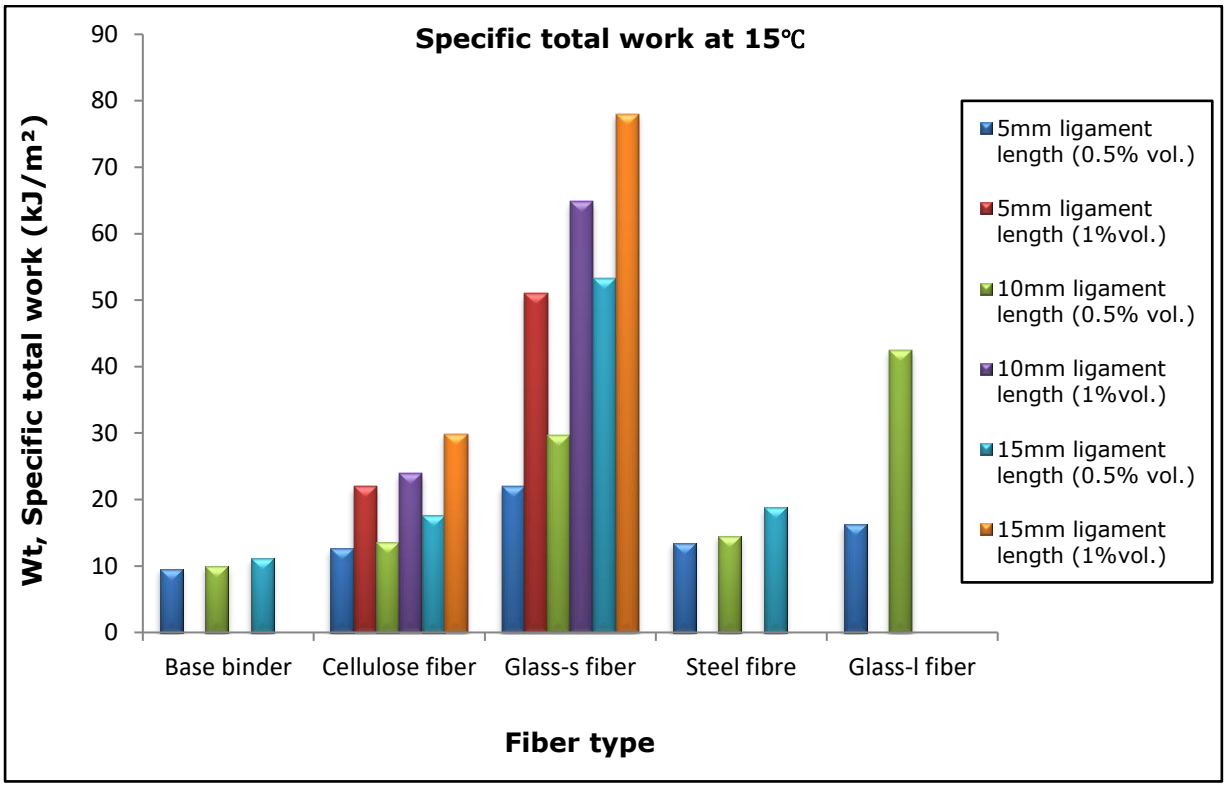


Figure 4-10 Specific total work of fracture

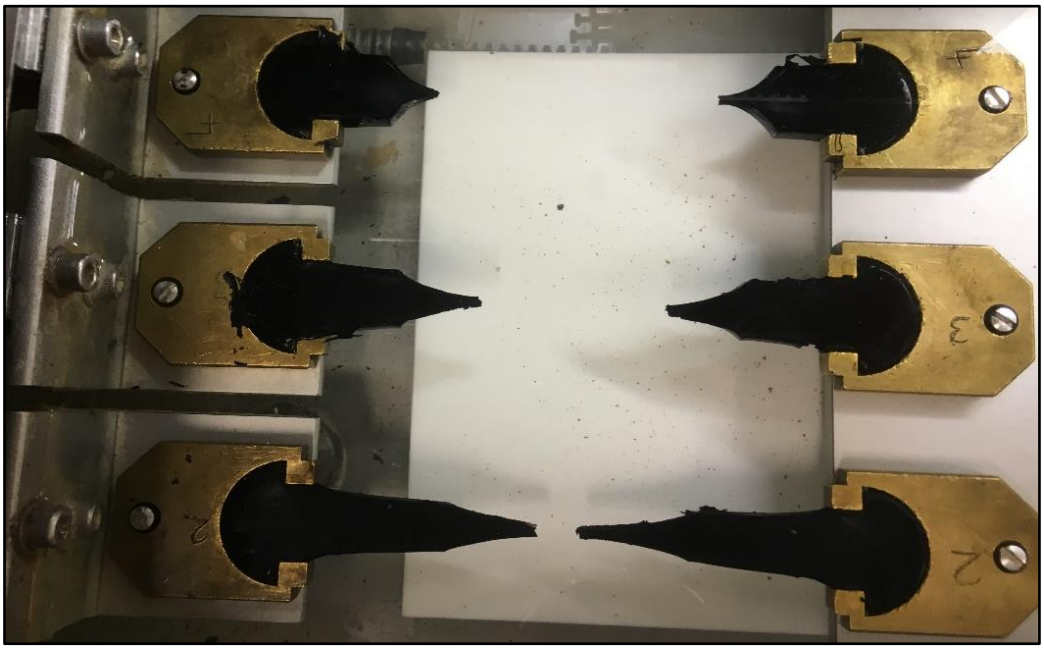


Figure 4-11 DENT samples of fibre reinforced mastic after the test

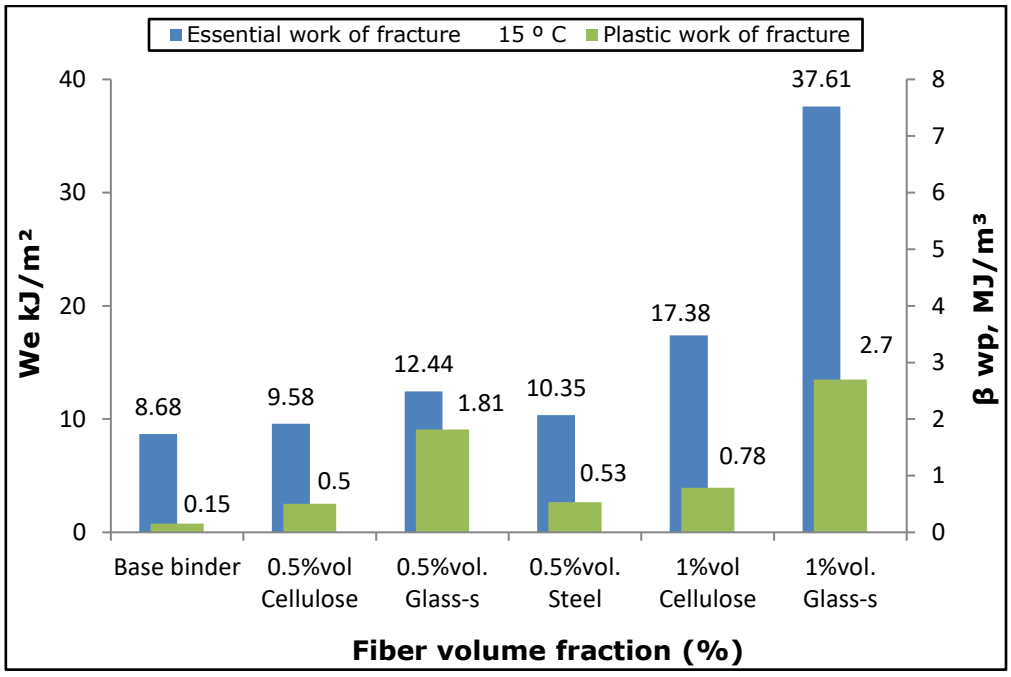


Figure 4-12 Essential and plastic works of fracture

4.7 Summary and conclusions

In this chapter, the influence of fibres on the conventional and more fundamental rheological properties of bitumen have been investigated, based on penetration, softening point, viscosity, double edge notch tension and dynamic shear rheometer tests over a wide range of test temperatures and loading frequencies. In the following chapter, the influence of filler ratio on the fibre reinforced mortar performance will be investigated. The following conclusions are offered from this chapter:

- Fibre properties such as shape, size and microstructure were observed using a scanning electron microscope (SEM). These properties will influence how fibres can reinforce bitumen through the formation of three dimensional networks within the modified mastics. Glass fibre forms such a network as shown in Figure 4-3. These networks provide support to the mastic structure by holding the components together and spreading stresses.
- Fibres can significantly improve bitumen mastic penetration, softening point and viscosity values. Long glass fibre showed the greatest increase in terms of viscosity, softening point and decrease in penetration. This indicates an improvement in bitumen stiffness mainly at high temperatures, which is beneficial to mastic strength. High viscosity and softening point could lead to reduced drain down and permanent deformation of asphalt mixture.
- Complex modulus master curves showed that the stiffening effect of fibre additives is more significant at low frequency and high temperature, which is important to increase permanent deformation resistance of asphalt mixtures.
- Phase angle master curves showed three different patterns, but cellulose fibre exhibited different behaviour to glass and steel fibres and led to a significant decrease in the phase angle at both high and low frequencies.

This decrease in phase angle implies a significant improvement in bitumen elasticity.

- The rutting parameters increased significantly with the increase in fibre content, at moderate and high temperatures. This indicates that the addition of fibres may lead to improved rutting resistance of asphalt mixtures. However, the DSR results for the glass and steel fibre mastics may influenced by the size and geometry of the samples.
- The addition of fibre significantly improves bitumen toughness. A 1.0% by volume addition of short glass fibre leads to a marked increase in essential and plastic works of fracture. This is because glass fibre has high tensile strength and good adhesion with the bitumen (Matthews and Rawlings, 1999). This increase in toughness may contribute to increasing the resistance of an asphalt mixture to cracking. However, the DENT sample geometry limits the test conditions for fibre reinforced mastics.

Chapter 5 Mortar properties

Influence of fibres on modified asphalt mortars

5.1 Introduction

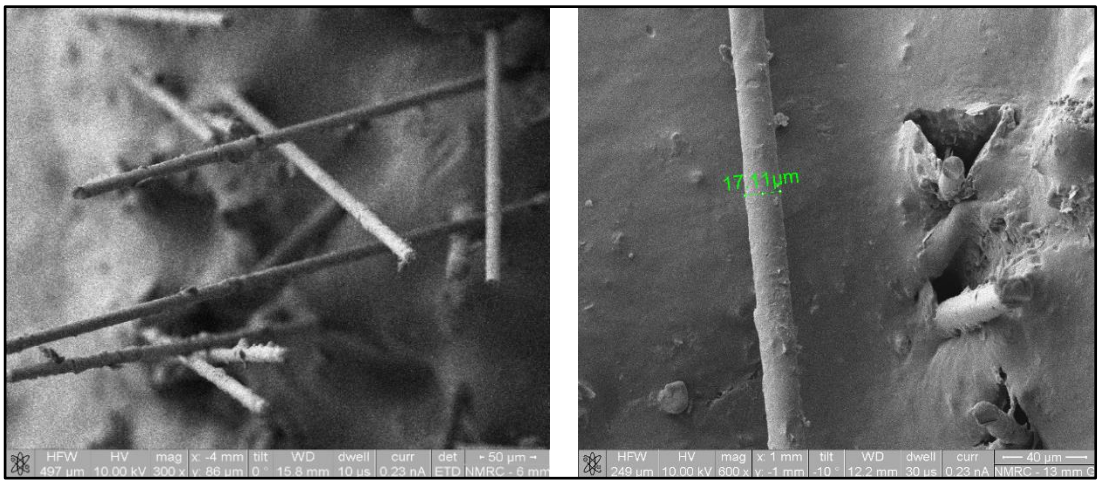
The bitumen-mineral filler mortar is the composite used to bond the aggregate particles in the bituminous mixtures. Data from a previous study pointed out that asphalt mixture distress is highly dependent on the properties of asphalt mortar such as complex modulus, moisture stability and the interaction of the asphalt bitumen and filler (Yi-qiu et al., 2010). Therefore, the investigation of asphalt mortar is important to gain a better understanding of the performance and response of asphalt mixtures.

The experimental work in this study focuses on the evaluation of conventional and more fundamental rheological parameters of fibre reinforced asphalt mortar. A combination of one penetration grade bitumen (40/60), limestone filler with maximum size less than 0.063 mm, three filler to bitumen ratios (0.8, 1.0, 1.2) by weight, four fibre types and three fibre concentrations of 0.5%, 1.0% and 2.0% by bitumen volume was selected to (1) assess the fibre effect on rheological properties of bitumen-fibre- filler mortars (2) the reinforcing effects of various factors such as dimensions, shape, content of fibres and filler to bitumen ratio and (3) provide fundamental information for the behaviour and optimisation of fibre reinforced mortar.

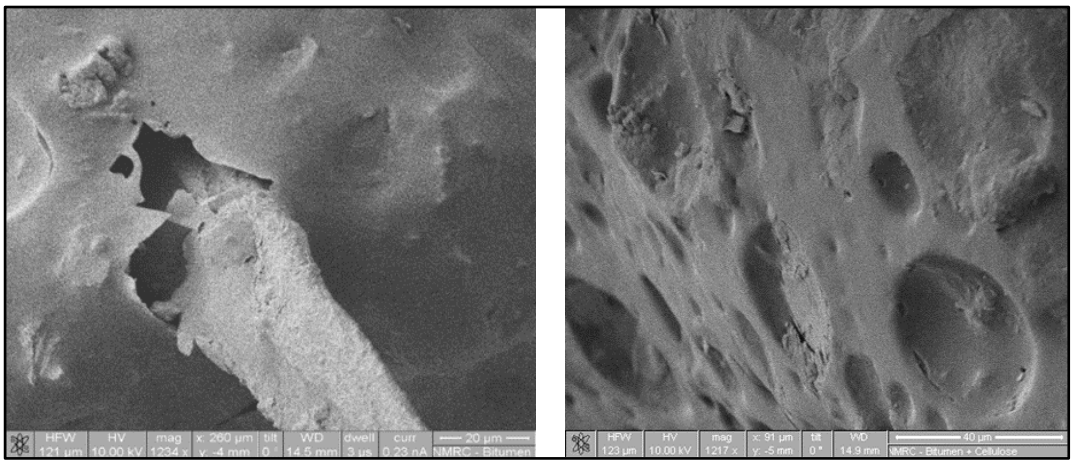
5.2 The microstructure of fibre modified asphalt mortar

Scanning electronic microscope (SEM) images of the three fibre modified asphalt mortars are shown in Figure 5-1. These images were taken from the DENT test samples in the notch area. In chapter three, the microstructures of these fibres were observed. This analysis will try to explain how fibre microstructure affected the distribution and entanglement of fibres into the asphalt mortar. These images show the microstructure of continuous networks of fibre shown in Figure 5-1 (a and c). The formed network by the interlacing of the fibre (steel and glass) horizontally and vertically and good distribution in the asphalt mortar may lead to the spread of the load stresses and reduces stress concentration.

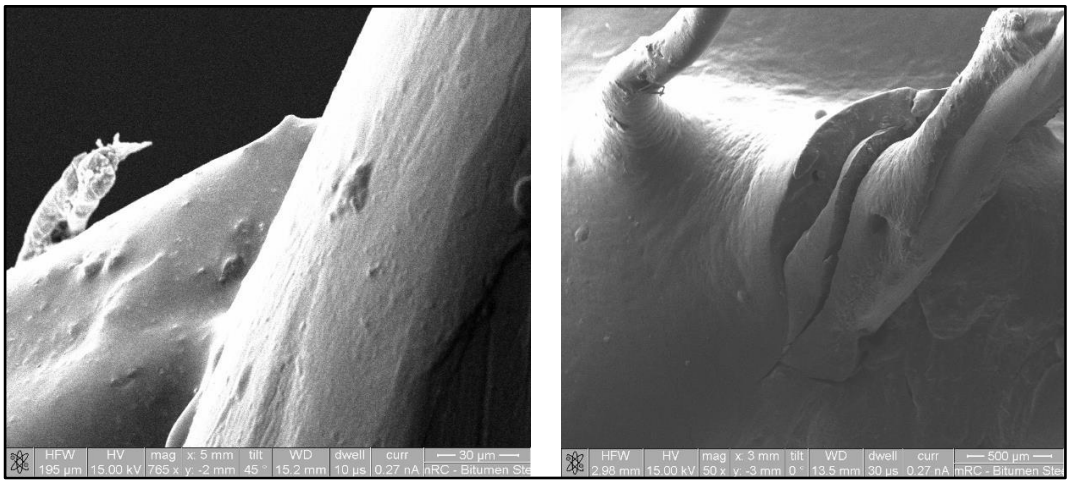
With regard to cellulose fibres, the scanning electronic microscope could not show a lot of information about the entanglement of cellulose fibres through asphalt mortar as shown in Figure 5-1 (b). However, cellulose fibres showed good interaction with the asphalt mortar as shown in Figure 5-1 (b). These figures show the needle-like structure of glass fibres; the spongy and flexible nature of cellulose; and the thick steel fibres coated with mortar.



(a) Glass fibre modified asphalt mortar



(b) Cellulose fibre modified asphalt mortar



(c) Steel fibre modified asphalt mortar

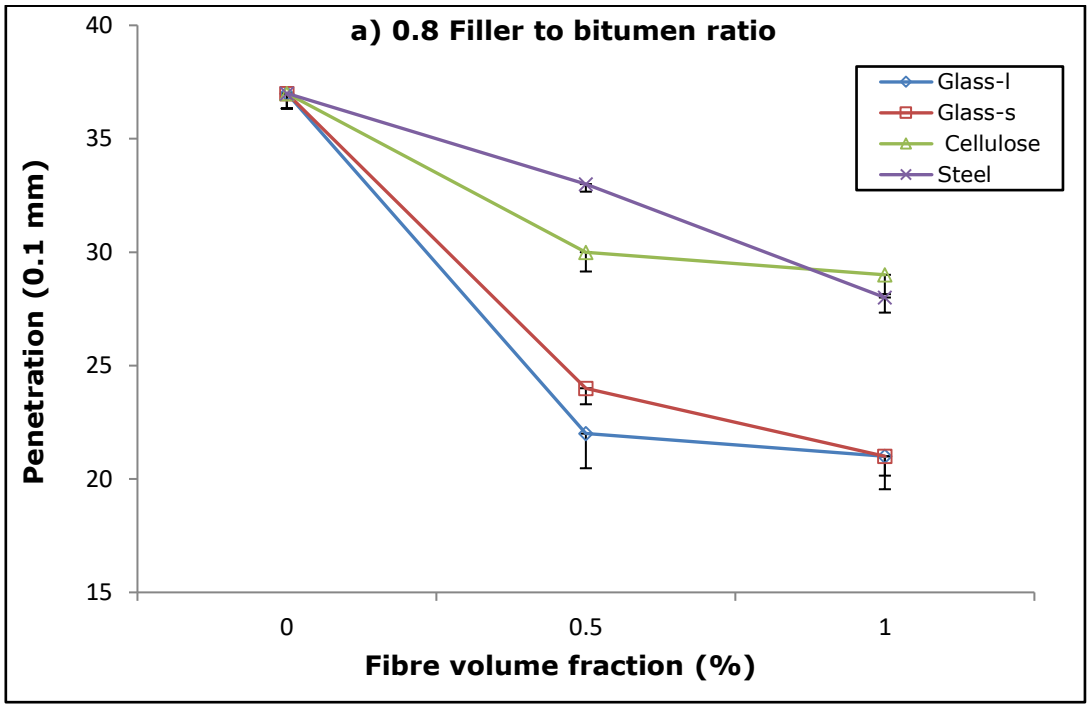
Figure 5-1 (a, b and c) SEM images of fibre modified asphalt mortars

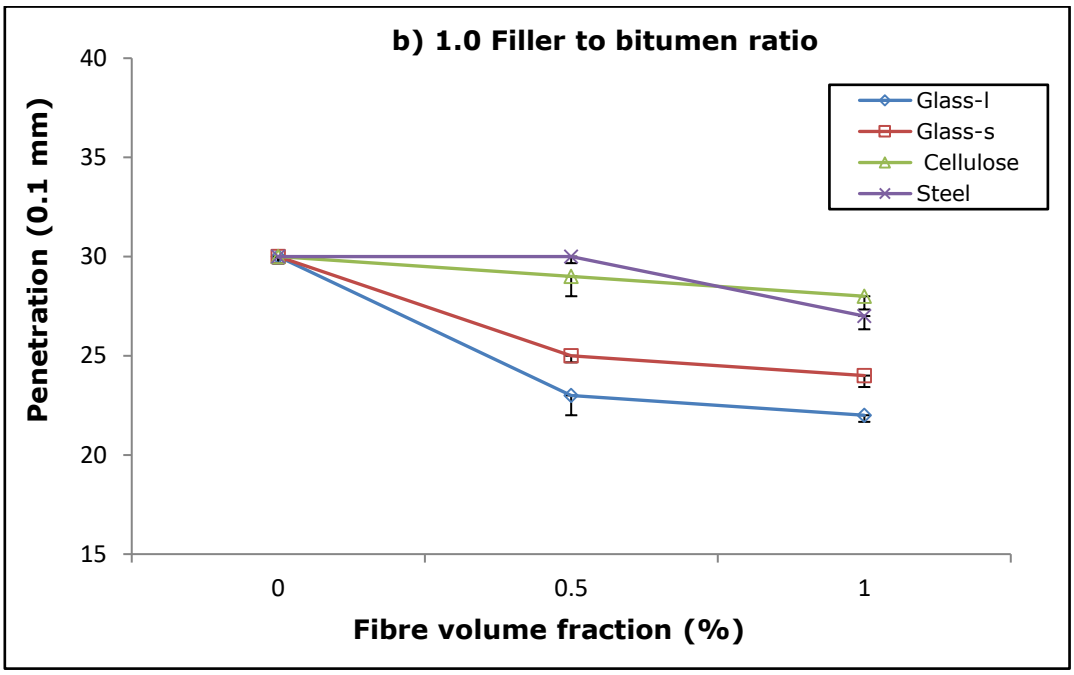
5.3 Results and analysis

5.3.1 Penetration test results

Penetration is a common test used to measure bitumen hardness. The penetration value was taken as the average of three readings, and the error bars in the following Figures represent plus and minus one standard error. It can be observed that the penetration value of modified asphalt mortar decreases significantly with 0.5% and 1.0% addition of glass-l and glass-s fibres, while slight decreases with 1.0% addition of cellulose and steel fibres, as shown in Figure 5-2. Moreover, the

increase in filler to bitumen ratio led to decreased penetration value of modified asphalt mortar by cellulose and steel fibres, while this increase led to very small effect on penetration value of modified asphalt mortar by glass fibres. Therefore, the significant decrease in penetration value was due to adding glass fibres. This could be due to the length of glass fibre more than cellulose fibres. These two features may have helped glass fibres to entangle with each other to form a continuous network (see Figure 5-1 (a)). This may not have applied for steel fibre due to the high density of steel fibre, seven times higher than bitumen and three time higher than filler, which led the steel to sink to the bottom of the sample. However, these results are consistent with the results obtained from modified mastic by fibres in the previous chapter.





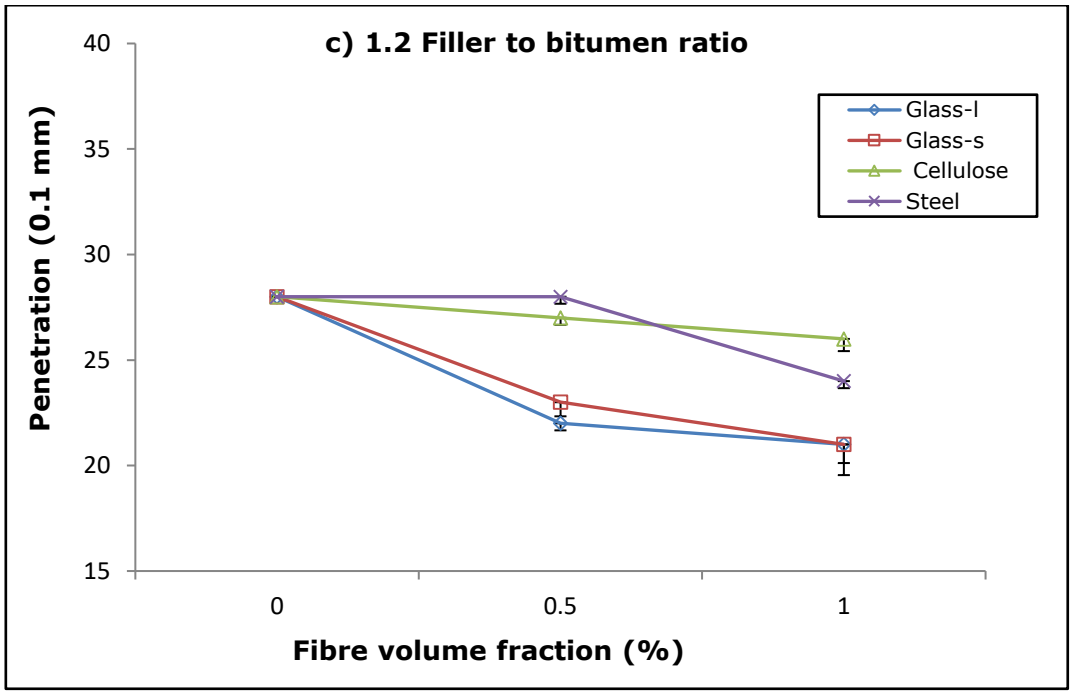


Figure 5-2 Penetration of asphalt mortar mixing with four fibre types and three filler bitumen ratios

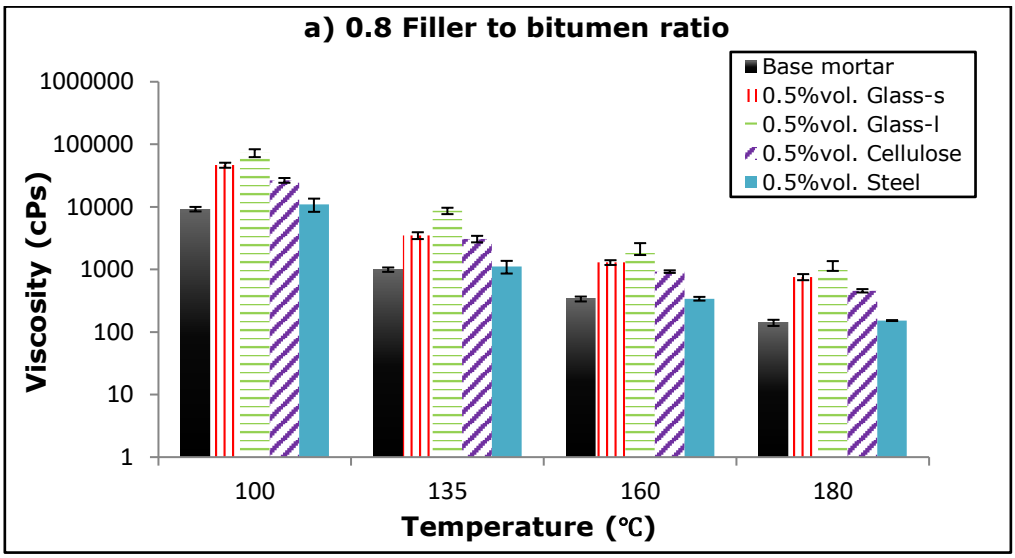
5.3.2 Viscosity test results

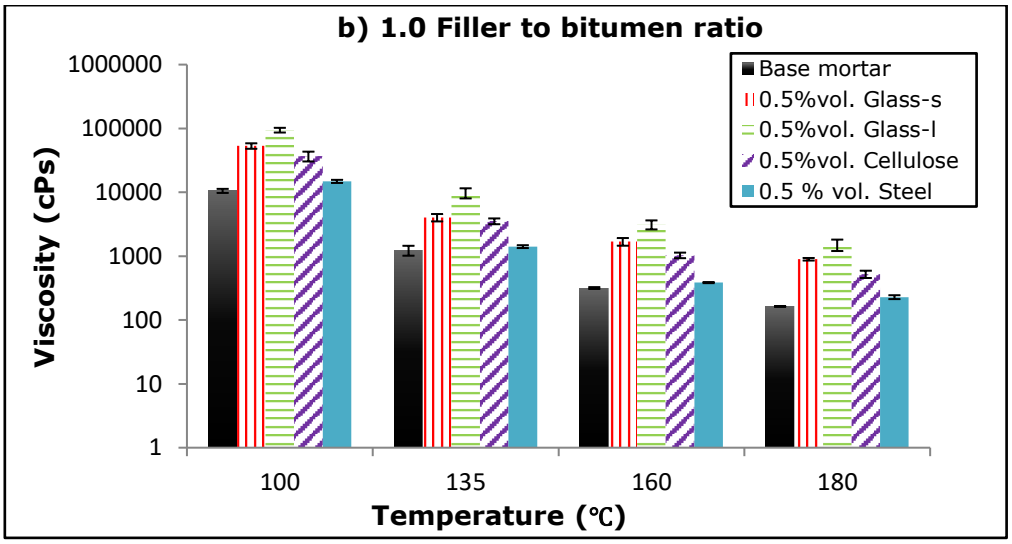
The addition of fibres increased the viscosity of base mortar measured in a Brookfield viscometer as shown in Figure 5-3 and Figure 5-4; and all data from three repeated tests were averaged and the error bars represent plus and minus one standard error. It is clear that the viscosity decreased with increasing temperature, but it increased with the increase of filler to bitumen ratio, indicating that the stiffening effect of filler led to increasing in composite stiffness resulted in an increased viscosity of bitumen, also the adhesion between bitumen and filler may have been good. There was a marked increase in base mortar viscosity at 0.5% glass and cellulose fibres content. At 1.0% glass and cellulose fibre content, the viscosity greatly increased since the cellulose fibre absorb/adsorb more bitumen as shown in drain down results in the following chapter, and glass fibre may have started to entangle with each other to form a continuous mat reinforcing the bitumen as appeared in scanning electronic microscope (SEM) of the fibre reinforced mortar. This network might provide support to the composite structure by holding the components together and resisting deformation (see Figure 5-1 (a)) (Tapkın et al., 2010).

It is interesting to note, the addition of steel fibres led to a slight increase in the viscosity of base mortar contain 0.8 and 1.0 filler to bitumen ratio. This may be due to the high density of steel fibre led to a high part of steel fibre to sink to the bottom of the Brookfield sample. Therefore, the entanglement effect of steel fibres is not dominant. This finding is consistent with the previous chapter.

In conclusion, adding glass and cellulose fibres improved asphalt mortar viscosity, implying an improvement in rutting resistance and reduced drain down of asphalt mixtures (Chen and Lin, 2005). Moreover, the viscosity increased most for glass-l follow by glass-s and then cellulose and at the end steel fibre, which had little

impact of the modified asphalt mortar, possibly due to it sinking to the bottom of the specimens.





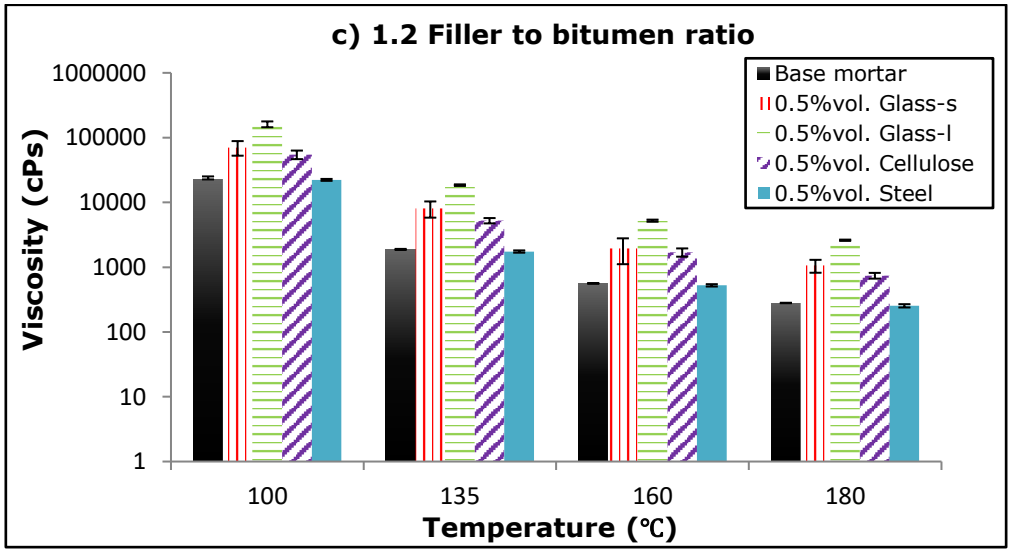
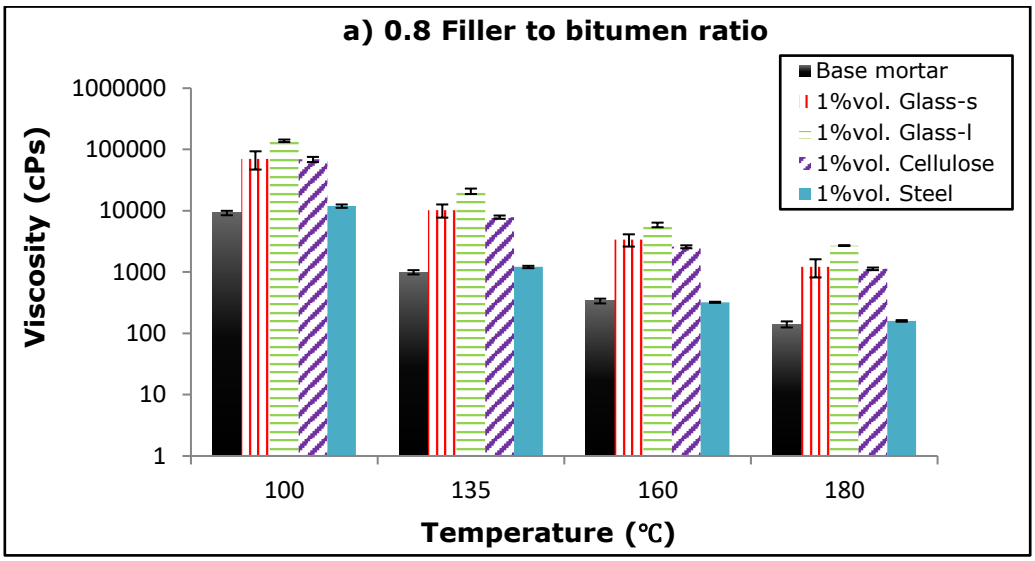
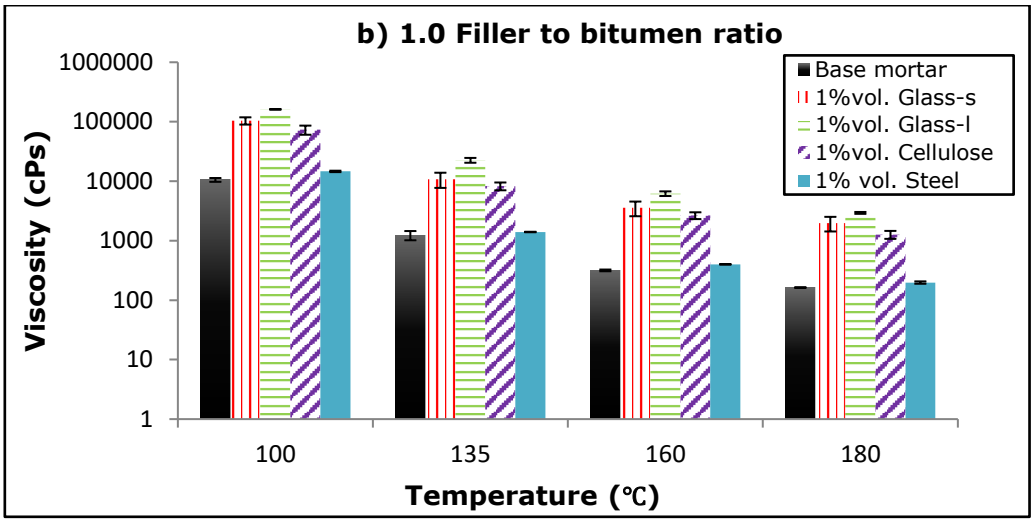


Figure 5-3 (a, b and c) Viscosity for base mortar and 0.5% mortar-fibre





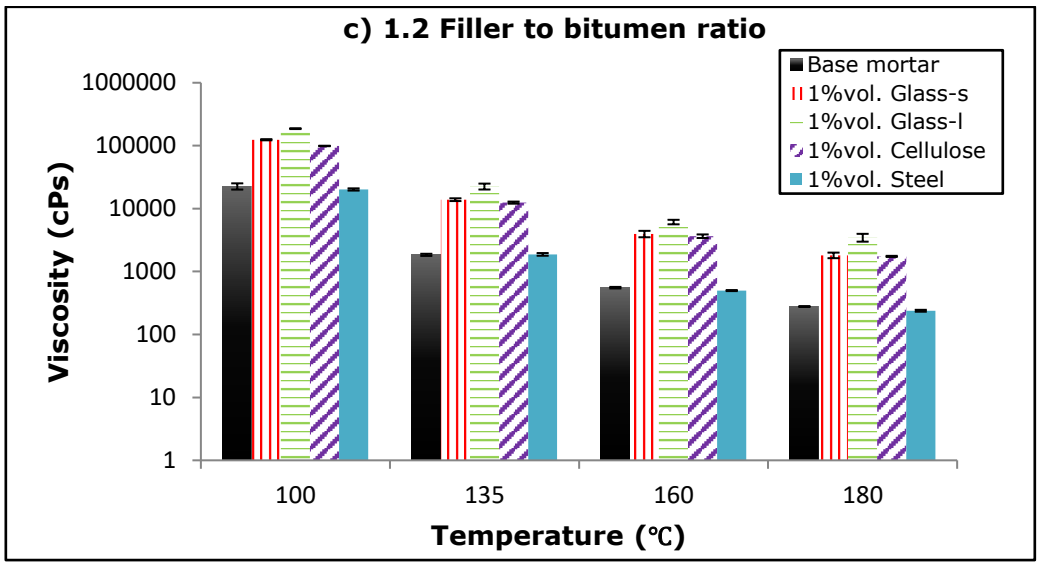


Figure 5-4 (a, b and c) Viscosity for base mortar and 1.0% mortar-fibre

5.3.3 Complex modulus master curve of base and modified mortar

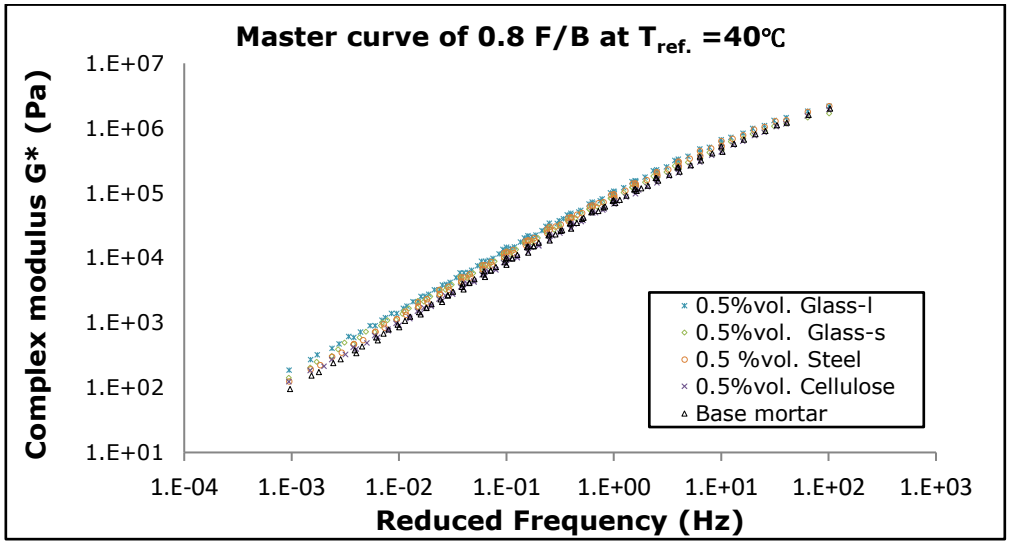
Figure 5-5 shows the complex modulus master curves for the base mortar and mortar containing different types of fibres. It is clear that the higher filler to bitumen ratio exhibited the highest complex modulus at all test temperatures and frequencies due to the influence of the filler (Liao, 2007). The values of complex modulus for mortar containing a different type of fibres of 0.5% by bitumen volume were slightly higher than that of base mortar in the whole range of frequencies and temperatures.

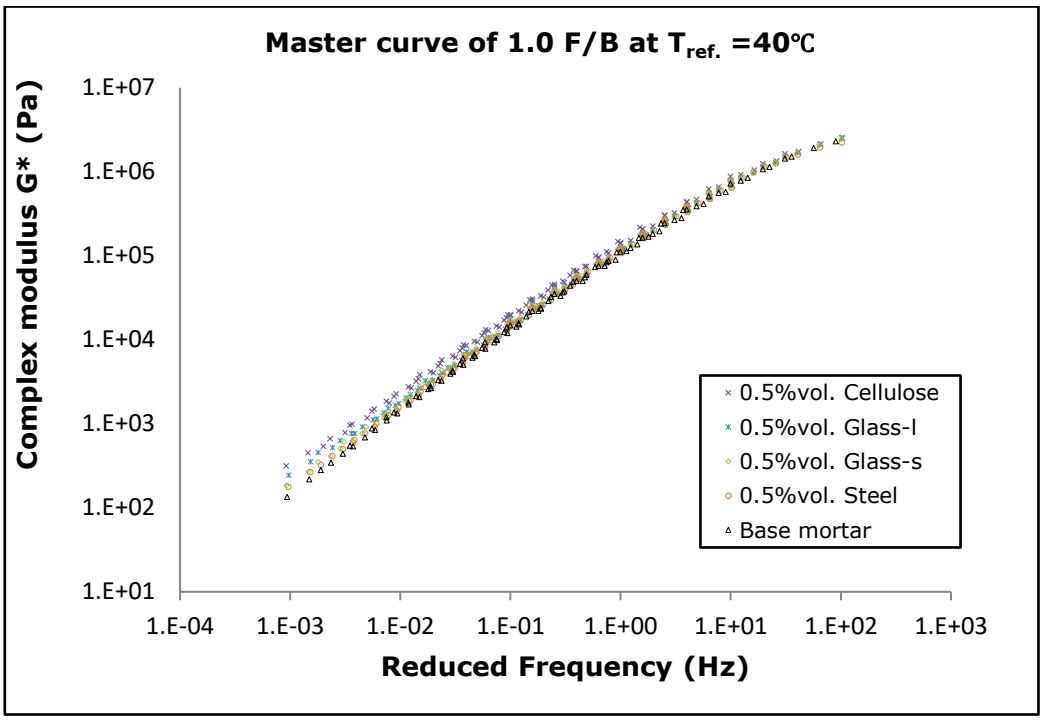
The master curves showed a marked effect of fibres on complex modulus for the 1.0% and 2.0% fibre at low frequencies and high temperatures (50-70℃) as shown in Figure 5-6 and Figure 5-7. The complex modulus master curves exhibited slightly different behavioural trends between base and fibre modified mortars. For the fibre modified mortars, there were a significant increase in G* at low frequencies and high temperatures where the fibre network was particularly dominant with a slight plateau being formed especially at the high fibre content. It seems possible that these results were due to the stiffness of base mortar being low enough to allow the continuous network of the fibre to affect the rheological properties of the modified mortars. While, at high frequencies and low temperatures, the high stiffness of the base mortar controls the stiffness and the differences between base and modified mortar were not as noticeable. However, the high fibre contents may have helped to entangle with each other to form a continuous network. This network stabilises the composite by absorption/adsorption, swelling or adhesion effects (Wu et al., 2014).

At the 0.8 and 1.2 filler to bitumen ratios, glass-l fibre has the highest value followed by cellulose then steel and glass-s, at low frequencies and high temperatures for 1.0 and 2.0% addition of fibres. At 1.0 filler to bitumen ratio the increase in complex modulus found in this order (steel, glass-l, glass-s and cellulose)

at low frequencies and high temperatures for 2.0% addition of fibre. Steel fibre showed the highest complex modulus among all fibre types and all filler to bitumen ratios at low temperatures. The reason for this behaviour might be due to the high modulus value of steel fibre controlling the increased stiffness of base mortar. The highest increase in complex modulus for 2.0% addition of glass-l, glass-s and steel fibre at low frequencies and high temperatures was found at 1.0 filler to bitumen ratio, while for cellulose fibre was found at 0.8 filler to bitumen ratio.

These findings imply a significant improvement in the resistance of asphalt mortar to deformation, especially at high temperatures. The reason for this could be due to the stiffening effect of fibres and its ability to resist repeatedly applied impact loading. In addition, fibres can entangle with each other to form networks to stabilise composite component by absorption/adsorption, reinforcing and adhesion effect of fibres to bitumen and filler (Wu et al., 2014), (see Figure 5-1). At the same time, the stiffness of base mortar became low enough at these temperatures to allow the fibre reinforcement to dominate the rheological behaviour of base mortar. Moreover, the absorption/adsorption of bitumen by fibres led to increase the viscosity and the interfacial adhesion between bitumen and fibres or filler (Wu et al., 2015) also see section 6.4.4. However, the inconsistency in the test results ranking may be due to the irregularities in the DSR test samples caused by fibre.





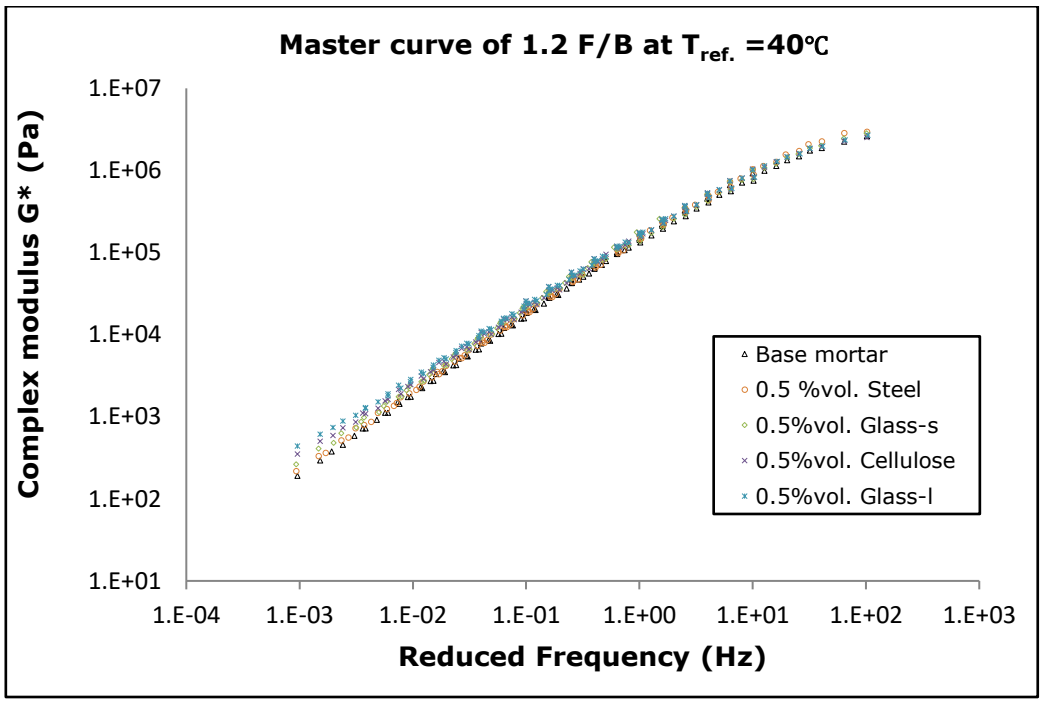
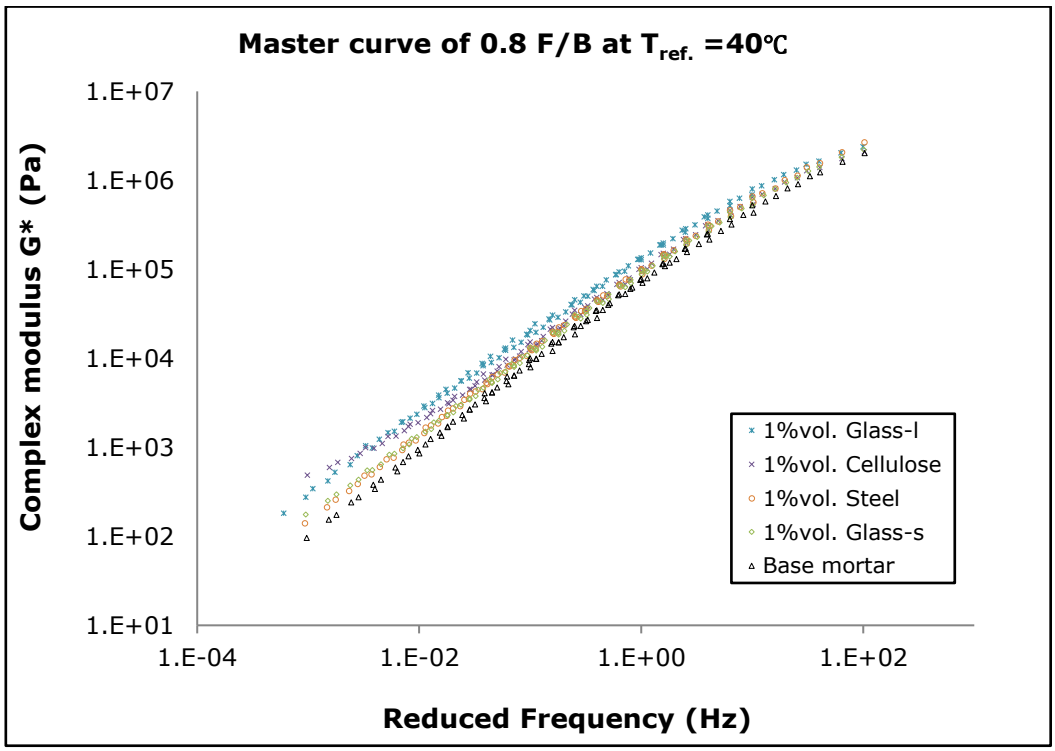
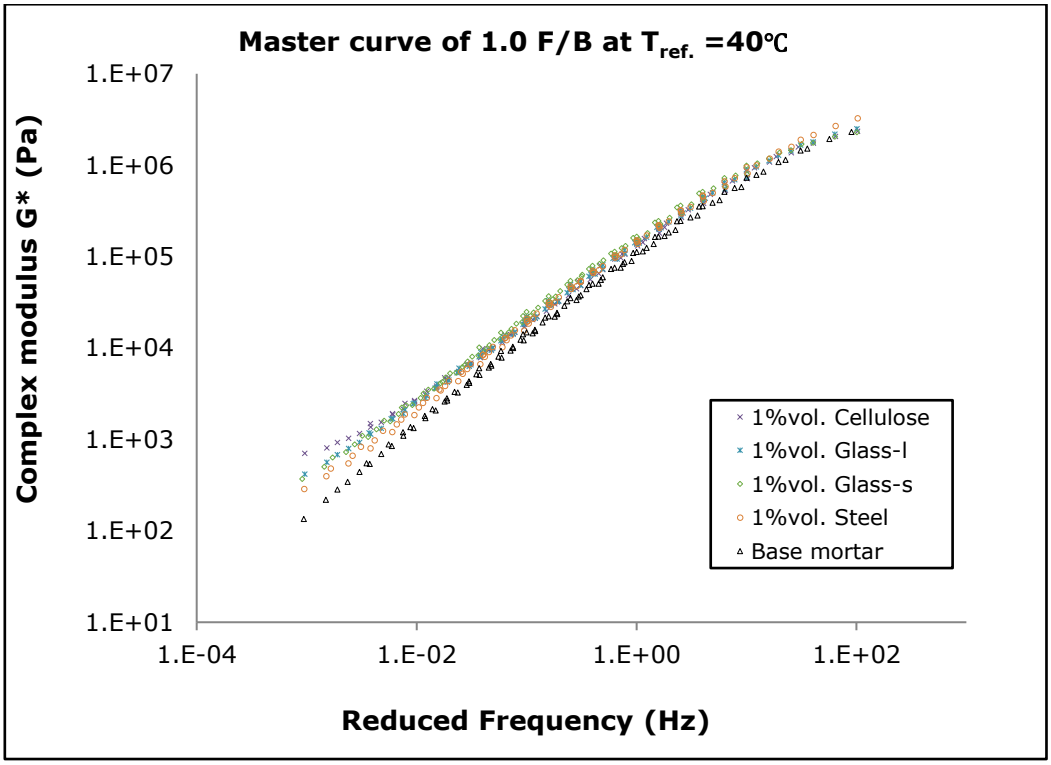


Figure 5-5 Complex modulus master curves for base mortar and 0.5% fibre modified mortar


Master curve of 0.8 F/B at T ref. =40℃
Complex modulus G* (Pa)
1.E+07
1.E+06
1.E+05
1.E+04
1.E+03
1.E+02
1.E+01
1.E-04
1.E-02
1.E+00
1.E+02
Reduced Frequency (Hz)
1%vol. Glass-l
1%vol. Cellulose
1%vol. Steel
1%vol. Glass-s
Base mortar


Master curve of 1.0 F/B at T ref. =40℃
Complex modulus G* (Pa)
1.E+07
1.E+06
1.E+05
1.E+04
1.E+03
1.E+02
1.E+01
1.E-04
1.E-02
1.E+00
1.E+02
Reduced Frequency (Hz)
1%vol. Cellulose
1%vol. Glass-l
1%vol. Glass-s
1%vol. Steel
Base mortar

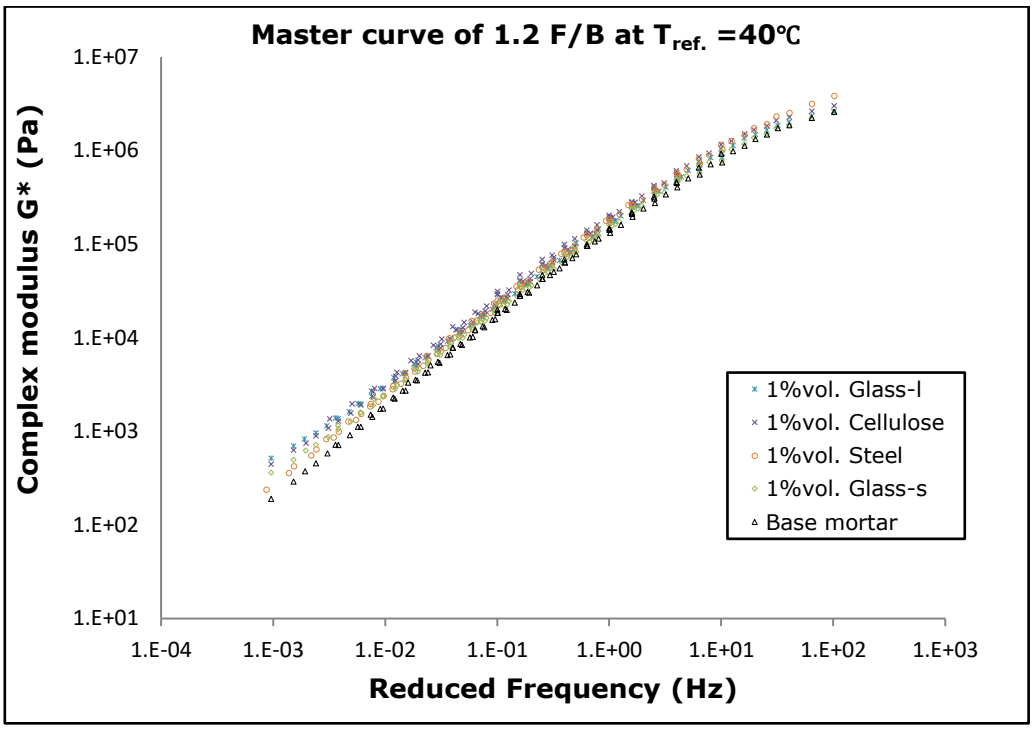
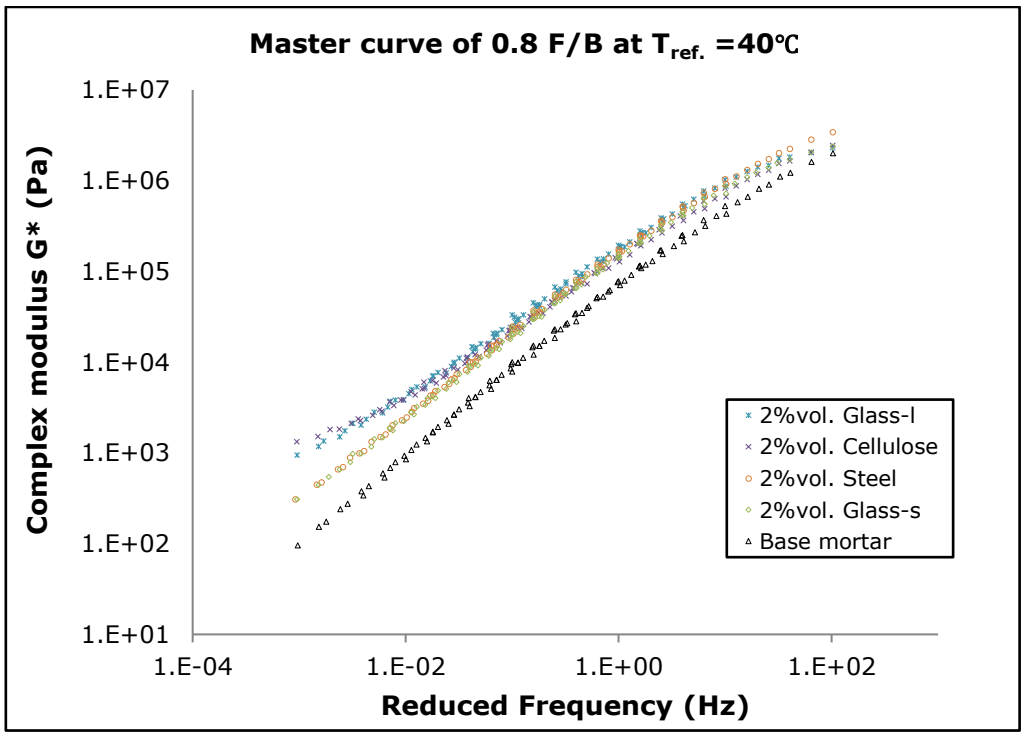
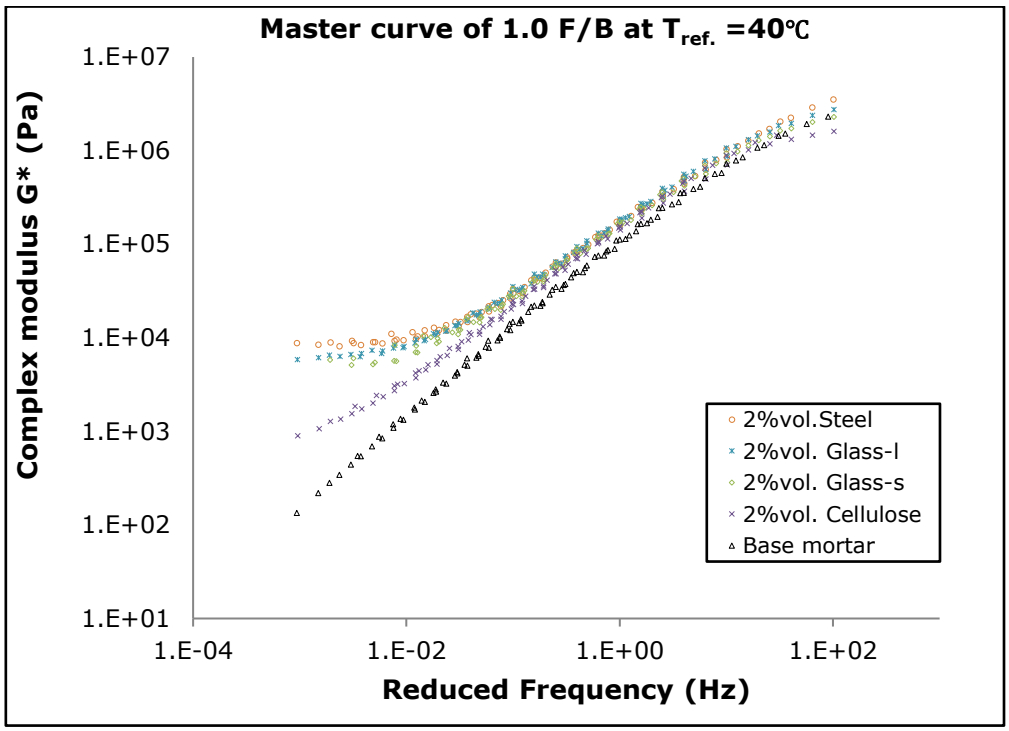


Figure 5-6 Complex modulus master curves for base mortar and 1.0% fibre modified mortar





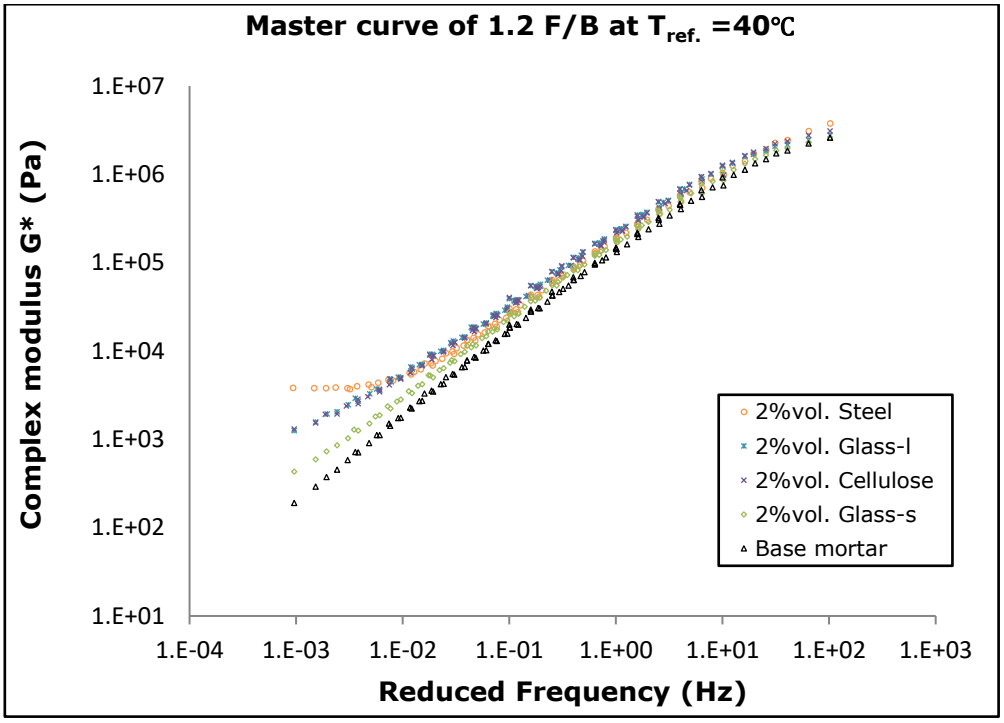
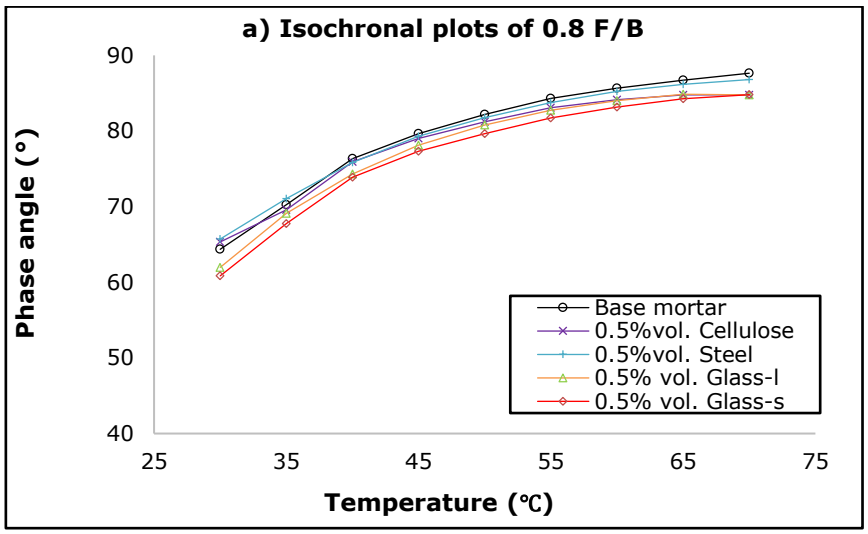
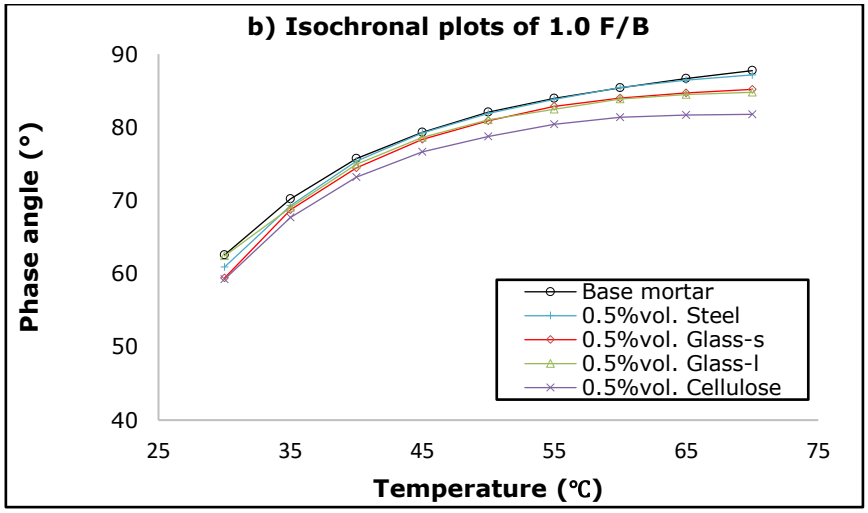


Figure 5-7 Complex modulus master curves for base mortar and 2.0% fibre modified mortar

5.3.4 Phase angle isochronal plots

Phase angle δ isochrones at 1.58 Hz for the base and fibre modified mortars are shown in Figure 5-8, Figure 5-9 and Figure 5-10. The phase angle isochrones showed a noticeable decrease in the phase angles (higher elastic response) of the highly modified mortars compared to the base mortar. It was noticeable that the considerable difference in the extent of the 1.0% modification for the δ values was found at high temperatures (> 50℃) particularly for 0.8 and 1.0 filler to bitumen ratio. While the phase angle of the base mortar approached 90° (viscous behaviour) with the increase of temperatures, the fibres significantly improve the elastic response. Also, there was a considerable difference in the extent of the 2.0% modification for the δ values, particularly at high temperatures (> 50℃) for 0.8, 1.0 and 1.2 filler to bitumen ratio. It seems possible that these results were due to the viscosity of base mortar becoming low enough to permit the continuous network of the fibre to affect the rheological properties of the modified mortars (Goodrich, 1991) (see Figure 5-1). This also means that the addition of fibre may have changed the chemical composition of the binder by absorption/adsorption fraction. This was investigated in the following chapter, by examining binder drainage for each fibre mastic type then measured the asphaltene content in the drained binder, in addition to investigating the complex modulus and phase angle of the drained binder by using the dynamic shear rheometer test.





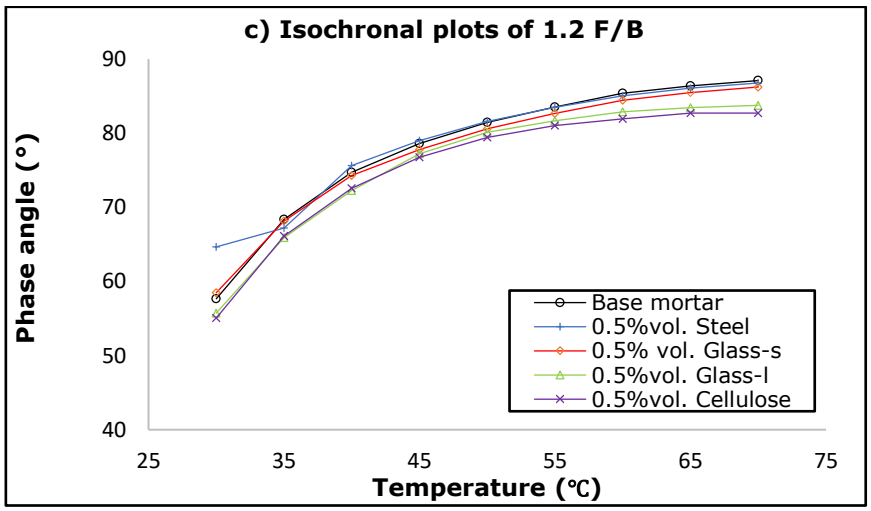
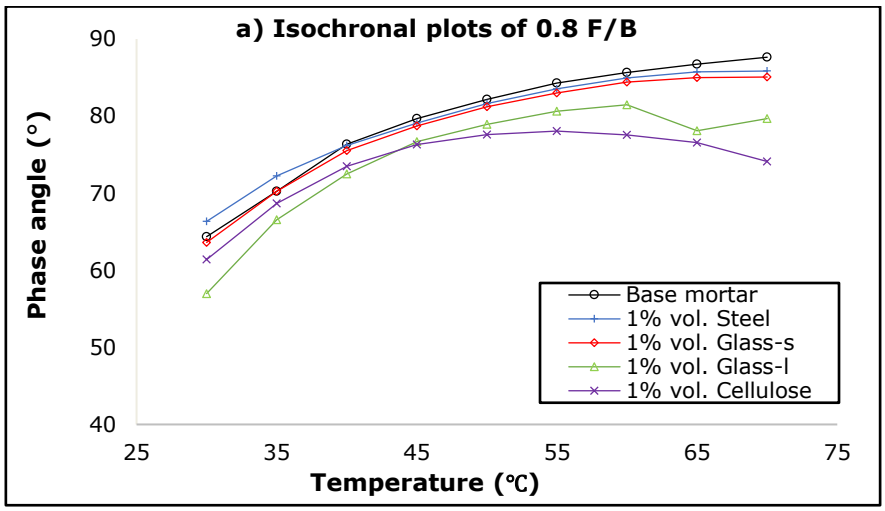
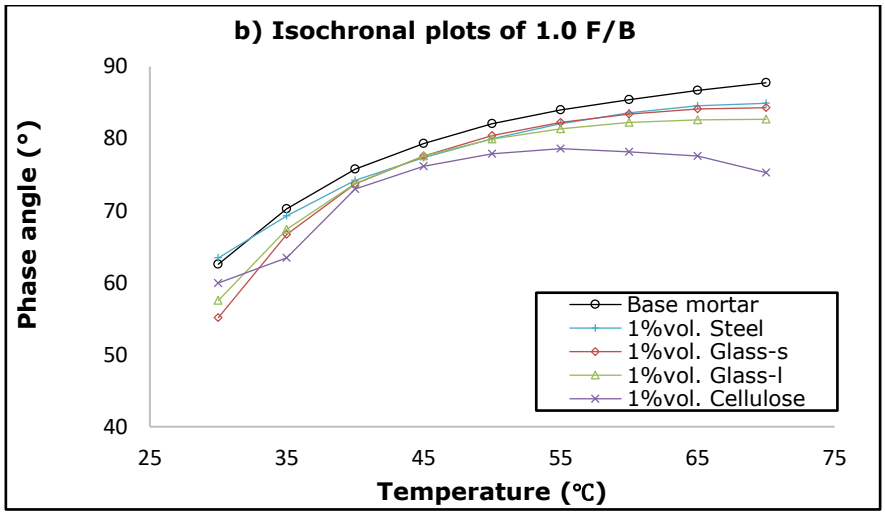


Figure 5-8 (a, b and c) Isochronal plots of phase angle at 1.58 Hz for the base and 0.5% fibre modified mortars





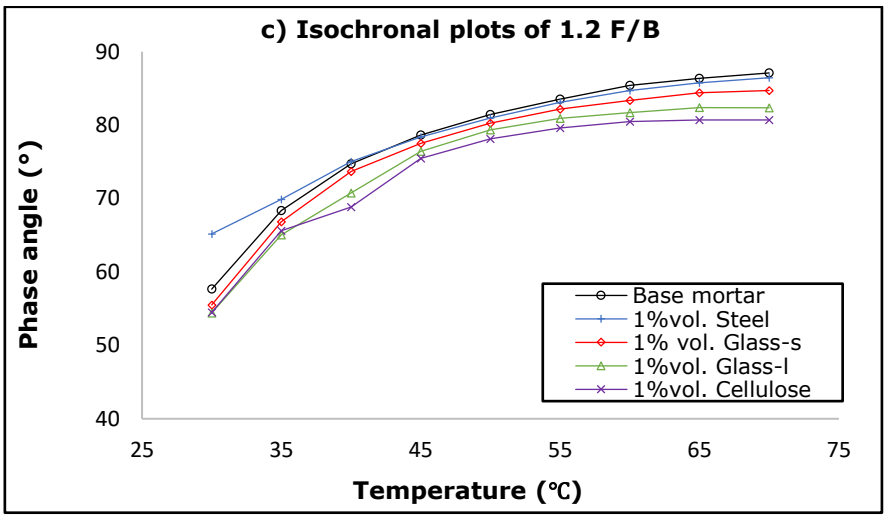
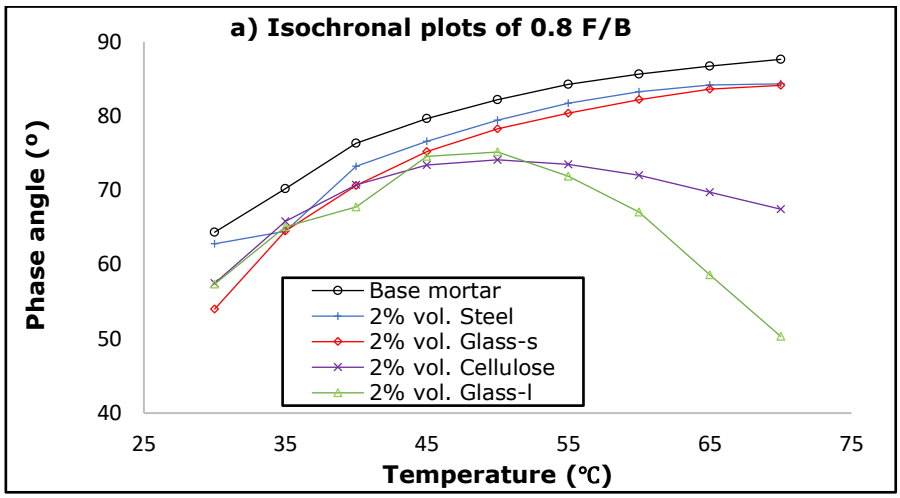
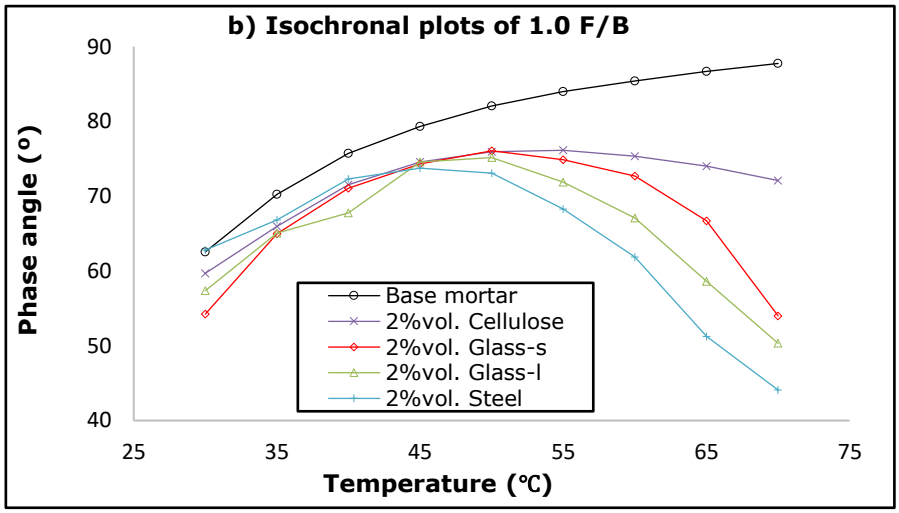


Figure 5-9 (a, b and c) Isochronal plots of phase angle at 1.58 Hz for the base and 1.0% fibre modified mortars





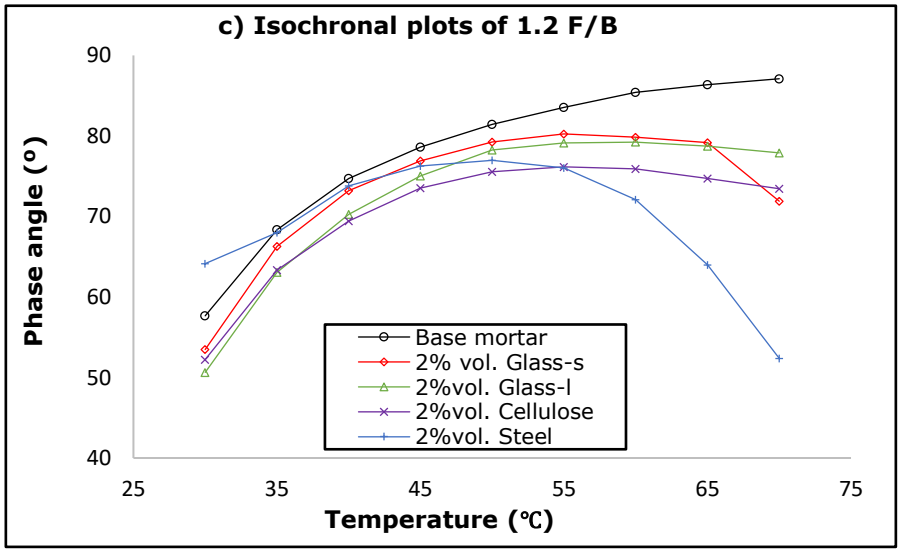


Figure 5-10 (a, b and c) Isochronal plots of phase angle at 1.58 Hz for the base and 2.0% fibre modified mortars

5.3.5 Phase angle master curve

Phase angle is an important property of viscoelastic materials because it indicates whether viscous or elastic behaviour is more dominant. Phase angle of 0° exhibits pure elastic behaviour, while the 90° phase angle shows pure viscous behaviour (Mezger, 2011). Figure 5-11 shows that the phase angle master curves for the 0.5% fibre content displays an effect mainly for glass-l and cellulose fibre modified asphalt mortars and only on high temperatures and low frequencies. The effect of 1.0% and 2.0% addition of fibres on the phase angle master curves of asphalt mortar are shown in Figure 5-12 and Figure 5-13.

The phase angle master curves for 2.0% fibre addition exhibited a significant reduction in phase angle. The phase angles of the modified mortars were significantly lower than the phase angle of base mortar within the range of temperatures (45-70℃) and low frequencies, exhibiting a higher elastic behaviour than viscous behaviour. However, at the range of low temperatures (< 45℃) and higher frequencies, where the increased stiffness of the base mortar dominated the influence of the fibre network, the differences between the base and modified mortar were not as marked.

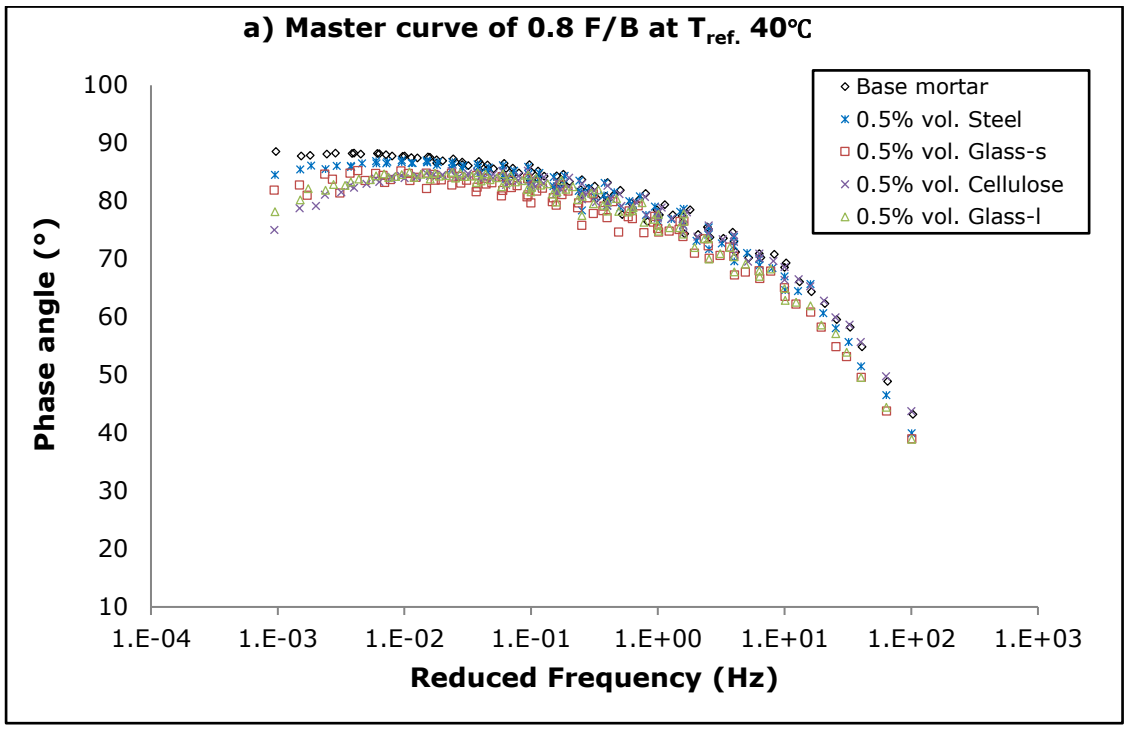
The most interesting finding was that the phase angle master curves for highly modified mortars exhibited different behaviour from the base mortar with the presence of plateau zones at the middle. These results match those observed in chapter four of this study, which evaluated the effect of fibre on rheological properties of mastic. Previous studies suggested that the plateau zone gives an indication of the existence of elastic networks of modification in polymer modified bitumen , in addition the differences in the phase angle master curves may have related to differences in the molecular interaction (adhesion, swelling and absorption/adsorption) between the modifier and bitumen or filler (Asgharzadeh et al., 2015, Airey, 2003). Moreover, simple rheological behaviour represented by a

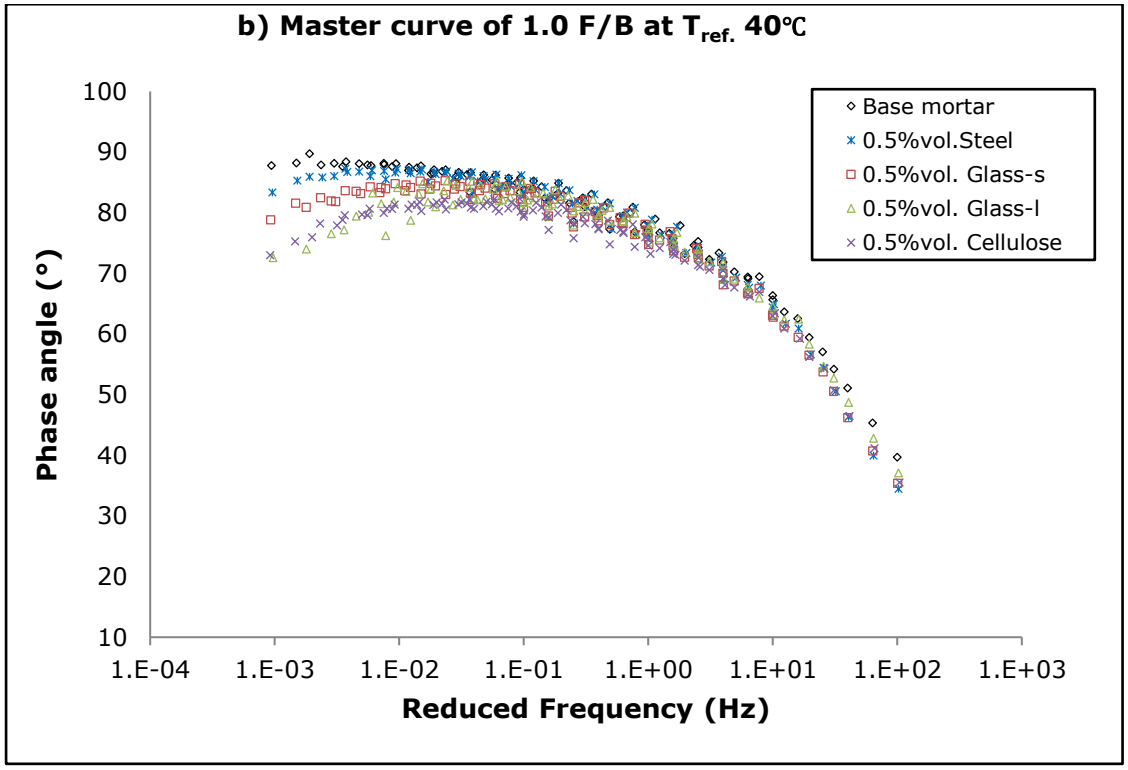
smooth, continuous master curve as usually appeared for base bitumen (Airey and Rahimzadeh, 2004). These findings may help us to understand how fibres may have affected the rheological properties of asphalt mortar when temperature and loading time change.

It should be noted that at 1.0 and 1.2 filler to bitumen ratio steel fibre showed the largest decrease in the phase angle of highly modified mortar (2.0%) among all fibre types within the range of high temperatures and low frequencies, while in the range of low temperatures (30-40℃) and high frequencies an opposite trend was observed.

The highest decrease in phase angle for 2.0% addition of glass-l, glass-s and steel fibre was found at 1.0 filler to bitumen ratio while 0.8 filler to bitumen ratio showed the highest decrease for cellulose fibre. According to the results of complex modulus and phase angle 1.0 filler to bitumen ratio is recommended for glass-l, glass-s and steel fibres.

In general, a reduction in the phase angle values of fibre modified asphalt mortars implies that more deformation energy is stored in this rigid structure and the elastic behaviour becomes increasingly dominant. Therefore, adding fibres may significantly improve asphalt mortar resistance to deformation (Yi-qiu et al., 2010, Ab-Wahab, 1993). The predominant effect is due to the composition change due to cellulose or the mechanical effect of ling fibres. At high fibres content, the mechanical effect predominates for all fibres. This is particularly the case at high filler to bitumen ratio where the high level of fibres and fillers contains to have a more significant mechanical effect.


a) Master curve of 0.8 F/B at T ref. 40℃
Phase angle (°)
100
90
80
70
60
50
40
30
20
10
1.E-04
1.E-03
1.E-02
1.E-01
1.E+00
1.E+01
1.E+02
1.E+03
Reduced Frequency (Hz)
Base mortar
0.5% vol. Steel
0.5% vol. Glass-s
0.5% vol. Cellulose
0.5% vol. Glass-l


b) Master curve of 1.0 F/B at T ref. 40℃
Phase angle (°)
100
90
80
70
60
50
40
30
20
10
1.E-04
1.E-03
1.E-02
1.E-01
1.E+00
1.E+01
1.E+02
1.E+03
Reduced Frequency (Hz)
Base mortar
0.5%vol.Steel
0.5%vol. Glass-s
0.5%vol. Glass-l
0.5%vol. Cellulose

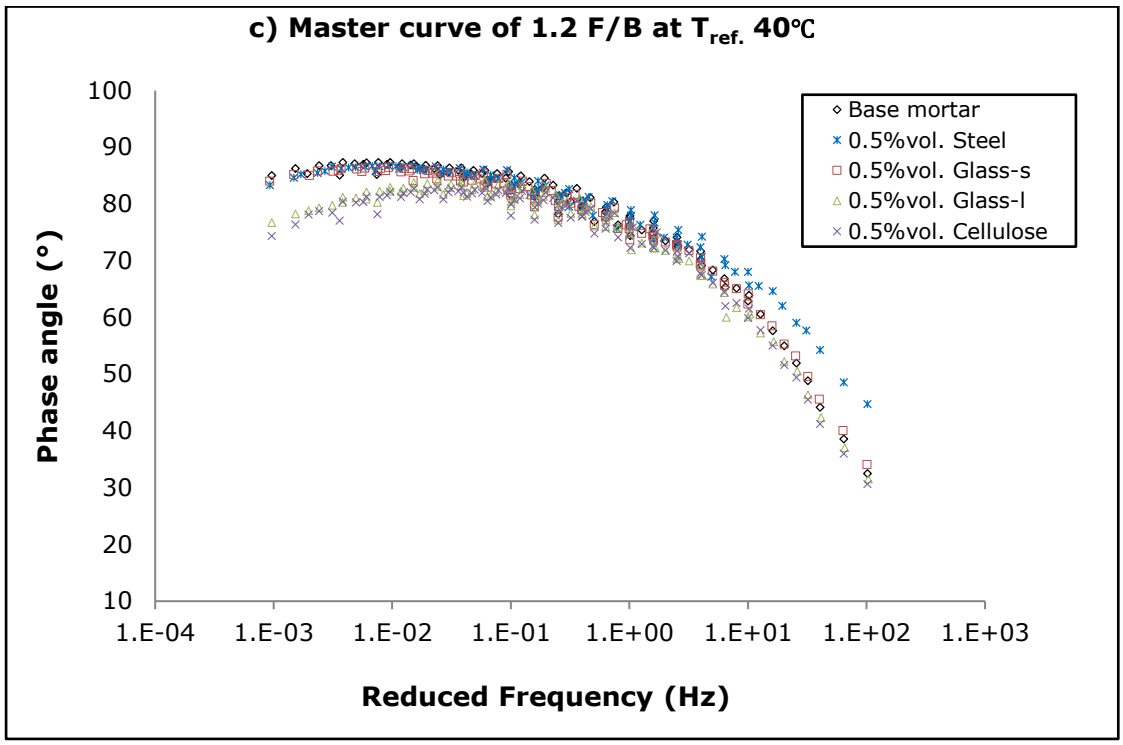
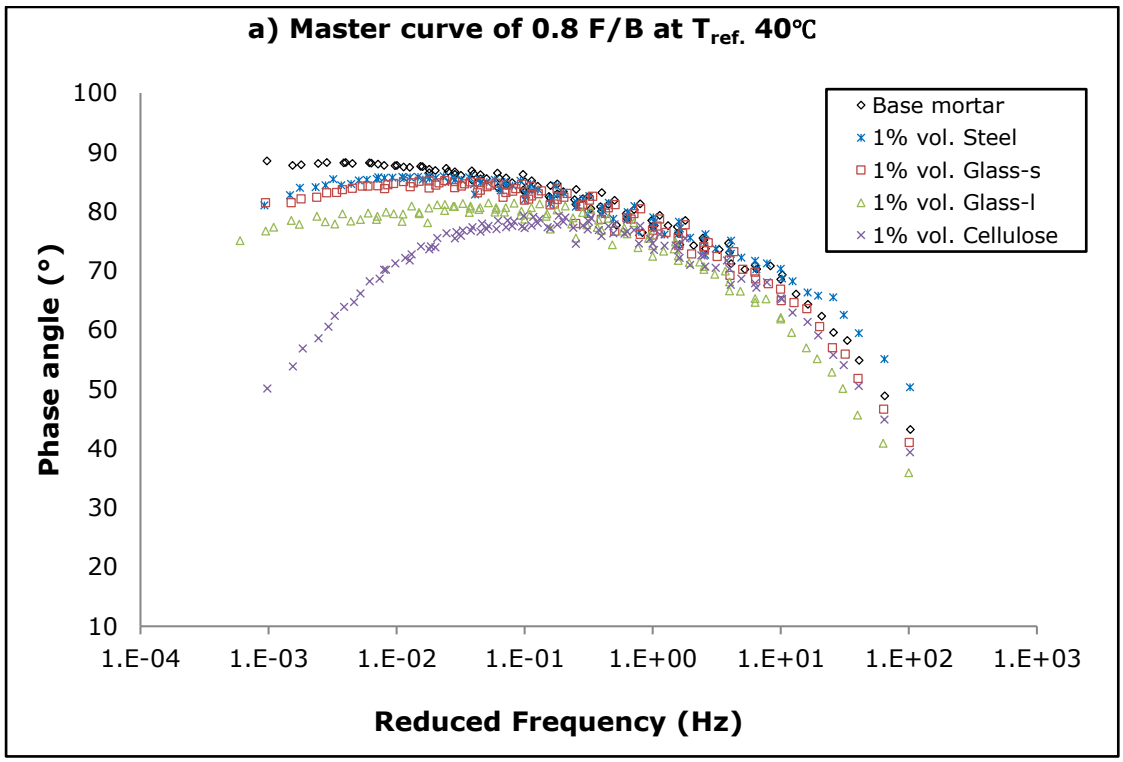
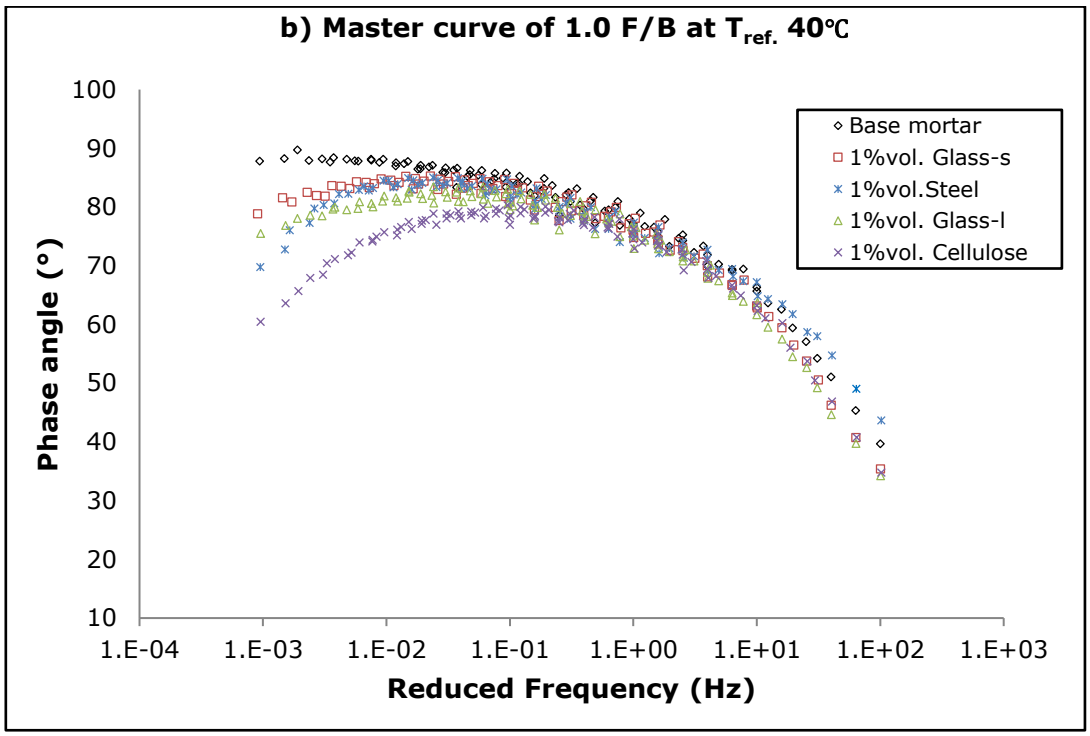


Figure 5-11 (a, b and c) Phase angle master curves for base mortar and 0.5% fibre modified mortar





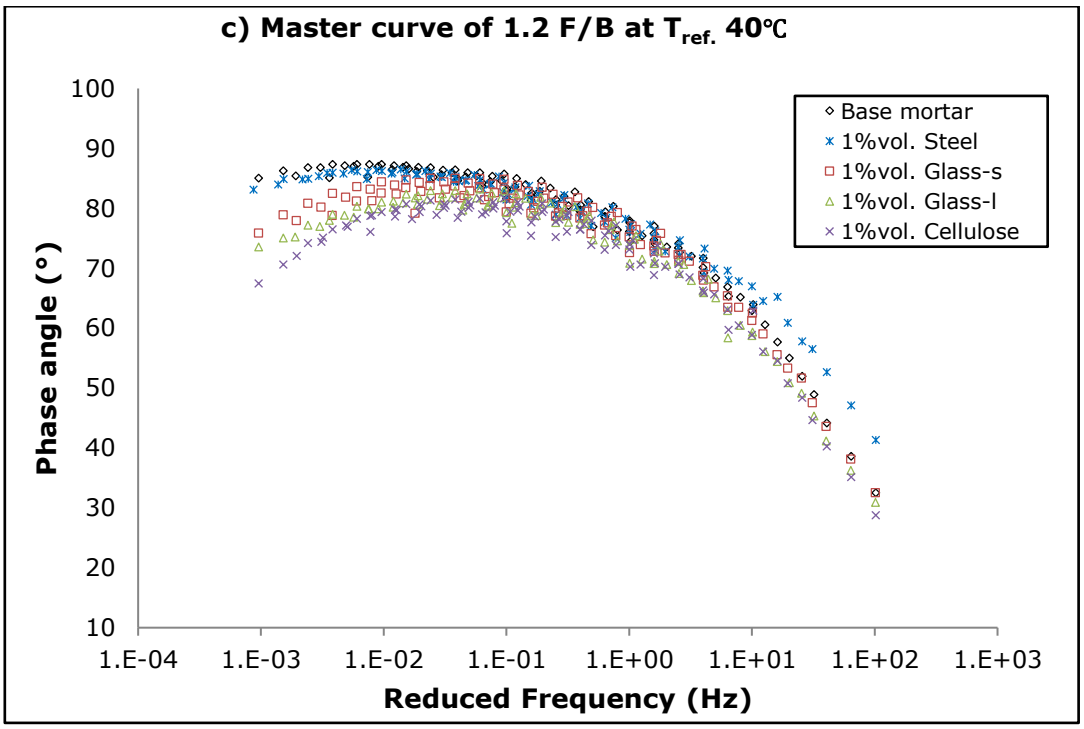
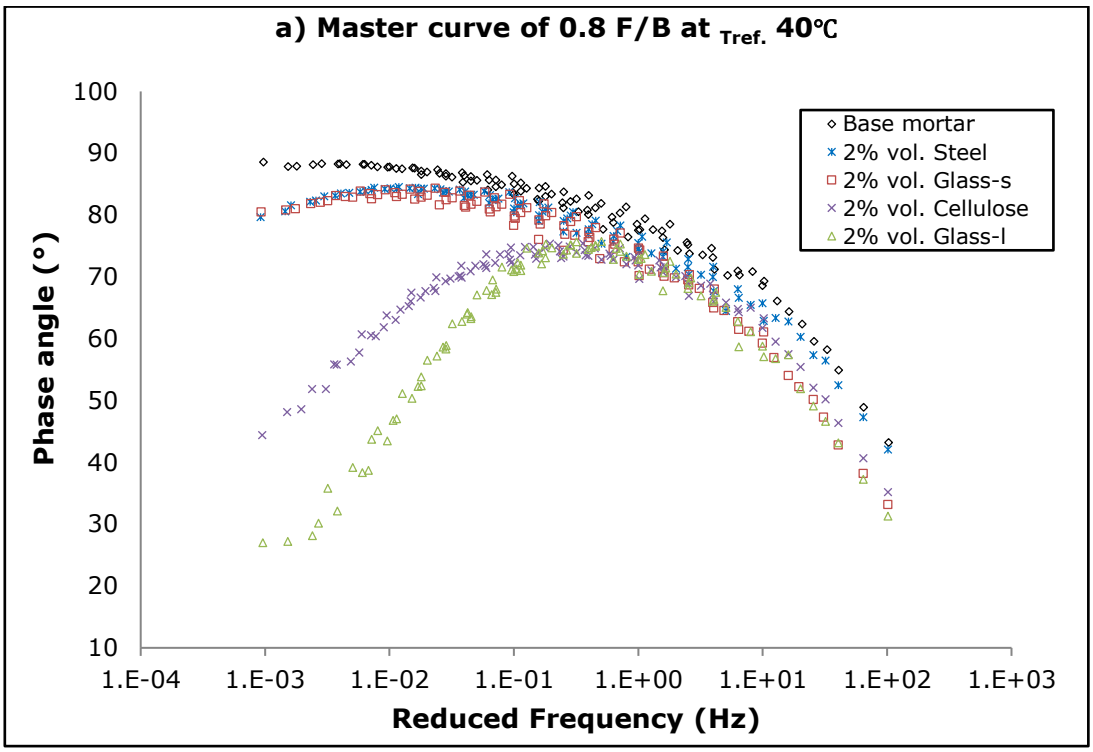
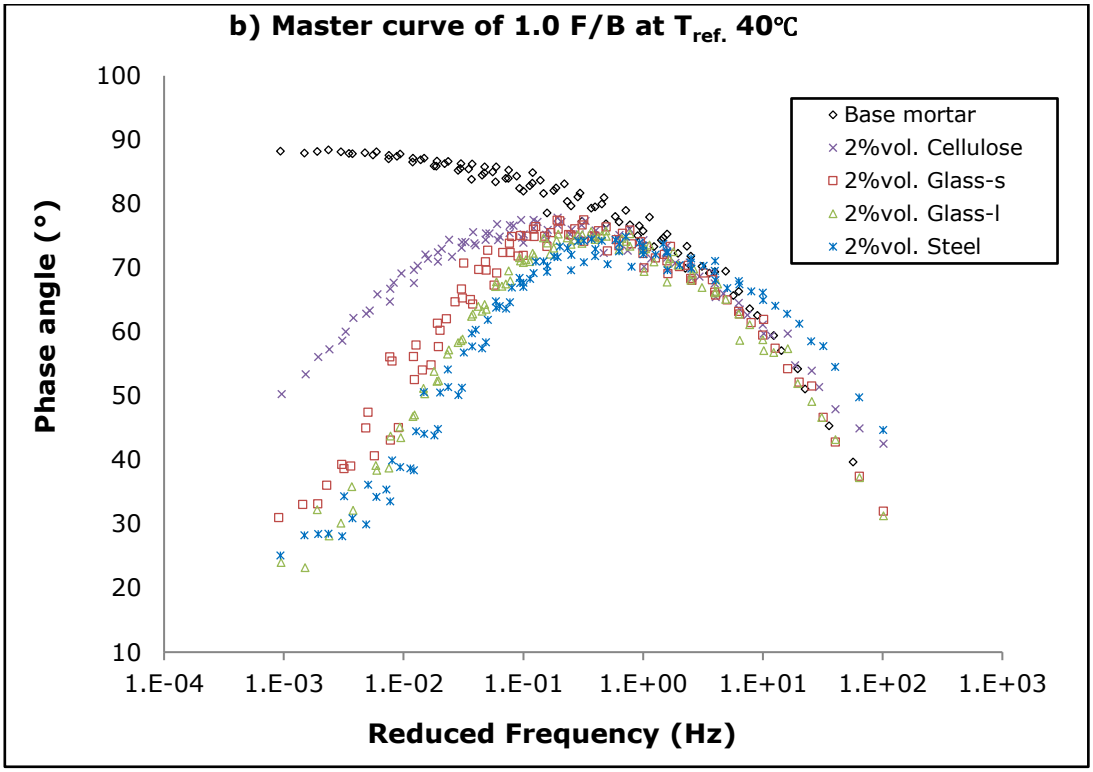


Figure 5-12 (a, b and c) Phase angle master curves for base mortar and 1.0% fibre modified mortar


a) Master curve of 0.8 F/B at Tref. 40℃
Phase angle (°)
100
90
80
70
60
50
40
30
20
10
1.E-04
1.E-03
1.E-02
1.E-01
1.E+00
1.E+01
1.E+02
1.E+03
Reduced Frequency (Hz)
Base mortar
2% vol. Steel
2% vol. Glass-s
2% vol. Cellulose
2% vol. Glass-l


b) Master curve of 1.0 F/B at Tref. 40℃
Phase angle (°)
100
90
80
70
60
50
40
30
20
10
1.E-04
1.E-03
1.E-02
1.E-01
1.E+00
1.E+01
1.E+02
1.E+03
Reduced Frequency (Hz)
Base mortar
2%vol. Cellulose
2%vol. Glass-s
2%vol. Glass-l
2%vol. Steel

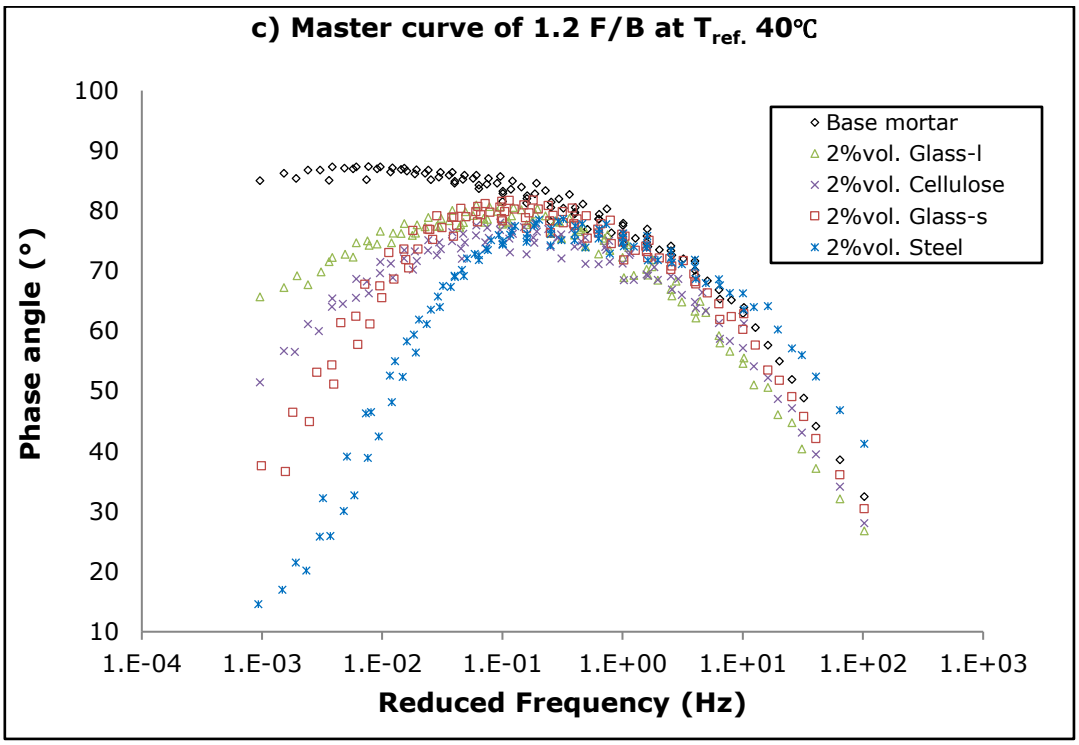


Figure 5-13 (a, b and c) Phase angle master curves for base mortar and 2.0% fibre modified mortar

5.3.6 Rutting parameter

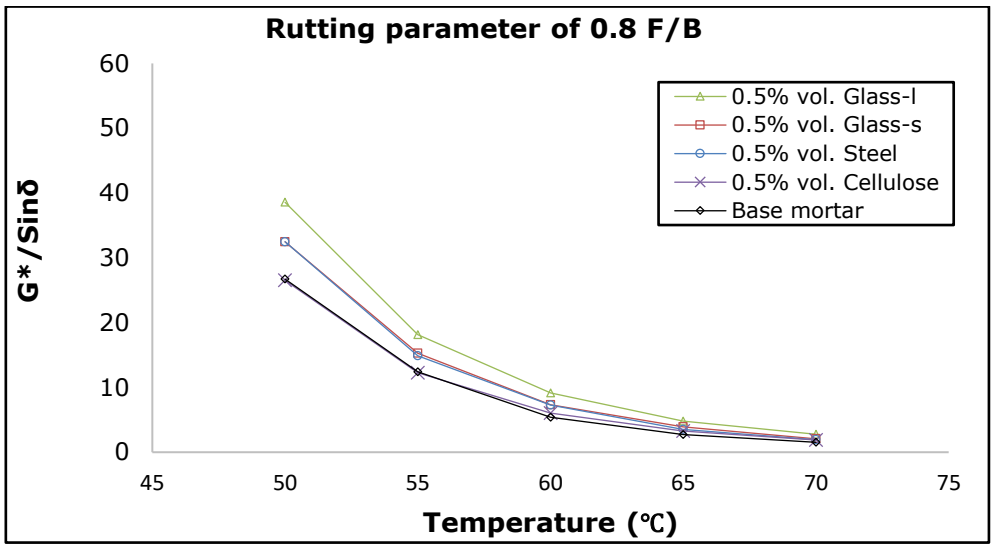
The rutting parameter G*/Sinδ was used to evaluate the effect of different fibre types on rutting resistance of asphalt mortar according to the SHRP specification (Wu et al., 2015, Al-Mansob et al., 2014). It is well known that higher G*/Sinδ values indicate higher permanent deformation resistance of asphalt mortar. The rutting factor of three filler to bitumen ratios with four fibre types at different testing temperatures was evaluated in this investigation. The rutting parameter increased with the addition of fibre, implying a significant improvement in permanent deformation resistance at moderate and high temperatures, as shown in Figures 5.14-5.16. The 2.0% of glass-l fibre for all filler to bitumen ratios showed the highest increase in rutting parameter followed by cellulose for 0.8 and 1.2 filler to bitumen ratio, followed by steel fibre for 1.0 filler to bitumen ratio. This result may be explained by the fact that glass-l fibre could tangle with each other to form

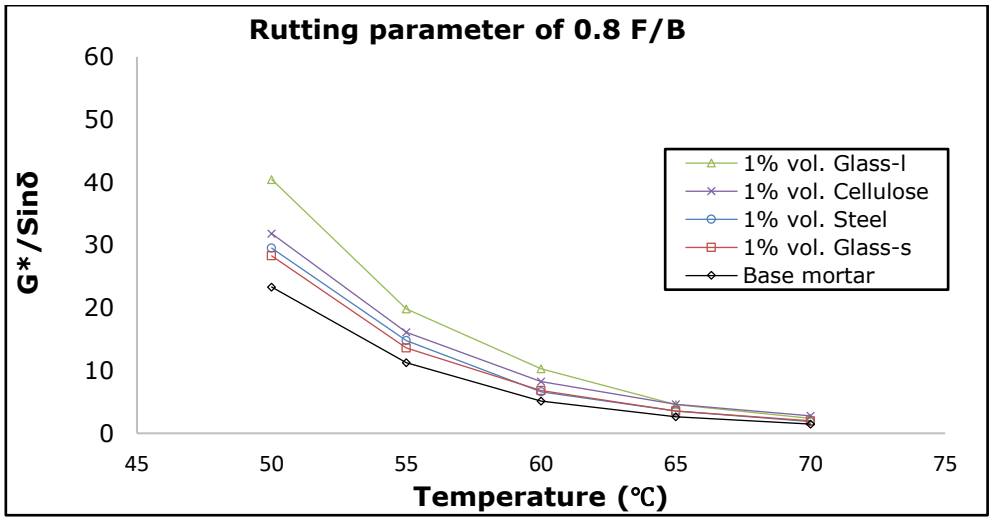
a network throughout the small composite sample more effectively than steel fibre due to glass-l fibre longer and thinner than steel fibre. This network held and reinforced the matrix components and increased its ability to withstand repeated applied, impact loading (see Figure 5-1) (Wu et al., 2014). Moreover, SEM microphotographs showed cohesive failure in DENT specimens, which means high adhesion between glass-l fibres and bitumen or filler (see Figure 5-1).

It is interesting to note that glass-l fibres behaviour in asphalt mortar was different from the behaviour of glass-l fibres when added to bitumen mastic in this study. The glass-l fibres showed higher rutting parameters than cellulose fibres when added to asphalt mortar, while cellulose fibres showed the highest increase in rutting parameters when added to bitumen mastic. Asphalt mortar is a multi-phase system affected by a combination of both fibre and filler.

The rutting parameter decreased with the increase in temperature for base and fibre modified asphalt mortar. All fibre types indicated an improvement in permanent deformation resistance of asphalt mortar.

According to rheological parameter results 1.0 filler to bitumen ratio and 2.0% addition recommended for glass and steel fibres and 0.8 filler to bitumen ratio and 2.0% addition for cellulose fibre.





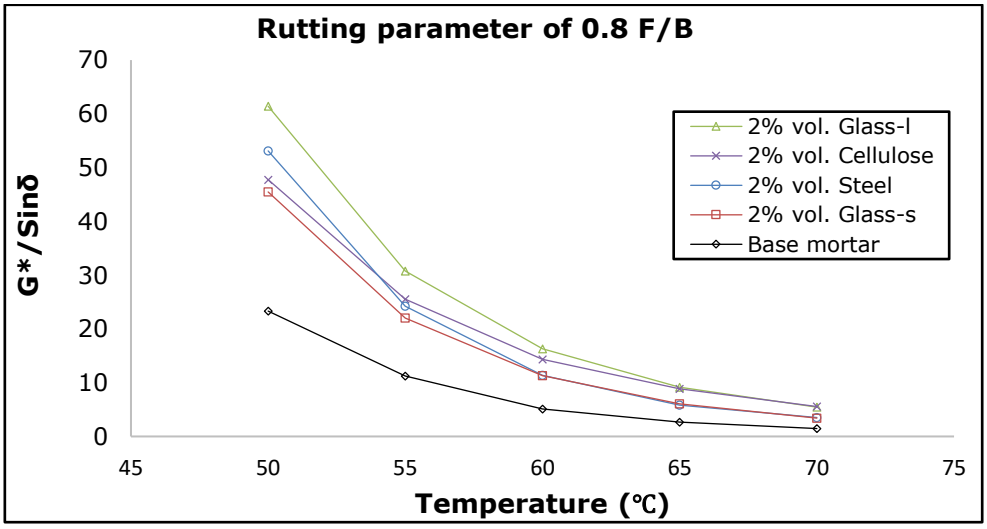
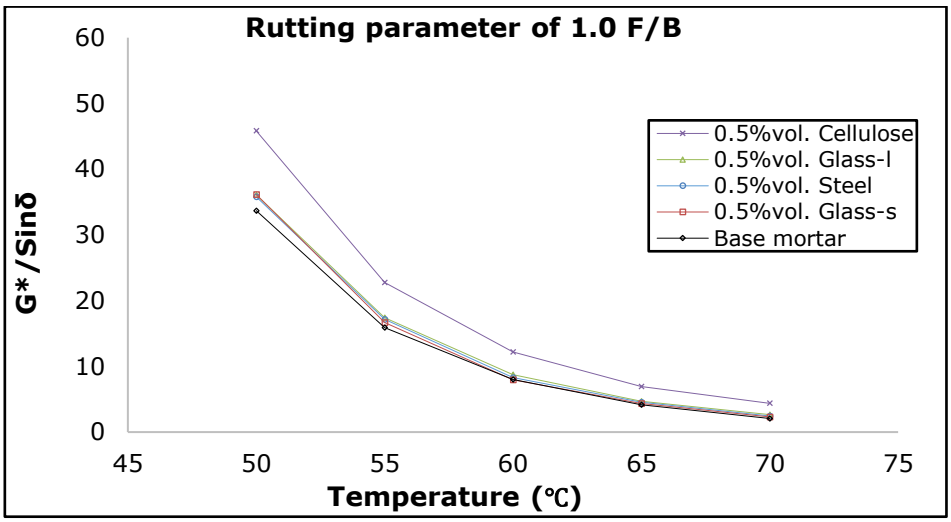
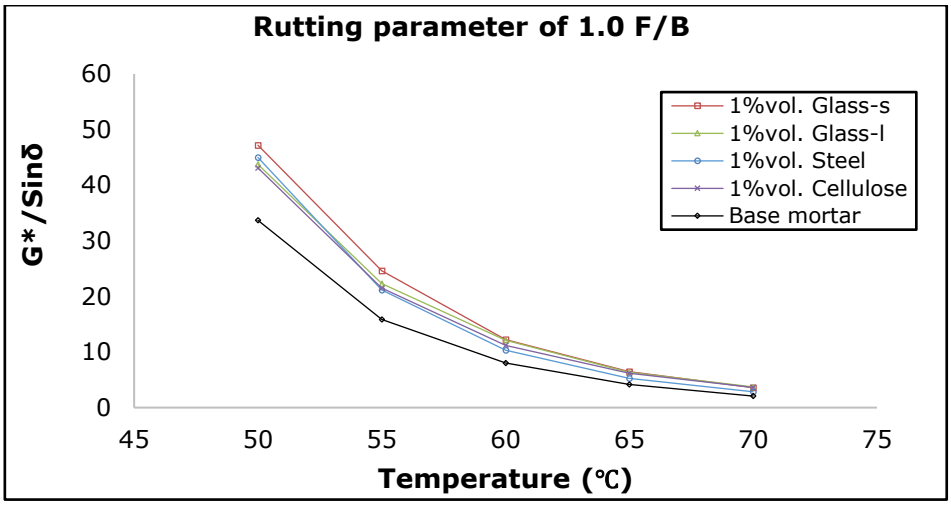


Figure 5-14 Rutting parameter for base mortar and fibre modified mortar





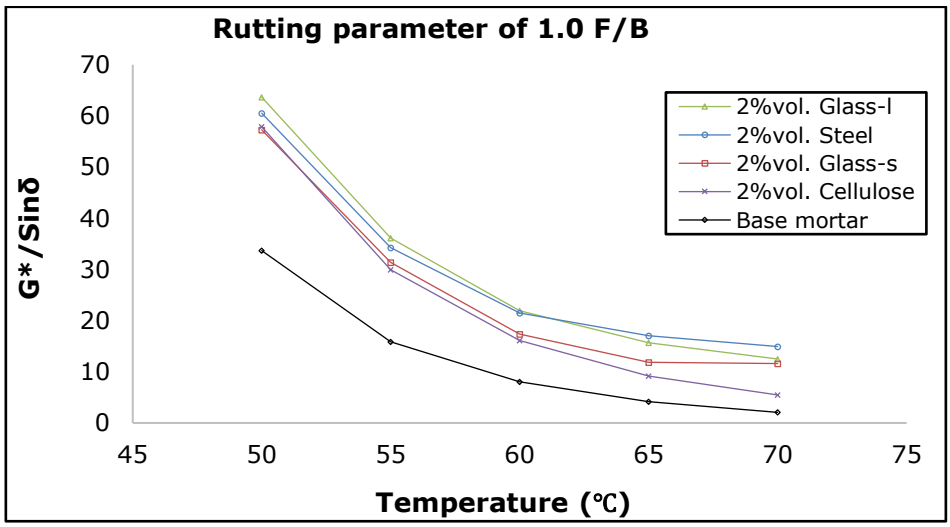
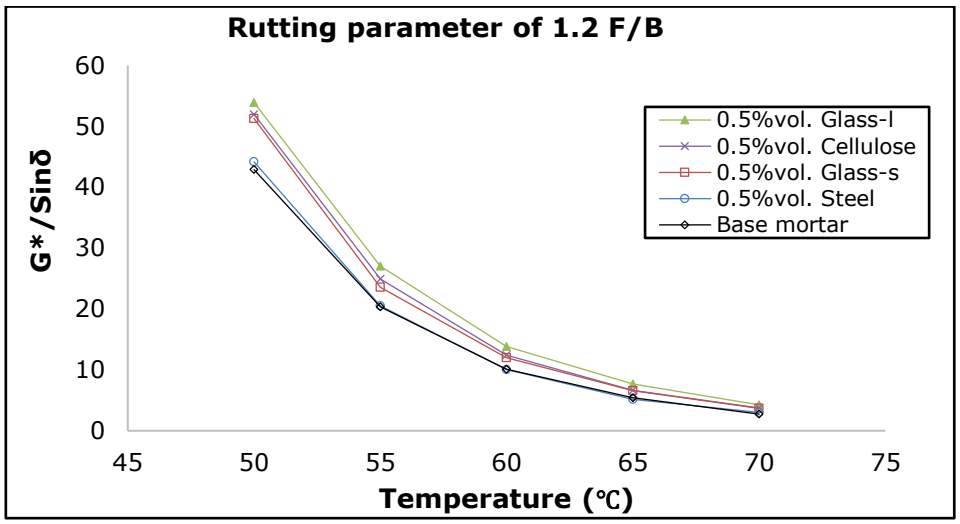
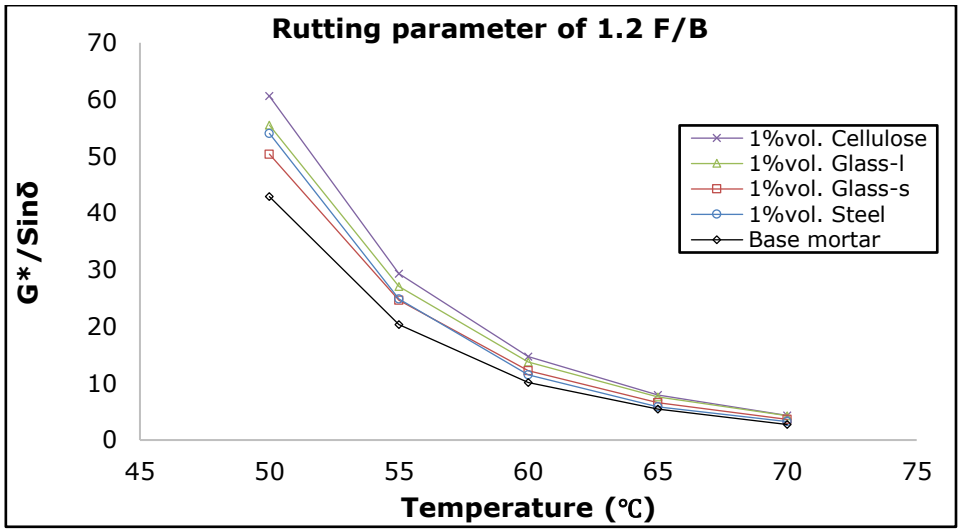


Figure 5-15 Rutting parameter for base mortar and fibre modified mortar





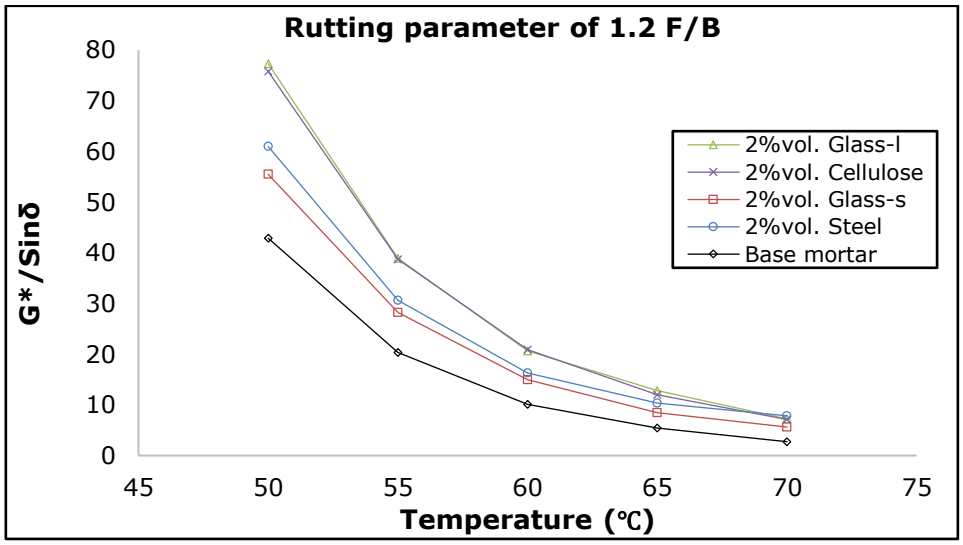


Figure 5-16 Rutting parameter for base mortar and fibre modified mortar

5.3.7 Double edge notch tension (DENT) test

A double edge notch tension test with 45° notch angle on both sides of the specimen and three different notch lengths was evaluated. The specimens were tested at 15℃, with a rate of displacement of 20 mm/min and the fracture energy of base and fibre modified asphalt mortars were measured, in order to predict fatigue performance. It should be noted that this test was done at a different rate of displacement due to the high stiffness of asphalt mortar compared to asphalt mastic. As a result, it is recommended to use a lower rate of displacement for stiffer materials. In most recent studies, the essential work of fracture method has been used to evaluate the fracture resistance of asphalt binders or mortars. This method developed by Cotterell and Reddel (1977) to estimate the fracture resistance by dividing the strain energy into the essential work of fracture (we) (which is the energy required to fracture or break the sample without plastic deformation away from the fracture zone) and the plastic work of fracture (wp) (which is the non-essential work dissipated during the deformation of a volume of asphalt around the fracture zone) (Cotterell and Reddel, 1977, Marasteanu, 2007).

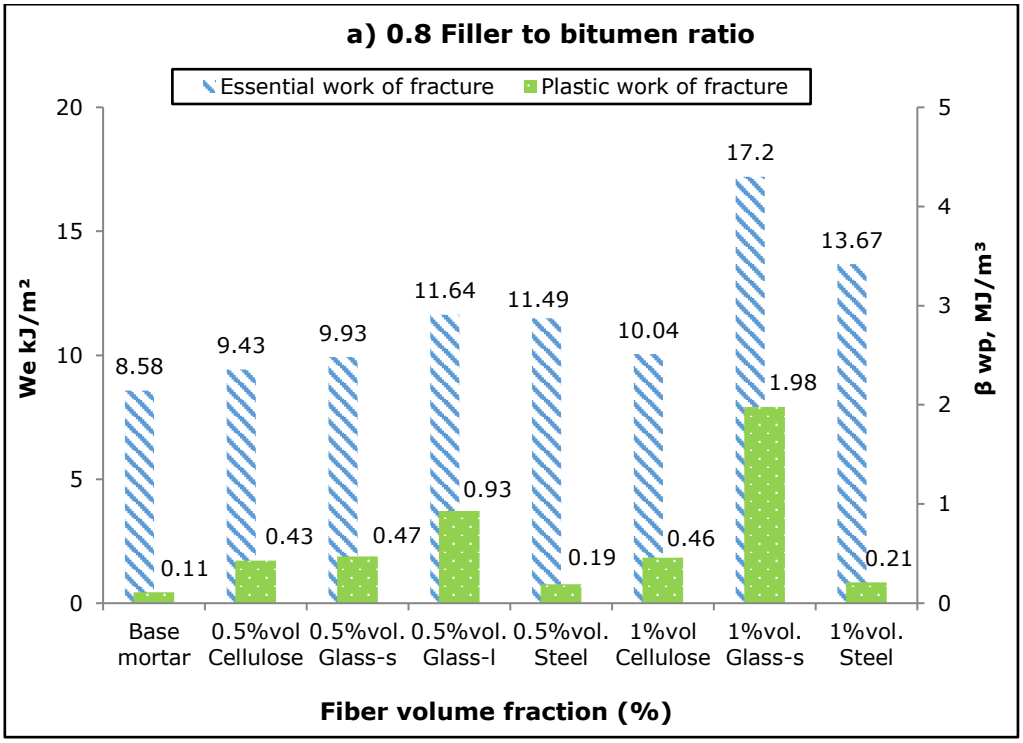
The results obtained from the analysis of the double edge notch tension test for three filler to bitumen ratios by weight (0.8, 1.0 and 1.2) and four fibre types are shown in Figure 5-17. There were marked differences in essential and plastic work of fracture between base mortar and 0.5% modified asphalt mortars by (cellulose, steel and glass-s) fibres. One interesting finding was only 0.5% asphalt mortar modified by glass-l fibres showed a significant effect in essential and plastic work of fracture indicating improvement in fatigue resistance of asphalt mortar (Marasteanu, 2007, Andriescu and Hesp, 2009). This result may be explained by the fact that glass-l fibres have high tensile strength and length, with small diameter and the sample thickness being smaller or similar to glass fibre length. This may help the glass fibre to distribute into the DENT test sample in such a way that the applied load is parallel to the direction of the fibres, thus the tensile force

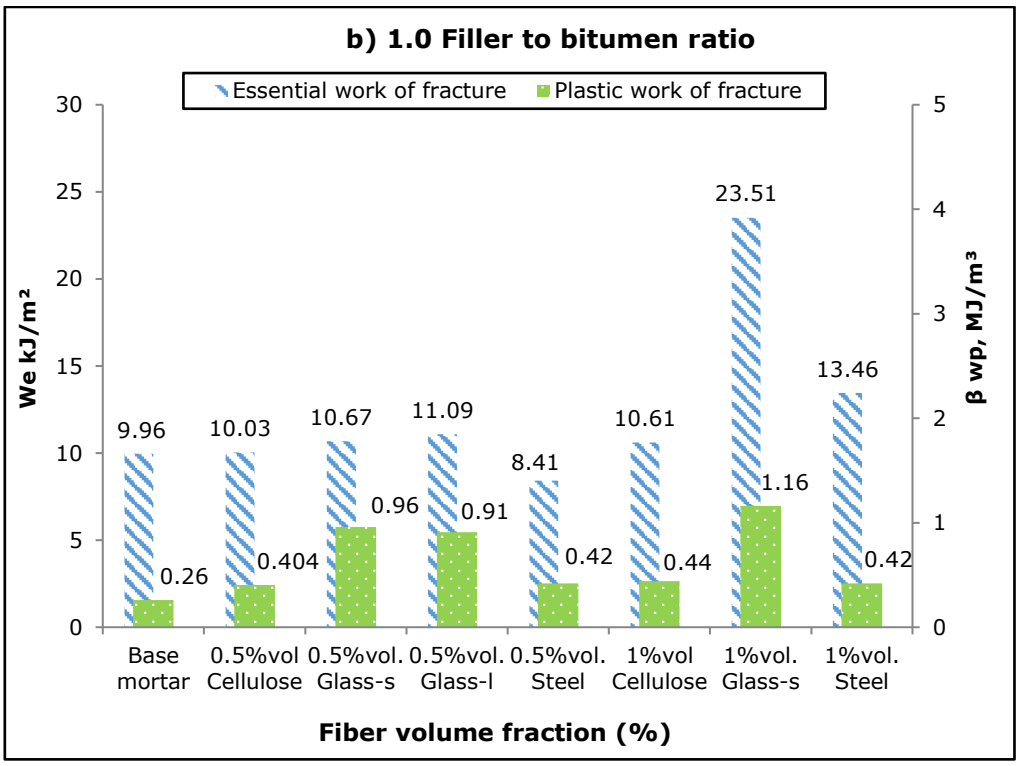
approaches that of the fibres. This is in agreement with the fact that composite anisotropic materials and anisotropic materials have different material properties in all directions at any point in the structure. In addition, the glass-l fibres may have entangled with each other to form a continuous network reinforcing the sample (see Figure 5-1) in the notch area more effectively than steel fibre due to the dimension of glass fibre and surface texture. The high thickness of steel fibres means a small number of steel fibres exist in the small notch area of DENT specimen. This reinforcement led to an increase in the fracture force required to fracture the sample, which leads to high toughness composite.

The results of this study indicated that the addition of 1.0% of fibres led to a marked effect in asphalt mortar toughness by increasing the essential and plastic work of fractures, as shown in Figure 5-17. This result may be explained by the fact that glass and steel fibres have high tensile strength and also due to the reinforcement effect of these fibres by forming a network through the composite; this network supported the composite and held the component by strong fibre-matrix adhesion along with interfaces (see Figure 5-1). With regards to cellulose fibre the technical properties of cellulose fibre which is high absorption/adsorption and retention of liquid media and high tensile strength may have led to increased asphalt mortar toughness by absorption/adsorption of the light fraction of bitumen and increasing asphalt mortar toughness (Payne et al., 2012). Also, basket drainage and asphaltene test results showed that drained binder after mixing with cellulose fibre exhibited improvement in rheological properties and asphaltene content, as shown in the following chapter.

In summary, these results showed that the addition of fibres led to increased asphalt mortar toughness which will minimise or prevent the occurrence of longitudinal and transverse cracking (Andriescu and Hesp, 2009). Although these results were in line with those of the previous chapter which evaluated the effect

of fibres on mastic toughness, the percentage of increase in toughness was lower in the case of asphalt mortar modified by fibres.





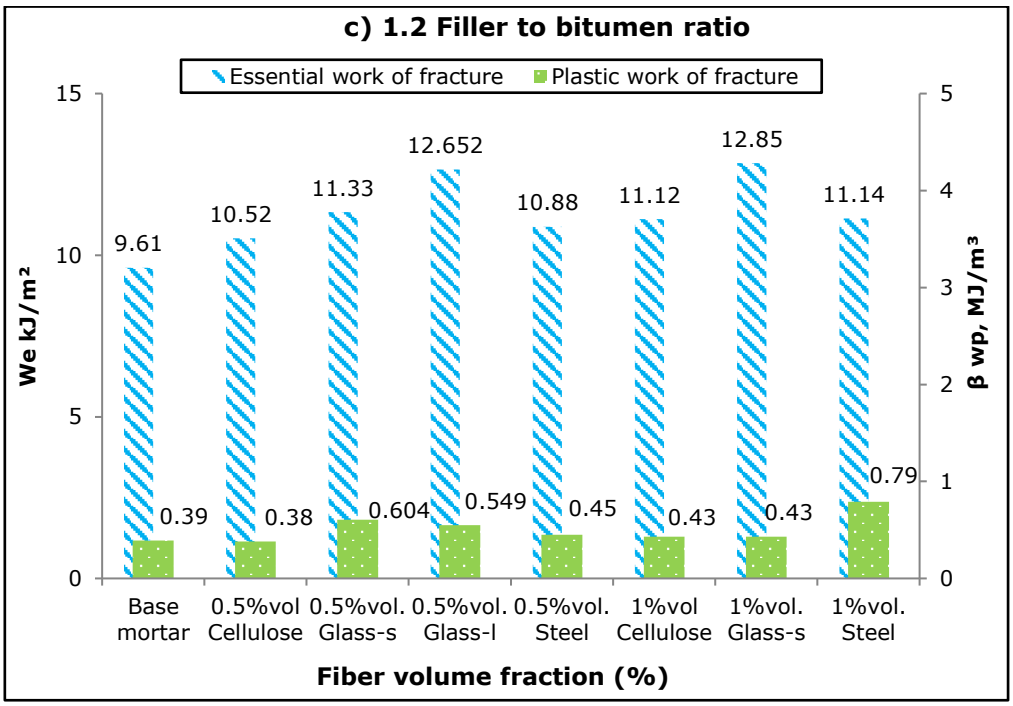


Figure 5-17 (a, b and c) Essential and plastic works of fracture at 15℃

5.4 Summary and conclusions

A combination of multiple phase system (fibre, filler and bitumen) has been investigated in this chapter. The influence of different filler to bitumen ratios and fibre types on the mechanical properties of base and fibre modified mortar was examined by means of high temperature viscosity, penetration, DENT test and dynamic shear rheometer tests. The following summary and conclusions are presented:

- The rheological properties of mortar (bitumen and filler) are enhanced by adding fibres as recognised by both common (penetration and viscosity) and Dynamic Shear Rheometer (DSR) parameters.
- Fibre properties such as shape, size and microstructure were observed using a Scanning Electron Microscope (SEM). Also, fibre interlacing

horizontally and vertically, was observed. This is particularly the case for the glass fibres.

- Generally, the differences in rheological properties between the base and modified mortars are more noticeable at higher temperatures. Under these circumstances, the viscosity of mortar is low enough to allow the fibre entanglement to control the rheological properties of fibre reinforced mortars. This may lead to increased load bearing capacity and service life of the pavement.
- The addition of fibre significantly improves the rutting parameter G*/Sinδ, at moderate and high temperatures. This implies that the addition of fibres may lead to improved rutting resistance of asphalt mixtures.
- The dynamic shear rheometer results indicate that 1.0 filler to bitumen ratio and 2.0% addition of glass and steel fibres showed the highest potential improvement, while 0.8 filler to bitumen ratio and 2.0% addition showed the best performance for cellulose fibre. These results are consistent with the mastic test results in the previous chapter as high fibre contents showed the best performance.
- Fibre reinforced asphalt mortars showed higher fracture toughness compared to the base mortar. This increase in toughness of fibre reinforced mortar was consistent with the increase in fibre reinforced mastic toughness examined in the previous chapter.

Chapter 6 Bond Strength

Bond strength of bitumen fibre mortar

6.1 Introduction

The loss of bond strength in road pavement surfacing due to high traffic loads or moisture is a recurring problem, creating distress such as ravelling, fatigue and rutting. It is, therefore, important to find a way to prevent or at least delay the loss of bond strength in asphalt mixtures. Such an improvement would lead to longer service life and a more comfortable drive for road users.

In an asphalt mixture, the aggregates are much stiffer and stronger than other components such as bituminous binder or mastic. Therefore, the possibility of failure is expected to be very small through the aggregates themselves, while there is a high possibility of failure in the material that bonds adjacent particles, particularly at high and moderate temperatures (Mo, 2010). The loss of strength of cohesive bonds within the bitumen itself is termed cohesive failure, and adhesive failure is the breaking of the adhesive bonds between aggregate and bitumen or mastic materials, mainly due to the effect of water or low temperatures (Caro et al., 2009). Under the effect of traffic loading forces, the aggregate particles tend to separate from each other. As these forces increase, failure occurs at the interfaces between the aggregate and mastic and/or inside the mastic film (Hossain and Tarefder, 2015). The loss of bond strength then compromises pavement integrity, and this could lead to different pavement failure types such as permanent deformation, ravelling and fatigue (Cho and Kim, 2010). It is, therefore, important

to investigate this phenomenon and find a way to prevent or at least reduce such deterioration in the bond strength.

The pull-off tensile strength test is commonly used to investigate the bond strength and failure type of a bitumen-aggregate mix. Past studies found that dry samples showed a cohesive failure, while moisture-conditioned samples showed a hybrid or adhesive failure (Mo, 2010, Kanitpong and Bahia, 2003, Copeland et al., 2006). The physicochemical properties of bitumen and aggregate surfaces, their surface energies, can be used to estimate the adhesive bond strength between the two (Ahmad, 2011). Also, adding modification (polymer, acid, stripping additive) to bitumen will influence the physicochemical properties and bond strength of bitumen (Moraes et al., 2017).

Fibres have the potential to strengthen the bitumen phase; however, studies have found that different types and amounts of fibre strengthen the modified asphalt in different ways (Chen et al., 2008, Mohammed et al., 2017). Past studies (Serfass and Samanos, 1996, Chen et al., 2009, Mahrez et al., 2005) have suggested that some fibres can absorb the light fraction of bitumen, in addition to the fact that adding fibres such as those of polyester, polyacrylonitrile, lignin and asbestos would change the optimum bitumen content of an asphalt mixture. It is important to note that the mechanism of possible chemical modification of binder in contact with fibres remains in large part unknown. The binder drainage test can provide results that may help in understanding such modification by examining the drained binder properties such as asphaltene content and complex modulus.

This chapter explores the influence of different types and percentages of fibre on the pull-off tensile strength of bituminous mastic. These samples are not conditioned in water, in order to investigate the effect of fibre on mastic strength and bond strength in dry condition. The effect of different filler to bitumen ratios on the pull-off tensile strength of fibre reinforced mastic is also investigated. To

gain a better understanding of the possible chemical effect of fibre on the binding properties of bitumen, the asphaltene content, the rheological properties and the work of cohesion and work of adhesion of drained binder, before and after mixing with fibres are calculated from surface energy components. The relationship between the work of cohesion and the pull-off tensile strength results of fibre reinforced mastic are investigated.

6.2 Characterisation

6.2.1 Binder drainage test basket method

In this work, the basket method (BS EN, 2004) was used to measure the binder drainage of fibre-reinforced mastic; 2.0% by volume of fibres in 80 g of the binder. Each resulting composite was placed into a steel mesh basket with sieve size 250 microns, which was then placed on a pre-wrapped tray in the oven at 160℃ for 3 hours. Binder flowed and drained through the mesh into the pre-wrapped tray. After 3 hours, the steel mesh basket and pre-wrapped tray were removed from the oven and the mesh basket separated from the pre-wrapped tray. Once cooled, the weight of the tray and drained binder was measured and the weight of drained material (D) calculated in percent.

6.2.2 Determination of asphaltene content

Asphaltene content in the drained binders was measured according to BS 143 (2000). In this method, the drained binder was mixed with heptane and heated under reflux, separating the binder into three components (asphaltenes, waxy substances and inorganic material). The remaining material was extracted by chromatographic separation.

6.2.3 Complex modulus test

A Bohlin Gemini 200 (DSR) was used in this study for measuring the rheological properties of base and drained binder. Eleven testing frequencies ranging from 0.1 to 10.0 Hz were used in the DSR tests with nine testing temperatures between 30 and 70℃ (at increments of 5℃).

6.2.4 Pneumatic adhesion tensile testing instrument (PATTI) test

The pneumatic adhesion tensile testing instrument (PATTI) is used to measure the cohesive and adhesive properties of a bitumen-aggregate system by measuring pull-off strength. The PATTI consists of a portable pneumatic adhesion tester, piston and reaction plate, air hose, camera and steel pull-out stub as shown in Figure 6-1. Aggregate substrates and pull-stubs have to be cleaned and dried at room temperature for at least 24 hours. Then, in order to remove any dust, the aggregate substrates and pull-stubs were wiped carefully using a damp paper towel. After that, all aggregate substrates and pull-stubs were placed in an oven at 80℃ for one hour. The fibre reinforced mortar was placed in an oven at 160℃ for 30 minutes, and by this time the mortar was fluid enough to coat the aggregate substrate. Then fibre reinforced mortar was poured onto the aggregate substrate, and a pull-stub was immediately pressed into it to achieve good mortar-aggregate adhesion (ASTM D 4541-17, 2002). Washers and three raised edges on the pull-stub were used to control the film thickness.

Samples were left for 24 hours at room temperature before testing in order to allow enough time for the aggregate and mortar to adhere and for the sample to reach the test temperature. After the mortar and substrate had cooled down the excess mortar at the edge of the pull-stub was carefully removed using a heated pallet knife. The test then consists of applying an upward pressure to the asphalt mortar by the movement of the pull-out stub. Air pressure rate was fixed during the test

in order to achieve repeatable results. The pull-off tensile strength of mortar indicates when the applied pressure exceeds the cohesive strength of the mortar or the adhesive bond strength between mortar and aggregate.

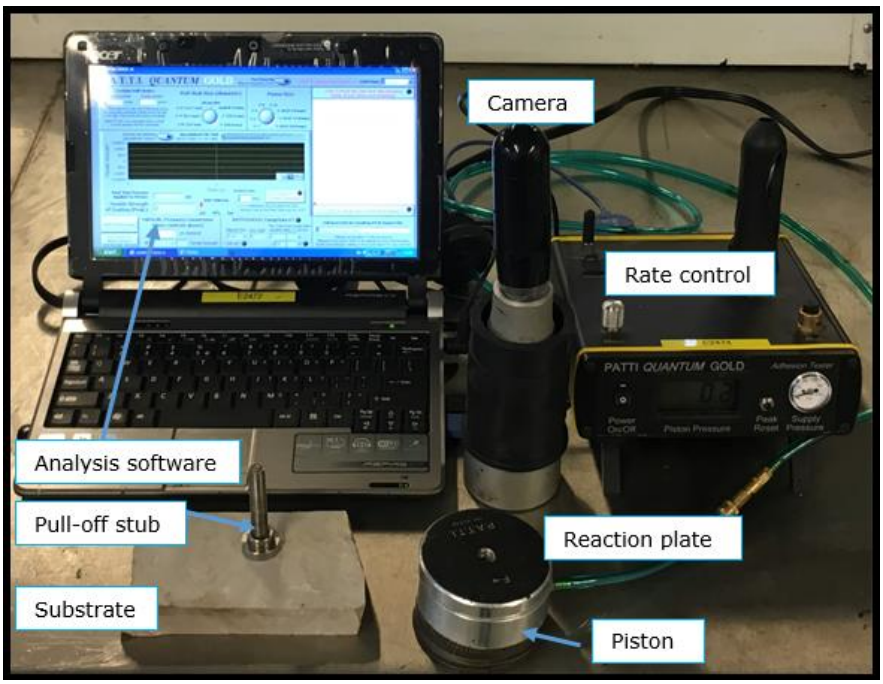


Figure 6-1 General representation of PATTI test

6.2.5 Surface energy measurement

Thermodynamic (adsorption) theory is widely accepted as an approach to explain the interfacial adhesion of a liquid-solid contact. This theory is based on the principle that an adhesive (the liquid) will adhere to a solid depending on the physical forces established at the interface, so long as contact is maintained. The interfacial forces are van der Waals and Lewis acid-base interactions. These forces are generally related to fundamental thermodynamic quantities, in particular, the

surface free energies of the materials involved (Mittal., 2003). The contact angles of binders and limestone aggregate were measured by using three selected probe liquids, distilled water, glycerol and diiodomethane (Ahmad, 2011).

6.3 Surface energy

According to past studies, the cohesive and adhesive strengths of bitumen-aggregate systems have been successfully determined from the surface free energy (γ) (Little and Bhasin, 2006, Masad et al., 2006). Previous research investigated the technical criteria of test methods, such as accuracy, precision and the ability to provide all three surface energy parameters and recommended the Whilhelmy plate method (dynamic contact angle) for routine use (Little and Bhasin, 2006). Another study focused on the evaluation of the resistance of asphalt mixtures to moisture damage, through understanding the mechanisms that influence the surface energy of aggregates and binders in addition to the fracture behaviour of asphalt mixture. They found that the ratio of the adhesive bond energy under dry conditions to the adhesive bond energy under wet conditions is related to the asphalt mixture resistance to moisture damage (Masad et al., 2006). The surface free energy is a measure of the amount of energy needed to form a unit area of new surface at the interface of the material (Ahmad, 2011).

The surface free energy ($\boldsymbol{\gamma}$) of a material comprises two components, a dispersive or Lifshitz-van der Waals component ($\boldsymbol{\gamma}^{LW}$) of electrodynamic origin, and a polar component ($\boldsymbol{\gamma}^{AB}$) caused by Lewis acid-base interactions (Van Oss et al., 1987) as shown in the following equation:

$$\gamma^{total} = \gamma^{LW} + \gamma^{AB} \qquad \text{Equation 6-1}$$

The acid-base components can be subdivided into a Lewis acid parameter of surface free energy (γ^+) and a Lewis base parameter of surface free energy (γ^-) as shown in the following equation:

$$\gamma^{AB} = 2(\sqrt{\gamma^+\gamma^-}) \quad \text{Equation 6-2}$$

By combining equations (6.1) and (6.2) the surface free energy (mJ/m^2) or (erg/cm^2) of a material can be defined as:

$$\gamma^{total} = \gamma^{LW} + 2(\sqrt{\gamma^+\gamma^-}) \quad \text{Equation 6-3}$$

6.3.1 Work of cohesion

The work of cohesion (W_C) can be defined as the energy required to separate the liquid or solid from itself, and this depends on the attraction between molecules. The following equation describes the work of cohesion (Moraes et al., 2017):

$$W_C = 2\gamma^{total} \quad \text{Equation 6-4}$$

6.3.2 Work of adhesion

The work of adhesion (W_a) can be defined as the energy required to create new surfaces between two materials (solid-liquid); therefore, work of adhesion represents the amount of intermolecular interaction between two materials (Reynolds and Cosgrove, 2005).

The work of adhesion is a dependent property of a solid-liquid pair. Accordingly the interfacial surface free energy of a material (binder or aggregate) is the combination of these non-polar (Lifshitz-van der Waals) and polar (Lewis acid/base) forces as shown in the following equation:

$$\gamma_{BA} = \gamma_{BA}^{LW} + \gamma_{BA}^{AB}$$ Equation 6-5

where B and A represent bitumen and aggregate, respectively. The adhesive Lifshitz-van der Waals and Lewis acid/base bond strength can be determined by the following equations, respectively (Bhasin, 2006).

$$W^{LW} = \gamma_B^{LW} + \gamma_A^{LW} - \gamma_{BA}^{LW}$$ Equation 6-6

$$W^{AB} = \gamma_B^{AB} + \gamma_A^{AB} - \gamma_{BA}^{AB}$$ Equation 6-7

The Lifshitz-van der Waals solid-liquid surface energy is described by the following equations (Bhasin, 2006):

$$\gamma_{BA}^{LW} = (\sqrt{\gamma_B^{LW}} - \sqrt{\gamma_A^{LW}})^2$$ Equation 6-8

$$\gamma_{BA}^{AB} = 2(\sqrt{\gamma_B^{+}} - \sqrt{\gamma_A^{+}})(\sqrt{\gamma_B^{-}} - \sqrt{\gamma_A^{-}})$$ Equation 6-9

By substituting these two equations (6-8) and (6-9) into equations (6-6) and (6-7), the following equation is obtained:

$$W_a = 2(\sqrt{\gamma_B^{LW}\gamma_A^{LW}} + \sqrt{\gamma_B^{+}\gamma_A^{-}} + \sqrt{\gamma_B^{-}\gamma_A^{+}})$$ Equation 6-10

Where W^{LW} is the Lifshitz-van der Waals work of adhesion and W^{AB} is the Lewis acid/base work of cohesion.

In this chapter, the work of cohesion and work of adhesion, computed in this way, will be used to interpret the pull-off test data.

6.4 Results and Discussions

6.4.1 Binder drainage test results

The results of the binder drainage tests are the average of three values, as shown in Table 6-1. The results have a low coefficient of variation, although higher for cellulose fibres due to having a similar level of variability and lower average drained binder percentage. The percentage of drained material reflects bitumen stability, which may be a function of the mechanical interaction of the fibres in the binder and absorption/adsorption of certain bitumen fractions by the fibres.

Cellulose fibre showed by far the highest stabilisation and absorption/adsorption effect compared to the other fibre types, as expected due to the surface texture and large surface area of cellulose fibre (see Table 3-2), giving high absorption and retention of liquid media. Other fibre types (glass and steel) held lower amounts of bitumen. These results may reflect the amount of bitumen adhering to the fibre surfaces. Samples of base binder and drained binders were taken for analysis of asphaltene content and surface energy components.

Table 6-1 Results of binder drainage test (basket method)

Fibre type	Percent of drained material (average of three results) (%)	Coefficient of variation %	Standard error
Base binder	97.0	0.7	0.41
Cellulose	43.4	3.0	0.74
Glass-s	74.9	2.2	0.96
Glass-l	71.1	2.4	0.97
Steel	72.1	1.2	0.49

6.4.2 Asphaltene test results

Asphaltenes are the bitumen fraction that is insoluble in low molecular weight paraffin, such as propane, n-butane, n-pentane, n-heptane and n-hexane (Oyekunle, 2007). It is relatively high in heteroatoms such as nitrogen, oxygen, carbon and hydrogen with sulphur. Asphaltenes are the largest fraction of bitumen, responsible for the increase in thickening, strength and stiffness of the bitumen and non-Newtonian rheological behaviour (Oyekunle, 2007). This study measured the influence of different fibre types on the asphaltene content of base binder to explore the effect on bitumen chemistry of adding fibres. A previous study indicated that high asphaltene content might have led to increased cohesive and adhesive strength of base binder (Canestrari et al., 2010).

Two tests were performed for each fibre type, and the average asphaltene content is reported in Table 6-2. The drained binders showed higher asphaltene content compared to the base binder. As noted in the introduction, previous studies showed that fibres can adsorb /absorb the light fraction of bitumen (Serfass and Samanos, 1996, Chen et al., 2009, Mahrez et al., 2005), and it is important to note that the cellulose fibres retained over 50% of the bitumen in the drainage test while the other fibres retained about 25%, compared to 3% for the sample without fibres. Preferential adhesion of the lighter binder fraction would lead to higher asphaltene content in the drained binder. Also, steel fibre, as a thermal conductor, may influence the bitumen heating process and lead to more ageing of the bitumen during the draining process and hence, lead to higher asphaltene content. The results suggest that the presence of fibres leads to higher asphaltene content; however, due to the variability in the asphaltene test results, it is hard to draw conclusions about any differences. For this reason, the rheological properties of the drained binders were evaluated by creating complex modulus master curves (more details in chapter four section 4.2.5) because stiffening of the binder would provide further evidence of higher asphaltene content.

Table 6-2 Asphaltene content test results

Binder type	Asphaltene content (%)	Coefficient of variation (%)	Standard error
Base binder	12.7	1.1	0.10
Drained base binder	14.7	0.5	0.05
Drained Cellulose	15.9	3.3	0.26
Drained Glass-s	14.9	4.0	0.57
Drained Glass-l	15.7	5.1	0.46
Drained Steel	15.5	5.0	0.55

6.4.3 Complex modulus and phase angle master curves of base and drained binder

Figure 6-2 shows the complex modulus master curves for base binder, drained base binder and drained binder after mixing with fibres. A considerable difference in the complex modulus values of drained binder after mixing with fibres, compared to both base and drained base binder can be seen. This increase in complex modulus could be due to the fibre affecting the chemical composition of the binder by adsorption/absorption of different fractions, mainly lighter fractions. A previous study, using chromatography, indicated that the fibre coating could influence the absorption of different fractions, particularly lighter fractions (Putman, 2011). Figure 6-3 shows the phase angle master curves for base binder, drained base binder and drained binder after mixing with fibres. Also, there is a clear difference in the phase angle values of both drained base binder and drained binder after mixing with fibre compared to the base binder. These results reflect the asphaltene content results, as the asphaltene content increased for drained binder after mixing with fibres, as shown in Table 6-2.

It is important to note that the complex modulus and phase angle values of drained binder after mixing with glass and steel fibre were almost the same. Cellulose fibre

showed higher complex modulus and lower phase angle compared to other fibre types. This increase in complex modulus may be because cellulose fibre had lower drained binder percentage (Table 6-1), indicating retention of more of the lighter fraction of the bitumen.

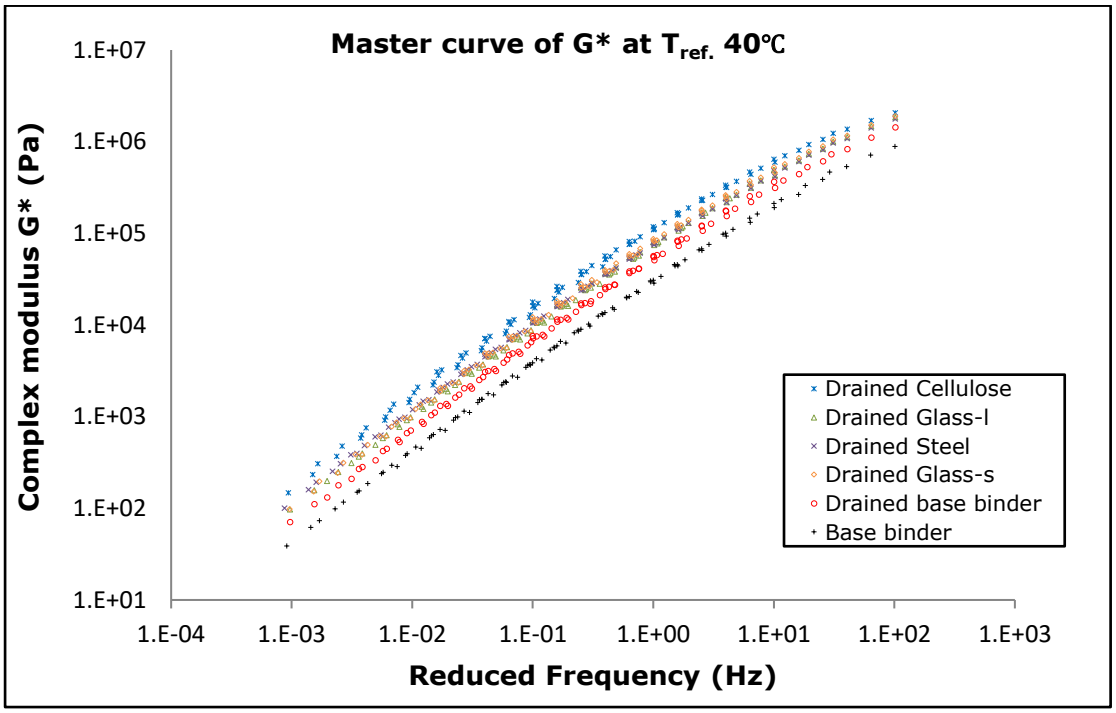


Figure 6-2 Complex modulus master curves for drained binders (2.0% fibre by volume)

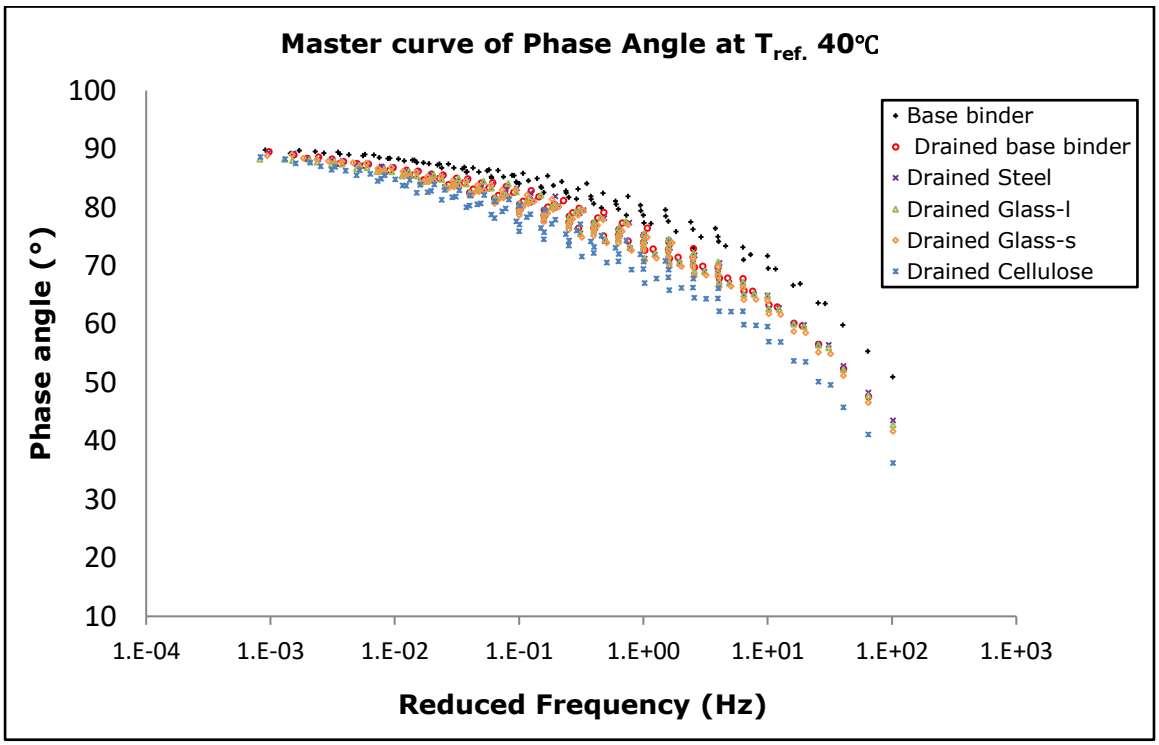


Figure 6-3 Phase angle master curves for drained binders (2.0% fibre by volume)

6.4.4 Pneumatic adhesion tensile testing instrument (PATTI)

The PATTI test was used to measure the influence of fibres on mortar bond strength. Three filler to bitumen ratios (0.8, 1.0 and 1.2 by weight) and three fibre contents (0.5, 1.0 and 2.0% by bitumen volume) were used in this investigation. Failure strength results are shown in Figure 6-4 and the mode of failure in Table 6-3, as illustrated in Figure 6-5 and Figure 6-6.

Table 6-3 Failure mode in fibre modified asphalt mortar

Mortar type	f/b*	Failure type			
		0.0% vol.	0.5% vol.	1.0% vol.	2.0% vol.
Base mortar	0.8	Cohesion	-	-	-
	1.0	Cohesion	-	-	-
	1.2	Cohesion	-	-	-
Cellulose fibre mortar	0.8	-	Cohesion	Hybrid	Hybrid
	1.0	-	Cohesion	Hybrid	Hybrid
	1.2	-	Cohesion	Hybrid	Hybrid
Glass-s fibre mortar	0.8	-	Cohesion	Cohesion	Cohesion
	1.0	-	Cohesion	Hybrid	Hybrid
	1.2	-	Cohesion	Hybrid	Hybrid
Glass-l fibre mortar	0.8	-	Cohesion	Cohesion	Cohesion
	1.0	-	Hybrid	Hybrid	Hybrid
	1.2	-	Hybrid	Hybrid	Hybrid
Steel fibre mortar	0.8	-	Cohesion	Cohesion	Cohesion
	1.0	-	Hybrid	Hybrid	Hybrid
	1.2	-	Hybrid	Hybrid	Cohesion

*f/b: filler-bitumen ratio

6.4.4.1 Influence of fibre content and type

Three tests were performed for each mortar type, and the average tensile strength was reported, as shown in Figure 6-4, where error bars represent plus and minus one standard error. The tensile strengths of different fibre types and filler to bitumen ratios were reasonably repeatable, indicating that the application of a constant rate of air pressure was successful for these tests. The specimens exhibited a linear response to the increase in pressure until the pressure overcame

the cohesive strength of the mortar and the adhesive strength of the mortar-aggregate interface and then rapidly decreased to zero.

It can be seen that on average, all fibre types increased the pull-off tensile strength compared to the base mortar. Table 6-4 gives the average results along with t-test results, comparing fibre mortars to the base mortar, for the three filler to bitumen ratios. Most fibre percentages and types show statistically significant increases in the pull-off strength.

The glass-l fibre showed the highest increase in bond strength among all fibre types. This increase may be due to two reasons. Firstly, glass fibre contains silicon dioxide (SiO_2) and aluminium oxide (Al_2O_3). This chemical combination can form strong chemical bonds with sulfoxides and carboxylic acids in bitumen (Zhang et al., 2015a, Moraes et al., 2011). Secondly, glass fibre dimensions (length and width) may help the fibres to cross over each other to form three dimensional networks. These networks then provide support to the composite structure by holding the components together and spreading stresses (Tapkın et al., 2010).

Base mortars with different filler to bitumen ratios showed cohesive failure (failure within the mortar). The failure type changed from cohesive to a hybrid (partly adhesive failure between aggregate and mortar) with an increase in the pull-off strength when 1.0 and 2.0% cellulose and glass-s fibres were used as a modification for 1.0 and 1.2 filler to bitumen ratios. This implies an improvement in the cohesive strength of the mortar with the increase in fibre content, as shown in Figure 6-4 (b and c). This behaviour may be explained by the higher fibre content both mechanically stabilizing the material and/or absorbing/adsorbing the bituminous binder (see Table 6-1) (Chen and Xu, 2010). The latter is likely with cellulose fibre since the surface texture of cellulose fibres comprises many interweaving branches with non-uniform sizes and rough surfaces, which will increase the specific surface area and hence the absorption/adsorption capability

(see Table 3-2), as shown in SEM images (see Figure 5-1 b). These features of cellulose fibre might explain the hybrid failure at 0.8 filler to bitumen ratio for mortar modified by cellulose fibre, whereas other fibre types exhibited a cohesive failure, as shown in Table 6-3 and Figure 6-5 a.

On the other hand, the longer steel and glass-l fibre samples showed a hybrid failure for all fibre percentages at 1.0 and 1.2 filler to bitumen ratios. This could be due to the dimensions of these fibres, leading to a more effective network and therefore enhanced reinforcement effects.

6.4.4.2 Influence of filler-bitumen ratio

The results (Figure 6-4) showed that the pull-off tensile strength increased with the increase in the filler to bitumen ratio. A possible explanation for this might be that adding more filler enhanced the interaction between the bitumen and the filler particles (Faheem and Bahia, 2010). Bituminous binders are non-polar, while molecules of limestone are more polar. This may help to satisfy the energy demand of the aggregate surface by improving the adhesion between the aggregate and the mortar (Hicks, 1991, Moraes et al., 2011).

There is a decrease in the pull-off tensile strength of the 1.2 filler to bitumen ratio at 2.0% fibre content, particularly for cellulose, glass-l and steel fibres. This may indicate that adding more fibre with a high absorption/adsorption and/or large surface area led to an increase in the percentage of voids in the matrix (Kim et al., 1999, Tapkin et al., 2009). The stress applied to the specimen may have been concentrated around these voids, and the fracture may have begun at these points. Moreover, as the percentage of filler and fibre increased, the composite became stiffer and was, therefore, more likely to show brittle behaviour. This suggests that when adding more fibre and filler, there should be enough binder in the mix to reduce the voids in the mortar.

It is important to note that the modulus and Poisson's ratio of steel and glass fibres are very large compared to the matrix, and therefore, a concentration of stress will occur at the interface. Also, steel fibre has large thickness and according to previous studies, the stress concentration area depends on the fibre thickness and this area will increase as fibre thickness increases (Chen and Lin, 2005), therefore the stress will be high at this area, and probably the failure will start at these points.

Only the 0.5% cellulose fibre samples show cohesive failure at all three filler to bitumen ratios, and this means they can be more directly compared for the base mortars (which also showed cohesive failure). Both showed an increase in cohesive pull-off tensile strength with increase in filler to bitumen ratio.

Table 6-4 Pull-off tensile strength t-test results

f/b ratio*	Fibre	Mean (MPa)	t-stat	p-value	Significant**
0.8	Base mortar	1.19	-	-	-
	0.5% Glass-s	1.61	4.828	0.0202	Yes
	0.5% Glass-l	1.71	5.677	0.0054	Yes
	0.5% Cellulose	1.56	4.121	0.0271	Yes
	0.5% Steel	1.44	2.731	0.0359	Yes
	1% Glass-s	1.76	4.139	0.0072	Yes
	1% Glass-l	1.78	6.394	0.0038	Yes
	1% Cellulose	1.64	4.703	0.0091	Yes
	1% Steel	1.76	4.117	0.0073	Yes
	2% Glass-s	1.85	6.403	0.0038	Yes
	2% Glass-l	1.95	8.388	0.0069	Yes
	2% Cellulose	1.84	6.348	0.0039	Yes
	2% Steel	1.81	6.275	0.0041	Yes
1.0	Base mortar	1.25	-	-	-
	0.5% Glass-s	1.61	3.775	0.0317	Yes
	0.5% Glass-l	1.78	3.350	0.0393	Yes
	0.5% Cellulose	1.69	4.525	0.0101	Yes
	0.5% Steel	1.55	3.641	0.0339	Yes
	1% Glass-s	1.78	3.798	0.0160	Yes
	1% Glass-l	2.06	5.222	0.0068	Yes
	1% Cellulose	1.76	6.398	0.0038	Yes
	1% Steel	1.88	5.446	0.0060	Yes
	2% Glass-s	2.10	8.518	0.0017	Yes
	2% Glass-l	2.16	8.794	0.0015	Yes
	2% Cellulose	2.09	11.947	0.0034	Yes
	2% Steel	1.90	10.204	0.0047	Yes
1.2	Base mortar	1.72	-	-	-
	0.5% Glass-s	1.93	2.174	0.0808	No
	0.5% Glass-l	2.08	4.087	0.0274	Yes
	0.5% Cellulose	1.99	3.410	0.0907	No
	0.5% Steel	2.00	2.617	0.0601	No
	1% Glass-s	2.03	2.372	0.0705	No
	1% Glass-l	2.47	7.338	0.0090	Yes
	1% Cellulose	2.10	3.353	0.0219	Yes
	1% Steel	2.12	3.242	0.0238	Yes
	2% Glass-s	2.06	2.368	0.0493	Yes
	2% Glass-l	2.17	4.786	0.0204	Yes
	2% Cellulose	2.06	4.316	0.0724	No
	2% Steel	2.05	3.405	0.0764	No

*f/b: filler-bitumen ratio.
** indicates significant at the 95 percent confidence interval.

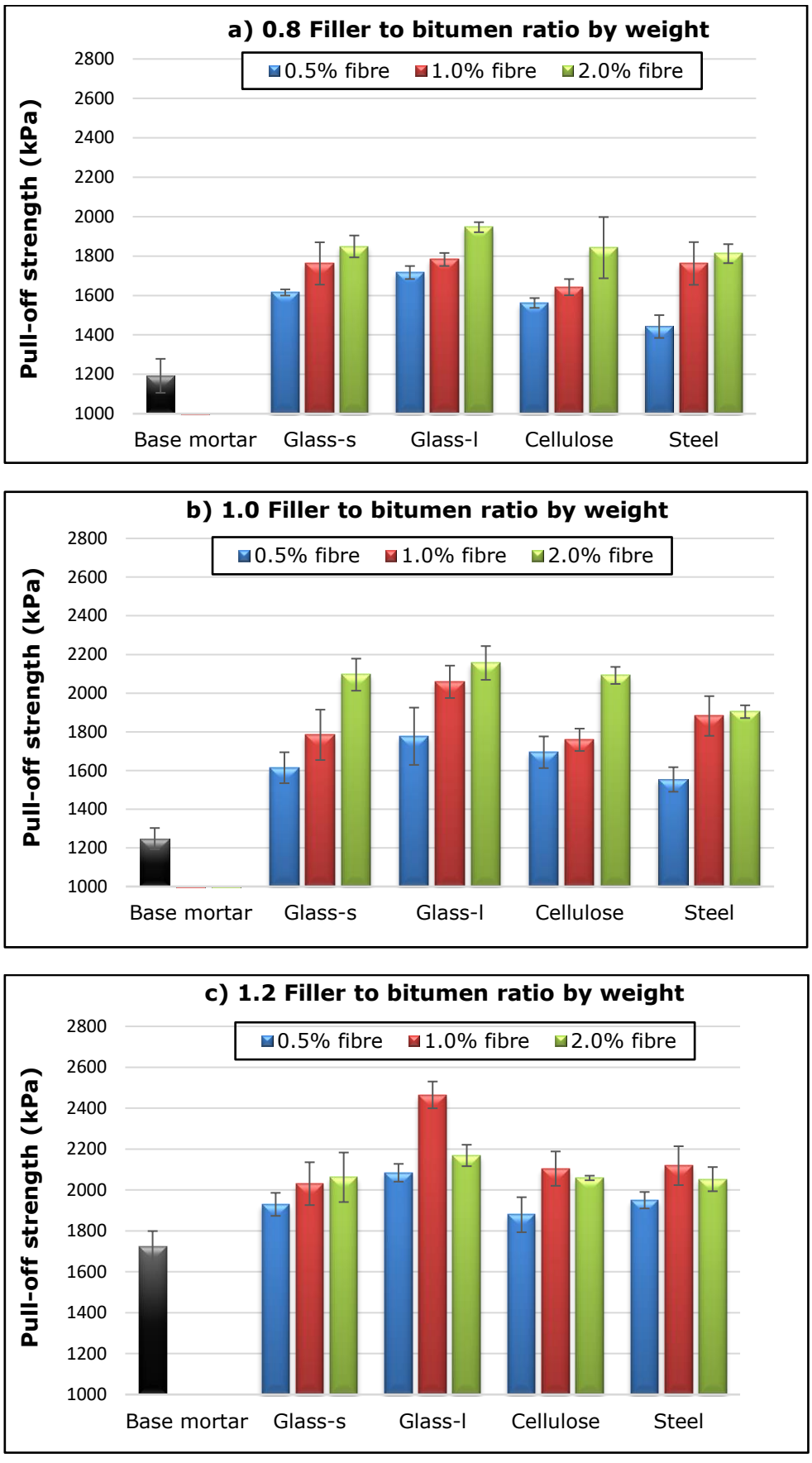


Figure 6-4 Pull-off tensile strength of the base and modified mortars

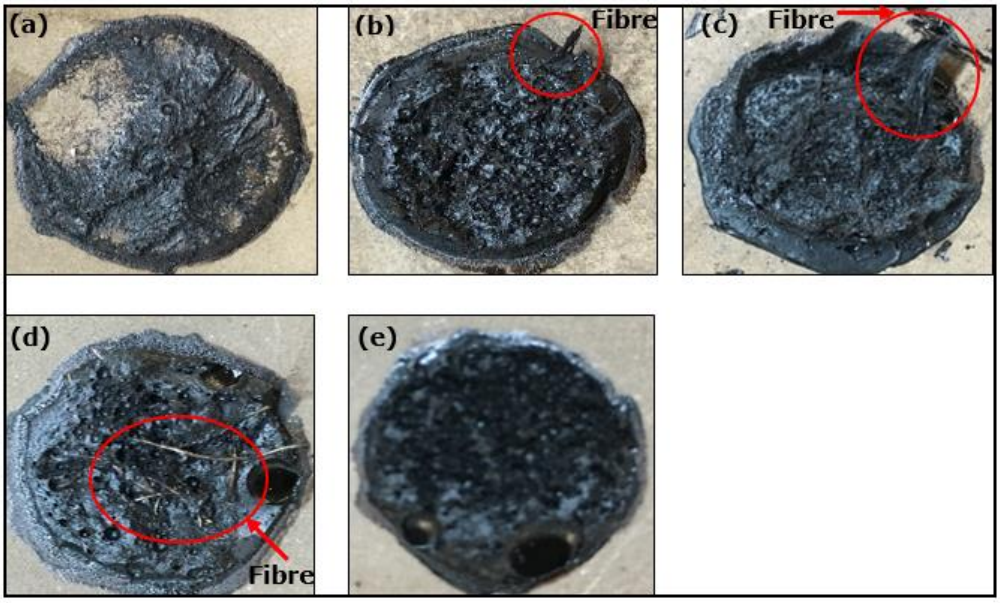


Figure 6-5 Failure surfaces of 0.8 filler to bitumen ratio asphalt mortar with limestone aggregate with different fibre types: (a) Cellulose, (b) Glass-s, (c) Glass-l, (d) Steel and (e) base mortar.

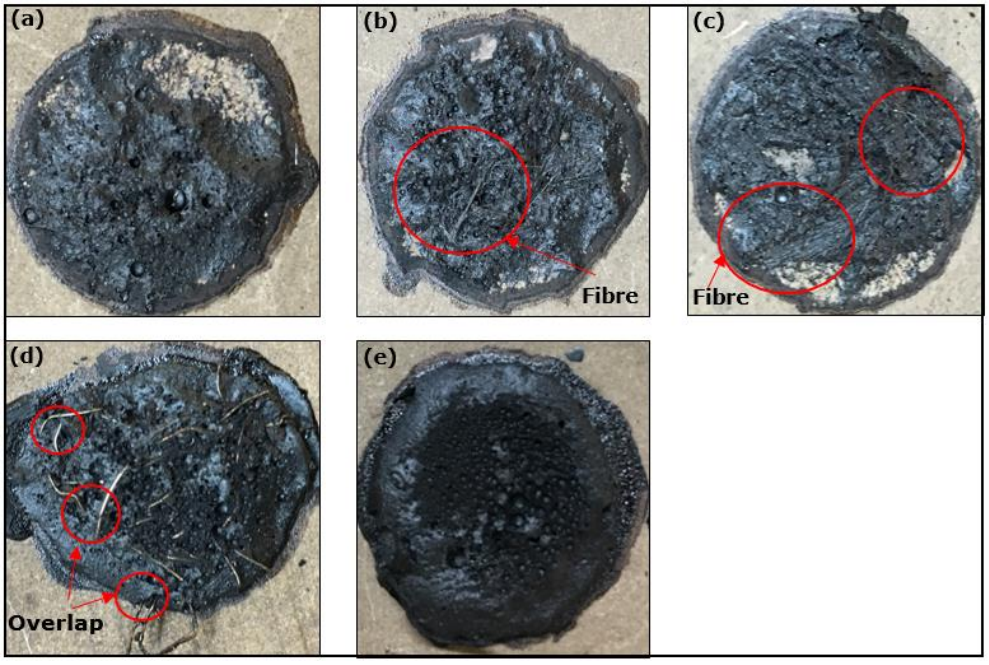


Figure 6-6 Failure surfaces of 1.2 filler to bitumen ratio asphalt mortar with limestone aggregate with different fibre types: (a) Cellulose, (b) Glass-s, (c) Glass-l, (d) Steel and (e) base mortar.

6.4.5 Surface energy

The dynamic contact angle (DCA) measurement of bitumen was used in this study. The contact angles were measured for each drained binder for each probe liquid, and the contact angle was taken as the average of four or five replicates, and the variation between results was low, as shown in Table 6-5. The results for the surface energy components of the drained binders are shown in Table 6.6 in which γ_s^{AB} represents the polar surface energy component of the solid and γ_s^{LW} represents the non-polar (Lifshitz-van der Waals) surface energy component of the solid. The results for the surface energy components of the drained binders showed more variation in the γ_s^{AB} values than the γ_s^{LW} values, ranging from 0.19 to 1.78 mJ/m^2, as shown in Table 6-6. The results showed that the bituminous binder molecular constituent forces are mainly Lifshitz-van der Waals (non-polar) in character (Hefer, 2005).

The surface energy components of limestone aggregate were determined by using a dynamic vapour sorption (DVS) approach, and the results are shown in Table 6-7. This method is usually used for high surface energy materials such as aggregate, and the advantage of this method is that it takes into consideration the irregular shape and surface texture of the aggregate (Ahmad, 2011). The surface energy of limestone aggregate was found to be 104.19 mJ/m^2.

Table 6-5 Contact angle measurement of the bitumen binder

Sample	Contact Angle in Diiodomethane		Contact Angle in Glycerol		Contact angle in Water	
	Average (º)	CV* (%)	Average (º)	CV (%)	Average (º)	CV (%)
Drained base binder	82.99	1.05	92.12	1.18	101.54	0.52
Drained Cellulose	80.23	1.32	92.56	0.08	101.58	1.36
Drained Glass-s	78.22	2.69	94.26	1.08	95.32	1.19
Drained Glass-l	75.99	1.36	94.96	0.33	98.09	0.67
Drained Steel	79.58	2.28	95.23	0.45	97.25	0.54

*CV: coefficient of variation

Table 6-6 Surface energy components of the drained binder

Binder type	γ_s^{LW}	$\gamma_s^{AB} = 2\sqrt{\gamma^+\gamma^-}$	γ^{total} (mJ/m²)
Drained base binder	15.99	1.78	17.77
Drained Cellulose	17.38	1.30	18.68
Drained Glass-s	18.41	0.46	18.88
Drained Glass-l	19.59	0.59	20.18
Drained Steel	17.71	0.19	17.90

Table 6-7 Surface energy components of limestone aggregate

Aggregate	γ_s^{LW}	$\gamma_s^{AB} = 2\sqrt{\gamma^+\gamma^-}$	γ^{total} (mJ/m²)
Limestone	65.81	38.38	104.19

6.4.6 Work of cohesion and adhesion

The results for work of cohesion ($2\gamma^{total}$) of the base drained binder and drained binder after mixing with fibres are shown in Table 6-8. Table 6-3 shows the mode

of failure in the PATTI tests and reveals that the 0.8 filler to bitumen ratio mortars consistently failed by fully cohesive failure at 0.5% fibres. It is, therefore, interesting to compare the pull-off strength for these mortars to the work of cohesion of the drained binders. The pull-off strengths are included in Table 6-8 and Figure 6-7 shows a comparison between the work of cohesion and pull-off tensile strength. Error bars in Figure 6-7 represent plus and minus one standard error. The work of cohesion results cover just a small range of values, but it was found that higher pull-off tensile strength corresponds to higher work of cohesion. These results are consistent with data obtained in another recent study (Moraes et al., 2017).

One consistent finding in this study is that all drained binders after mixing with fibres showed higher values for work of cohesion compared to that of the drained base binder. Also, it is noted that all unmodified mortars showed a cohesive failure, while highly modified mortars for 1.0 and 1.2 f/b ratios showed a hybrid failure (partially between aggregate and mortar) together with an increase in pull-off strength. These observations indicate that adding fibre increases the cohesive strength of the mortar leading to hybrid failure.

The work of adhesion results is shown in Table 6-9. It is interesting to note that drained binder after mixing with cellulose fibre had the lowest value of work of adhesion. This is due to the low value of the Lewis base parameter of surface free energy of the drained binder after mixing with cellulose fibre. This finding may explain the hybrid failure for mortar modified with cellulose fibre at 0.8 filler to bitumen ratios and 1.0 and 2.0% fibre, while other modified mortars showed cohesive failure at this filler to bitumen ratio (see Table 6-3). These surface energy results support the ability of the PATTI test to detect differences in bond strength. However, none of the pull-off tensile strength samples showed purely adhesive failure because pull-off tensile strength tests were done at room temperature (20℃) and in dry conditions. These conditions eliminate the possibility of adhesive failure

(Zhang et al., 2017, Caro et al., 2009). Therefore, this study was not able to find a relationship between the pull-off tensile strength and the work of adhesion.

Table 6-8 Work of cohesion (2 γ^{total}) and pull-off tensile strength values (0.8 filler to bitumen ratios and 0.5% fibre)

Sample	Pull-off tensile strength (MPa) 0.8 f/b ratio	Work of cohesion (mJ/m^2)
Drained base binder	1.19	35.53
Drained Cellulose	1.84	37.35
Drained Glass-s	1.85	37.76
Drained Glass-l	1.95	40.36
Drained Steel	1.81	35.80

Table 6-9 Work of adhesion results

Sample	Work of adhesion (mJ/m^2)
Drained base binder	122.69
Drained Cellulose	125.18
Drained Glass-s	172.88
Drained Glass-l	158.64
Drained Steel	163.21

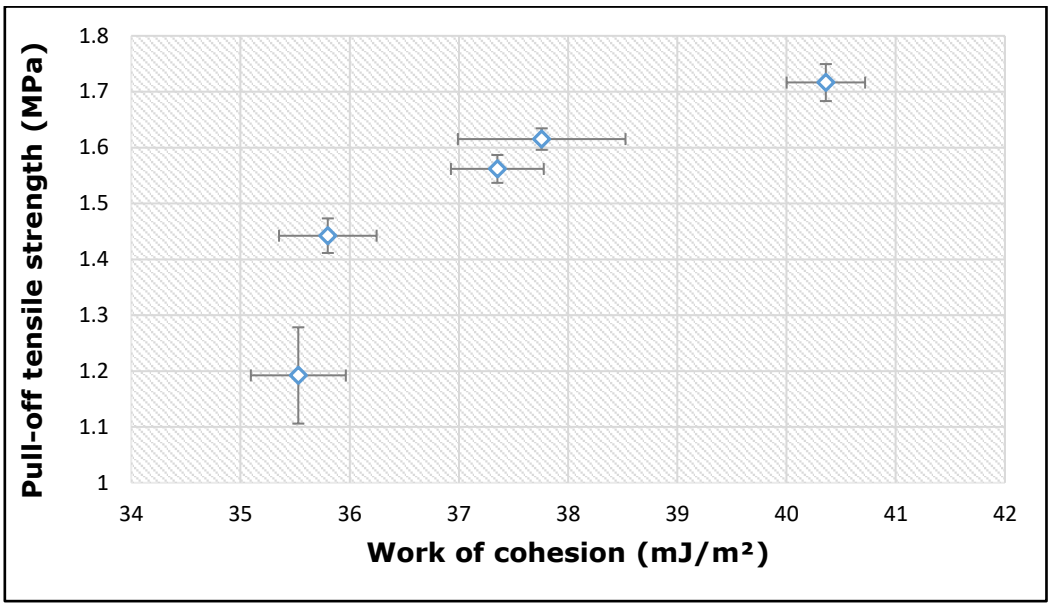


Figure 6-7 Comparison between work of cohesion of drained binders and pull-off tensile strength of 0.8 filler to bitumen ratio and 0.5% fibre mortars (specimens undergoing cohesive failure)

6.5 Summary and conclusions

This chapter has explored the potential for chemical modification of the binder due to the presence of fibres, by means of work of cohesion and work of adhesion calculations, based on surface energy parameters and a binder drainage test. The study also evaluated the influence of different filler to bitumen ratios and fibre percentages on pull-off tensile strength based on the PATTI test results. Based on the discussion and analysis described in this chapter, the following conclusions can be drawn:

- The drainage test results showed that cellulose fibre can retain more than 55% of binder. Other fibre types (glass and steel) can retain up to 30% of binder.
- All fibre types increased asphaltene content and complex modulus of the drained binder compared to the base binder. However, the differences

between asphaltene contents for different fibre types were too small to discriminate between them with confidence.

- Adding fibre led to an increased pull-off tensile strength of the mortars, at the same time changing the failure mode from cohesive to hybrid, implying an improvement in cohesive strength of the mortar.
- There was a general reduction in the pull-off tensile strength of the 1.2 filler to bitumen ratio at high fibre content (2.0%).
- The surface energy of drained binder after mixing with fibres was estimated by dynamic contact angle (DCA) measurements. The contact angle results for each drained binder varied within a narrow range, making this a useful test for characterising the differences in the surface energy of different binder types.
- In general, there is a good agreement between work of the cohesion and pull-off tensile strength for 0.8 filler to bitumen ratio and higher work of cohesion results in higher pull-off tensile strength where the mode of failure is cohesive.
- Exploring the influence of these fibres on adhesive strength would require different test conditions.

Chapter 7 Permanent deformation

Permanent deformation resistance

7.1 Introduction

Permanent deformation is a phenomenon where pavement deforms plastically, due to residual strains occurring under the wheel paths. Under repetitive load, this accumulates and appears in the pavement as permanent deformation. The residual strains are mainly due to the compaction of different pavement layers and shear strains. Therefore, this type of behaviour is a feature of every layer. Shear strains are greatest if the applied stress level and pavement temperature, under traffic loads, are higher (Laurinavicius and Oginskas, 2006).

Permanent deformation, or rutting, is a major concern for the integrity of road structures and traffic safety. It is considered dangerous for traffic, especially when the pavement is wet, increasing the risk of skidding (on water or ice). It also helps water to soak into the pavement, and this causes rapid pavement deterioration. In addition, rutting leads to increased friction between the pavement and the side of the tyre, thereby increasing the consumption of fuel and tyre wear. Rutting produces an uneven surface along the length of the road, and this leads to user discomfort (Olsson et al., 2000, Dawson and Kolisoja, 2006, Laurinavicius and Oginskas, 2006).

There are different methods to improve pavement rutting resistance. Studies show that rubber added to conventional binders leads to improvement in permanent deformation resistance (Way, 2003, Sebaaly et al., 2003). Another study found that 9%wt crumb tyre rubber added to bitumen enhanced the resistance to permanent deformation at high service temperatures (Navarro et al., 2004). Another way to improve pavement rutting resistance is by manipulating aggregate shape and studies have evaluated the effect of fine aggregate angularity (Topal and Sengoz, 2005). However, adding fibre represents a further way to improve rutting resistance of asphalt mastics and mixtures by improving the stiffness of the mastic and elastic response of the mixture (Tapkin et al., 2009, Mahrez et al., 2005, Mohammed et al., 2018).

This chapter investigates the influence of fibre on the multiple stress creep recovery (MSCR) of bituminous mastic in order to examine the influence of fibre on the elastic recovery of the bitumen at different stress levels. The performance of fibre reinforced asphalt mixtures is then examined in the immersed Hamburg wheel tracking test and repeated load axial test (RLAT).

7.2 Characterisation

Three different mechanical experiments were conducted; multiple stress creep recovery test (MSCR), repeated load axial test (RLAT) and immersed Hamburg wheel tracking test. The target air void level for all asphalt mixtures was 7%. All mixture specimens were compacted with the roller compactor.

7.2.1 Multiple stress creep recovery (MSCR) test

A Malvern instruments CVO model Dynamic Shear Rheometer (DSR) was used in this study for measuring the multiple stress creep recovery (MSCR) properties of base bitumen and fibre reinforced mastic as shown in Figure 7-1. The test consists of applying repeated shear stress cycles, with one second applied stress followed

by nine seconds rest period. The test results represent the average of two replicate tests. The tests were carried out according to the ASTM D7405 (2010) procedure. Ten shear stress levels were used to examine the stress sensitivity and strain recovery of base bitumen and fibre reinforced mastics. The following conditions were used for the MSCR test:

- Stress levels were 25, 50, 100, 400, 800, 1600, 3200, 6400, 12800 and 25600 Pa; there was no time lag between cycles
- Test temperature was 50℃
- Each stress level included 10 cycles
- 25 mm diameter and 1 mm gap parallel plate geometry was used
- The non-recoverable creep compliance (Jnr) and percent recovery (R) were calculated according to the following equations:

$$J_{nr} = \frac{\varepsilon_u}{\sigma}$$ Equation 7-1

$$R = \frac{\varepsilon_p - \varepsilon_u}{\varepsilon_p} \times 100\%$$ Equation 7-2

where ε_u is the non-recovered strain, σ is the shear stress level and ε_p the peak strain.

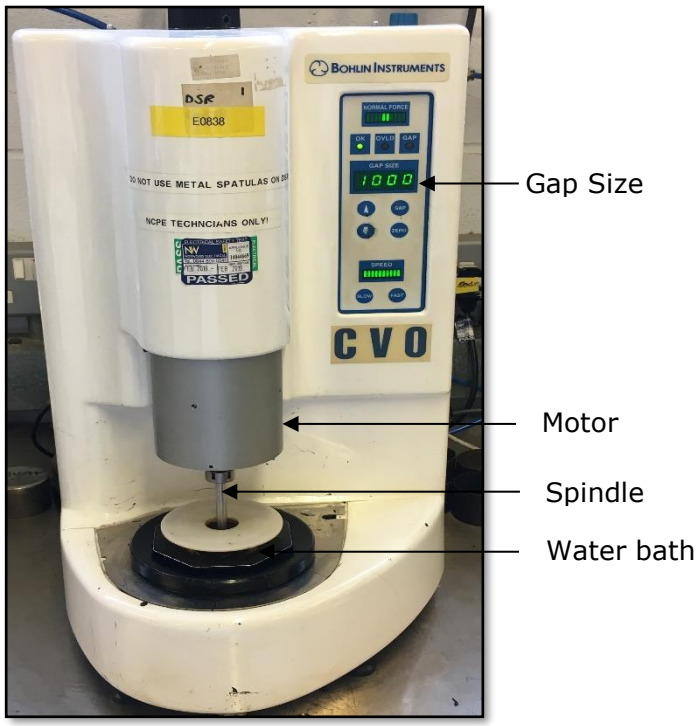


Figure 7-1 Malvern instruments CVO model dynamic shear rheometer (DSR)

7.2.2 Immersed Hamburg wheel tracking test

A wheel tracking testing machine according to BS EN 12697-22 (2003) standard was used for examining the permanent deformation resistance of control and 2.0% fibre reinforced asphalt mixtures immersed in water. Asphalt mixture was compacted into slabs with a laboratory steel roller compactor. Slab test specimens with dimensions of 300 mm width, 300 mm length and 50 mm height were tested. The test was performed at 50℃. A solid rubber wheel travels back and forth along the centre of the top surface of the test slab with a 230 mm total distance of travel at a constant rate (26.5 loading cycles per minute) to simulate traffic as shown in Figure 7-2. The test continues tracking until 20,000 load passes are applied or 20 mm rut depth forms, whichever occurs first.

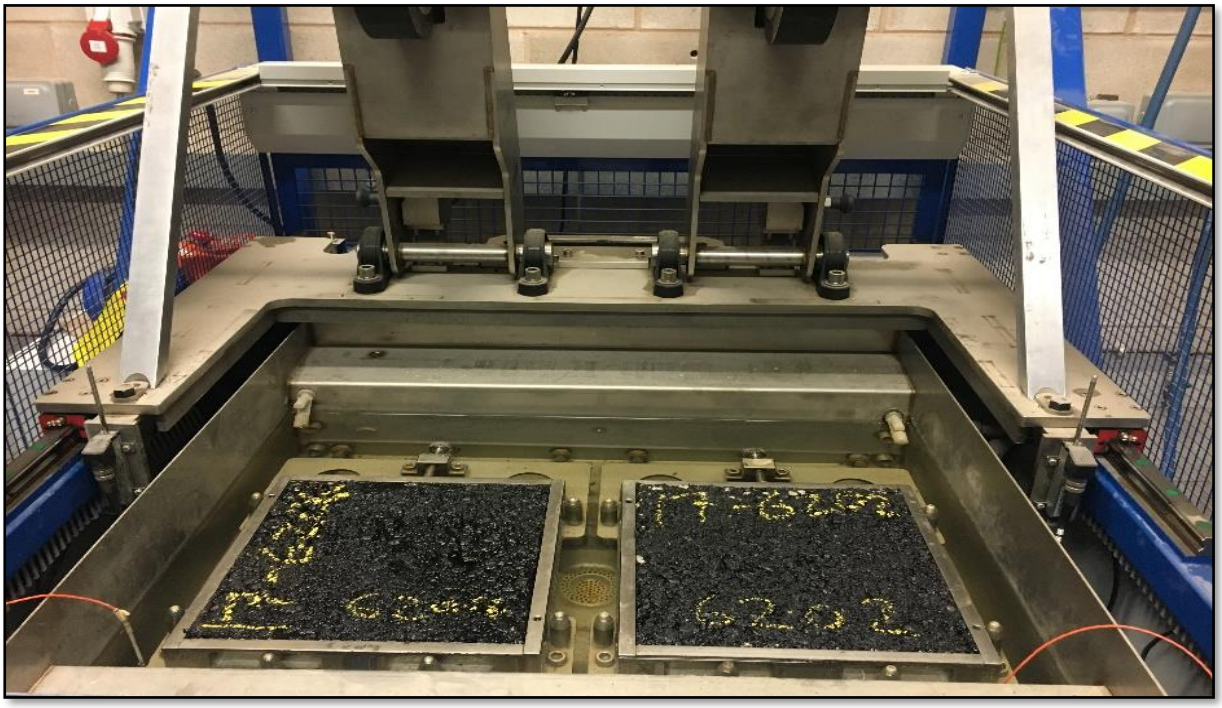


Figure 7-2 Immersed Hamburg wheel tracking test configuration

7.2.3 Repeated load axial test (RLAT)

The test was performed according to BS EN 12697-25 (2016) using the Nottingham Asphalt Tester (NAT) machine. Three replicate core specimens were tested with dimensions of 100 mm diameter and 45 mm thickness. After conditioning the specimen for four hours in a temperature controlled cabinet, the specimen and assembled platens were aligned concentrically with the loading axis and the actuator of the NAT attached to the platens. The machine applies a repetitive harversine load and measures the vertical deformation after each repeated load by means of two linear variable differential transformers (LVDTs) fixed on the surface of the loading frame as shown in Figure 7-3. The test was performed at 30℃, with 5000 cycles test duration, 1 second loading time followed by 1 second rest period and axial stress of 100 kPa. The following equation was used to calculate the accumulated strain:

$$\varepsilon = \left(\frac{\Delta h}{H_o}\right) \times 100 \qquad \text{Equation 7-3}$$

where ε: is the cumulative axial strain (%), Δh is the average axial deformation (mm) and Ho is the average initial specimen height (mm).

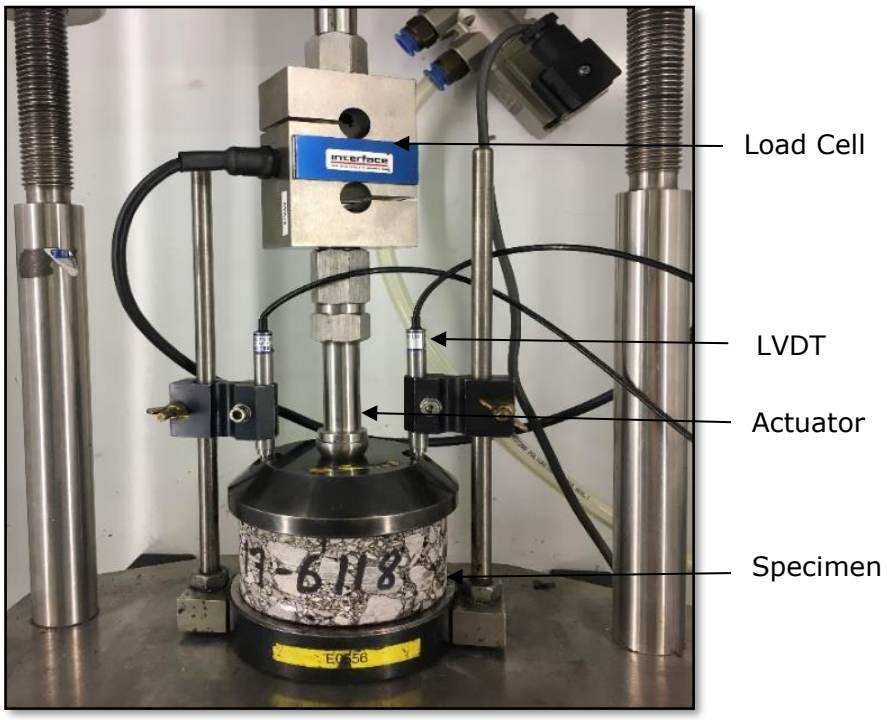
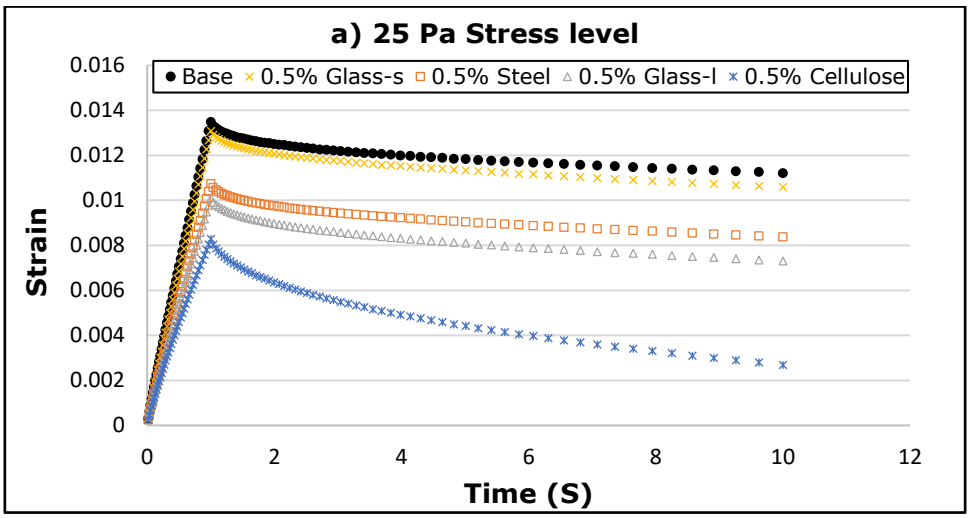


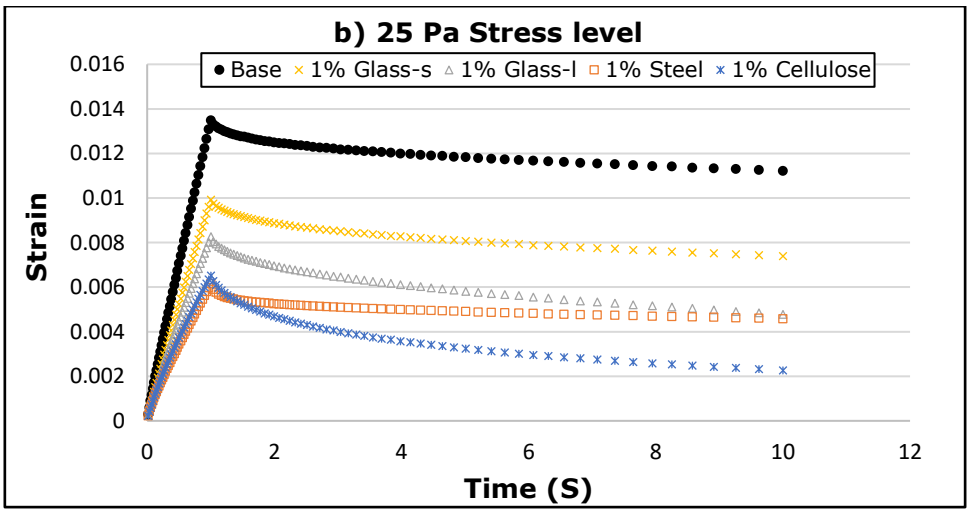
Figure 7-3 RLAT test configuration

7.3 Results and analysis

7.3.1 Multiple stress creep recovery (MSCR) results

MSCR tests were conducted on the base (un-aged) binder and fibre reinforced (un-aged) binders at 50℃. Figure 7-4 (a, b and c) and Figure 7-5 (a, b and c) show the instantaneous and peak strains of the base binder and fibre modified mastics at 25 and 3200 Pa stress levels, respectively. Figure 7-6 shows the % recovery (%R) at different stress levels, which gives an indication of the elastic response of the base and modified mastics. A high %R gives an indication that the asphalt mastic has a superior elastic response. Figure 7-7 illustrates non-recoverable creep compliance (Jnr) at different stress levels.





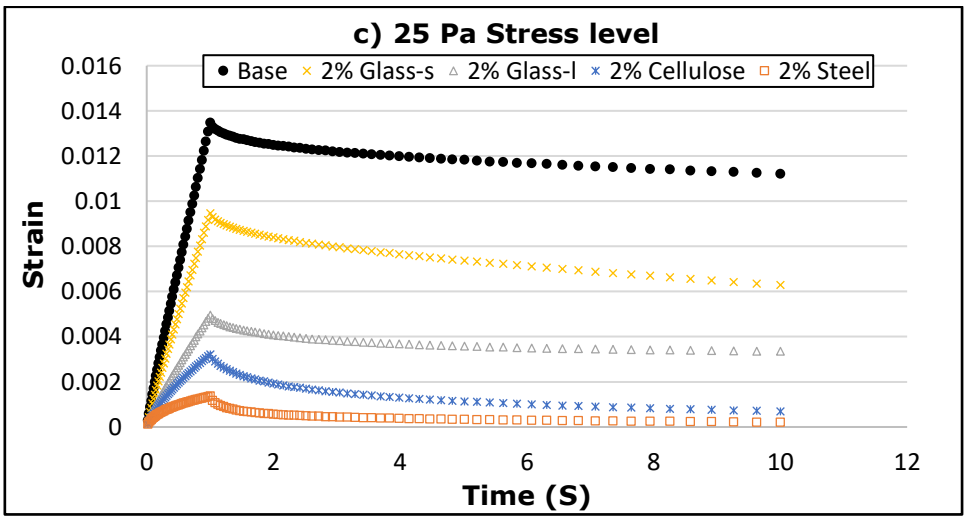
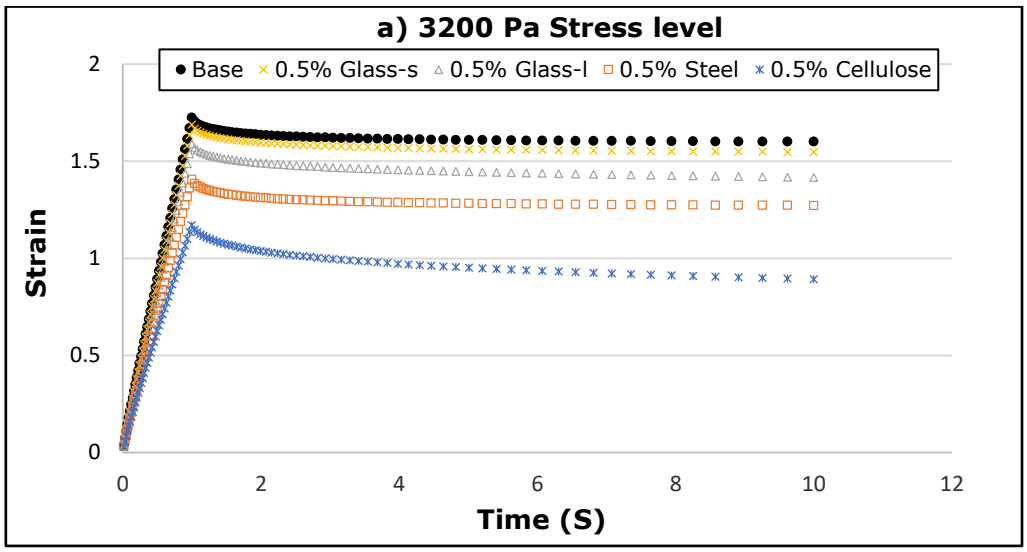
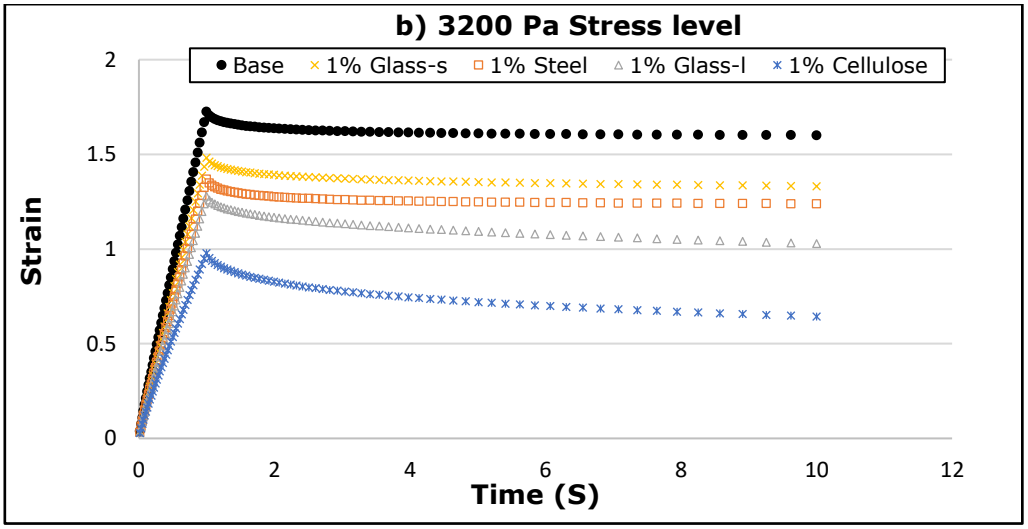


Figure 7-4 a, b and c Deformation recovery for the base and fibre modified asphalt mastic at 50℃





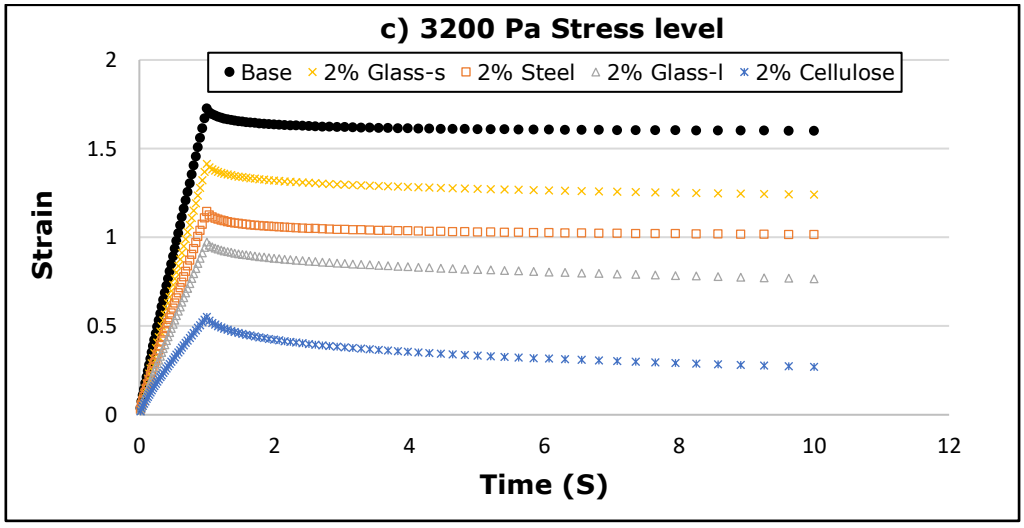


Figure 7-5 a, b and c Deformation recovery for the base and fibre modified asphalt mastic at 50℃

7.3.1.1 Effect of fibre content

The peak strain after loading at one second and the irrecoverable strain after unloading for nine seconds, decrease with the increase in fibre content, as shown in Figure 7-4 and Figure 7-5. The peak strains of fibre modified mastics are lower than that of the base bitumen. This indicates that adding fibre improves the stiffness and the elastic recovery of bitumen and this improvement increases with the increase in fibre content. These results are in line with the complex modulus results that were obtained by the dynamic oscillatory test, as shown earlier in chapter four. It is clear from Figure 7-4 and Figure 7-5 that cellulose fibre shows the highest improvement in mastic rutting resistance followed by steel fibre at low stresses and glass long fibre at high stresses.

7.3.1.2 Effect of stress level

It is clear from Figure 7-6 and Figure 7-7 that stress level has a significant effect on the high-temperature performance of base binder and modified mastics. Asphalt mastic irrecoverable creep compliance (Jnr) increases, and recovery rate (%R) decreases with the increase in stress from 25 Pa to 25600 Pa. Cellulose fibre has a significant influence on %R and Jnr, especially at stresses lower than 6400 Pa compared to the other fibre types and base binder. The results, as shown in Figure 7-7, indicate that at a certain stress level, the sensitivity to stress increases and differences in mastic response were marked. Several reports have shown that a high Jnr value indicates poor resistance to permanent deformation (Gajewski et al., 2015, Krol and Matraszek, 2012, Zhang et al., 2015b).

A previous study recommended the Jnr over the rutting parameter ($G^*/\sin\delta$) when evaluating the rutting resistance of the different binders (D'Angelo et al., 2007). The sensitivity of the Jnr value to the applied stresses on the base and modified binder makes this parameter suitable for specification purposes for both (Tabatabaee and Tabatabaee, 2010, D'Angelo, 2009). It seems reasonable to

examine the performance of binder at high stresses and outside the linear viscoelastic region due to the fact that the strains in binder films on aggregate surfaces can be several times greater than the average strain of the mixture.

The MSCR test results show a slightly different ranking from the rutting parameter obtained by the dynamic oscillatory test (see chapter four), and this difference is mainly associated with steel fibre. Steel fibre showed poor influence on the rutting parameter when added to the asphalt mastic, while it has a marked influence on the Jnr, %(R) and peak strain values over a wide range of stresses at the 50℃ test temperature. The difference in ranking between the two tests is not surprising for various reasons. Many factors related to the two tests are not equal. For instance, the stress value, loading and recovery times and nonlinearity may all play an important role in affecting the response of mastics tested under dynamic oscillatory, or, under MSCR conditions. Further investigation on the effect of those binders on the rutting resistance of asphalt mixtures has been examined and is presented in the next section.

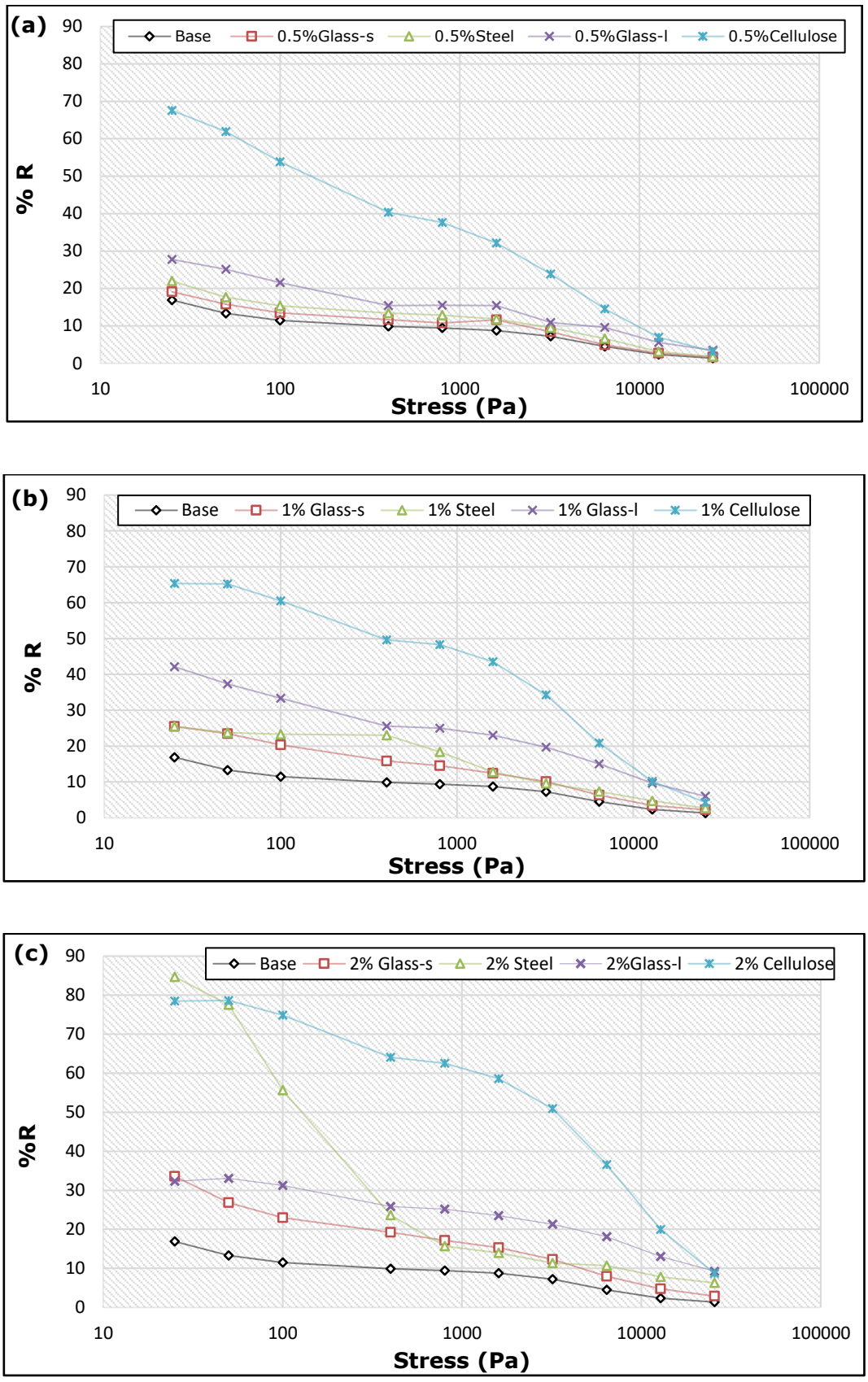


Figure 7-6 Relationship of stress with %R at different fibre types and contents at 50℃

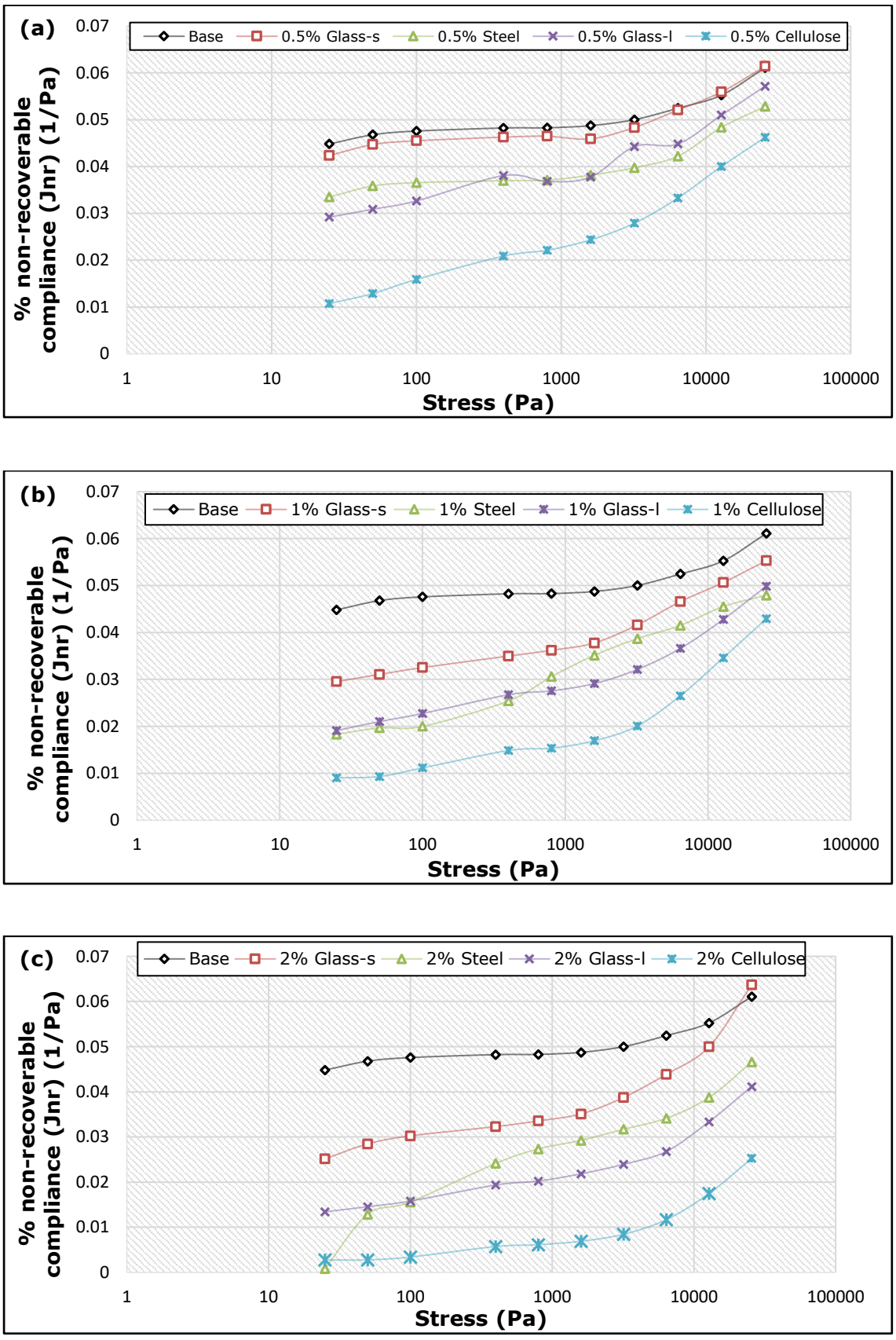


Figure 7-7 Non-recoverable creep compliance (%Jnr) obtained from MSCR tests at 50℃

7.3.2 Immersed Hamburg wheel tracking test results

7.3.2.1 Permanent deformation curve

Figure 7-8 presents the rut depth curves of control and fibre reinforced asphalt mixtures immersed in water for one slab specimen. None of the asphalt mixtures reached 10 mm rut depth during the loading period of 20,000 passes at the 50℃ test temperature.

It can be seen that the rut depth of the control asphalt mixture increased significantly with a number of load cycles. The fibre reinforced asphalt mixtures show much lower permanent deformation increase rate after the first 4000 cycles. None of the asphalts showed the third stage of accelerated rutting associated with weaker mixes (Zhou et al., 2004). It is important to note that the difference between the rut depths of fibre reinforced asphalt mixtures and control mixture reached its highest value at 20,000 passes. This indicates that there is probably more improvement in rutting resistance with further increase in the number of passes (see Figure 7-8).

A comparison between the control and reinforced slabs shows that the reinforcement exhibited significant resistance to deformation and, therefore, the build-up of rut depth. An analysis of both the graph and test data clearly show that in the specimens containing fibres the rut depth is significantly lower than in control asphalt mixtures. The reduction in rut depth was found to be as high as 43.5, 40.2, 39.8 and 33.0% with the addition of 2.0% cellulose, glass-l, steel and glass-s fibres, respectively, into the original mixture. Previous studies have found that stone mastic asphalt shows good resistance to permanent deformation (Cooley Jr and Brown, 2001). The presence of cellulose fibre may be one of the reasons for this high permanent deformation resistance, not only the aggregate gradation.

Although there are agglomerations of glass fibres at 2.0% addition at some places in the slab, glass-l fibres led to a significant decrease in rut depth.

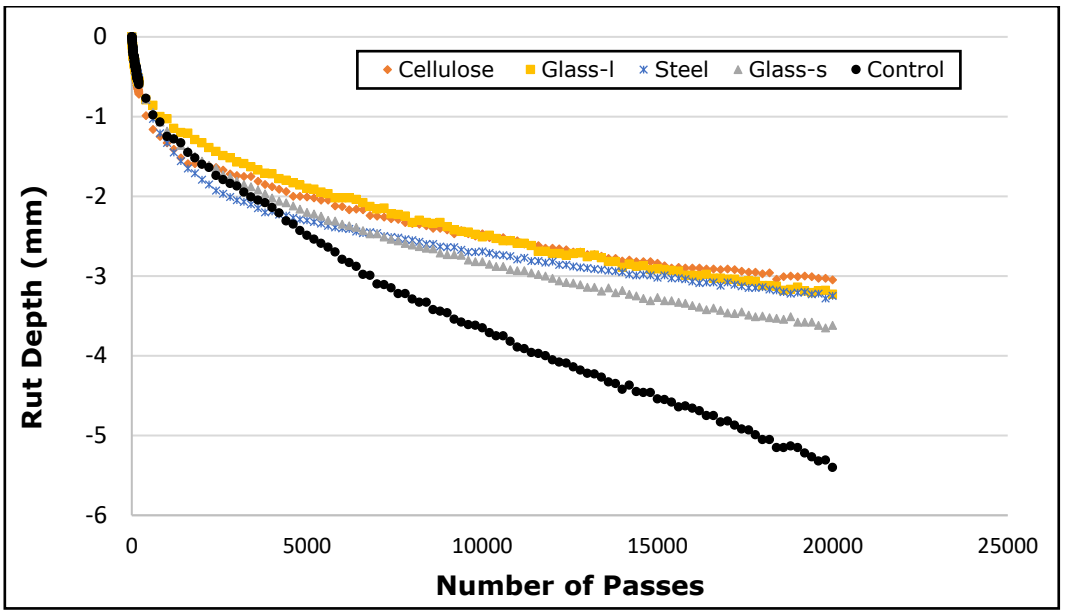


Figure 7-8 Immersed Hamburg wheel tracking results at 50℃ for control and 2.0% fibre reinforced asphalt mixture

7.3.2.2 Dynamic stability (DS)

Dynamic stability (DS) was used as an index of high temperature stability for control and fibre reinforced asphalt mixtures (Fakhri and Hosseini, 2017). Dynamic stability was calculated as follows:

$$DS = \frac{(t_2 - t_1) \times N}{d_2 - d_1}$$ Equation 7-4

where t_1 and t_2 are times, 45 and 60 minutes respectively, N is the rate of the wheel track test in cycles per minute and d_1 and d_2 are the deformations at t_1 and t_2, respectively.

The higher the DS values, the higher the permanent deformation resistance of the asphalt mixture. Several studies have recommended specific values for DS depending on the highest expected temperature and the highest expected traffic load. For instance, the DS of mixes experiencing daily temperatures higher than 30℃, from 20℃ to 30℃ and lower than 20℃ are recommended to have a minimum DS of 1500 cycles/mm, 1000 cycles/mm and 800 cycles/mm, respectively (JTG E20, 2011, Li and Li, 2012). Another study recommended that the DS should be minimum 3000 for heavy traffic and 800 for light and medium traffic (Poulikakos and Partl, 2003). On the other hand, if two mixtures have similar secondary rutting rate (the stage when rut depth per cycle tends to reach a constant value), the DS would not be able to distinguish between mixtures (Tarefder, 2003).

Figure 7-9 shows the DS of control and fibre reinforced asphalt mixtures. Compared with the control mixture, the value of DS for the cellulose fibre asphalt mixture is increased by 90.0%.

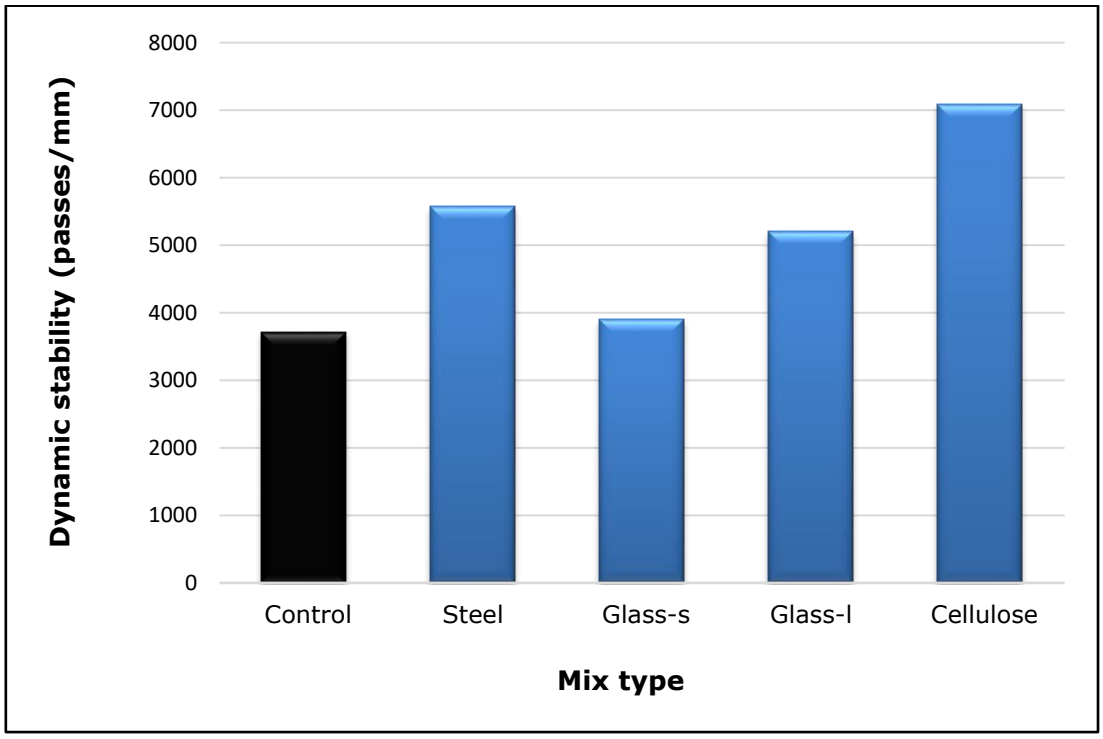
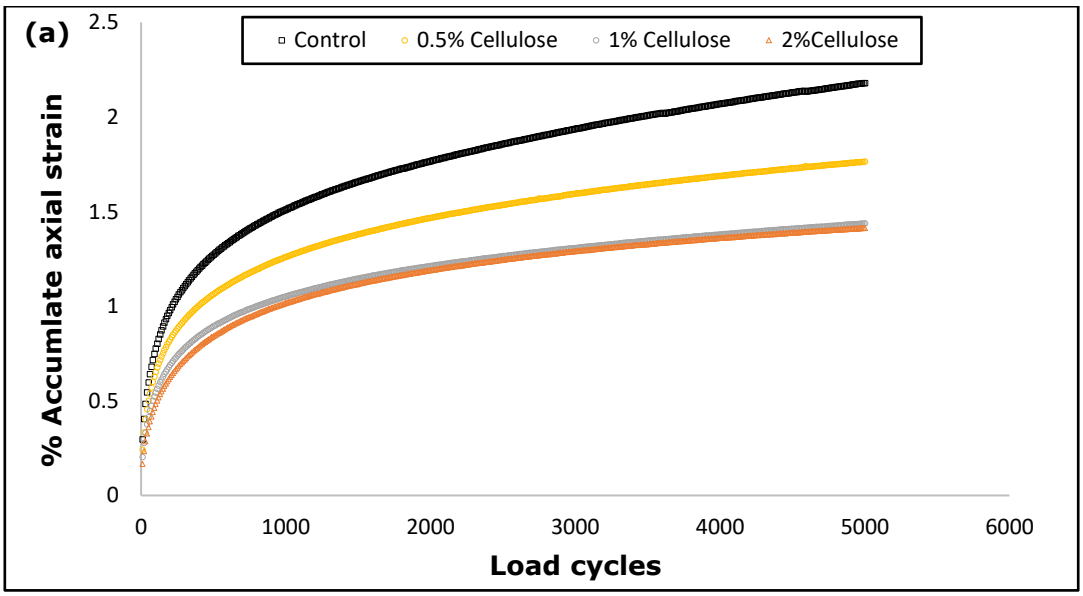


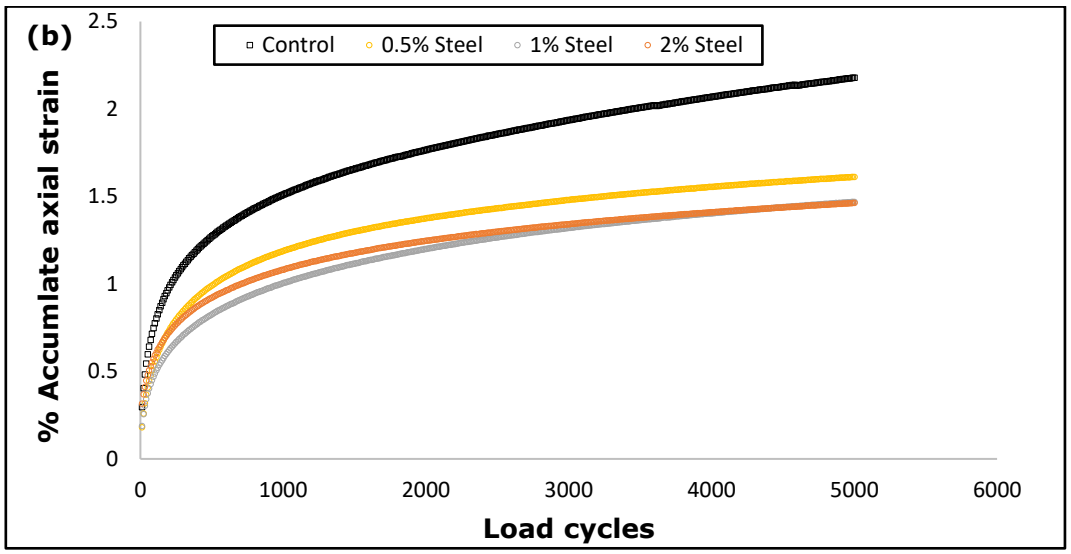
Figure 7-9 Dynamic stability of control and 2.0% fibre reinforced asphalt mixtures

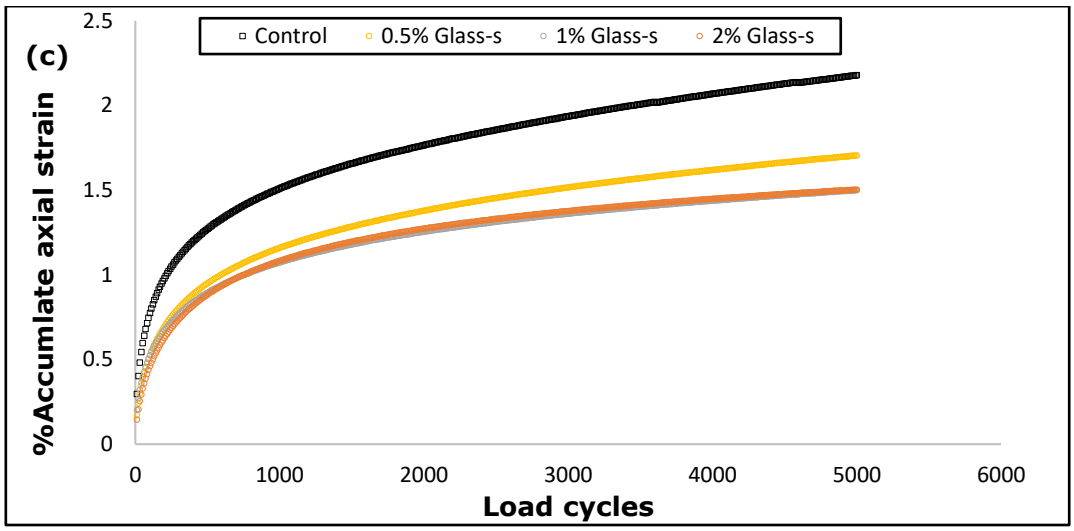
7.3.3 Repeated Load axial test (RLAT)

7.3.3.1 Permanent strain curve

The permanent strain curves of control and fibre reinforced asphalt mixtures are shown in Figure 7-10. In general, permanent strain curves consist of three stages, primary, secondary and tertiary. The primary stage may be defined as the densification stage, while the secondary stage approaches a constant value of strain accumulation rate. The tertiary stage shows a rapid increase in accumulated strain per cycle (Zhou et al., 2004). The asphalt mixtures in this study did not show a tertiary stage during the loading period of 5000 cycles at 100 kPa stress level and 30℃. Lower permanent axial strain values indicate that mixtures have higher rutting resistance potential. It is clear from Figure 7-10 that the fibre reinforced asphalt mixtures showed lower cumulative permanent strain compared to the control mixture. Although the permanent strain curves for 1.0% and 2.0% cellulose fibre asphalt mixtures were almost the same, it is possible that more severe test conditions such as higher temperature, stress level or a number of cycles would show a difference between them.







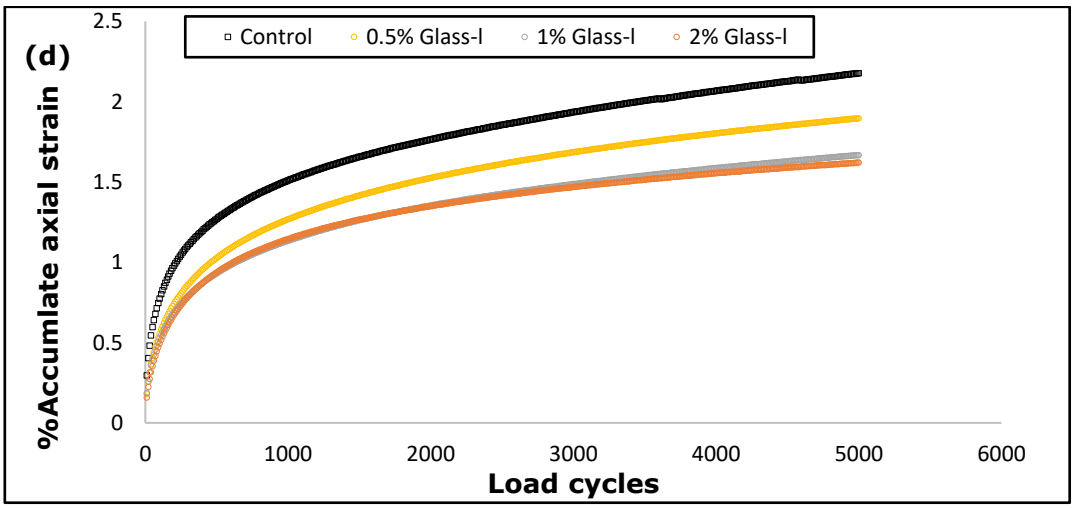


Figure 7-10 (a, b, c and d) Accumulate axial strain versus load cycle for control and fibre reinforced asphalt mixture

7.3.3.2 Ultimate strain

Figure 7-11 shows the results of strain after 5000 load cycles, where error bars represent plus and minus one standard error. It is clear that the ultimate strain of fibre reinforced asphalt mixtures improves significantly compared to the control mixture. The ultimate strain values of fibre reinforced asphalt mixtures containing 2.0% cellulose, steel, glass-s and glass-l fibre are about 35, 33, 31 and 26% lower than the value of the control mixture, respectively. This indicates that adding fibre to the asphalt mixtures makes a significant impact on the susceptibility of the mixtures to permanent deformation.

The strain rate (micro-strain per cycle) during the secondary stage was used to gain a better understanding of the rutting resistance performance of the asphalt mixtures. This gives a more reliable indication of the permanent deformation of the asphalt mixtures because it is not dependent on the initial densification stage. The strain rate (με/cycle) over the steady state phase of the accumulated axial strain curve was calculated between 1800 to 3600 pulses (Brown and Gibb, 1996). It may be noted that the strain rate for 1.0% and 2.0% fibre reinforced asphalt mixtures was lower than that of the control mixture, as shown in Figure 7-12. This implies that the control mixture will transition to the tertiary stage more rapidly than the fibre reinforced asphalt mixtures, which would mean that adding fibre will delay deterioration in asphalt mixtures, leading to longer service life and a more comfortable drive for road users when used in pavement construction.

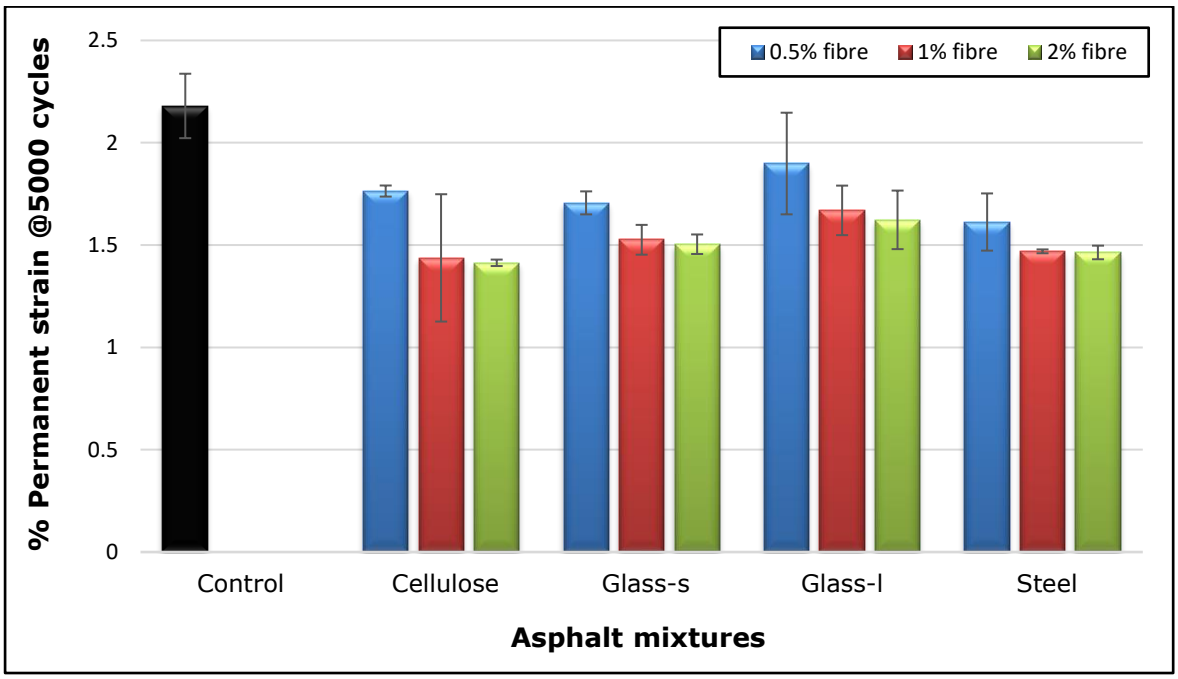


Figure 7-11 Ultimate strain of control and fibre reinforced asphalt mixtures

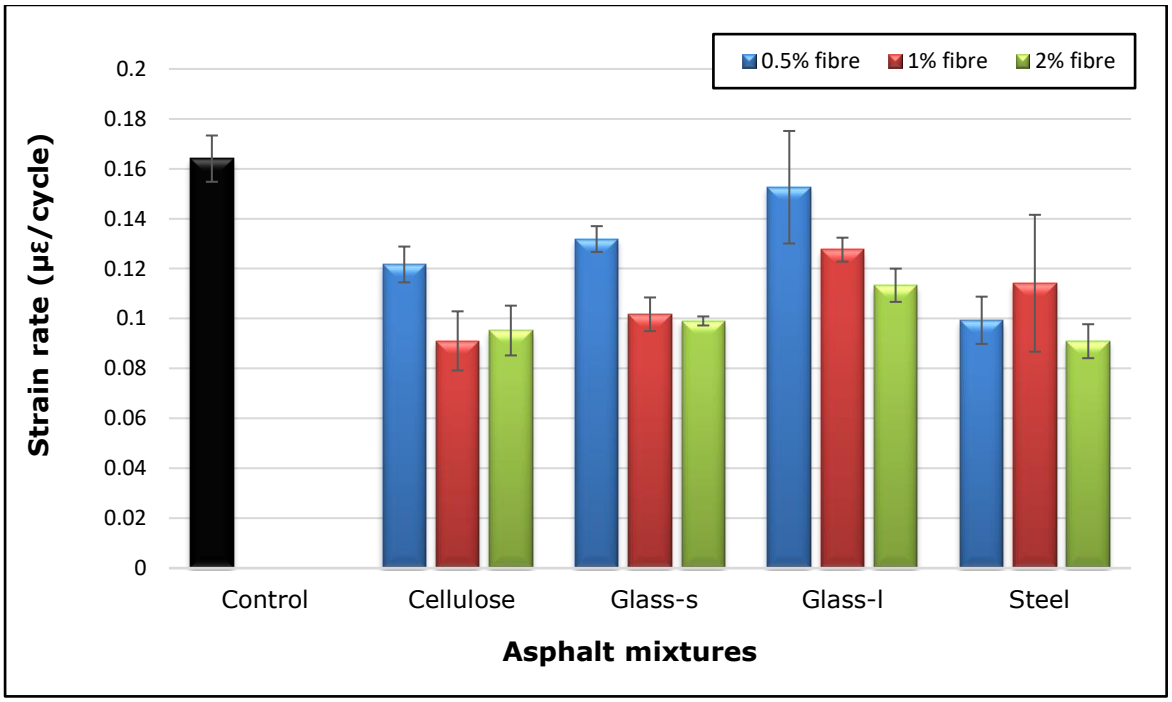


Figure 7-12 Strain rate of control and fibre reinforced asphalt mixtures

7.4 Discussion

Analysis of the multiple stress creep recovery (MSCR) parameters, as measured with the DSR, has shown that adding fibre led to improved temperature and stress sensitivity (elastic recovery) of modified mastic compared to the base binder and with benefits in terms of permanent deformation resistance (increased stiffness and elastic response). This is likely to be due to two mechanisms, firstly asphalt and cellulose fibre having good absorption/adsorption and adhesion ability (Silva, 2008, Mohamadzadeh et al., 2014). Cellulose absorbs/adsorbs and stabilises free asphalt, and therefore, asphalt viscosity and cohesive strength increases as shown earlier in drain down results (see chapter six). Secondly, the ability of fibres (steel, glass and cellulose) to form three dimensional networks may further enhance permanent deformation resistance and encourage elastic recovery (see SEM images in chapters four and five) (Mohammed et al., 2018, Fu et al., 2000, Thanh et al., 2011). Increasing the fibre content led to greater reinforcement effect, thereby reducing the amount and risk of irrecoverable flow (Putman, 2011).

The improvement in permanent deformation resistance of the mixtures mirrors the improvement in high temperature performance as predicted by MSCR and dynamic oscillatory tests on mastics. At high temperature (50℃) the immersed Hamburg wheel tracking test result is also likely to be related to the ability of cellulose fibre to absorb/adsorb bitumen, which would reduce the flow of bitumen. The anti-shearing capacity of the mastic is increased. Moreover, the rough and interwoven surface texture of cellulose fibre, as shown in SEM images (see chapter three), may also improve the bonding strength of the mastic. The interlacing of the fibre (steel, glass and cellulose) horizontally and vertically and good distribution in the asphalt mixture may lead to the spread of the load stresses, which may also help to reduce permanent deformation as shown earlier in SEM images of the mastics and CT X-ray of fibre reinforced asphalt mixture in the following chapter.

Also, RLAT test results show that the ultimate strain of fibre reinforced asphalt mixtures improves significantly compared to the control mixture which is in agreement with the test results of MSCR and rutting parameters of the asphalt mastics.

7.5 Summary and conclusions

The resistance of fibre reinforced asphalt mastics and mixtures at moderate and high temperatures to permanent deformation has been examined in this chapter. The MSCR test has been used to investigate the influence of different fibre types and amounts, on the irrecoverable creep compliance and percent recovery of the binder. Immersed Hamburg wheel tracking and RLAT tests are used to investigate the permanent deformation resistance of asphalt mixtures incorporating these binders. The following conclusions can be drawn from this chapter:

- Adding fibre led to significant improvement in permanent deformation resistance of the modified mastics; decreasing the irrecoverable creep compliance (Jnr) and increasing the recovery (%R) value.
- The influence of fibre on permanent deformation resistance of asphalt mastics was more marked at low stresses compared to high stresses.
- Immersed Hamburg wheel tracking test results showed that the rut depth of 2.0% cellulose, glass-l, steel and glass-s fibre reinforced asphalt mixture was significantly lower than that in the control asphalt mixture and the reduction in rut depth was found to be 43.5, 40.2, 39.8 and 33.0%, respectively.
- Adding fibre led to a significant improvement in the dynamic stability (DS) of asphalt mixture.
- The study results indicated that there is a good agreement between MSCR test results and immersed Hamburg wheel tracking test results.

- Repeated load axial test (RLAT) results confirm the improvement in permanent deformation resistance of fibre reinforced asphalt mixtures.
- Reported cellulose fibre absorption/adsorption of bitumen, and the reinforcement mechanism of interlacing steel and/or glass fibres results in lower permanent deformation in the asphalt mixtures.
- The combined MSCR, immersed Hamburg wheel tracking and RLAT tests led to the same conclusion, which is that adding fibre significantly delays the build-up of rut depth in an asphalt mixture, which may lead to longer service life and a more comfortable drive for road users.
- Cellulose fibre showed the highest improvement in permanent deformation resistance of mastic and/or asphalt mixture compared to other fibre types.

Chapter 8 Other Mechanical properties

Microstructure and mechanical properties

8.1 Introduction

In the previous chapter, it was found that fibre reinforced asphalt mixtures tested in the repeated load axial test (RLAT) at 30℃ and immersed Hamburg wheel tracking test at 50℃ showed a significant improvement in permanent deformation resistance compared to asphalt mixture without fibres. Further investigation into the mechanical properties of fibre reinforced asphalt mixtures would increase the level of confidence of using these mixtures.

A good quality pavement is fundamental to guarantee a long service life. Such a pavement must be capable of providing a smooth ride and high resistance to thermal cracking, withstand large traffic volumes and effectively transfer the load to the underlying support. This chapter examines the influence of different types and percentages of fibre on asphalt mixture stiffness, fatigue cracking resistance based on the indirect tensile fatigue test (ITFT), moisture damage resistance based on indirect tensile strength ratio (ITSR), and fracture toughness at low and moderate temperatures using the semi-circular bending test (SCB). Furthermore, X-ray CT is used to observe the presence of fibres and their entanglement in the asphalt mixture in order to provide a better understanding of the fibre reinforcing mechanism.

8.2 Experimental programme

The experimental programme used in this chapter is shown in Table 8-1. These tests are focused mainly on evaluating the most important mechanical properties of asphalt mixtures, in addition to the microstructure of these mixtures. The number of replicates and variables are shown in Table 8-1.

Table 8-1 Experimental programme

Materials	Variables	Test methods	Test replicate	Test temperature
Fibre reinforced asphalt mixture	Fibre content 0.5% 1.0% 2.0%	Indirect tensile stiffness modulus (ITSM)	10	20℃
		Indirect tensile fatigue test (ITFT)	1	20℃
	Fibre type Glass-l Glass-s Cellulose Steel	Dry indirect tensile strength (ITS)	2	20℃
		Wet indirect tensile strength (ITS)	3	20℃
		Moisture damage	5	20℃
		Moisture damage for RLAT specimens	2	20℃
		Semi-circular bending test (SCB)	3	0℃ and 20℃
		X-ray CT	-	-

8.3 X-ray computed tomography imaging

Fibre reinforced asphalt mixtures are complex, heterogeneous, multiple phase composites of, fibres, mastics, aggregates and air voids. The performance of fibre reinforced asphalt mixture is highly dependent on the proportion of these components, in addition to their physical properties, presence and distribution (Mahrez et al., 2005, Cleven, 2000, Alvarado et al., 2007). In asphalt mixtures, the fibre distribution and the way they interact with each other contribute

significantly to their ability in spreading traffic loads. Therefore, their microstructure and distribution play a significant role in performance.

A few studies have explored fibre distribution and entanglement within bituminous binder by using a scanning electronic microscope SEM (Xiong et al., 2015, Chen and Xu, 2010, Mohammed et al., 2018). These studies found that fibre dimensions and surface textures have an influence on the formation of three dimensional networks. The network formed provides support to the composite structure by holding the components together and reducing stress concentration in addition to retaining bitumen at high temperatures (Wiljanen, 2003).

X-ray computed tomography is a non-destructive test. It is a very useful test in medical diagnosis since the first tomographies were constructed in 1973. This technology has gained increasing interest in engineering material research. Thus far, several studies have used X-ray CT for a non-destructive investigation of soils, concrete and asphalt mixtures. A recent study used X-ray CT to assess the distribution and direction of steel fibres in steel fibre self-compacted concrete for a chosen structural model (Ponikiewski and Gołaszewski, 2016). A number of researchers have used X-ray CT together with image analysis techniques to investigate the air voids content, distribution and microstructure before and after testing the specimen (Aboufoul and Garcia, 2017, Masad et al., 2002, Gopalakrishnan et al., 2007).

However, so far, no research effort has been specifically dedicated to investigating the challenges of measuring the actual distributions of different types of fibres in the asphalt mixture. The aim was to explore the usefulness of using X-ray CT along with image analysis techniques to investigate the distribution, orientation and presence of different fibre types in the asphalt mixtures. The advanced imaging facilities will help to achieve a better understanding of the asphalt mixture micro-

structure and define the various parameters that may influence the internal structure and to link them to the asphalt mixture mechanical properties.

8.3.1 General procedure for X-ray CT imaging

X-ray computed tomography (CT) was used in this investigation for the non-destructive characterisation of fibre distribution, orientation and presence in asphalt mixture core specimens with 48 mm thickness and 46 mm diameter that were taken from slabs prepared using a roller compactor. The components of an X-ray CT are shown in Figure 8-1. The test specimen is positioned between a source and a detector. The source emits X-rays which pass through the specimen, and this generates a series of CT images. The intensity value of the X-rays is measured before and after they pass through the specimen. The scanning process is finished when the intensity measurement collection for a full rotation of the specimen has been completed.

The X-ray image represents the distribution of the linear attenuation coefficient. The linear attenuation coefficient represents the amount of photons that are absorbed or removed from the X-rays per unit detector thickness. The higher values of the coefficient are characterised by brighter areas. The analysis is based on the fact that the coefficient value depends directly on the density of the sample at that point. Therefore, it is possible to recognise different features within the specimen. Once the images of X-ray CT are extracted, they show the differences in density at each point in each slice through the specimen. A number of studies have claimed that X-ray CT is highly sensitive to small density differences as low as 1.0% between materials (Dennis, 1997, Masad et al., 1999). One study has pointed out that although a difference in density is essential, the particle size and distribution in the mixture is also important to find out the region of interest. For instance, a gap graded mixture shows higher resolution of grey levels assigned to the different

material phases compared to a dense bitumen mixture as the penetration of X-rays beams will be easier through the gaps (Hassan et al., 2012).

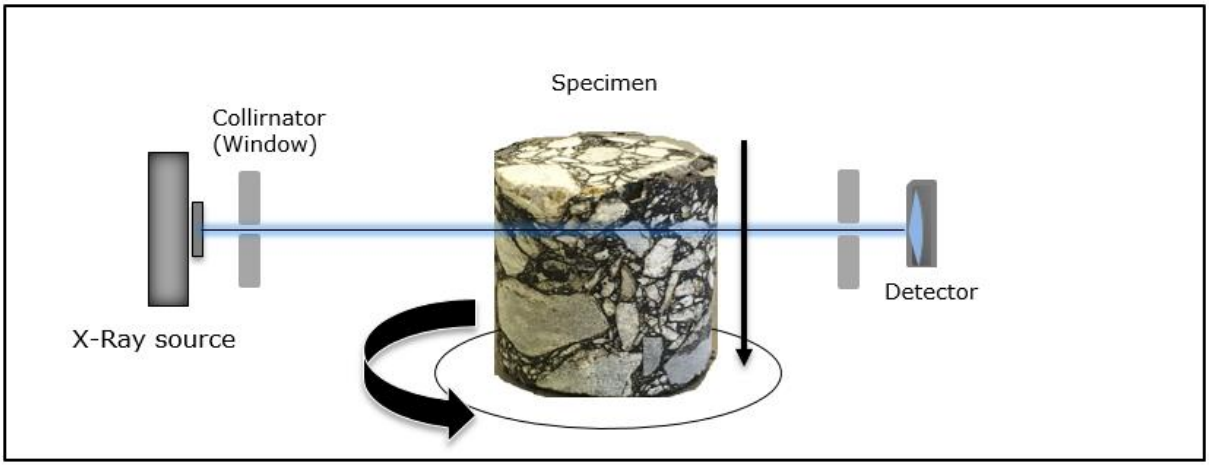


Figure 8-1 Simple configuration for the components of the X-ray system

8.3.2 Results and Discussion

The imaging process can be summarised in three steps: image acquisition, followed by image processing, and then image analysis. An advantage of using X-ray CT imaging is that by creating cross-sectional images, they can be used by specific programs, such as Image J, in the rebuilding of a volumetric (three dimensional) image of any specimen. A greyscale 8-bit image consisting of 256 levels was used in this study. The intensity value used in this study ranged from 0 (black) to 256 (white) for each element in the image. Image quality plays a significant role in the accuracy of the information extracted from an image. Therefore, great care was taken in this study to enhance the image and filter out the noise. This was done by using a Gaussian filter and also by excluding points with very small areas from the results. The Image J program was used to analyse the results and to rebuild a volumetric three-dimensional distribution of fibres, as shown in Figure 8-2.



Figure 8-2 Three dimensional distribution of steel fibres inside asphalt mixture

Although there is slight noise in rebuilding the volumetric distribution of steel fibres, it can be seen from Figure 8-2 that, in the case of steel fibres, the individual fibres were oriented in different directions (horizontal, vertical and inclined at different angles) inside the asphalt mixture specimen. It is clear from Figure 8-3 that steel fibres exist almost everywhere in the asphalt mixture specimen. It should be noted that the area of steel fibres is slightly higher in the middle of the specimen compared to the top and the bottom of the specimen. The aspect ratios (the ratio of the width to the height of an image) of steel fibres are shown in Figure 8-4. The aspect ratio values were higher than 1.5.

It should be noted that this study attempted to investigate the distribution of other fibre types (glass and cellulose) in the same way. The test results were not clear enough to analyse due to the similarity in the density of these fibres and other asphalt mixture components.

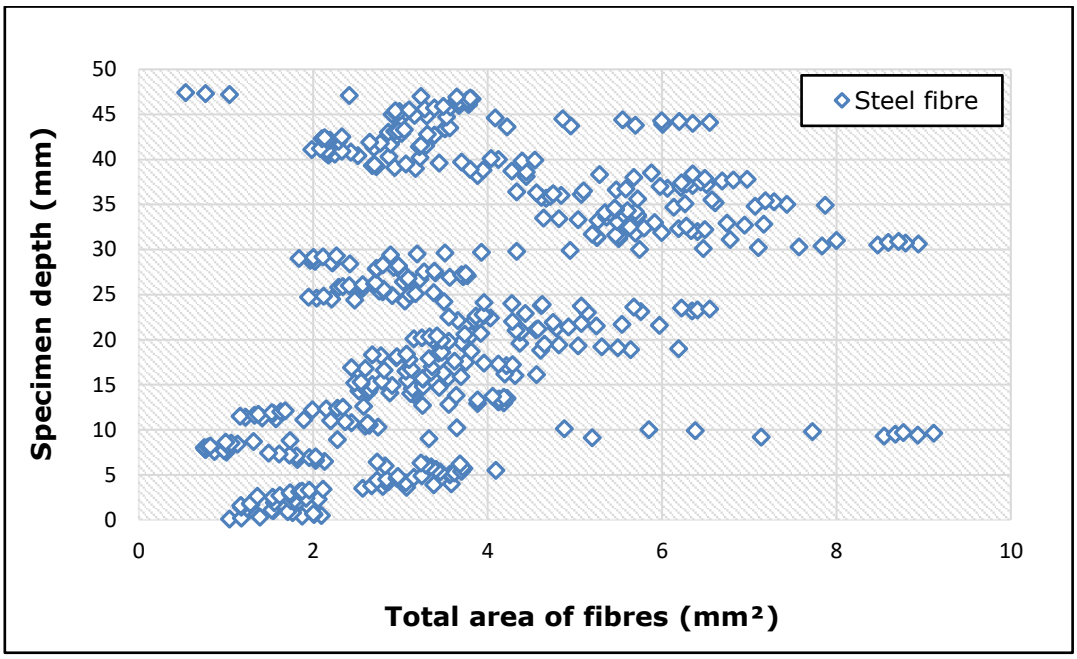


Figure 8-3 Total areas of fibres along with the specimen depth

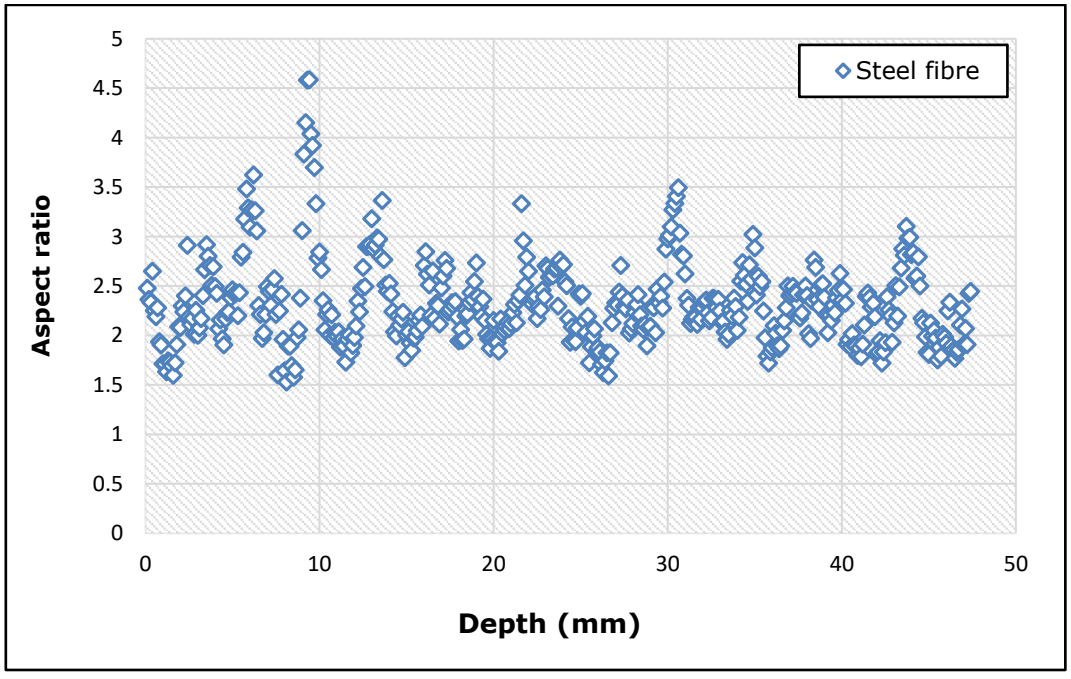


Figure 8-4 Aspect ratio of steel fibres

8.4 Indirect tensile stiffness modulus (ITSM) test

The indirect tensile stiffness modulus test is considered an important property of asphalt mixtures. This test gives an indication of the ability of the pavement to withstand traffic-induced stresses and strains (Asphalt Institute, 2007). The stiffness test is an easy, non-destructive, quick and inexpensive test and can be easily conducted by using the Nottingham Asphalt Tester (NAT). In addition, according to a previous study, stiffer mixtures at high temperatures show higher resistance to permanent deformation, whereas asphalt mixtures with low stiffness at low temperatures indicate higher resistance to thermal cracking (Pszczola et al., 2018). Temperature and loading frequency have a significant effect on asphalt mixture stiffness (Read and Whiteoak, 2003).

8.4.1 Experimental setup

The stiffness test (ITSM) as shown in Figure 8-5, was used to evaluate the stiffness modulus of control and fibre reinforced asphalt mixtures according to BS EN 12697-26 (2012). The Nottingham Asphalt Tester (NAT) machine is used for this test. In accordance with BS EN 12697-26, a compressive load pulse was applied with a rise time of 124±4 ms in order to get a target horizontal deformation of 5±2 μm. The testing machine system needs at least ten conditioning pulses to adjust the load value and the duration to achieve the specific horizontal strain and time, followed by five load pulses. The load and horizontal strain were measured and stored for each load pulses to calculate the stiffness modulus. These measurements were repeated along two diameters; therefore, stiffness modulus value was the average for the two tests. The stiffness modulus was calculated, as shown in the following equation:

$$ITSM = \frac{F}{(z\,h)} \times (\upsilon + 0.27) \qquad \text{Equation 8-1}$$

where ITSM is the stiffness modulus (MPa), F is the maximum load (N), ν is Poisson's ratio, z is the horizontal deformation (mm), and h is the specimen thickness (mm).

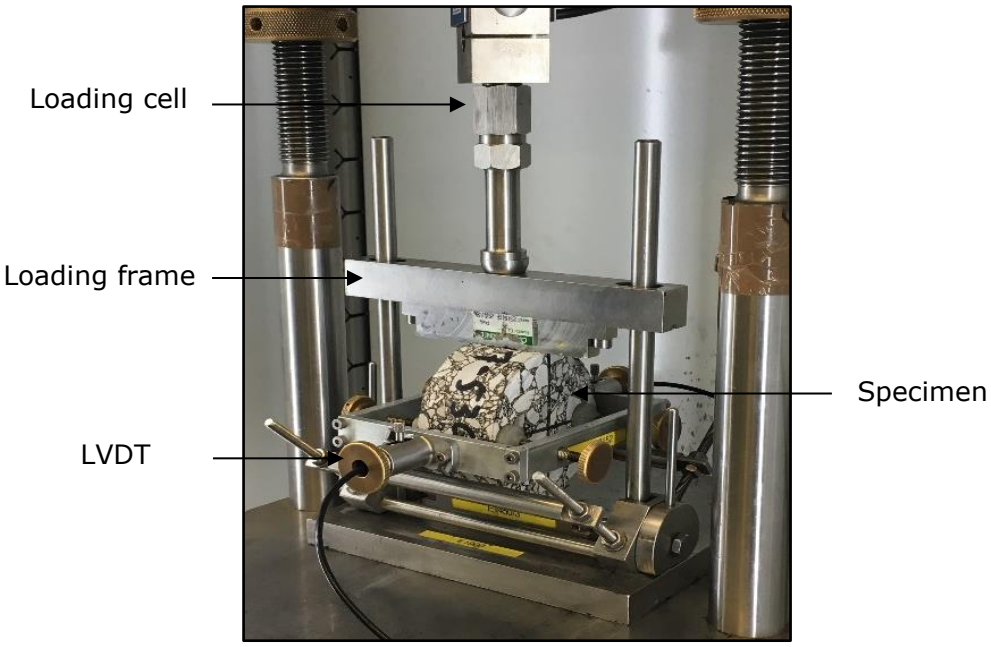


Figure 8-5 ITSM test configuration

8.4.2 Sample preparation

The mixing proportions and processes, also specimen coring and cutting are reported elsewhere (section 3.5.2 and 3.5.3 of chapter three, respectively). Roller compactor used to compact control and fibre reinforced asphalt mixtures. Specimens with 100 mm diameter and 45 mm thickness were used for this test. Prior to testing, all asphalt mixture core specimens were conditioned for four hours at the test temperature (20℃).

8.4.3 Results and Discussion

Figure 8-6 shows the indirect tensile stiffness test results of the control and fibre reinforced asphalt mixtures at 20℃. Error bars represent plus and minus one standard error (standard deviation divided by the square root of the number of the samples (ten replicates for stiffness test)). Adding more fibres led to significant increases in stiffness values of asphalt mixture, especially for short glass fibre and cellulose fibre at the 20℃ test temperature. T-test results showed that the stiffness value of fibre reinforced asphalt mixture significantly increased, compared to control specimens, as show in Table 8-2. Stiffness modulus values of asphalt mixtures containing 2.0% (glass-l, steel, cellulose and glass-s fibre) are about 21%, 26%, 28% and 32% higher than the stiffness modulus value of the control mixture, respectively.

This increase in stiffness modulus value of fibre reinforced asphalt mixture may be due to two reasons. Firstly the influence of fibre on bitumen by absorption/adsorption of the bitumen fraction led to increased bitumen stiffness (Chen et al., 2009, Mahrez et al., 2005). Also, this study evaluated the asphaltene content in the drained binder after mixing with fibre, and it was found that asphaltene content increased compared to the base binder, as shown earlier in chapter six. Moreover, the complex modulus value of drained binder after mixing with fibres showed a marked increase compared to the base binder, as explored in chapter six. The second reason is the reinforcement mechanism of the fibre by separating the stresses over a large area due to the three-dimensional network as shown earlier in SEM images and those of the X-ray CT (see Figure 8-2). Fibres entangle with each other to form networks which are important to stabilise the composite component (bitumen, fibre and filler) by reinforcing and adhesion effect of fibres to bitumen and aggregate (Wu et al., 2014).

Table 8-2 T-test for stiffness of control and fibre reinforced asphalt mixtures

Asphalt mixtures	Mean (MPa)	T-stat	P-value	Significant*
Control	2629.8	-	-	-
0.5% Glass-S	2910.2	2.652	0.0226	Yes
0.5% Glass-L	2860.2	2.699	0.0122	Yes
0.5% Cellulose	2757.1	1.458	0.0842	No
0.5% Steel	3119.6	6.476	0.00003	Yes
1% Glass-S	3113.7	2.923	0.0111	Yes
1% Glass-L	3086.6	3.882	0.0012	Yes
1% Cellulose	3300.3	5.950	0.0009	Yes
1% Steel	3238.0	4.307	0.0062	Yes
2% Glass-S	3481.4	3.447	0.0068	Yes
2% Glass-L	3184.3	6.684	0.00002	Yes
2% Cellulose	3371.6	2.928	0.0163	Yes
2% Steel	3317.8	6.103	0.0001	Yes

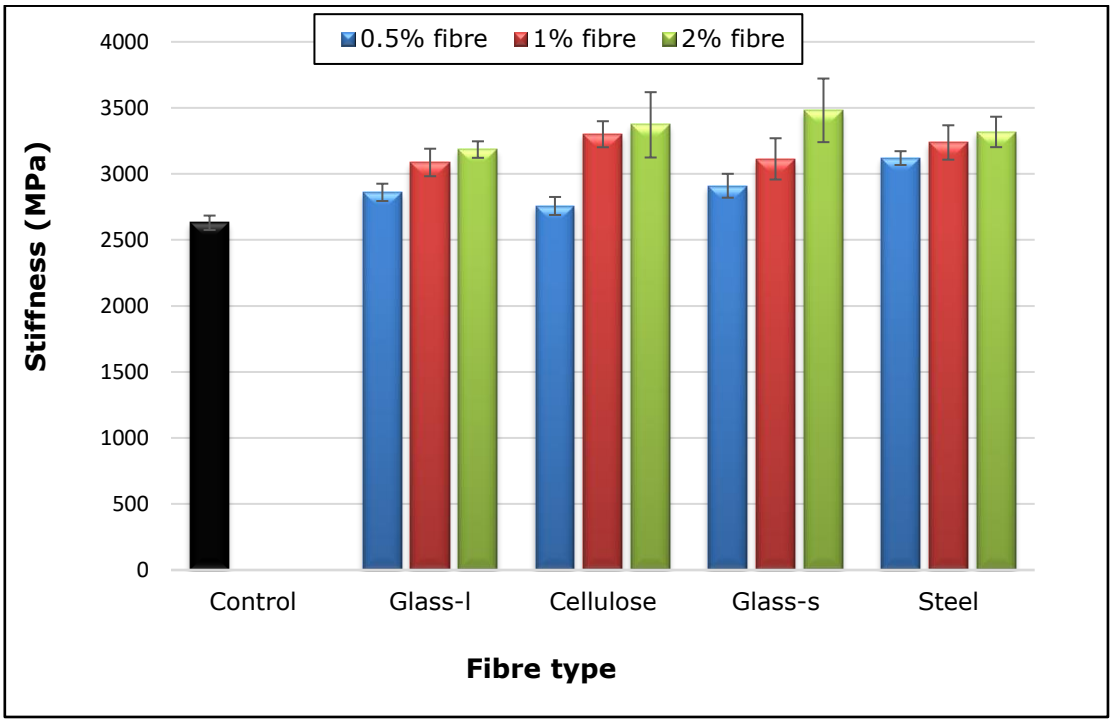


Figure 8-6 Stiffness values of control and fibre reinforced asphalt mixtures

8.5 Indirect tensile fatigue test (ITFT)

Fatigue can be defined as the slow development and propagation of a crack due to tensile strains generated in the bituminous mixture under the effects of repeated loading and temperature variations. These cracks can be seen at the pavement surface after a specific number of years (Arabani et al., 2010). Fatigue cracking can be bottom top cracking or top-down cracking. In thin asphalt pavements, the high tensile stress at the bottom of the asphalt mixture layer will initiate the crack and then the crack will propagate to the surface as one or a group of cracks. In thick asphalt pavements, the crack will start most likely from the top where there is high tensile stress as a result of traffic loading and binder ageing (Suchismita, 2009).

8.5.1 Experimental setup

In this study, the fatigue life of the asphalt mixtures was obtained through the indirect tensile fatigue test (ITFT). The test configuration is shown in Figure 8-7. This test was done at 124 ± 4 ms of repeated constant loading time and 1.5 ± 0.1s of a pulse repetition time according to the Draft British standard Draft BS (2003).

The tests were done in stress control loading mode in that case, the applied load range is kept constant during the test. Five different stress levels (150, 200, 300, 400 and 600 kPa), were applied for each mixture. In stress controlled loading mode the test will stop when the sample breaks or the vertical deformation has reached 10 mm, whichever occurs first (Draft BS, 2003).

The speed of crack propagation depends on the stress intensity in the vicinity of the crack. The crack propagates much faster in stress controlled mode than in strain controlled mode for a given value of initial strain. The applied stress in strain control mode gradually decreases after crack initiation as a result of an effective decrease

in the material stiffness, which leads to a longer fatigue crack propagation period. Therefore, the stress controlled mode test is more conservative and failure criteria more easily defined. On the other hand, the accumulation of vertical deformation in the stress controlled test is a big concern (Read, 1996, Airey, 2004).

A past study (Brown, 1978) cited in (Read, 1996) has explained the difference between the stress and strain modes of loading in a pavement structure. A pavement layer which has considerable thickness and stiffness is subjected to a stress controlled loading as a whole system, while those layers with low thickness are mostly moved by the lower layers that have a considerable structural significance, which results in a strain controlled mode. This explanation gained credence from a study done by Monismith and Salam (1973), who used multilayer elastic theory to analyse a pavement structure and demonstrated that:

- Asphalt pavement layers with a thickness less than 50 mm are subjected to strain controlled loading,
- Asphalt pavement layers with a thickness greater than 150 mm are subjected to stress controlled loading and
- Asphalt pavement layers with a thickness range from 50 mm to 150 mm are subjected to an intermediate mode of loading.

It is important to note that there is a possibility for a mode of loading between controlled strain and controlled stress in a pavement which will exhibit an intermediate fatigue life.

The test results can be expressed in two ways, and the relationships should be linear. In the first method, log stress is plotted against log fatigue life, and in the other log strain is plotted versus log fatigue life. The second method requires the calculation of the tensile strain for each stress level generated at the middle of the specimen according to the following equation:

$$\varepsilon_{xmax} = \frac{\sigma_{xmax}(1+3\nu)}{S_m} \times 1000$$ Equation 8-2

where ε_{xmax} is the maximum horizontal tensile strain (micro-strain), σ_{xmax} is the maximum tensile stress at the middle of the specimen (kPa), S_m is the stiffness of the specimen at σ_{xmax} in (MPa) and ν is the Poisson's ratio (assumed 0.35).

The ITFT test results of the bituminous mixtures are characterised as a function of the applied strain according to equation (8-3) or as a function of the applied stress, as shown in equation (8-4).

$$N_f = a\varepsilon_0^{-b}$$ Equation 8-3

$$N_f = k_1\sigma_0^{-k_2}$$ Equation 8-4

where N_f is the number of load cycles to failure, ε_0 is the initial tensile strain at the middle of the specimen (micro-strain), a and b are the coefficients obtained from the laboratory test, σ_0 is the tensile stress at the middle of the specimen (kPa) and k_1 and k_2 are coefficients obtained from the laboratory test.

The resistance of asphalt mixtures to fatigue cracking was assessed in this study by the following two parameters depending on the fatigue equations obtained for the mixtures (Read and Collop, 1997, Draft BS EN 12697-24 2015).

- Strain value at one million cycles (micro-strain), and
- Fatigue life at one hundred micro-strain.

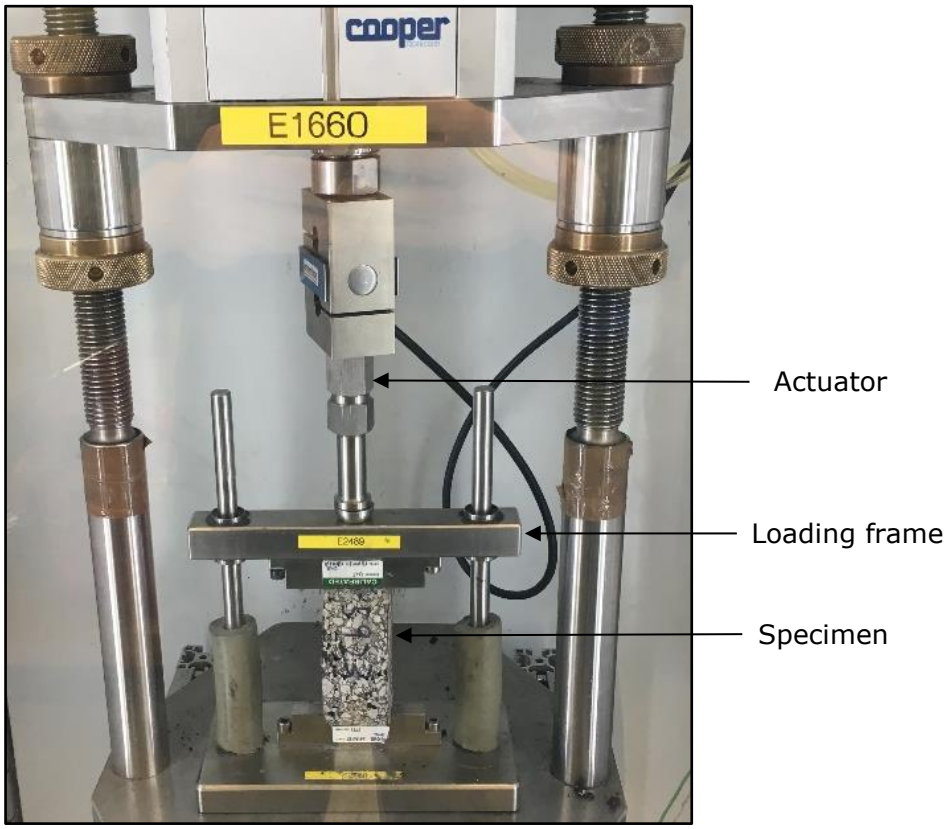


Figure 8-7 ITFT test configuration

8.5.2 Sample preparation

A roller compactor was used to prepare slab samples with dimensions of 306 mm in length, 306 mm in width and 65 mm in height. Each slab was then saw-cut to obtain five core specimens with the dimensions of 100 mm diameter and 45 mm thickness as detailed elsewhere (section 3.5.2 and 3.5.3 of chapter three). A total of 13 slabs (13 mixes) were compacted and cut in order to get 65 core specimens for conducting indirect tensile fatigue tests (ITFT), (see Figure 8-8). Before the test, a controlled air cabinet is used for conditioning the specimens for four hours at the test temperature (20℃).



Figure 8-8 Roller compacted slabs and core specimens

8.5.3 Results and Discussion

8.5.3.1 ITFT test results as a function of the applied strain

The fatigue results for the control and fibre-reinforced asphalt mixtures are presented in Figure 8-9, Figure 8-10 and Figure 8-11, while the fatigue equation (8-3), for all control and fibre reinforced asphalt mixtures together and their R^2 values are shown in Table 8-3. The fatigue equations of the asphalt mixtures have been determined with a high degree of accuracy (high R^2 values) for both control and fibre reinforced asphalt mixtures. They were established from a data set (five specimens) of the asphalt mixtures. Five specimens were used since testing more samples will be time consuming and may not change the fatigue equation degree of accuracy (R^2) significantly.

With regard to the fatigue performance of control and fibre reinforced asphalt mixtures, the fatigue life in Figure 8-9 and Figure 8-10 and the fatigue parameters for the fibre modified asphalt mixtures in Table 8-3 confirm the difference in the fatigue performance of fibre modified asphalt mixtures at 0.5% and 1.0% fibre content, particularly for steel fibres. At the 100 micro-strain level, the 0.5% and 1.0% fibre reinforced asphalt mixtures showed approximately 1.5, 2.5 and 1.8, 2.8,

times higher fatigue life for long glass and steel fibres, respectively and these became 2.30 and 1.07, times higher for 1.0% cellulose and short glass fibres respectively, compared to the control mixture at 20℃ test temperature. A 2.0% the cellulose fibre was the only fibre that showed higher fatigue life compared to the control mixture at the 100 micro-strain level and 20℃ test temperature. However, at the high strain level, the control mixture in general exhibited higher fatigue life than the fibre reinforced mixtures. This finding indicates that the fibre reinforced asphalt mixtures perform better at low strain values only and this in agreement with a previous study (Kaloush et al., 2010), offered results are based on limited data, and further investigation at low strain values recommended. The improvement in fatigue life is due to the fibre reinforcement effect, as shown in X-ray 3D image analysis (see Figure 8-2) and SEM images (see chapters four and five). Fibre networks may perform as bridges, relocating and spreading stresses which may delay crack propagation and maintain greater strain before material failure, resulting in longer fatigue life. The improvement in fatigue cracking resistance could also be attributed to the fibre's cohesion and adhesion in the mastic.

It is noted that adding high fibre content (2.0%) resulted in lower fatigue life compared to other fibre contents used in this study. This finding was unexpected and suggested that high fibre contents may lead to increase asphalt mixture stiffness which results in lower strain value (see Equation 8-2). The results were represented as log strain versus log number of cycles in a control stress mode. This method of expressing the result may be disadvantageous for a stiffer material such as fibre reinforced asphalt mixture. This is because stiffer materials will show low strain value, and this will affect the fatigue life slope as shown in the following figures.

Table 8-3 Summary data for all the asphalt mixtures tested during this study using the ITFT

Mixture type	Fatigue equation	ε@10^6 cycles ($\mu\varepsilon$)	Rank	Fatigue equation	N_f @100$^{\mu\varepsilon}$	Rank	R^2
Control	$\varepsilon = 5219\ N_f^{-0.345}$	44.4	8	$N_f = 3\times10^{10}\ \varepsilon^{-2.794}$	77,468	8	0.97
0.5%Steel	$\varepsilon = 2853.9\ N_f^{-0.274}$	64.8	3	$N_f = 2\times10^{12}\ \varepsilon^{-3.481}$	218,288	1	0.95
0.5%Gl-l	$\varepsilon = 2588.1\ N_f^{-0.274}$	58.7	4	$N_f = 1\times10^{12}\ \varepsilon^{-3.462}$	119,124	5	0.95
0.5%Gl-s	$\varepsilon = 3663.7\ N_f^{-0.318}$	45.3	7	$N_f = 1\times10^{11}\ \varepsilon^{-3.128}$	55,463	12	0.99
0.5%Cell	$\varepsilon = 5075.4\ N_f^{-0.350}$	40.3	10	$N_f = 2\times10^{10}\ \varepsilon^{-2.726}$	70,637	9	0.96
1%Steel	$\varepsilon = 3788.5\ N_f^{-0.292}$	67.1	2	$N_f = 1\times10^{12}\ \varepsilon^{-3.355}$	194,984	2	0.98
1%Gl-l	$\varepsilon = 3827.1\ N_f^{-0.309}$	46.0	6	$N_f = 4\times10^{11}\ \varepsilon^{-3.230}$	138,695	4	0.99
1%Gl-s	$\varepsilon = 4495\ N_f^{-0.336}$	43.3	9	$N_f = 5\times10^{10}\ \varepsilon^{-2.890}$	82,979	7	0.97
1%Cell	$\varepsilon = 1920.5\ N_f^{-0.241}$	68.8	1	$N_f = 2\times10^{13}\ \varepsilon^{-4.024}$	179,073	3	0.97
2%Steel	$\varepsilon = 4001.3\ N_f^{-0.333}$	40.2	11	$N_f = 6\times10^{10}\ \varepsilon^{-2.978}$	66,397	10	0.99
2%Gl-l	$\varepsilon = 4519.4\ N_f^{-0.353}$	34.4	13	$N_f = 7\times10^{9}\ \varepsilon^{-2.619}$	40,467	13	0.92
2%Gl-s	$\varepsilon = 4215.3\ N_f^{-0.339}$	39.0	12	$N_f = 3\times10^{10}\ \varepsilon^{-2.860}$	57,164	11	0.97
2%Cell	$\varepsilon = 3271.5\ N_f^{-0.296}$	55.0	5	$N_f = 2\times10^{11}\ \varepsilon^{-3.175}$	89,337	6	0.94

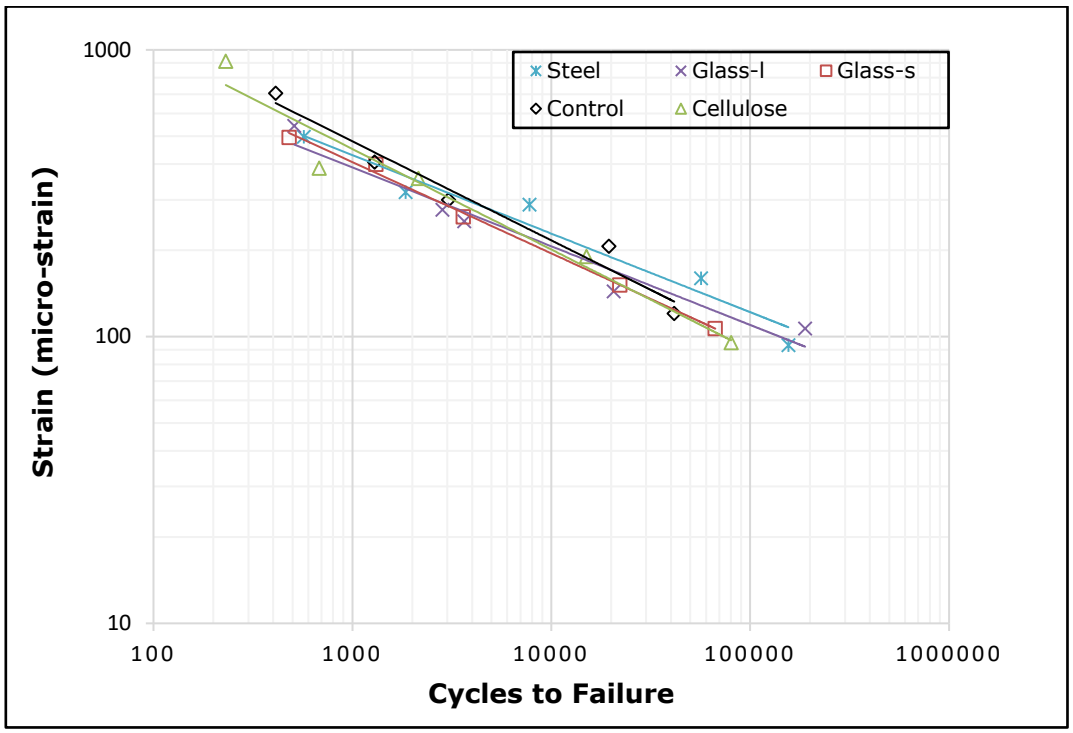


Figure 8-9 Fatigue life of 0.5% fibre reinforced asphalt mixtures versus strain

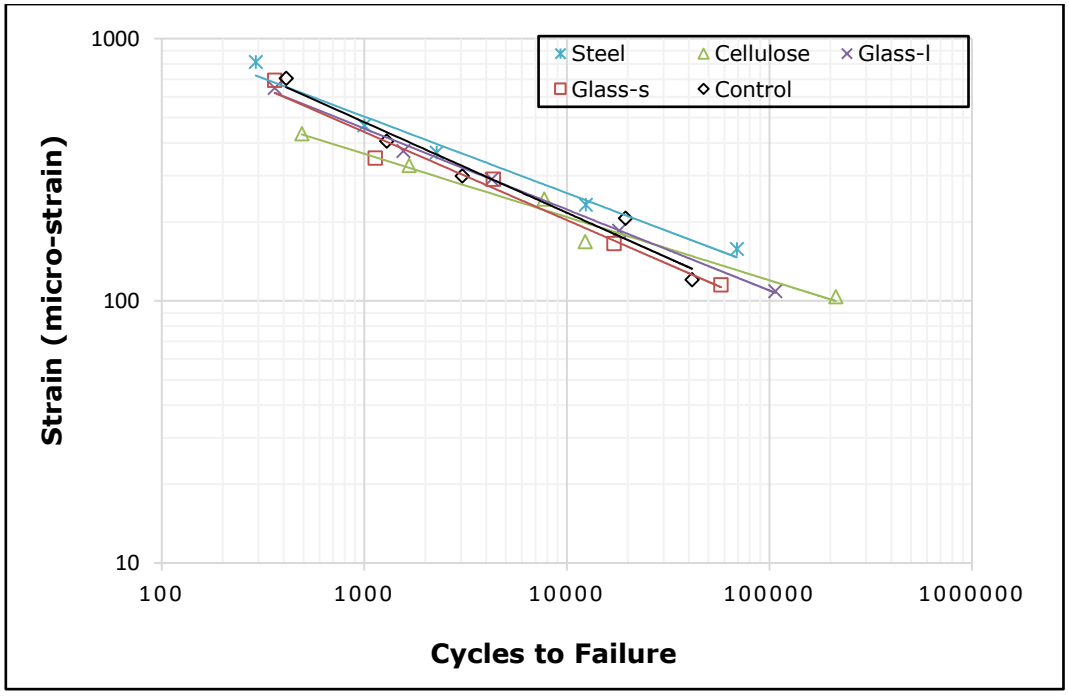


Figure 8-10 Fatigue life of 1.0% fibre reinforced asphalt mixtures versus strain

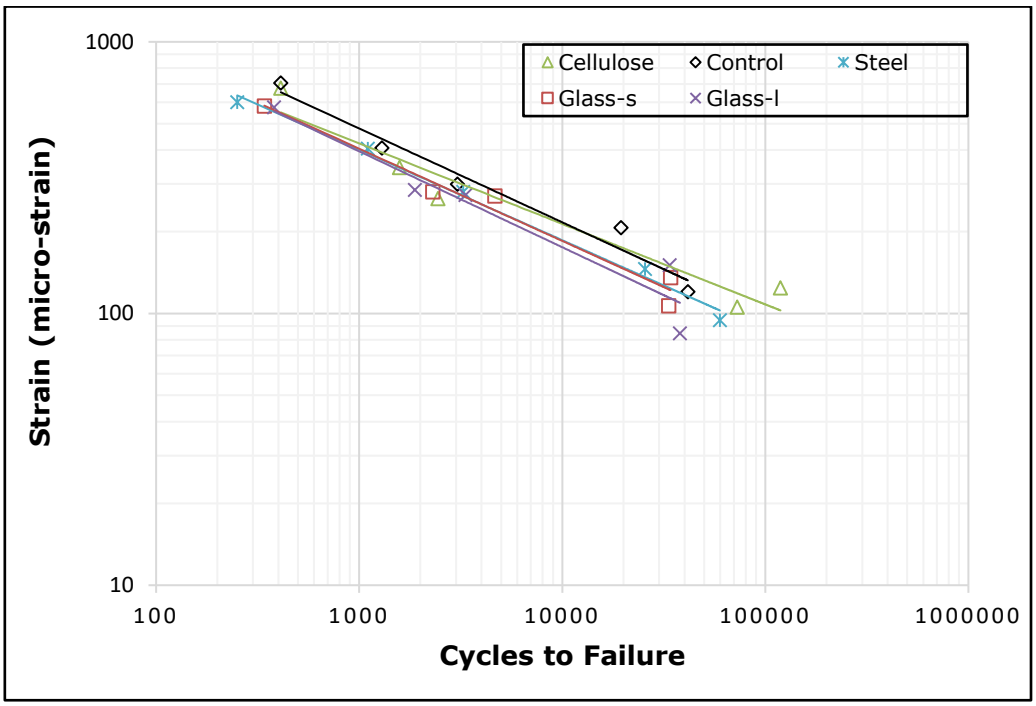


Figure 8-11 Fatigue life of 2.0% fibre reinforced asphalt mixtures versus strain

8.5.3.2 ITFT test results as a function of the applied stress

For this stress controlled mode test the intuitive way to express the results is to use log stress versus log number of cycles, which produces a formula as shown in (Equation 8-4). Figure 8-13 and Figure 8-14 (Equation 8-4), for all asphalt mixtures together with their R^2 values, are presented in Table 8-4. The fatigue equations of the asphalt mixtures have been determined with a high degree of accuracy (high R^2 values) for all asphalt mixtures.

From the Figures 8-12 to 8-14 and Table 8-4, it is clear that fibre reinforced asphalt mixtures showed higher fatigue life, compared to the control mixture. At 100 kPa stress level, the fibre reinforced asphalt mixtures showed approximately 1.5 to 6.0 times higher fatigue life compared to the control mixture at the 20 ℃ test temperature. Cellulose fibre showed the highest increase in fatigue life, followed then by steel, long glass and short glass fibres. In addition, at 10^6 loading cycles, the fibre-reinforced asphalt mixtures support stress values 11% to 70% greater

than the control asphalt mixture. This indicates an improvement in the performance of fibre reinforced asphalt mixture when considering the resistance to fatigue cracking. Moreover, this implies that there is more stress-dependency in stiffness for fibre reinforced mixtures.

Table 8-4 Summary data for all the asphalt mixtures tested during this study using the ITFT

Mixture type	Fatigue equation	σ@10^6 cycles	Rank	Fatigue equation	N_f @100kPa	Rank	R^2
Control	$\sigma = 3209.7\ N_f^{-0.287}$	60.9	13	$N_f = 1\times10^{12}\sigma^{-3.452}$	124,738	13	0.99
0.5%Steel	$\sigma = 2514.3\ N_f^{-0.235}$	97.8	2	$N_f = 2\times10^{14}\sigma^{-4.218}$	732,875	2	0.99
0.5%Gl-l	$\sigma = 2440.2\ N_f^{-0.238}$	91.1	4	$N_f = 5\times10^{13}\sigma^{-3.975}$	561,009	3	0.95
0.5%Gl-s	$\sigma = 3663\ N_f^{-0.27}$	70.5	8	$N_f = 5\times10^{12}\sigma^{-3.128}$	244,889	8	0.99
0.5%Cell	$\sigma = 1900.3\ N_f^{-0.231}$	78.1	6	$N_f = 1\times10^{14}\sigma^{-4.25}$	316,228	7	0.98
1%Steel	$\sigma = 2317.2\ N_f^{-0.253}$	70.3	9	$N_f = 1\times10^{13}\sigma^{-3.868}$	183,654	11	0.98
1%Gl-l	$\sigma = 2477\ N_f^{-0.248}$	80.5	5	$N_f = 3\times10^{13}\sigma^{-3.977}$	333,520	6	0.99
1%Gl-s	$\sigma = 2809.5\ N_f^{-0.269}$	68.3	12	$N_f = 6\times10^{12}\sigma^{-3.698}$	241,074	9	0.99
1%Cell	$\sigma = 2240.1\ N_f^{-0.23}$	93.4	3	$N_f = 6\times10^{13}\sigma^{-4.024}$	537,219	4	0.92
2%Steel	$\sigma = 2253.2\ N_f^{-0.244}$	77.4	7	$N_f = 5\times10^{13}\sigma^{-4.072}$	358,897	5	0.99
2%Gl-l	$\sigma = 3013.4\ N_f^{-0.274}$	68.4	11	$N_f = 2\times10^{12}\sigma^{-3.523}$	179,900	12	0.96
2%Gl-s	$\sigma = 3133.6\ N_f^{-0.276}$	69.2	10	$N_f = 2\times10^{12}\sigma^{-3.463}$	237,154	10	0.96
2%Cell	$\sigma = 1832.2\ N_f^{-0.208}$	103.5	1	$N_f = 3\times10^{14}\sigma^{-4.288}$	796,382	1	0.89

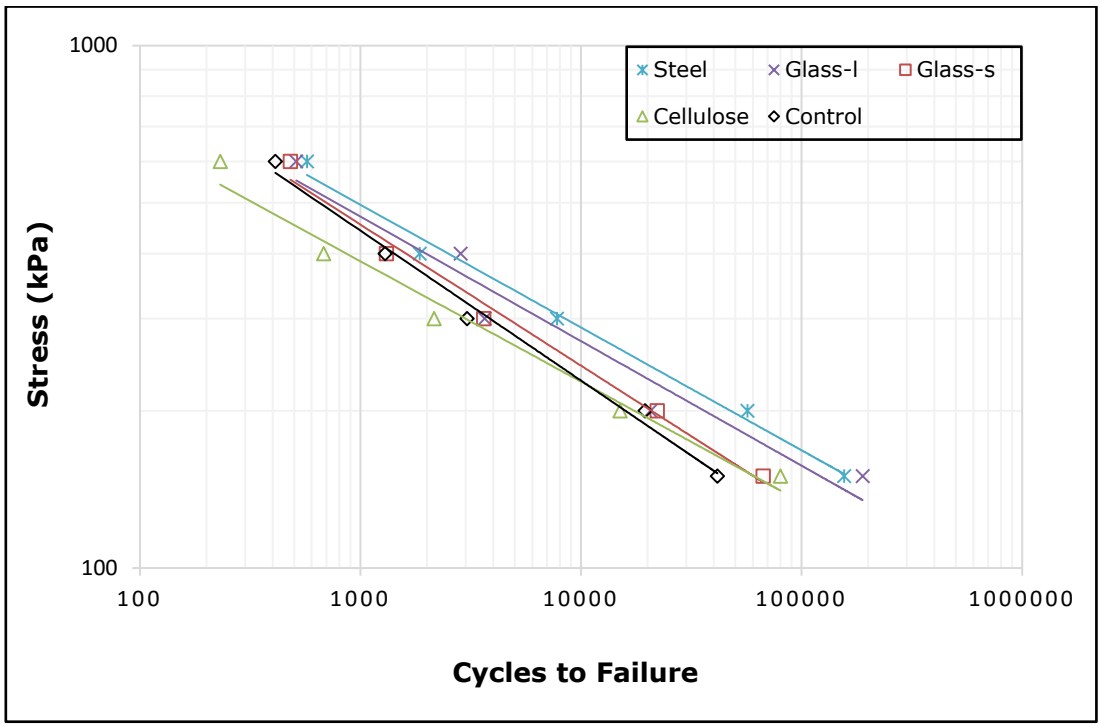


Figure 8-12 Fatigue life of 0.5% fibre reinforced asphalt mixtures versus stress

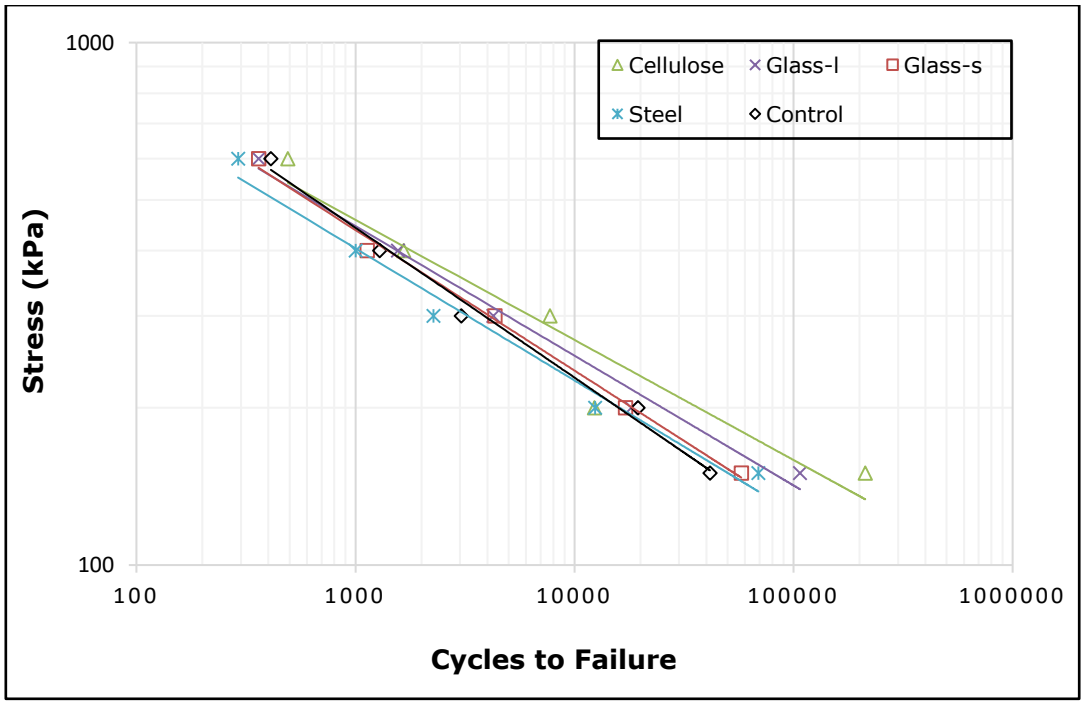


Figure 8-13 Fatigue life of 1.0% fibre reinforced asphalt mixtures versus stress

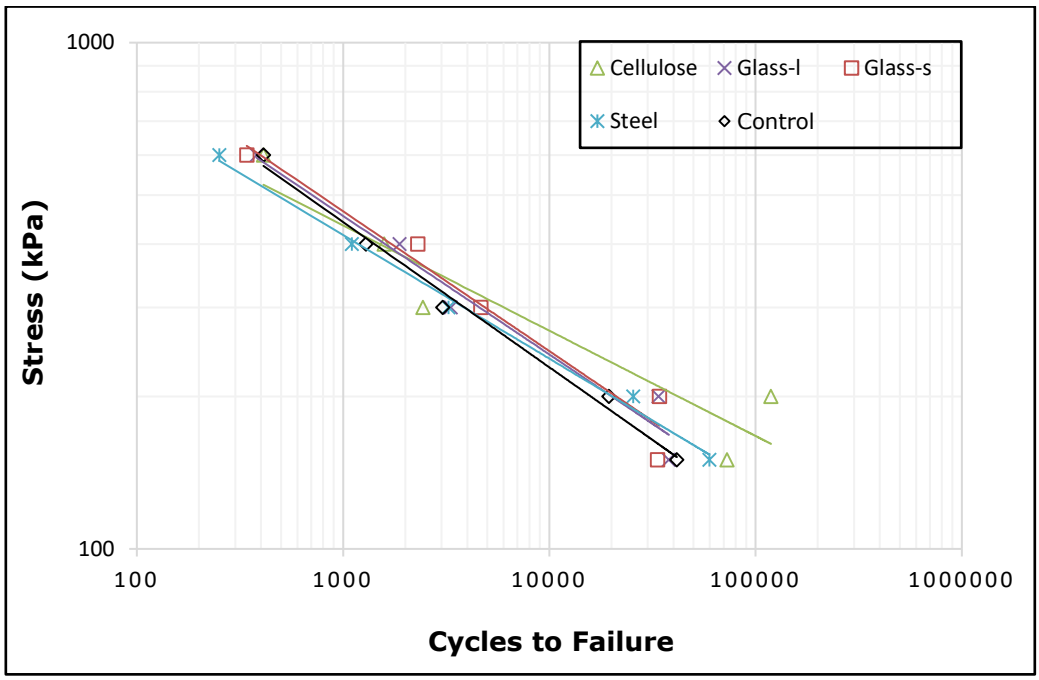


Figure 8-14 Fatigue life of 2.0% fibre reinforced asphalt mixtures versus stress

8.6 Indirect tensile strength test (ITS)

It is known that asphalt mixture is not as strong in tension as it is in compression. Asphalt mixture tensile strength is important to pavement engineers as it is further associated with the cracking properties of roads. It is believed that asphalt mixtures with high tensile strength show higher resistance to cracking. They are able to resist higher strain prior to failure compared to low tensile strength asphalt mixtures (Tayfur et al., 2007). Several studies have related tensile strength to the performance of asphalt pavements (Roque et al., 1999, Zhang et al., 2001). A previous study found that higher tensile strength asphalt mixture showed higher resistance to low temperature cracking (Huang et al., 2003).

8.6.1 Experimental setup

An Instron 1332 hydraulic loading frame testing machine according to BS EN 12697-23 standard was used for evaluating the indirect tensile strength of control

and fibre reinforced asphalt mixtures (BS EN 12697-23, 2017). The Instron loading frame fitted with a 50 kN loading cell was used to apply compressive loading through the vertical axis of the specimen with a 50 mm/min displacement rate. The experimental setup of the ITS test is shown in Figure 8-15. The ITS was calculated for each specimen as shown in the equation below:-

$$ITS = \frac{2F}{(\pi \times d \times t)}$$ Equation 8-5

where F is the vertical load (N), d is the specimen diameter (mm), and t is the thickness of the specimen (mm).

8.6.2 Sample preparation

The mixing proportions and processes, also specimen coring and cutting are reported elsewhere (section 3.5.2 and 3.5.3 of chapter three, respectively). Control and fibre reinforced asphalt mixtures were compacted by roller compactor. Core specimens with 100 mm diameter and 45 mm thickness were used in this study after conditioning at 20℃ for four hours.

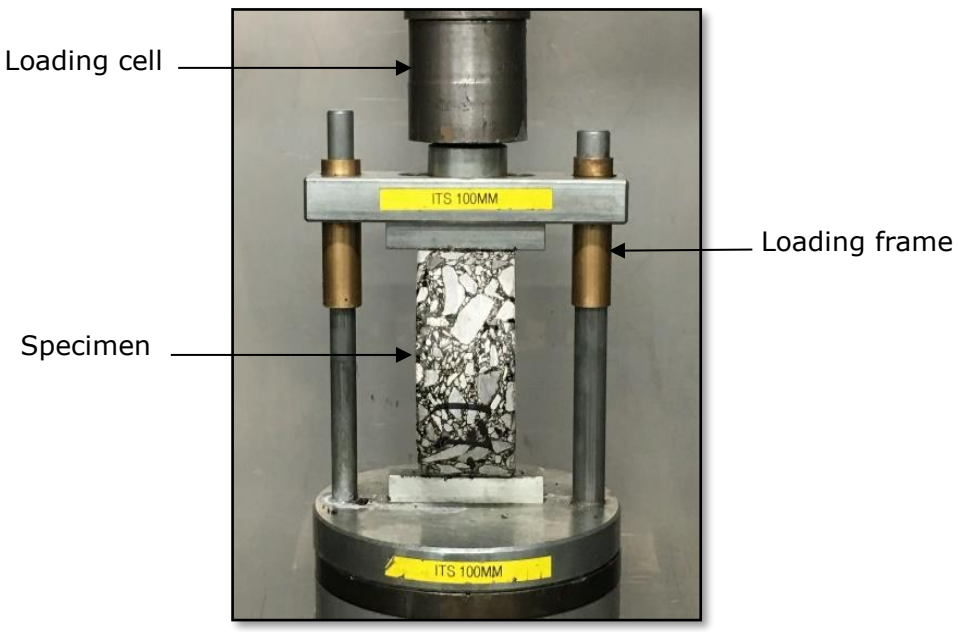


Figure 8-15 Experimental setups of ITS

8.6.3 Results and Discussion

Indirect tensile strength of control and fibre reinforced asphalt mixtures at 20℃ are shown in Figure 8-16. The error bars represent plus and minus one standard error. It can be seen that glass-s and cellulose fibre reinforced asphalt mixtures showed a slight increase in the indirect tensile strength and only steel fibre reinforced asphalt mixture showed a marked increase, reaching 32% higher than the control mixture. It is interesting to note that most glass and steel fibre reinforced samples after testing at 20℃ did not split in two, while all control and most cellulose fibre reinforced asphalt mixture samples spilt at the end of the test. This is due to the residual strength provided by the fibres, as shown in Figure 8-17.

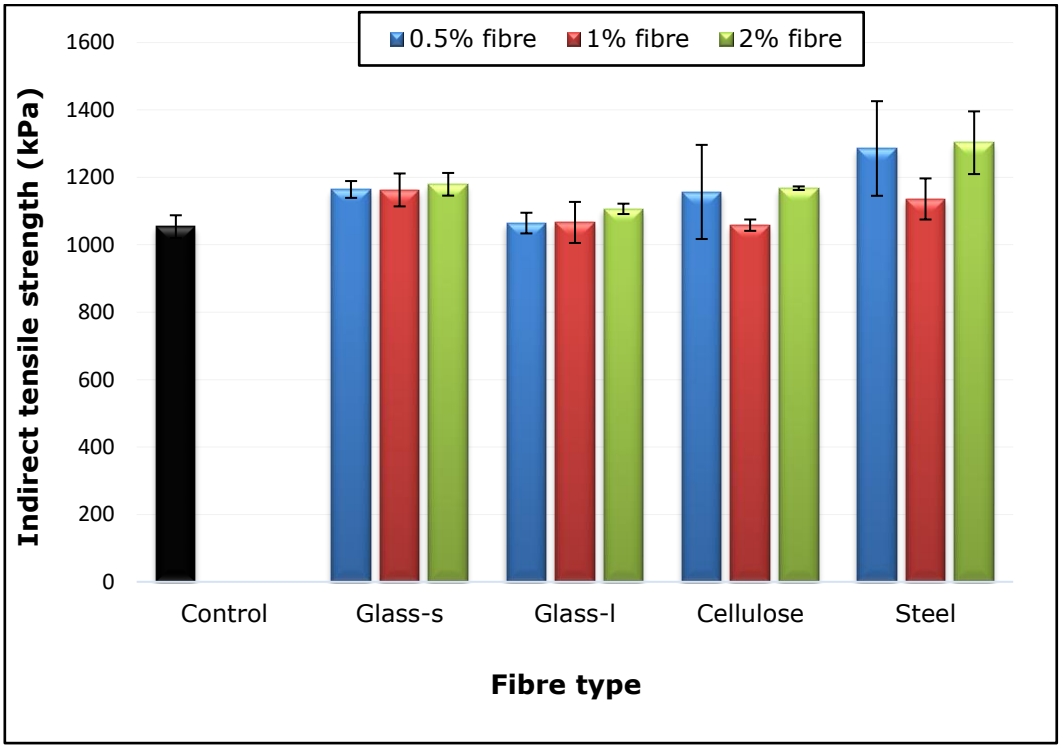


Figure 8-16 Indirect tensile strength of control and fibre reinforced asphalt mixtures

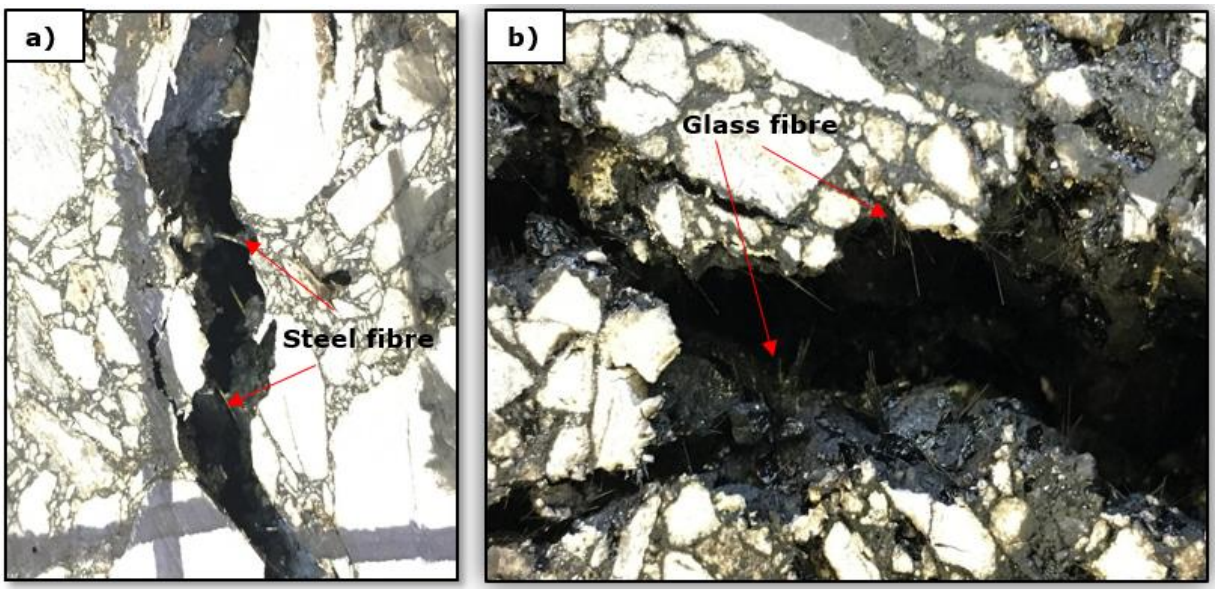


Figure 8-17 (a) Steel, (b) glass fibre reinforced asphalt mixtures

8.7 Moisture damage test

Moisture damage is a primary reason for distress in asphalt pavements that most transportation engineers face. Moisture susceptibility depends on many factors in asphalt pavement and complicated mechanisms. The moisture sensitivity test was done according to BS EN 12697-12 (2003). Five core specimens for each mixture were obtained from roller compacted slabs. These were divided into two groups. Two dry specimens were placed in a water bath at 40℃ for a period of 68 to 72 hours, wrapped in plastic wrap, in a sealed bag, followed by conditioning in a 20℃ thermostatically controlled air cabinet for more than three hours.

The moisture conditioned specimens (three samples) were previously subjected to vacuum in water for thirty minutes under 6.7 kPa pressure and then conditioned at 40℃ in a water bath for 68 hours, followed by conditioning in a 20℃ water bath for more than three hours prior to testing. Then, the dry and wet specimens were tested for indirect tensile strength, according to BS EN 12697-23 (2017), with a 50 mm/min constant displacement rate. The moisture damage test results are

reported as an Indirect Tensile Strength Ratio (ITSR), which is the ratio of the wet strength to the dry strength, expressed as a percentage by BS EN 12697-12 (2003) and Indirect Tensile Strength (ITS) by BS EN 12697-23 (2017), as shown in the following equation:

$$ITSR\ (\%) = \frac{ITS_{wet}}{ITS_{dry}} \times 100 \qquad \text{Equation 8-6}$$

8.7.1 Results and Discussion

The changing of the indirect tensile strength (ITS) and indirect tensile strength ratio (ITSR) follow no clear trend as shown in Figure 8-18, Figure 8-19 and Figure 8-20. These show that 0.5% of fibre did not influence the ITSR of asphalt mixtures. However, all asphalt mixtures showed high resistance to a water attack. What is surprising is that their properties even seem to improve when they are exposed to the moisture damage procedure. Nevertheless, these results are in line with those of previous studies (Xiao et al., 2007, Lu and Harvey, 2006, Putman and Amirkhanian, 2004). A possible explanation for this might be that the limestone aggregate chemistry (hydrophobic) and the action of conditioning in warm water may have led to slight ageing of the dense bitumen mixture, which plays a role in increasing the internal friction between the aggregate and the binder (McDaniel et al., 2002). This finding may indicate that the water conditioning is not harsh enough for dense bitumen mixture made with limestone aggregate and low air voids.

Another issue is that the failure mode in the ITS test is not pure tension, but it is a combination of tensile, compressive and shear failures. It is clear that compression and shear failures occur at locations near to the loading cell at the top of the specimen during the ITS test (Apeagyei et al., 2006) (see Figure 8-21). The plastic deformation on the top of the specimen under the loading cell may redistribute the stress and may change the effective straining rate in the centre of the specimen where tension occurs. Therefore, the influence of moisture damage on tensile

strength measured from the maximum load may be quite complex and unpredictable (Apeagyei et al., 2006).

These unexpected results led this study to investigate the influence of the moisture damage procedure on weaker specimens. Therefore, RLAT specimens after being exposed to 5000 pulses at 30℃ were used in order to examine their moisture resistance, and this is detailed in the following section.

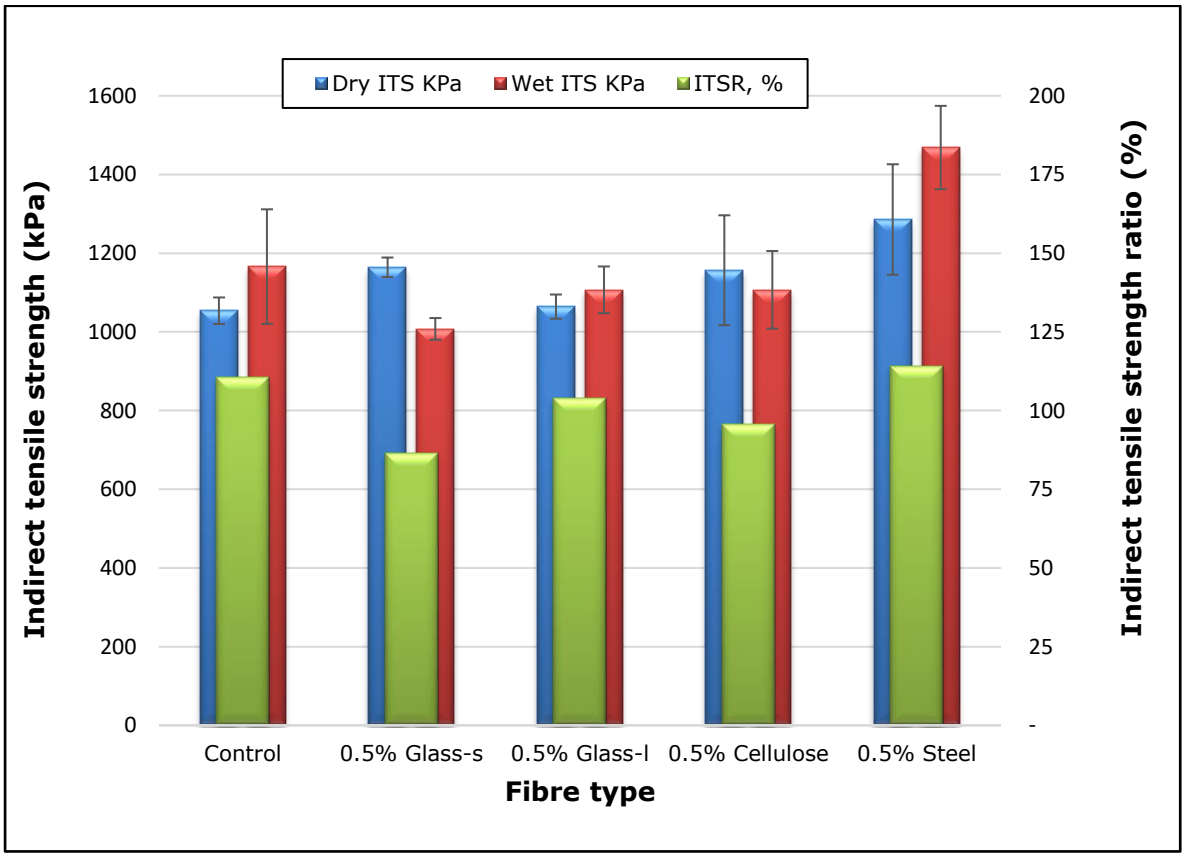


Figure 8-18 Moisture damage results of control and 0.5% fibre reinforced asphalt mixtures

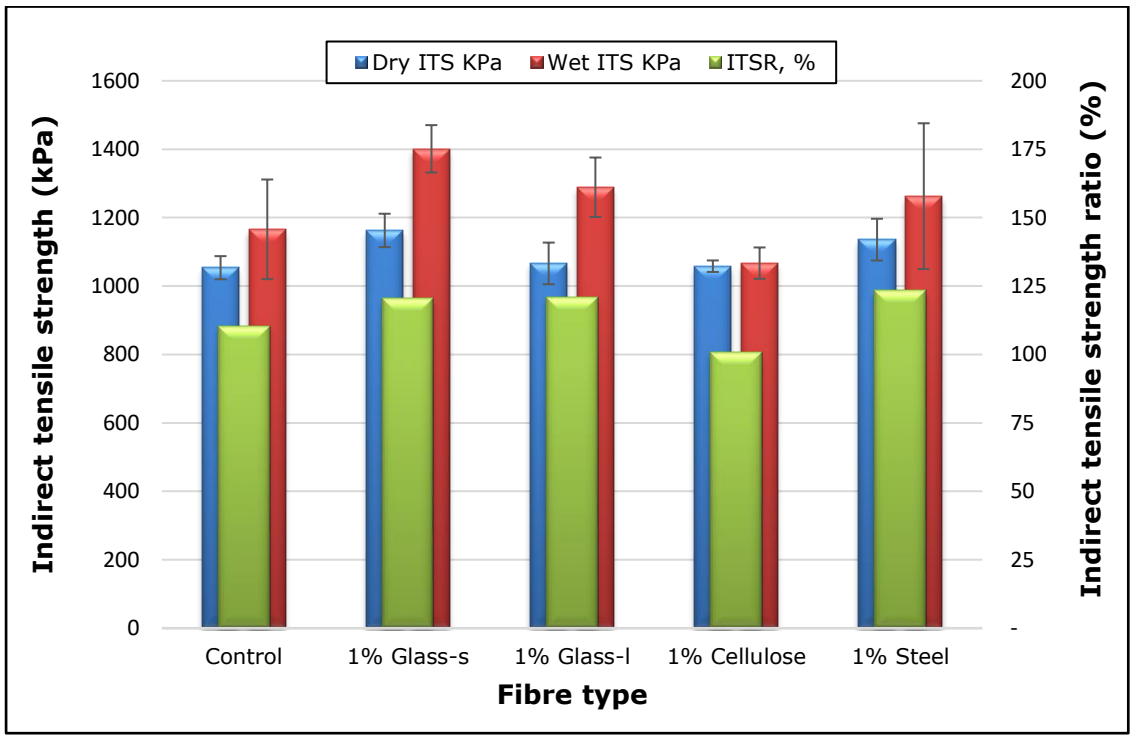


Figure 8-19 Moisture damage results of control and 1.0% fibre reinforced asphalt mixtures

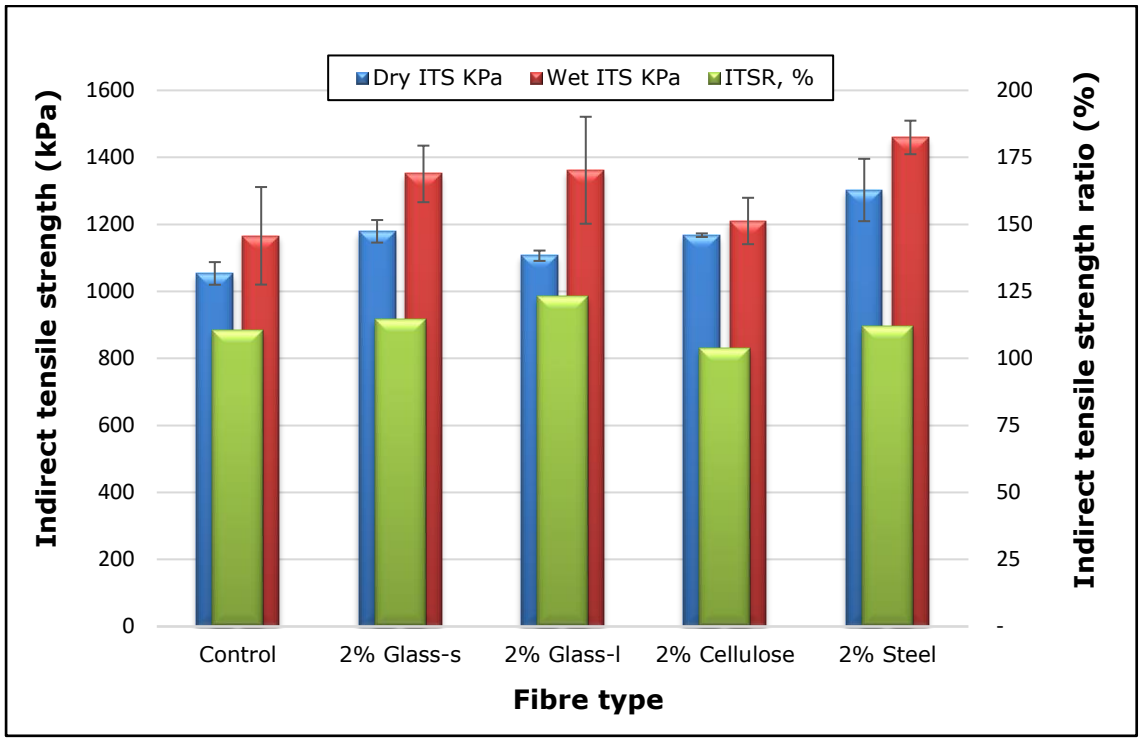


Figure 8-20 Moisture damage results of control and 2.0% fibre reinforced asphalt mixtures

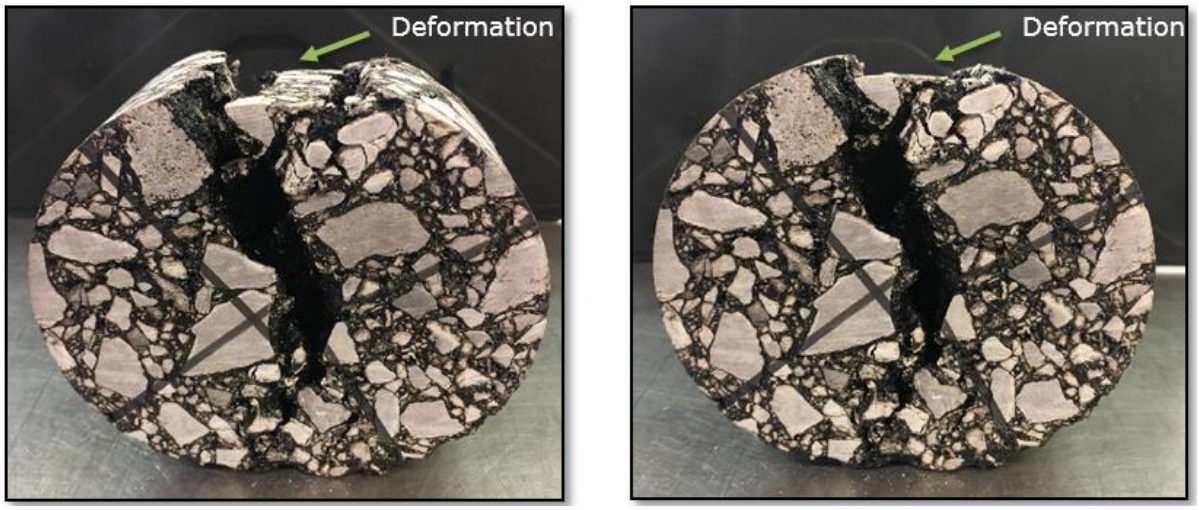


Figure 8-21 Asphalt mixture samples after ITS test

8.7.2 Results and discussion of moisture damage for RLAT specimens

As shown in, Figure 8-22, Figure 8-23 and Figure 8-24, all specimens showed good resistance to moisture damage with an ITSR higher than 80%. In general, there is a slight reduction in moisture damage resistance of asphalt mixtures examined after RLAT testing compared to virgin (new) specimens. It can be inferred from this observation that moisture resistance of specimens used after RLAT testing can be decreased after exposing to the same moisture damage procedure (BS EN 12697-12, 2003). This is reasonable since these samples have cracks after being exposed to 5000 load pulses. This might help water to penetrate further inside these specimens and cause more damage compared to virgin (new) specimens. However, due to the limited number of specimens used in this investigation, it would be worth doing more investigation into this issue. It is important to note that both control and fibre reinforced asphalt mixtures performed very well regards to moisture damage resistance.

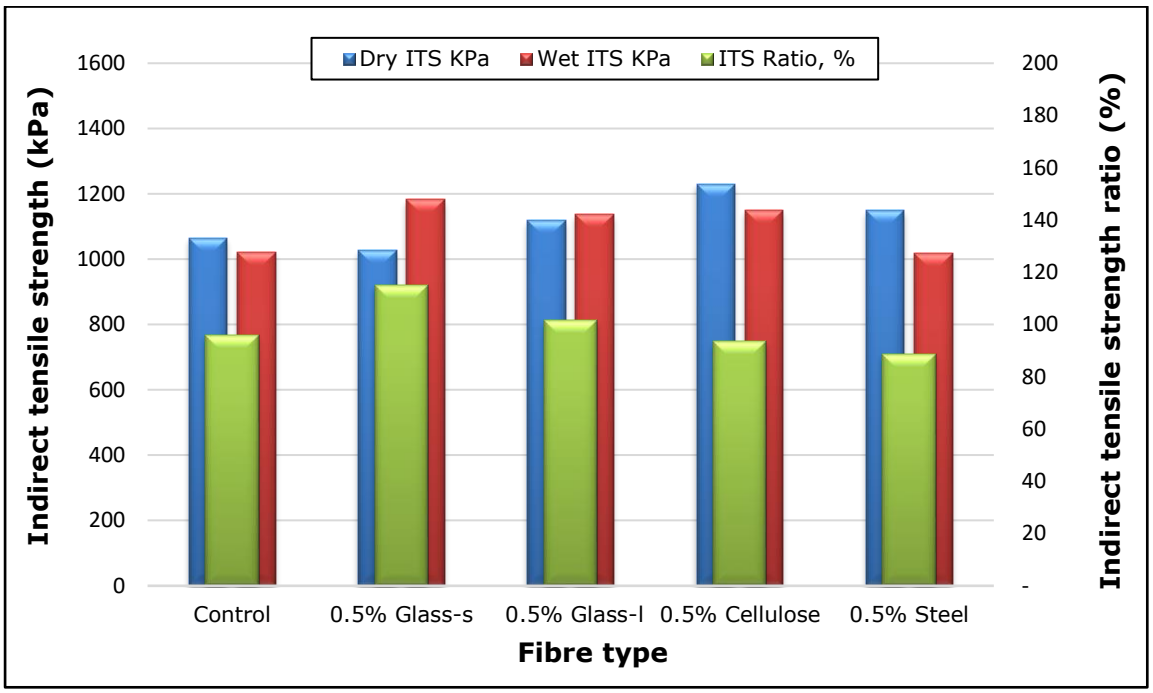


Figure 8-22 Moisture damage results of control and 0.5% fibre reinforced asphalt mixtures after RLAT test

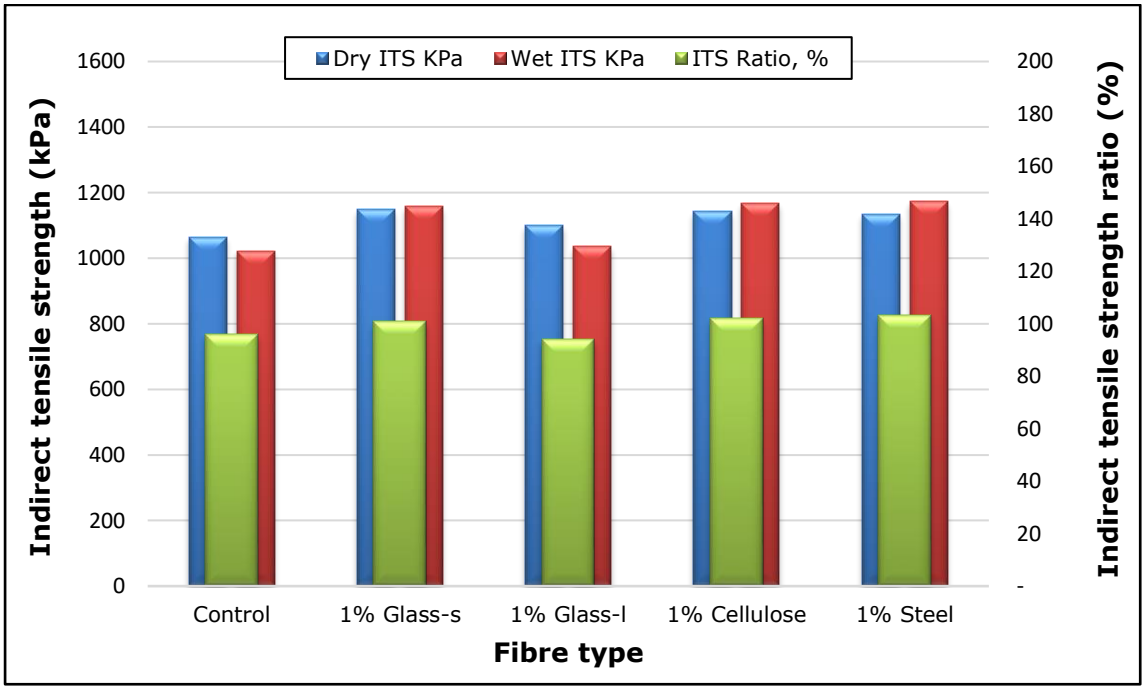


Figure 8-23 Moisture damage results of control and 1.0% fibre reinforced asphalt mixtures after RLAT test

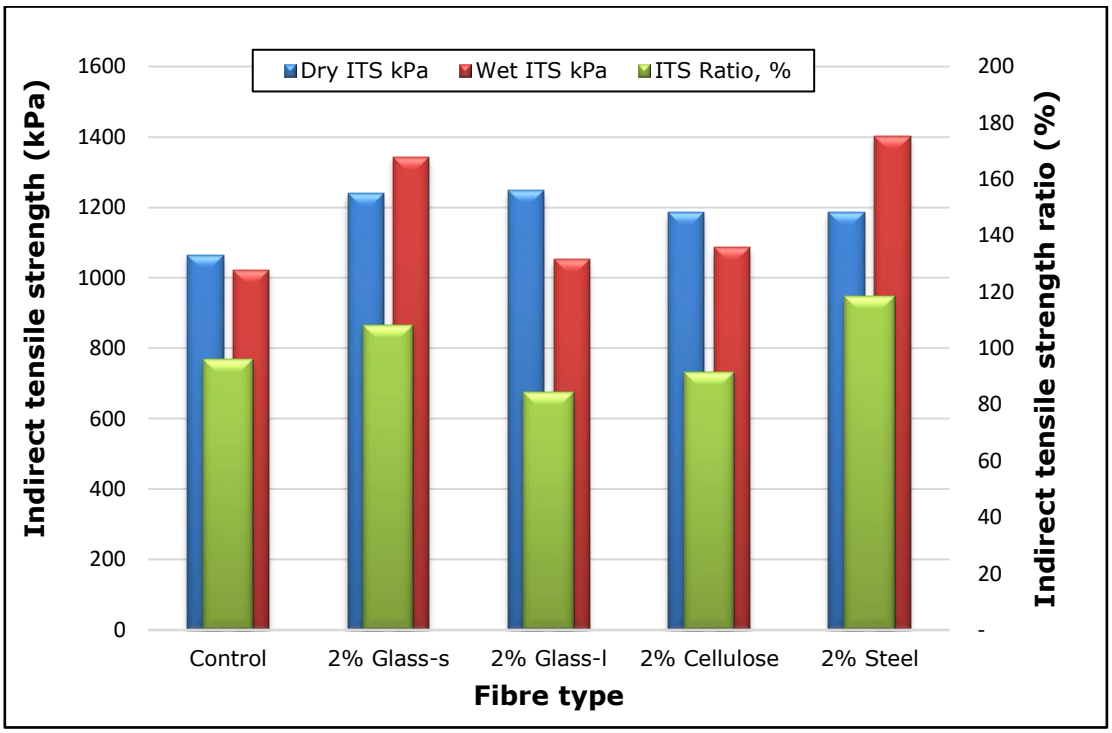


Figure 8-24 Moisture damage results of control and 2.0% fibre reinforced asphalt mixtures after RLAT test

8.8 Semi-circular bending test (SCB)

Semi-circular bending is a simple test developed in the Netherlands to assess the resistance against cracking and crack propagation rate of asphalt mixtures. Also the SCB test is important to examine the ability of asphalt mixtures to resist thermal cracking, which is the main failure type in cold regions (Hofman et al., 2003). It is significant to investigate the resistance of asphalt mixture against cracking due to the increase in the number of vehicles and axle loads, in addition to extreme environmental conditions that asphalt roads are subjected to. These extreme conditions will lead to the initiation and propagation of cracks; after a period of time, these cracks gradually expand and let water penetrate the pavement causing a rapid deterioration in the roads (Zegeye et al., 2012).

The SCB test method is fundamentally a three-point bending test of a semi-circular shaped specimen with an introduced notch. This geometry induces tension at the

bottom of the sample resulting in crack propagation through the specimen. The SCB specimen geometry is suitable for the evaluation of the fracture properties of both field cores and laboratory-compacted samples (Huang et al., 2013). The only difficulty in preparing the specimen is getting a consistent notch length. A few studies have investigated the SCB test and its relation to the asphalt mixture fracture performance (Saha and Biligiri, 2016).

8.8.1 Experimental setup

The semi-circular bending test (SCB), as shown in Figure 8-25, was used to examine the fracture toughness (K_i) (crack growth toughness) and maximum stress (σ) at the failure of asphalt mixtures according to BS EN 12697-44 (2010). Experiments were conducted on specimens simply supported by two rollers with a span length equal to 0.8 times the diameter under three-point bending load configuration. A previous study recommended using rollers as supports so that the friction between the specimen and the support is reduced (van de Ven et al., 1997). The Nottingham Asphalt Tester (NAT) machine was used for this test. This machine applied a monotonic load with a constant rate of displacement (1 mm/min) until failure. It has the ability to capture the test results (load vs displacement). A camera was placed in front of the SCB specimen to capture the crack growth rate.

The maximum stress at failure (σ_{max}) was calculated according to the following equation:

$$\sigma_{max} = \frac{4.263 \times F_{max}}{D \times t} \quad (N/mm^2) \qquad \text{Equation 8-7}$$

where D is the diameter, t is the sample thickness, both in millimetres, and F is the maximum force on the sample in Newtons.

The fracture toughness (K_i) was calculated according to the following equation:

$$K_i = \sigma_{max} \times f\left(\frac{a_i}{W_i}\right) \quad (N/mm^{3/2}) \qquad \text{Equation 8-8}$$

where W_i is the height of the specimen, a_i is the notch depth, both in mm, and $f(a_i/W_i)$ is a geometric factor. The geometric value $f(\frac{a_i}{W_i})$ is 5.956, for $9 < a_i < 11$ mm and $70 < W_i < 75$ mm. For other a_i and W_i values, the geometric value can be calculated according to the following equation:

$$f\left(\frac{a_i}{W_i}\right) = -4.9965 + 155.58\left(\frac{a_i}{W_i}\right) - 799.94\left(\frac{a_i}{W_i}\right)^2 + 2141.9\left(\frac{a_i}{W_i}\right)^3 - 2709.1\left(\frac{a_i}{W_i}\right)^4 + 1398.6\left(\frac{a_i}{W_i}\right)^5$$

Equation 8-9

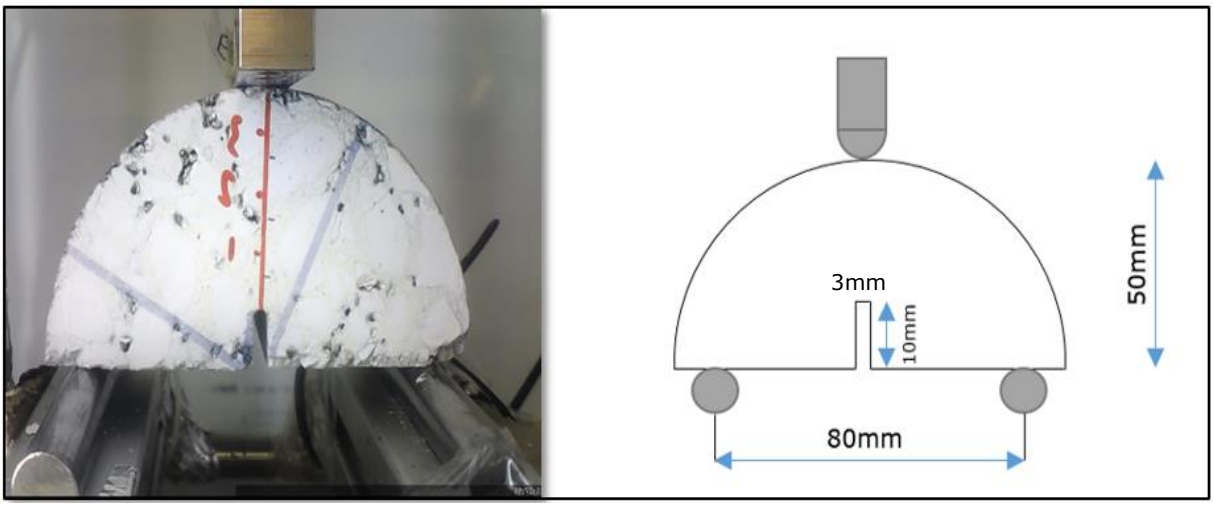


Figure 8-25 SCB test configuration

8.8.2 Sample preparation

The mixing proportions and processes, in addition to specimen coring and cutting, are reported elsewhere (section 3.5.2 and 3.5.3 of chapter three, respectively). These mixtures were compacted by roller compactor. The specimen with 100 mm diameter and 45 mm thickness was cut into two symmetrical halves by using a masonry saw. Then a notch of 10 mm ±2 mm in length was cut vertically in the middle of the bottom edge of the specimen using the masonry saw. All specimens

were conditioned overnight in a controlled air cabinet at the test temperature (0℃ and 20℃) before testing.

8.8.3 Results and Discussion

Fracture toughness (K_i) of asphalt mixture is considered the main outcome of the SCB test and it has been used as a fracture assessment parameter by several researchers under different test conditions. Fracture toughness (K_i) of thirteen asphalt mixtures with different fibre types and contents is illustrated in Figure 8-26 and Figure 8-27. Three replicates were used for each asphalt mixture. Error bars represent plus and minus one standard error. The SCB test was performed at two test temperatures (20℃ and 0℃). 20℃ was chosen to be similar to the previous investigation in the ITS and ITFT tests, while 0℃ was selected to examine the influence of fibre reinforcement on low temperature cracking of asphalt mixture.

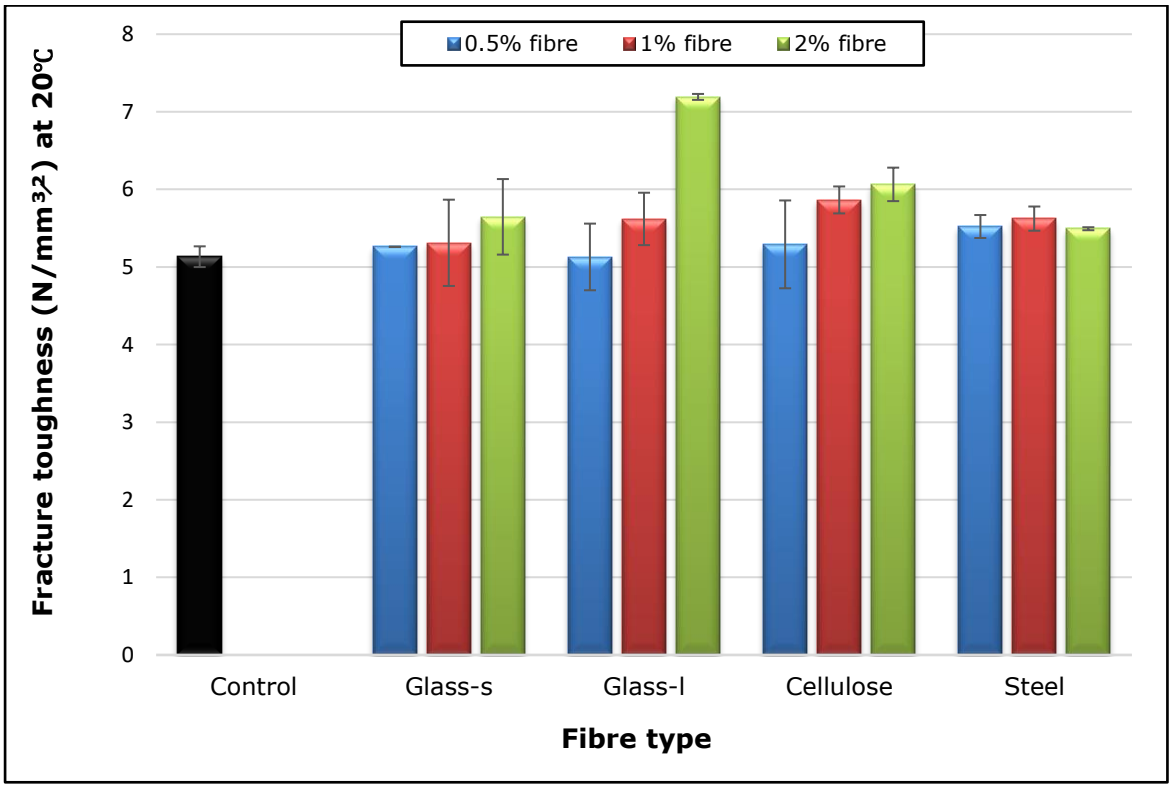


Figure 8-26 Fracture toughness of control and fibre reinforced asphalt mixtures at 20℃

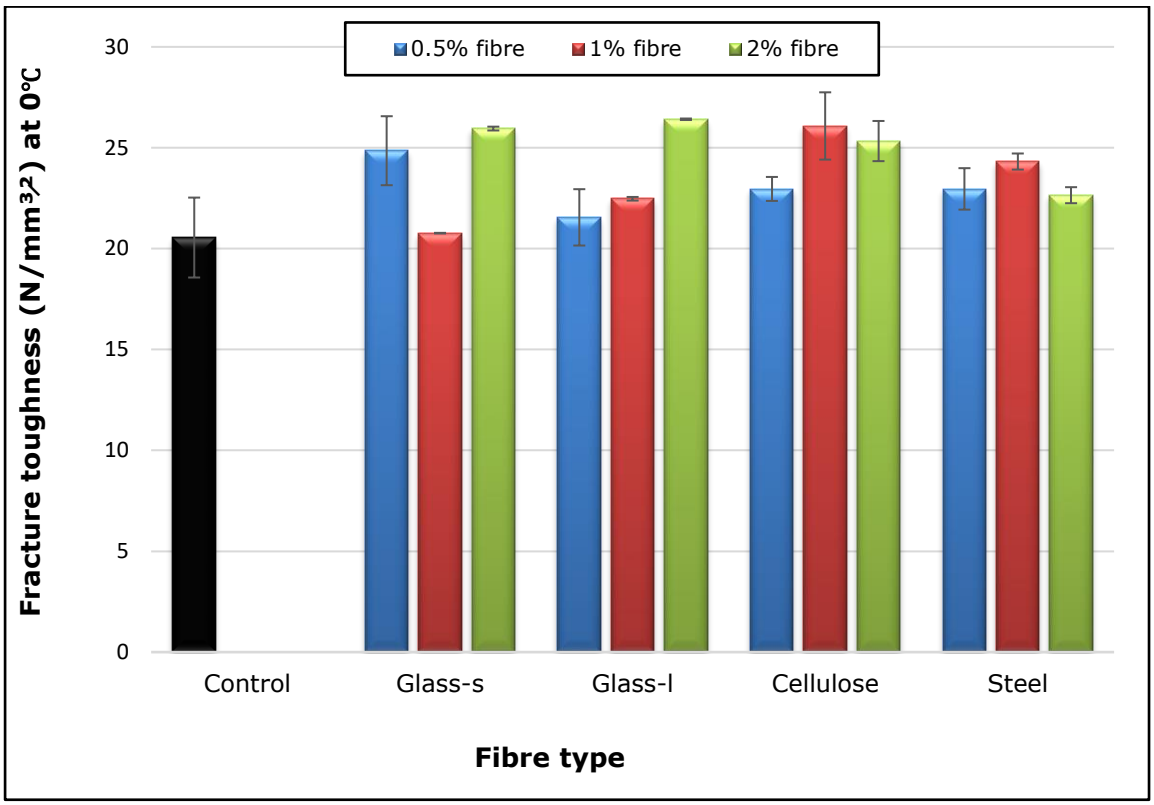


Figure 8-27 Fracture toughness of control and fibre reinforced asphalt mixtures at 0℃

In Figure 8-26 and Figure 8-27, there is a clear through the slight trend of increasing fracture toughness (Ki) for fibre reinforced asphalt mixtures compared to a control mixture. The fracture toughness at 20℃ increased gradually with the increase in fibre content and led to significant improvement mainly at 2.0%, as shown in Figure 8-26. This supports the finding from ITFT tests that adding fibre may improve the resistance of asphalt mixture against fatigue cracking. There are several possible explanations for this result. Firstly, the ability of fibre networks in delaying crack propagation by spreading the stress across a larger area may lead to a reduction in the stress concentration caused by the cracks which thus take more time to propagate (Razmi and Mirsayar, 2017). This is one of the reasons for significant improvement in fracture toughness at 20℃ of 2.0% long glass fibre reinforced asphalt mixture due to the presence of a large number of fibres in the notch area compared to glass-s and steel fibres. This was investigated by visual

observation after the test finished, as shown in Figure 8-28. Also, for fibre with a higher length/diameter ratio, the formation of a networking system will be more effective at interweaving (Xu et al., 2010). It should be noted that glass and steel fibre reinforced samples after testing at 20℃ did not split in two, while most cellulose and all control mixture samples spilt when the test finished.

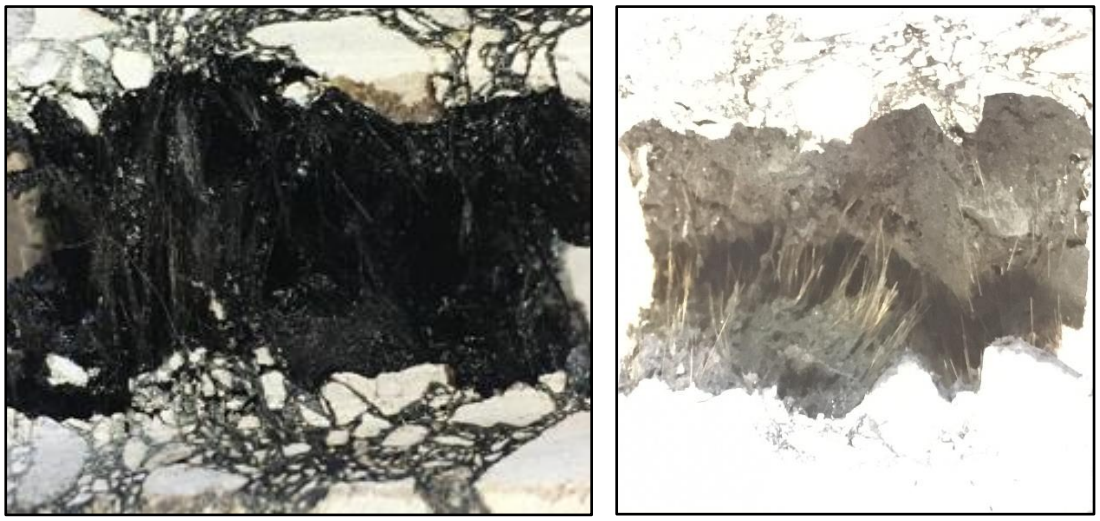


Figure 8-28 Long glass fibre into the notch area of asphalt mixture

Table 8-5 T-test for fracture toughness of control and fibre reinforced asphalt mixtures

Asphalt Mixtures	Mean ($N/mm^{3/2}$)	T-stat	P-value	Significant*
Control	5.132	-	-	-
0.5% Glass-s	5.260	0.957	0.219	No
0.5% Glass-l	5.129	0.007	0.497	No
0.5% Cellulose	5.291	0.273	0.414	No
0.5% Steel	5.521	1.951	0.061	No
1% Glass-s	5.311	0.313	0.392	No
1% Glass-l	5.619	1.340	0.136	No
1% Cellulose	5.864	3.338	0.014	Yes
1% Steel	5.623	2.132	0.037	Yes
2% Glass-s	5.646	1.017	0.247	No
2% Glass-l	7.192	14.819	0.002	Yes
2% Cellulose	6.064	3.674	0.033	Yes
2% Steel	5.593	2.951	0.023	Yes

* Indicates significant at the 95 percent confidence interval.

Another reason for these results is the ability of fibre to absorb/adsorb bitumen fractions resulting in stiffer bitumen, as shown in the drain-down test results in chapter six. Also adding fibre increases the cohesive strength of asphalt mortar as shown in pull-off tensile strength results earlier in chapter six. According to a previous study, it was found that binder with higher stiffness showed higher fracture toughness (Ki) (Biligiri et al., 2012). It is interesting to note that the fracture toughness increases with the increase in fibre contents at 20℃ test temperature, whereas at 0℃, the trend was more scattered. This is due to the fracture at 0℃ being through a combination of both aggregate and mastic as shown in Figure 8-29. Adding fibre to asphalt mixtures generally resulted in a slight improvement in the average fracture toughness at 0℃, although there is a large

degree of scattering in the results. Such an improvement can enhance the resistance of asphalt mixture to low temperature cracking.



Figure 8-29 Fracture face at 0℃ test temperature

The maximum stress and peak load were evaluated. As shown in Figure 8-30 and Figure 8-31, the maximum stress increased when fibres were added. The maximum stress increased with increase in fibre contents at the 20℃ test temperature. This confirms the improvement in fracture toughness and indicates an enhancement in mechanical properties of the asphalt mixture. The peak load increased with the addition of fibre, as shown in Figure 8-32 and Figure 8-33.

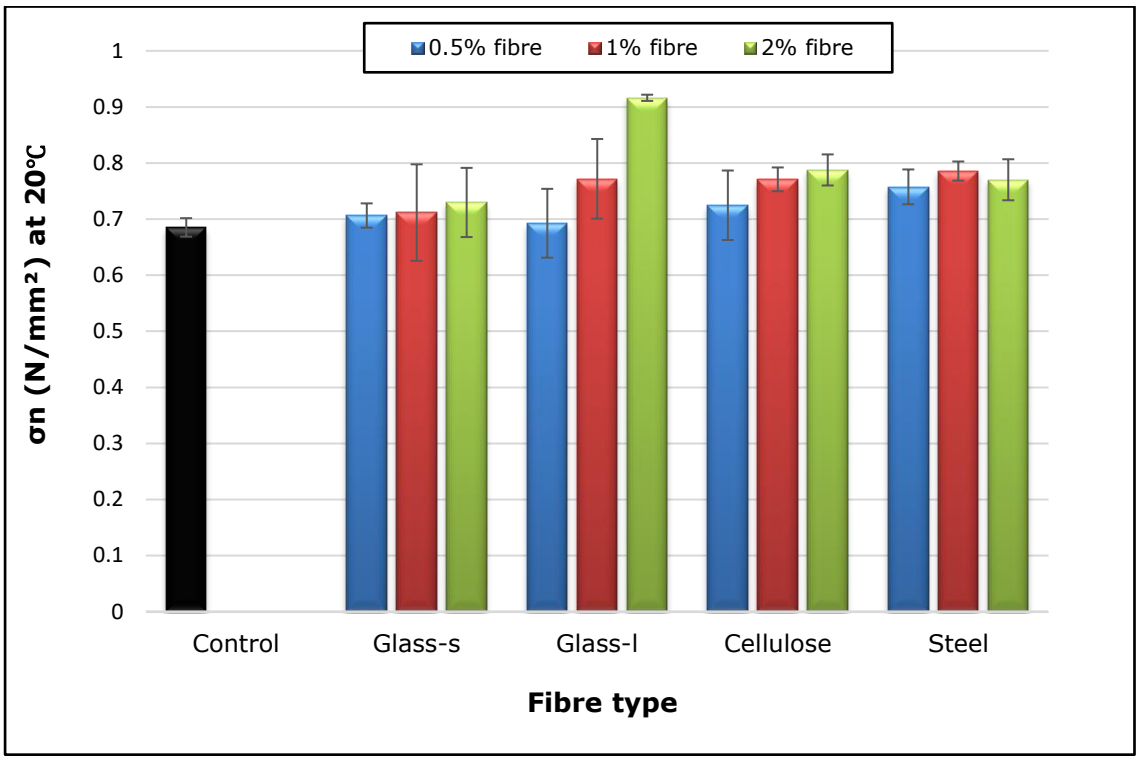


Figure 8-30 Maximum stress of control and fibre reinforced asphalt mixtures at 20℃

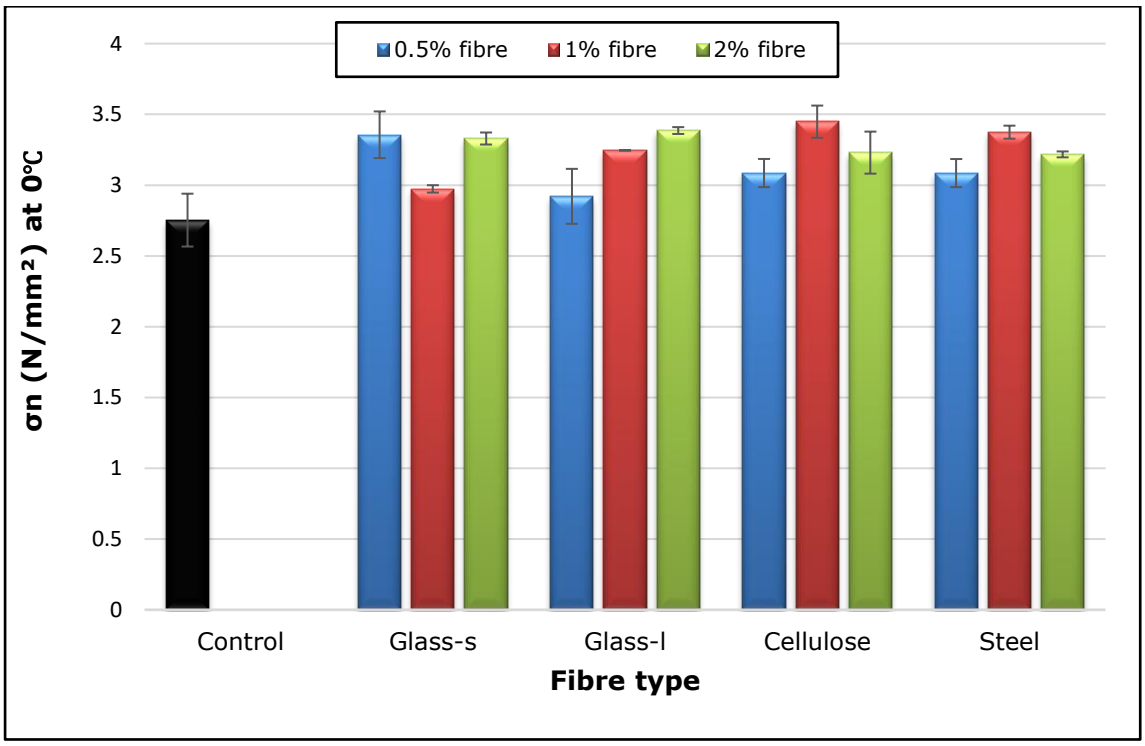


Figure 8-31 Maximum stress of control and fibre reinforced asphalt mixtures at 0℃

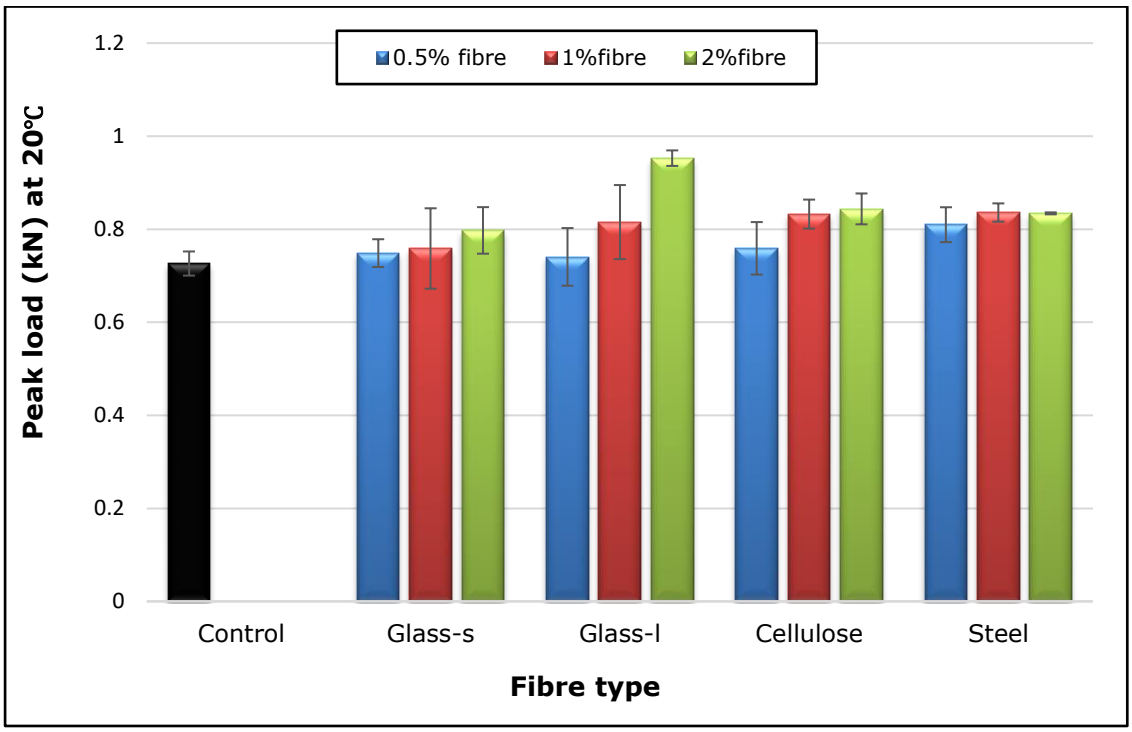


Figure 8-32 Peak load of control and fibre reinforced asphalt mixtures at 20℃

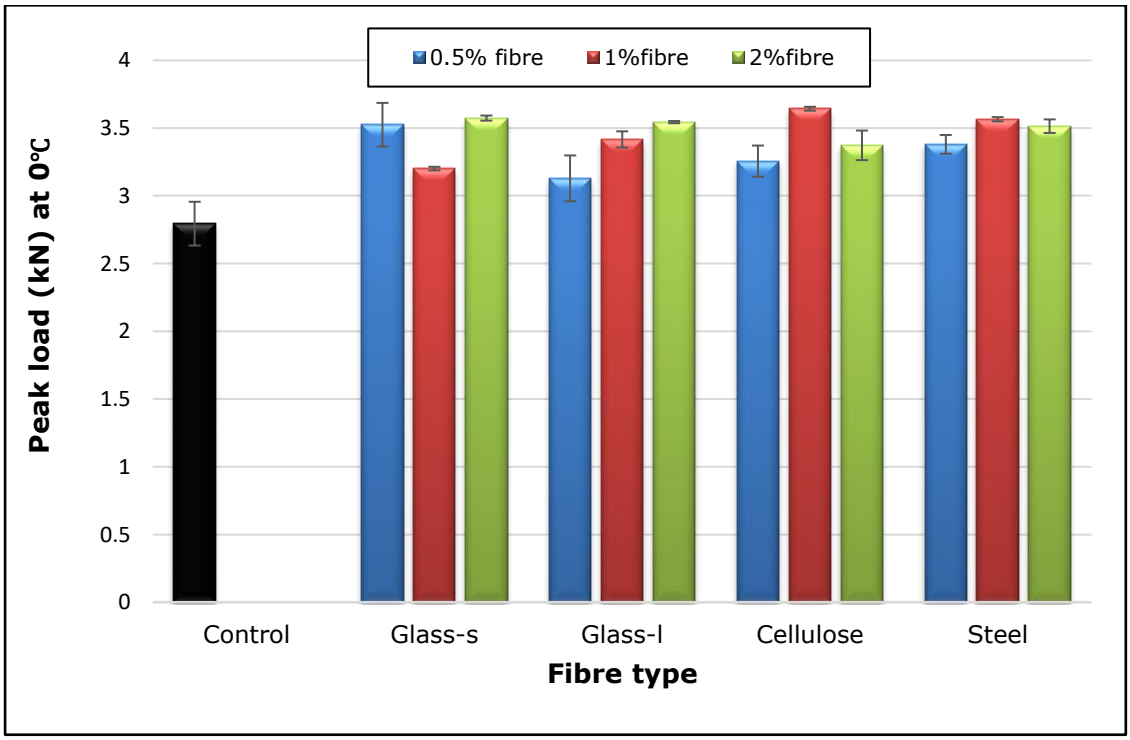


Figure 8-33 Peak load of control and fibre reinforced asphalt mixtures at 0℃

8.9 Summary and conclusions

This chapter has examined the influence of different fibre types and amounts on the mechanical properties of asphalt mixture, by means of fatigue cracking resistance, moisture damage resistance and fracture toughness based on ITFT, ITSR and SCB tests, respectively. The study has also explored the fibre presence and distribution in the asphalt mixture by using X-ray CT and image analysis. Based on the discussion and analysis presented in this chapter, the following conclusions are offered:

- Steel fibre distribution and orientation have been investigated successfully, using X-ray CT. This technique was not successful for glass or cellulose fibres, which have a density similar to other components of the mixture.

- It was found that steel fibres are present throughout the mixture, although there is some variability in their distribution through the sample. Images showed that the steel fibres are arranged at a variety of angles, forming a three-dimensional network throughout the sample.

- The fibres increased the stiffness of the asphalt mixtures, by modification of the bitumen mastic (as demonstrated by previous studies) and by spreading the load through the fibre networks throughout the sample.

- The fatigue life of modified asphalt mixtures was higher than the fatigue life of control mixture at low strain values at fibre contents 0.5% and 1.0%, while this was the other way around at high strain values.

- Adding fibre produced a marked influence on the fatigue life of fibre reinforced asphalt mixtures compared to a control mixture when the results were expressed as a function of the applied stress.

- Indirect tensile strength of asphalt mixture is improved when fibres are added. Steel fibres showed the highest improvement among all fibre types.

- Control and fibre reinforced asphalt mixtures exhibited higher resistance to moisture damage, and surprisingly, their properties seemed to improve after being exposed to the moisture damage procedure.

- Specimens after RLAT testing were more susceptible to moisture damage. No systematic difference was found between control and fibre reinforced specimens.

- Fibre reinforced asphalt mixtures showed higher fracture toughness than the control mixture. Fracture toughness at 20 ℃ shows statistically significant increase with the increase in fibre content. This supports the findings from ITFT tests.

- Adding fibres showed an improvement in the low temperature cracking resistance of asphalt mixtures as they exhibited higher fracture toughness and maximum stress compared to the control mixture at 0 ℃ test temperature.

- The extensive range of mechanical tests used in this study lead to one general conclusion: Adding these fibres enhances the properties of asphalt mixture in tests designed to assess their performance with respect to the predominant modes of deterioration in flexible pavements that is, stiffness, moisture damage, low thermal cracks and fatigue.

Chapter 9 Pavement design

Pavement analysis and design

9.1 Introduction

In the previous chapters, extensive investigation has been made, with regard to the mechanical properties of control and fibre reinforced asphalt mastics, mortars and mixtures. The results support the study of the influence of using these mixtures in pavement design. It is known that the pavement structure should be designed such that the critical levels of strains for the materials used should not be exceeded during the design life. In order to achieve this, pavement design depends on the mechanical properties of the materials (Brown, 1988). In addition to the mechanical properties, traffic volume and environmental conditions are also important factors in pavement design (Otte, 1977). However, there is still no single agreed method for pavement design (Thom, 2008).

Flexible pavements are engineered structures made of different layers such as wearing, binder and base course, subbase and subgrade. Each one of these layers has definite mechanical properties and a specific role. The road element that directly supports traffic loads is the wearing course. This layer usually has relatively high bitumen contents and maximum aggregate size less than 19 mm, which may help the wearing course to withstand traffic loadings and environmental attack, and provide a better ride comfort to road users. Underneath the wearing course layer is the binder course, then followed by the base course. In general, binder and base course are designed with larger aggregate sizes compared to the wearing course.

Also, these two layers are placed in thicker lifts compared to the wearing course. Such an aggregate size required less binder content with a greater thickness that may reduce the construction cost. These three layers together are known as bound layers due to the existence of the binder, which holds the components together. Usually, these three layers are supported by a subbase layer. The subbase layer is constructed from crushed stone or gravel with a thickness range from 100 to 300 mm and should be well compacted. Underneath the subbase layer is the subgrade which is the soil on which the road is constructed. These are the typical pavement layers (Jenks et al., 2011).

This chapter aims to evaluate the possibility of using fibre reinforced asphalt mixture (FRAM) as a road paving material. To achieve this goal asphalt mixtures modified by four fibre types (glass long and short, cellulose and steel fibres recovered from tires) with three different contents are used in pavement analysis and design as a binder layer, and then compared to a control mixture. In this chapter, a mechanistic-empirical approached is used in pavement analysis and design through the KENLAYER software.

9.2 Pavement structure

A pavement structure consisting of three layers has been used, and each layer is considered as a linear elastic material classified by specific properties such as stiffness modulus and Poisson's ratio, as shown in Figure 9-2. Traffic load is represented by a single axle with dual wheel load. Dual wheel load is expressed in this study as a uniformly distributed stress applied over a circular area. Various computer softwares have been used to estimate the strains, stresses and vertical deflections which occur in the pavement structure as a result of the applied load (Wardle, 1977, Dejong et al., 1973) cited in (Brown, 2013). In addition, these programs are able to deal with more complicated structures with regard to the load configuration and number of layers than the one used in this chapter.

In simple pavement design, the designers pay attention to only two locations in the pavement structure. The first one is at the bottom of the asphalt layer where the maximum tensile strain (ε_t) develops, and the other is at the top of the subgrade where the maximum compressive strain (ε_z) develops, as shown in Figure 9-1. If the tensile strain at the bottom of the asphalt layer becomes higher than the tensile strength of the asphalt material, a crack starts to initiate and propagates upward, causing failure (Brown, 2013). However, in this study the major and the minor strains were measured in all pavement layers.

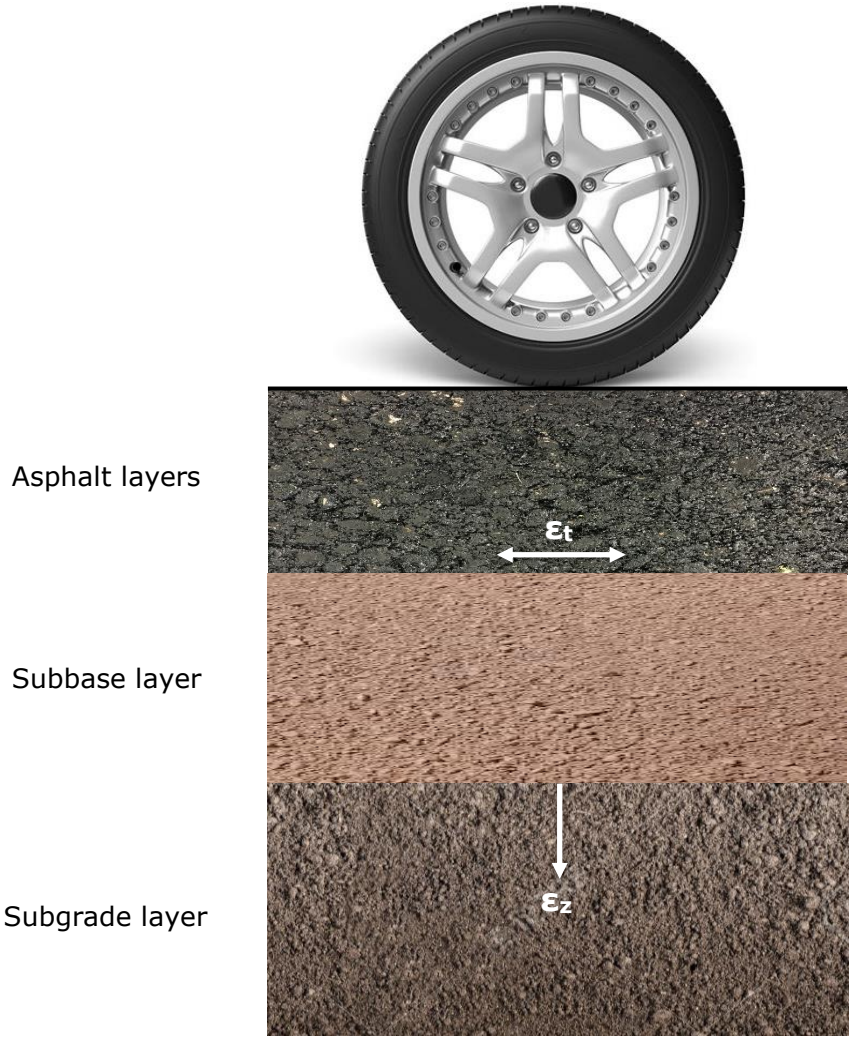


Figure 9-1 Structure of flexible pavement

Fatigue cracking in asphalt is initiated as a result of the strain level due to the applied traffic loads and not the stress. Therefore, the strain is normally used to characterise the fatigue cracking resistance of the asphalt material, as shown in the following equation:

$$\varepsilon_t = a(\frac{1}{N_f})^b \qquad \text{Equation 9-1}$$

where a and b are parameters dependent on the asphalt mixture properties such as binder content and binder properties, and these parameters are different from one test method to another (Brown, 2013).

9.3 Pavement structure and material properties

The pavement layer structural properties play a significant role in pavement design, in that the stresses and strains and the incidence of failure resulting from traffic load depend on the thicknesses of the designed layers and material properties. The elastic properties are the main factor which influences the strains, stresses and failure parameters. It is well known that the elastic properties of bituminous materials are influenced by the rate of loading and temperature, while granular materials and soils are usually affected by the moisture conditions and stress level (Brown, 2013).

The investigation of mechanical properties in the previous chapters indicated the potential improvement in the performance of fibre reinforced asphalt mixtures; therefore, an attempt is made in this chapter to examine the usefulness of these mixtures in pavement design. In this chapter fibre reinforced asphalt mixtures are used as binder course and base due to the steel fibre which cannot be used in the wearing course. The pavement analysis and design parameters of asphalt mixtures implemented in this study are shown in Table 9-1. Stiffness modulus values shown in Table 9-1, were measured in the laboratory for each mixture, as shown in chapter eight, and they are multiplied by a 1.5 shift factor to simulate field conditions (Thom,

2008), i.e. an approximate ten field increase in loading rate. The fatigue life equations illustrated in Table 9-1, were got from ITFT laboratory test for each mixture, as shown in the previous chapter.

Table 9-1 Control and fibre reinforced asphalt mixtures used in pavement analysis and design**

Mixture type	Stiffness modulus (MPa)* at 20℃	Stiffness modulus standard error bar	Fatigue life equations at 20℃
Control mixture	3945	54.5	$N_f = 3\times10^{10} \times \varepsilon^{-2.794}$
0.5% Glass-s	4365	90.6	$N_f = 1\times10^{11}\ \varepsilon^{-3.128}$
0.5% Glass-l	4290	65.6	$N_f = 1\times10^{12}\ \varepsilon^{-3.462}$
0.5% Cellulose	4136	68.1	$N_f = 2\times10^{10}\ \varepsilon^{-2.726}$
0.5% Steel	4680	52.4	$N_f = 2\times10^{12}\ \varepsilon^{-3.481}$
1.0% Glass-s	4671	156.2	$N_f = 5\times10^{10}\ \varepsilon^{-2.890}$
1.0% Glass-l	4631	104.2	$N_f = 4\times10^{11}\ \varepsilon^{-3.230}$
1.0% Cellulose	4950	98.6	$N_f = 2\times10^{13}\ \varepsilon^{-4.024}$
1.0% Steel	4857	130.2	$N_f = 1\times10^{12}\ \varepsilon^{-3.355}$
2.0% Glass-s	5222	240.9	$N_f = 3\times10^{10}\ \varepsilon^{-2.860}$
2.0% Glass-l	4776	62.5	$N_f = 7\times10^{9}\ \varepsilon^{-2.619}$
2.0% Cellulose	5057	247.4	$N_f = 2\times10^{11}\ \varepsilon^{-3.175}$
2.0% Steel	4977	115.2	$N_f = 6\times10^{10}\ \varepsilon^{-2.978}$

*Stiffness values shifted by 1.5 shift factor (see section 9.3)
**Poisson's ratio assumed 0.35

The pavement structure case study in this chapter consists of a conventional bituminous wearing course (40 mm), control and fibre reinforced asphalt mixtures as binder course and base (200 mm), a granular subbase (200 mm) and soft soil subgrade, as shown in Figure 9-2.

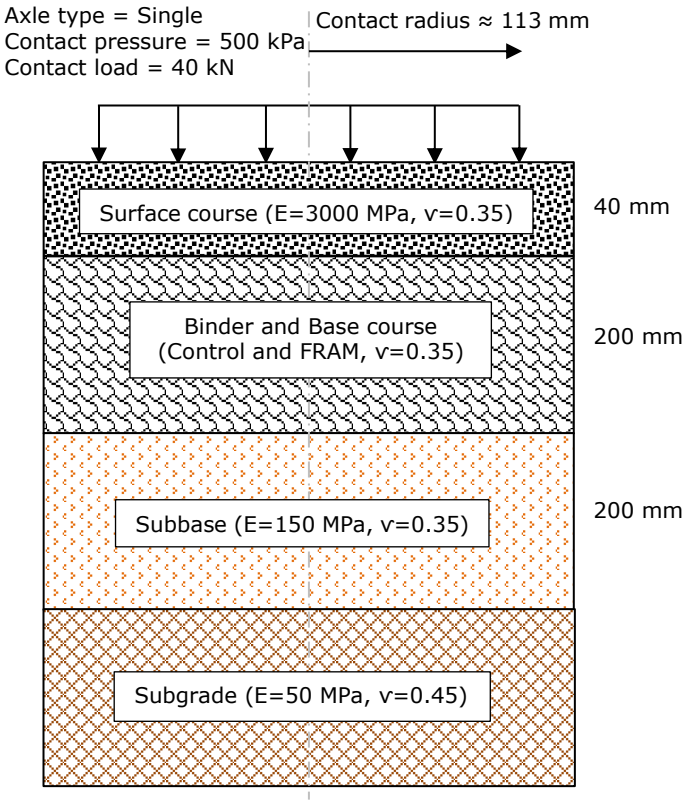


Figure 9-2 Pavement structure considered for the analysis

9.4 Design principle and analysis

The KENLAYER computer software developed by Huang (2004) was used in pavement analysis and design in this chapter. This program is widely available and considered a useful tool in terms of pavement design. The pavement structure used as a case study was shown in the previous section, and the focus was on the binder and base courses. A single axle with a dual tyre loading system per axle tyre, 40

kN, 500 kPa contact tyre pressure, giving a contact area radius of 113 mm, the dual tyres were 340 mm apart centre to centre.

The dual tyres give the possibility of the critical stress and strain position lying at three points (under the centre of the contact area, away from the centre by a distance equal to the radius of the contact area and at the point midway between the two tyres) (Huang, 2004).

In general, there are two main modes of failure that occur in the road, cracking in the bound layers as a result of repeated load and rutting in the wheel path. Therefore, it is important to consider both modes of failure in pavement design to make sure that the pavement can withstand these two types of failure (Brown, 2013). However, since chapter seven has already dealt with the rutting, the pavement design in this study was based on the fatigue criterion only. The horizontal tensile strain in the bottom of the asphalt layer was therefore used as the design parameter. Fatigue cracking in the asphalt layer under repeated traffic loads occurs as a result of tensile strain instead of stress. Consequently, the resulting strain is then implemented into a fatigue equation such as those in Table 9-1 and Equation 9-1 to characterise the fatigue life of the asphalt mixture (Kuna, 2015).

However, it should be noted that no laboratory fatigue testing can accurately simulate actual field performance due to a number of reasons. Therefore, different shift factors are usually applied in an attempt to account for the difference between laboratory test results and site conditions such as the effect of healing in the field, temperature, rate of loading, the pattern and lateral distribution of traffic loads (Singh et al., 2016, Thom, 2008).

9.5 Results and Discussions

9.5.1 Strain distribution in pavement layers

The pavement structure shown in Figure 9-2 was used in this analysis. The major and minor strain distributions through pavements layers containing a conventional bituminous mix of 40 mm thickness, control and fibre reinforced asphalt of 200 mm thickness, subbase layer of 200 mm and subgrade, are shown in Figures 9-3 and 9-4, respectively.

As shown in Figure 9-3 within the surface layer, the major strain distribution is not very different between control and fibre reinforced asphalt mixtures. However, in the binder/base and subbase layers, the difference is greater. This is because the fibre reinforced asphalt mixtures in the binder/base course resulted in a stiffer mixture compared to the control mixture. It is interesting to note that the difference in major strain between control and fibre reinforced asphalt mixtures increased with the increase in fibre content. Once again, this is because adding more fibres results in a stiffer mixture (see chapter 8).

With regards to minor strain, it was found that the value of minor strain was lower for fibre reinforced asphalt mixtures compared to a control mixture. This is because the stiffness values of fibre reinforced asphalt mixtures are higher than that of the control mixture. The difference in minor strain values between control and fibre reinforced asphalt mixtures increase with the increase in fibre contents as shown in Figure 9-4.

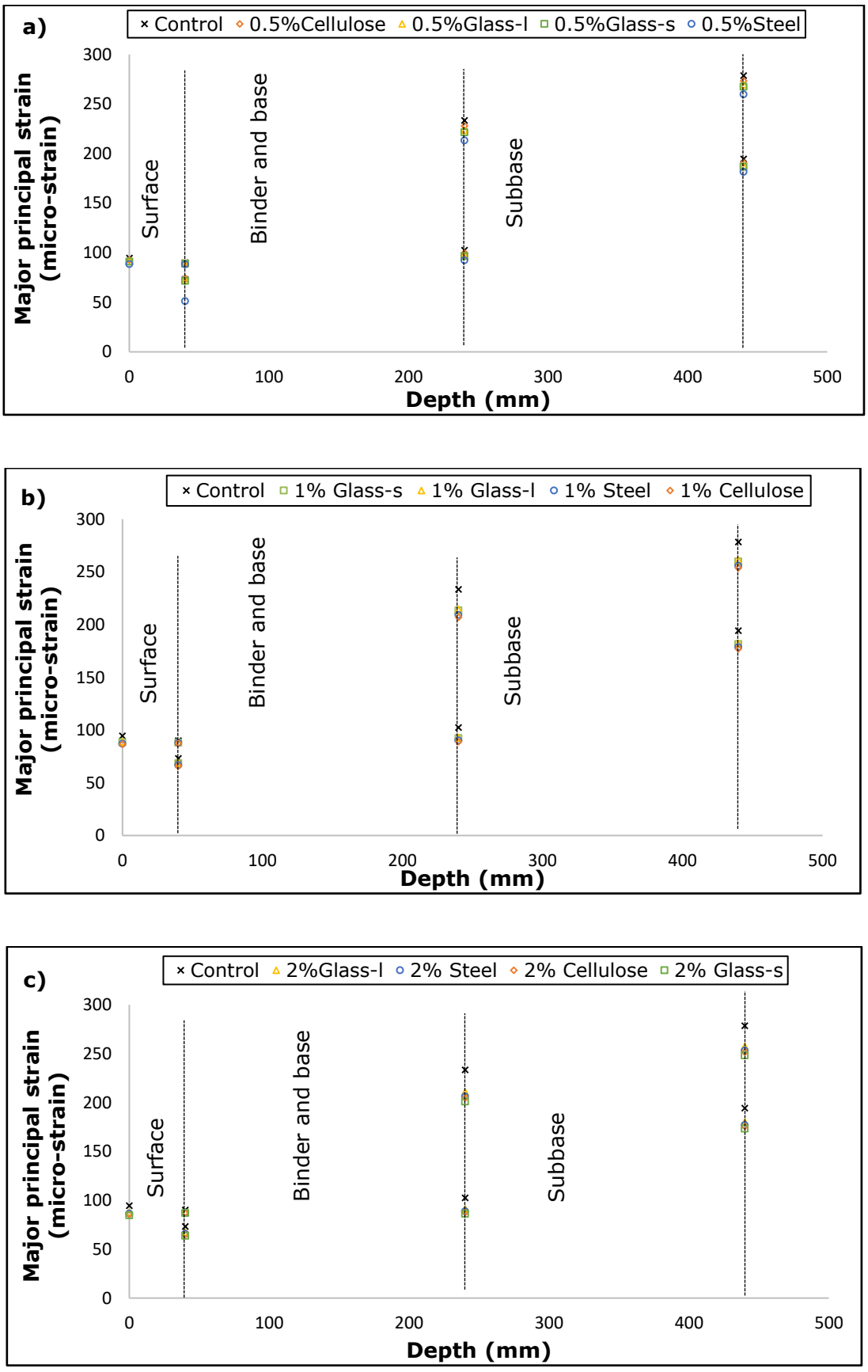
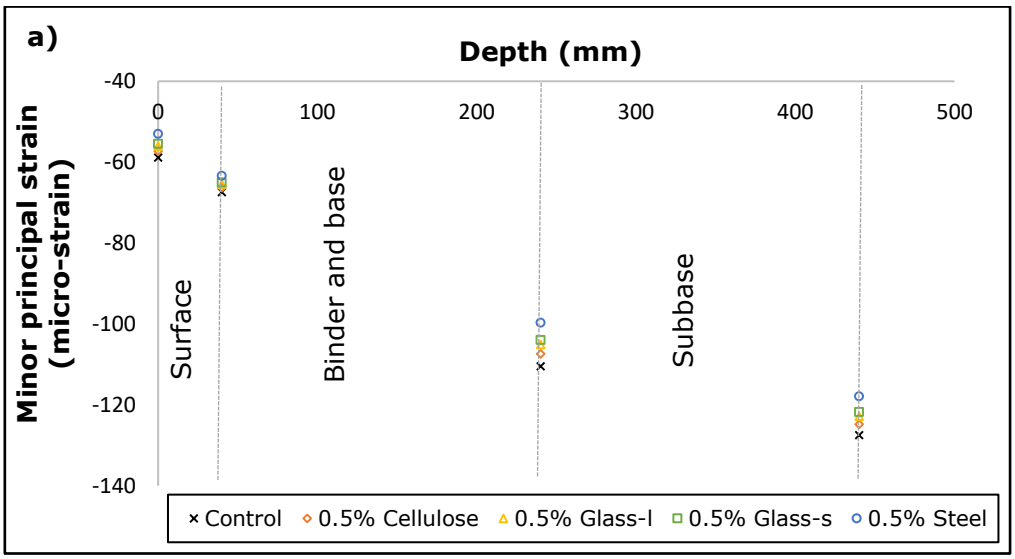
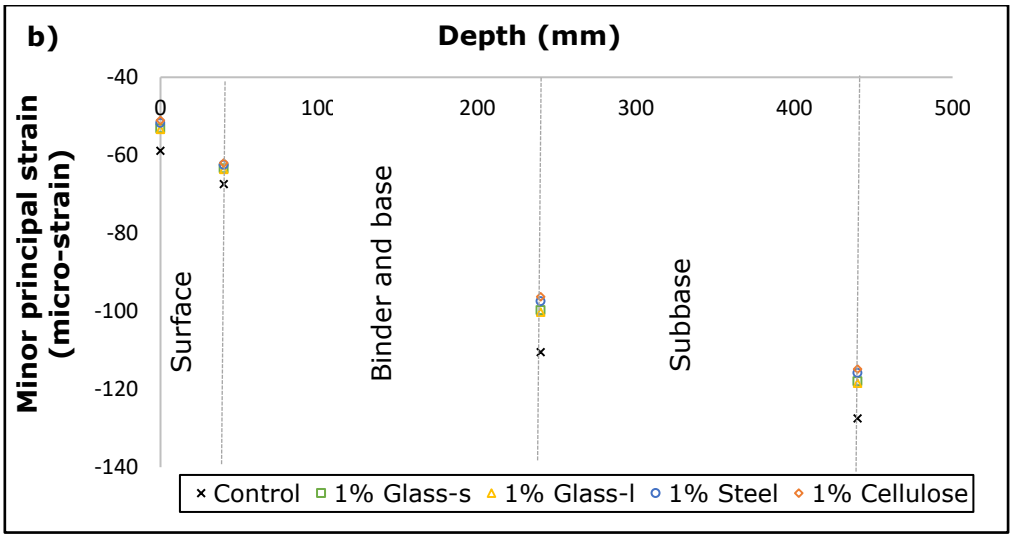


Figure 9-3 Major principal strain distribution through the pavement structure





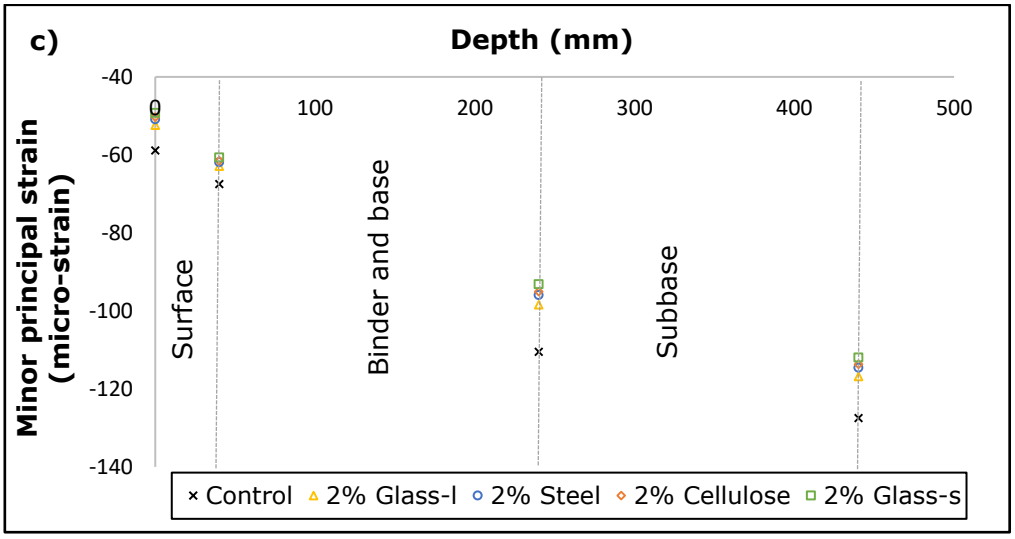


Figure 9-4 Minor principal strain distribution through the pavement structure

9.5.2 Design of FRAM binder course for fatigue life

The principal horizontal strain results of the analysis using the KENLAYER software at the bottom of the base layer are implemented in the fatigue equation shown in Table 9-1. Fatigue life equations conducted at 20℃ (see chapter 8) were used in the pavement design. A 3000 MPa stiffness value is assumed for the wearing course layer. It is important to note that the number of passes shown in Figure 9-5 has not been shifted by any factors. This is because the focus of this study is on the comparison between control and fibre reinforced asphalt mixtures and no specific shift factor value for fibre reinforced asphalt mixture can yet be proposed.

Figure 9-5 shows the number of passes to failure for each binder/base mixture based on the maximum horizontal strains at the bottom of the base course. The number of passes in Figure 9-5 were calculated for each mixture by using fatigue life equations in Table 9-1. The results clearly indicate that adding fibres especially steel, cellulose and glass-l led to an increase in the pavement life, as shown in Figure 9-5. Adding 1.0% cellulose, 0.5% and 1.0% of steel fibres showed the highest improvement in pavement life compared to other asphalt mixtures. The highest increase in pavement life reached almost four times the life of the control mixture, and this indicates an improvement in cost-effectiveness of using these fibres. These findings are promising and encouraging, especially for cellulose and steel fibres. However, using these modified asphalt layers in a pavement design has to be checked through full scale pavement tests. It should be note that these results are based on stiffness and fatigue life of the binder/base asphalt course.

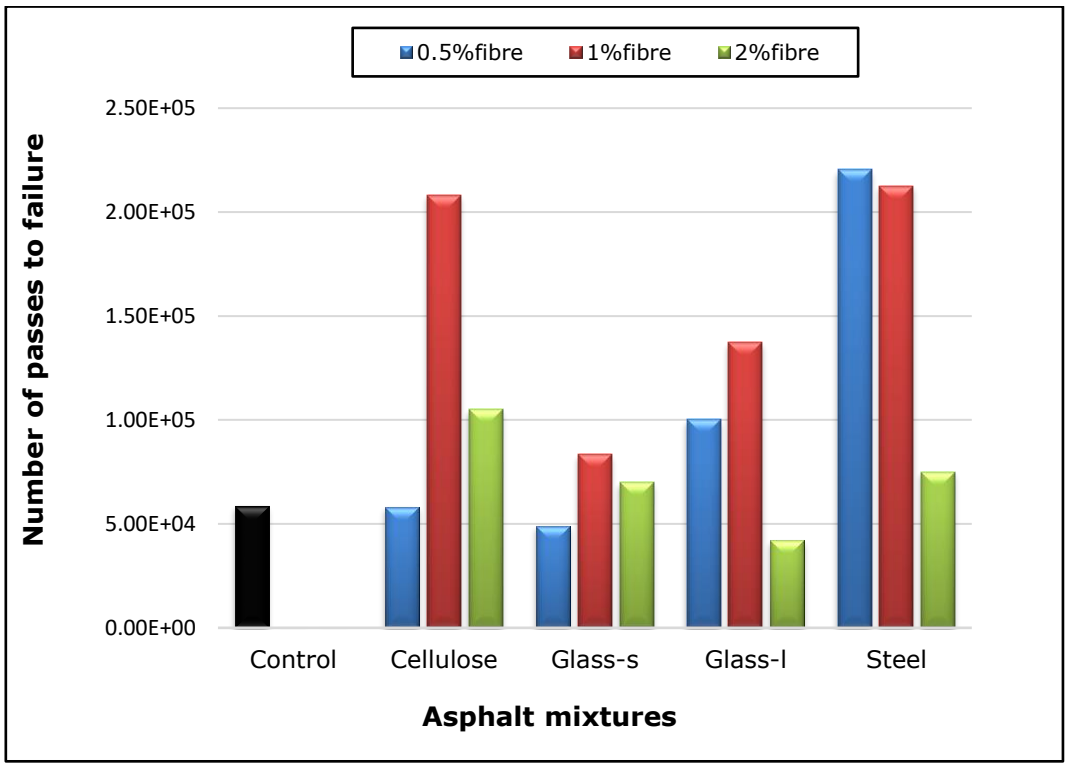


Figure 9-5 Number of passes to failure for control and fibre reinforced asphalt mixtures

9.6 Summary and conclusions

Flexible pavement analysis and design incorporating fibre reinforced asphalt mixtures have been successfully investigated in this chapter. The example used in this study is hypothetical in nature, but the finding showed clear differences between control and fibre reinforced asphalt mixtures. The conclusions in this chapter are offered below:

- The analysis result of KENLAYER software showed that adding fibre to the asphalt mixture resulted in lower horizontal strain value at the bottom of the binder layer where this mixture is implemented.
- Major and minor strain values of fibre reinforced asphalt mixtures in the pavement structure were lower than that of the control mixture.

- 1.0% cellulose, 0.5% and 1.0% of steel fibre reinforced asphalt mixtures showed the highest improvement in pavement life compared to other fibre types and amounts. This increase in pavement life reached almost four times compared to the pavement life of the control mixture, which indicates a marked improvement in cost-effectiveness. On the other hand, glass fibre, especially the short one, did not show good performance due to the poor fatigue life compared to other fibre types and the control mixture.

Chapter 10 Conclusions

Conclusions, implications and recommendations

10.1 Introduction

The main aims of this thesis were to explore and provide a deeper understanding of the effect of different fibre types on mastic, mortar and dense bitumen asphalt mixture properties. This study also aimed to determine which fibre type provides the best performance with regard to permanent deformation and cracking resistance, providing a better understanding of using fibres in asphalt construction.

The research in this thesis was divided into three areas

- Conventional and shear rheological testing of base and fibre reinforced mastics.
- Explanation of fibre reinforcement mechanisms associated with changes in conventional, rheological and bond strength of base and fibre reinforced asphalt mortars.
- Applicability of conventional mechanical performance tests and KENLAYER software at describing the performance and cost effectiveness of control and fibre reinforced asphalt mixtures.

10.2 Conclusions and implications

The conclusions in this thesis were based on three parts.

10.2.1 Conclusions are drawn from the literature review:

- A few researchers have used dynamic shear rheological testing to examine the influence of different fibre types on the rheological properties of bitumen. In general, they came to the same conclusion that adding fibres improves bitumen stability and stiffness. However, only one study found as much as a ten times increase in viscosity compared to pure bitumen.
- None of the previous researchers investigated important topics such as fibre length, orientation, geometry, cost effectiveness or possible chemical influence.
- Only one researcher examined the influence of adding fibre on the viscoelastic behaviour of asphalt mortar. Therefore, fibre reinforced asphalt mortar is relatively poorly characterised scientifically.
- There are two methods to introduce fibre to an asphalt mixture, namely dry and wet methods. There is no standard method stated by ASTM or BS. However, most researchers prefer the dry method, unless the fibre is brittle.

10.2.2 Characteristics of fibre reinforced asphalt mastics and mortars

Micrographs, conventional and more fundamental rheological properties of mastic and mortar reinforced by different fibre types and amounts are examined in this study. The main novel findings are explained below:

- Fibre shape, size, texture and microstructure play a vital role in the way that fibres influence the performance of modified asphalt mastics and mortars. In this study, these properties were investigated by using a scanning electronic microscope. These properties will influence how fibres

can reinforce bitumen through the formation of three dimensional networks within the modified mastics or mortars. Glass fibre forms such a network.

- The conventional properties of the mastic improved when fibre was added. Long glass fibre (13 mm) exhibited the greatest improvement in terms of viscosity, softening point and penetration. These results indicated that adding fibre could lead to improved bitumen stiffness, permanent deformation resistance of asphalt mixture and reduced drain-down.
- Using a Dynamic Shear Rheometer (DSR) together with rheological data in the form of complex modulus, phase angle master curves, isochronal plots and rutting parameters, when used in concert and correctly interpreted, provide a clear representation of the rheological properties of fibre reinforced mastics and mortars. Conventional tests such as penetration, viscosity and softening point, although able to suitably describe the influence of fibre on the rheological properties of base mastic and mortar, are unable to clarify the unique rheological behaviour of modified mastics and mortars.
- In general, the differences in rheological properties between the base and modified mastics and mortars are more noticeable at low frequency and high temperatures, which relate to increased permanent deformation resistance of asphalt mixtures. Under these circumstances, the viscosity of base mastic and/or mortar is low enough to allow the fibre entanglement to control the rheological properties of fibre reinforced mastics and/or mortars.
- Cellulose fibre mastic phase angle master curves showed different behaviour compared to other fibre types and base bitumen and led to a significant decrease in the phase angle at both high and low frequencies. While phase angle master curves of modified asphalt mortars with different fibre types were quite similar to each other but different from that of base mortars.

- Adding fibre to asphalt mastic and/or mortar led to a marked increase in rut resistance parameters mainly at moderate and high temperatures. The rut resistance parameters increased with the increase in fibre contents.
- The dynamic shear rheometer results of asphalt mastics indicate that 2.0% addition of cellulose fibre showed the highest potential improvement. Asphalt mortar test results indicate that 1.0 filler to bitumen ratio and 2.0% addition of glass and steel fibres showed the highest potential improvement, while 0.8 filler to bitumen ratio and 2.0% addition showed the best performance for cellulose fibre.
- The influence of fibre on mastic and mortar toughness has been investigated through the double edge notch tension test at 15℃ test temperature. It was found that the addition of fibres, particularly glass fibre, leads to a marked increase in essential and plastic work of fracture. This increase in mastic and/or mortar may contribute to improving the resistance of an asphalt mixture to cracking.
- To gain a better understanding of the possible chemical effect of fibre on the binding properties of bitumen, the drainage test was used. It was found that cellulose fibre can retain more than 55% of the binder. Other fibre types (glass and steel) can retain up to 30% of the binder. The asphaltene content and the rheological properties of the drained binder, before and after mixing with fibres were measured. The results indicated that all fibre types slightly increased asphaltene content and complex modulus of the drained binder compared to the base binder.
- The influence of fibre on the cohesive strength of the mortar and the adhesive strength between mortar and aggregate is still unknown. The results in this study indicated that adding fibre led to increased pull-off tensile strength of the mortar, at the same time changing the failure mode from cohesive to hybrid, implying an improvement in cohesive strength of the mortar.

- The dynamic contact angle (DCA) test was used to examine surface energy of drained binder after mixing with fibre. The results of the contact angle for each drained binder varied within a narrow range, making this a useful test for characterising the difference in the surface energy of these materials. It is important to note that there is a good agreement between the work of cohesion and pull-off tensile strength for 0.8 filler to bitumen ratio and higher work of cohesion results in higher pull-off tensile strength where the mode of failure is cohesive. These findings indicated that DCA is a useful test in evaluating binder bonding properties.

10.2.3 Microstructure, permanent deformation and mechanical properties of fibre reinforced asphalt mixture

- Steel fibre orientation and distribution have been examined by using X-ray CT and the Image J program. The results indicated that steel fibre was well distributed with a slightly higher percentage in the depth range from 25 to 40 mm of the specimen height (48 mm). It is important to note that individual fibres were distributed in different directions and thus provide an effective three-dimensional network through the composite. On the other hand, glass and cellulose fibres were hard to see in X-ray CT images.
- Multiple stress creep recovery (MSCR) results indicated that adding fibre enhanced the permanent deformation resistance of modified mastics significantly. However, the improvement was greater at low stresses compared to high stresses.
- Both immersed Hamburg wheel tracking test at 50℃ and repeated load axial (RLAT) test at 30℃ showed that the rut depths of fibre reinforced asphalt mixtures were significantly lower than that in the control asphalt mixture.

Cellulose fibre showed the highest reduction in rut depth compared to other fibre types and the control mixture.

- The combined MSCR, immersed Hamburg wheel tracking and RLAT tests led to the same conclusion, which is that adding fibre delays the build-up of rut depth in an asphalt mixture, which may lead to longer service life and a more comfortable drive for road users.
- Indirect tensile fatigue test (ITFT) results indicated that adding fibre led to a slight improvement in fatigue life of fibre reinforced asphalt mixtures compared to the control mixture, mainly at low strain values, while this was the other way around at high strain values.
- Adding fibre led to an increased indirect tensile strength of asphalt mixture. Steel fibre showed the highest increase in the indirect tensile strength among all fibre types. In terms of moisture damage, both control and fibre reinforced asphalt mixtures showed high indirect tensile strength ratio, which indicates high moisture resistance. Surprisingly, their properties seemed to improve after being exposed to the moisture damage procedure, which implies that the conditioning regime may be insufficiently aggressive in this test.
- Specimens after RLAT testing were more susceptible to moisture damage. No systematic difference was found between fibre reinforced and control specimens.
- Fracture toughness of fibre reinforced asphalt mixtures was higher than that of the control mixture at 20℃. Moreover, adding more fibre gave a statistically significant increase in fracture toughness which may indicate an improvement in asphalt mixture fatigue life.
- Semi-circular bending test results indicated an improvement in low temperature thermal cracking resistance of fibre reinforced asphalt mixture as they exhibited higher fracture toughness and maximum stress compared to the control mixture at 0℃ test temperature.

- The influence of fibre on pavement analysis and design has been examined by using the KENLAYER software. It was found that adding 1.0% cellulose, 0.5% and 1.0% of steel fibres showed the highest increase in pavement life compared to other fibre types and percentages and the control mixture.

10.3 Recommendations for future research

In this section, a list is given of areas where further research is needed, to provide a clear view and validation of the findings of the current study.

- ❖ The investigation in this thesis has concentrated on the moderate to high temperature testing of mastic and mortar. This is because the main concern for this study was permanent deformation, in addition to the difficulty of examining everything in a limited time. However, further experimental investigations are needed to examine the rheological and mechanical properties at low temperatures using bending beam rheometer (BBR), pull-off tensile strength and the direct tension test if possible. It is important to take fibre dimensions into consideration in choosing a suitable test method.
- ❖ The mechanism of possible chemical modification of binder in contact with fibres remains in large part unknown. The binder drainage test provided results that have helped in understanding such modification. Further research could usefully explore how fibre may change the chemical properties of the drained binder by using a saturates, aromatic, resin and asphaltene (SARA) analysis. Such a finding may help to establish a relationship between the chemical properties of modified bitumen and the rheological properties of fibre reinforced mastics.
- ❖ The pneumatic adhesion tensile testing instrument is considered a useful test to measure the cohesive and adhesive strength properties of a bitumen-aggregate system by measuring pull-off tensile strength. All fibre

modified and base mortars samples showed either cohesive or hybrid failure in this study. It is, therefore, recommended exploring the influence of these fibres on adhesive strength and that would require different test conditions such as low testing temperature and conditioning in water.

- The double edge notch tension (DENT) test is considered a useful test method and covers the determination of a bitumen's essential and plastic work of fracture. A 45° notch angle was used to facilitate ease of handling during the removal of the specimens from the mould. The tensile fracture force of modified mastics may be higher than the adhesion force between the mould and mastic, and the failure sometimes happened at the mould edge or away from the notch area instead. Due to this issue, this thesis recommends the design of a new mould that can provide higher bond strength between the mould edge and mastic sample. One solution is by increasing the contact area between the mould edge and the mastic such as using rectangular or ellipse shape instead of half circle and also using rougher surface that may increase the adhesion between the mastic and the mould.
- Fatigue failure is an important issue that influences pavement design life. This study has examined the influence of fibre reinforcement on fatigue life. It was found that the fatigue life was slightly improved, particularly at low strain values. However, these results may be inconclusive, and further investigation at low strain values is recommended using different test methods such as two-point bending, four-point bending test and at different test temperatures. These tests are less time consuming than ITFT and can be run at a wide range of loading frequencies.
- The influence of laboratory ageing was not examined in this study on either bitumen or mixture. Further research is required to determine the effect of ageing on the performance of fibre reinforced asphalt mastics and mixtures.

- Moisture damage depends on many factors in asphalt pavement and mechanisms are complicated. All asphalt mixtures in this study showed high resistance to water sensitivity. Surprisingly their properties even seemed to improve when exposed to the moisture damage procedure. Further work needs to be done to establish whether this finding is consistent in different moisture damage procedures. Although this study examined the water sensitivity of weaker specimens for a limited number, it is recommended doing more investigation for weaker specimens such as asphalt mixture specimens after repeated load axial test (RLAT) and then compare the results to water sensitivity of virgin (new) specimens.
- This study examined the differences in the compaction effort between control and fibre reinforced asphalt mixture. It was difficult to discriminate between these mixtures due to the inconsistency in the compaction efforts of roller compactor. Further work is needed to examine this effect by using different compaction methods such as Superpave gyratory compactor and Marshal Compaction mould.
- Pavement design in this study was based on fatigue criteria only. Further work is needed to fully understand the implications of other types of pavement distress, particularly permanent deformation. Such a study is needed to validate and provide more support to the current findings. Moreover, to minimise the gap between laboratory fatigue tests and field conditions such as loading frequency, healing effect and temperature variations, multipliers known as shift factors are usually applied. In the current study, these shift factors were not used. Further research should be carried out to establish appropriate shift factors that may be utilised for fibre reinforced asphalt mixtures.
- In this thesis, extensive investigation into the properties of materials from mastic, mortar and mixture has been carried out. Therefore, one of the most important implications of this study is to extend to full-scale pavement

trials. These will enrich the understanding of the behaviour of fibre reinforced asphalt mixtures and allow examination of their performance under realistic conditions.

References

AB-WAHAB, Y. B. 1993. Development of the simplified method to evaluate dynamic mechanical analysis data on asphalt-aggregate mixtures.

ABIOLA, O., KUPOLATI, W., SADIKU, E. & NDAMBUKI, J. 2014. Utilisation of natural fibre as modifier in bituminous mixes: A review. *Construction and Building Materials,* 54**,** 305-312.

ABOUFOUL, M. & GARCIA, A. 2017. Factors affecting hydraulic conductivity of asphalt mixture. *Materials and Structures,* 50**,** 116.

ABTAHI, S., HEJAZI, S., SHEIKHZADEH, M. & SEMNANI, D. 2008. An investigation on the use of textile materials to mechanical reinforcement of asphalt-concrete (AC) structures and analysis of results by an artificial neural network (ANN). *4th Nat Cong on Civil Eng*.

ABTAHI, S. M., ESFANDIARPOUR, S., KUNT, M., HEJAZI, S. M. & EBRAHIMI, M. G. 2013. Hybrid reinforcement of asphalt-concrete mixtures using glass and polypropylene fibers. *Journal of Engineered Fibers and Fabrics,* 8**,** 25-35.

ABTAHI, S. M., SHEIKHZADEH, M. & HEJAZI, S. M. 2010. Fiber-reinforced asphalt-concrete–a review. *Construction and Building Materials,* 24**,** 871-877.

AHMAD, N. 2011. *Asphalt mixture moisture sensitivity evaluation using surface energy parameters.* PhD thesis PhD, University of Nottingham.

AIREY, G. D. 1997. *Rheological characteristics of polymer modified and aged bitumens.* University of Nottingham.

AIREY, G. D. 2003. Rheological properties of styrene butadiene styrene polymer modified road bitumens. *Fuel,* 82**,** 1709-1719.

AIREY, G. D. 2004. Fundamental binder and practical mixture evaluation of polymer modified bituminous materials. *International Journal of Pavement Engineering,* 5**,** 137-151.

AIREY, G. D. & RAHIMZADEH, B. 2004. Combined bituminous binder and mixture linear rheological properties. *Construction and Building Materials,* 18**,** 535-548.

AL-MANSOB, R. A., ISMAIL, A., ALDURI, A. N., AZHARI, C. H., KARIM, M. R. & YUSOFF, N. I. M. 2014. Physical and rheological properties of epoxidized natural rubber modified bitumens. *Construction and Building Materials,* 63**,** 242-248.

AL-RIDHA, A., HAMEED, A. A. & IBRAHIM, S. 2014. Effect of steel Fibre on the Performance of Hot Mix Asphalt with Different Temperatures and Compaction. *Australian Journal of Basic and Applied Sciences,* 8**,** 123-132.

ALRAJHI, A. 2012. *Fiber Dosage Effects in Asphalt Binders and Hot Mix Asphalt Mixtures.* Arizona State University.

ALVARADO, C., MAHMOUD, E., ABDALLAH, I., MASAD, E., NAZARIAN, S., LANGFORD, R., TANDON, V. & BUTTON, J. 2007. Feasibility of quantifying

the role of coarse aggregate strength on resistance to load in HMA. *TxDOT Project No. 0-5268 and Research Report No. 0-5268*.

ALVAREZ, A. E., MARTIN, A. E., ESTAKHRI, C. & IZZO, R. 2008. Determination of volumetric properties for permeable friction course mixtures. *Journal of Testing and Evaluation,* 37**,** 1-10.

ANDERSON, D., MAURER, D., RAMIREZ, T., CHRISTENSEN, D., MARASTEANU, M. & MEHTA, Y. 1999. Field performance of modified asphalt binders evaluated with superpave test methods: I-80 test project. *Transportation Research Record: Journal of the Transportation Research Board***,** 60-68.

ANDRIESCU, A., HESP, S. & YOUTCHEFF, J. 2004. Essential and plastic works of ductile fracture in asphalt binders. *Transportation Research Record: Journal of the Transportation Research Board***,** 1-7.

ANDRIESCU, A. & HESP, S. A. 2009. Time–temperature superposition in rheology and ductile failure of asphalt binders. *International Journal of Pavement Engineering,* 10**,** 229-240.

ANURAG, K., XIAO, F. & AMIRKHANIAN, S. N. 2009. Laboratory investigation of indirect tensile strength using roofing polyester waste fibers in hot mix asphalt. *Construction and building materials,* 23**,** 2035-2040.

APEAGYEI, A., BUTTLAR, W. & DEMPSEY, B. 2006. Moisture damage evaluation of asphalt mixtures using AASHTO T283 and DC (T) fracture test. *Urbana,* 51**,** 61801.

ARABANI, M., MIRABDOLAZIMI, S. & SASANI, A. 2010. The effect of waste tire thread mesh on the dynamic behaviour of asphalt mixtures. *Construction and Building Materials,* 24**,** 1060-1068.

ASGHARZADEH, S. M., TABATABAEE, N., NADERI, K. & PARTL, M. N. 2015. Evaluation of rheological master curve models for bituminous binders. *Materials and Structures,* 48**,** 393-406.

ASPHALT INSTITUTE 2007. *The Asphalt Handbook MS-4,* Lexington, USA, The Asphalt Institute.

ASTM D 4541-17 2002. 4541, Standard Test Method for Pull-Off Strength of Coatings Using Portable Adhesion Testers. *ASTM International: West Conshohocken, PA*.

ASTM D7405 2010. Standard test method for multiple stress creep and recovery (MSCR) of asphalt binder using a dynamic shear rheometer. United State of America: American Society for Testing and Materials.

BAGHERPOUR, S. 2012. Fibre reinforced polyester composites. *Edited by Hosam El-Din M. Saleh***,** 167.

BAUMGARDNER, G. L., MASSON, J., HARDEE, J. R., MENAPACE, A. M. & WILLIAMS, A. G. 2005. Polyphosphoric acid modified asphalt: proposed mechanisms. *Journal of the Association of Asphalt Paving Technologists,* 74**,** 283-305.

BEHBAHANI, H., NOWBAKHT, S., FAZAELI, H. & RAHMANI, J. 2009. Effects of fiber type and content on the rutting performance of stone matrix asphalt. *Journal of Applied Sciences,* 9**,** 1980-1984.

BHASIN, A. 2006. *Development of methods to quantify bitumen-aggregate adhesion and loss of adhesion due to water.* Texas A&M University.

BILIGIRI, K. P., SAID, S. & HAKIM, H. 2012. Asphalt Mixtures. *International Journal of Pavement Research and Technology,* 5**,** 209-217.

BROWN, S. 1978. Material characteristics for analytical pavement design. *Developments in highway pavement engineering,* 1**,** 41-92.

BROWN, S., ROWLETT, R. & BOUCHER, J. Highway research: sharing the benefits. Proceedings, The United States Strategic Highway Research Program Conference, 1990.

BROWN, S. F. 1988. *An introduction to the analytical design of bituminous pavements,* Nottingham, University of Nottingham, Department of Civil Engineering.

BROWN, S. F. An introduction to asphalt pavement design in the UK. Proceedings of the Institution of Civil Engineers-Transport, 2013. Thomas Telford Ltd, 189-202.

BROWN, S. F. & GIBB, J. M. 1996. Validation experiments for permanent deformation testing of bituminous mixtures (with discussion). *Journal of the Association of Asphalt Paving Technologists,* 65.

BS 143 2000. Part 143. Determination of asphaltenes (heptane insolubles) in crude petroleum and petroleum products. London, United Kingdom: The institute of peteroleum and BSI 1996.

BS 4987-1 2005. Coated macadam (asphalt concrete) for roads and other paved areas. *Specification for constituent materials and for mixtures.* London, United Kingdom: British Standard, Standards Policy and Strategy Committee.

BS EN 1426 2007. Bitumen and bituminous binders—determination of needle penetration. London, United Kingdom: British Standard and European Committee.

BS EN 1427 2015. Bitumen and bituminous binders-Determination of the softening point-Ring and Ball method. London, United Kingdom: British Standard and European Committee.

BS EN 12697-5 2009. Bituminous mixtures— Test methods for hot mix asphalt. *Part 5: Determination of the maximum density.* London, United Kingdom: British Standard and European Committee.

BS EN 12697-6 2012. Bituminous mixtures — Test methods for hot mix asphalt. *Part 6: Determination of bulk density of bituminous specimens.* London, United Kingdom: British Standard and European Committee.

BS EN 12697-8 2003. Bituminous mixtures — Test methods for hot mix asphalt. *Part 8: Determination of void characteristics of bituminous specimens.* London, United Kingdom: British Standard and European Committee.

BS EN 12697-12 2003. Part 12: Determination of the water sensitivity of bituminous specimens. London, United Kingdom: British Standard and European Committee

BS EN 12697-22 2003. Bituminous mixtures —Test methods for hot mix asphalt. *Part 22: Wheel tracking.* London, United Kingdom: British Standard and European Committee.

BS EN 12697-23 2017. Bituminous mixtures - Test methods *Part 23: Determination of the indirect tensile strength of bituminous specimens* London, United Kingdom: British Standard and European Committee.

BS EN 12697-25 2016. Bituminous mixtures — Test methods. *Part 25: Cyclic compression test.* London, United Kingdom: British Standard and European Committee.

BS EN 12697-26 2012. Bituminous mixtures: Test methods for hot mix asphalt. *Part 26: Stiffness.* London, United Kingdom: British Standard and European Committee

BS EN 12697-33 2003. Bituminous mixtures —Test methods for hot mix asphalt. *Part 33: Specimen prepared by roller compactor.* London, United Kingdom: British Standard and European Committee.

BS EN 12697-35 2016. Bituminous mixtures — Test methods. *Part 35: Laboratory mixing.* London, United Kingdom: British Standard and European Committee.

BS EN 12697-44 2010. Bituminous mixtures — Test methods for hot mix asphalt. *Part 44: Crack propagation by semi-circular bending test.* London, United Kingdom: British Standard

BS EN 13302 2010. Bitumen and bituminous binders- determination of dynamic viscosity of bituminous binder using rotating spindle apparatus. London, United Kingdom: British Standard and European Committee

BS EN 2004. Bituminous mixtures - Test methods for hot mix asphalt - Part 18: Binder drainage. *basket method.* London, United Kingdom: British Standard and European Committee for Standardization.

BUSCHING, H. & ANTRIM, J. Fiber reinforcement of bituminous mixtures. Assoc Asphalt Paving Technol Proc, 1968.

BUSCHING, H., ELLIOTT, E. & REYNEVELD, N. A state-of-the-art survey of reinforced asphalt paving. Association of Asphalt Paving Technologists Proc, 1970.

CAMPBELL, F. C. 2010. *Structural Composite Materials*, ASM International.

CANESTRARI, F., CARDONE, F., GRAZIANI, A., SANTAGATA, F. A. & BAHIA, H. U. 2010. Adhesive and cohesive properties of asphalt-aggregate systems subjected to moisture damage. *Road Materials and Pavement Design,* 11**,** 11-32.

CARO, S., MASAD, E., BHASIN, A. & LITTLE, D. 2009. Coupled micromechanical model of moisture-induced damage in asphalt mixtures. *Journal of Materials in Civil Engineering,* 22**,** 380-388.

CASEY, D., MCNALLY, C., GIBNEY, A. & GILCHRIST, M. D. 2008. Development of a recycled polymer modified binder for use in stone mastic asphalt. *Resources, Conservation and Recycling,* 52**,** 1167-1174.

CASTRO, M. & SANCHEZ, J. A. 2008. Estimation of asphalt concrete fatigue curves–a damage theory approach. *Construction and Building Materials,* 22**,** 1232-1238.

CHEN, H.-X., LI, N.-L., HU, C.-S. & ZHANG, Z. 2004. Mechanical performance of fibers-reinforced asphalt mixture. *Journal of Chang'an University (Natural Science Edition)* 24**,** 1-5.

CHEN, H. & XU, Q. 2010. Experimental study of fibers in stabilizing and reinforcing asphalt binder. *Fuel,* 89**,** 1616-1622.

CHEN, H., XU, Q., CHEN, S. & ZHANG, Z. 2009. Evaluation and design of fiber-reinforced asphalt mixtures. *Materials & Design,* 30**,** 2595-2603.

CHEN, J.-S. & LIN, K.-Y. 2005. Mechanism and behavior of bitumen strength reinforcement using fibers. *Journal of Materials Science,* 40**,** 87-95.

CHEN, Z., WU, S.-P., ZHU, Z.-H. & LIU, J.-S. 2008. Experimental evaluation on high temperature rheological properties of various fiber modified asphalt binders. *Journal of Central South University of Technology,* 15**,** 135-139.

CHENG, Y., TAO, J., JIAO, Y., GUO, Q. & LI, C. 2015. Influence of diatomite and mineral powder on thermal oxidative ageing properties of asphalt. *Advances in Materials Science and Engineering,* 2015.

CHIU, C.-T. & LU, L.-C. 2007. A laboratory study on stone matrix asphalt using ground tire rubber. *Construction and Building Materials,* 21**,** 1027-1033.

CHO, D.-W. & KIM, K. 2010. The mechanisms of moisture damage in asphalt pavement by applying chemistry aspects. *KSCE Journal of Civil Engineering,* 14**,** 333-341.

CHONG, K. P. & KURUPPU, M. D. 1988. New specimens for mixed mode fracture investigations of geomaterials. *Engineering Fracture Mechanics,* 30**,** 701-712.

CLEVEN, M. A. 2000. *Investigation of the properties of carbon fiber modified asphalt mixtures.* Michigan Technological University.

COOLEY JR, L. & BROWN, E. 2001. Potential of using stone matrix Asphalt for thin overlays. *Transportation Research Record: Journal of the Transportation Research Board***,** 46-52.

COPELAND, A., YOUTCHEFF, J., KRINGOS, N., SCARPAS, A. & MAHADEVAN, S. Determination of bond strength as a function of moisture content at the aggregate-mastic interface. 10th International Conference on Asphalt Pavements-August 12 to 17, 2006, Quebec City, Canada, 2006.

COTTERELL, B. & REDDEL, J. 1977. The essential work of plane stress ductile fracture. *International journal of fracture,* 13**,** 267-277.

CRISPINO, M., MARIANI, E. & TORALDO, E. 2013. Assessment of fiber-reinforced bituminous mixtures' compaction temperatures through mastics viscosity tests. *Construction and Building Materials,* 38**,** 1031-1039.

D'ANGELO, J., KLUTTZ, R., DONGRE, R. N., STEPHENS, K. & ZANZOTTO, L. 2007. Revision of the superpave high temperature binder specification: the

multiple stress creep recovery test (with discussion). *Journal of the Association of Asphalt Paving Technologists,* 76.

D'ANGELO, J. A. 2009. The relationship of the MSCR test to rutting. *Road Materials and Pavement Design,* 10**,** 61-80.

DAWSON, A. & KOLISOJA, P. 2006. Managing rutting in low volume roads: Executive summary.

DE FILIPPIS, P., GIAVARINI, C. & SCARSELLA, M. 1995. Improving the ageing resistance of straight-run bitumens by addition of phosphorus compounds. *Fuel,* 74**,** 836-841.

DEJONG, D., PETUZ, M. & KORSWAGEN, A. 1973. Computer Program. *BISAR, Layered Systems under Normal and Tangential Surface Loads, Koninklijke Shell Laboratorium, External Report AMSR-000673, Amsterdam, Netherlands*.

DENNIS, M. J. 1997. Industrial computed tomography. *General Electric, NDE System and Service*.

DRAFT BS 2003. DD ABF Method for the determination of the fatigue characteristics of bituminous mixtures using indirect tensile fatigue London, United Kingdom: British Standard.

DRAFT BS EN 12697-24 2015. Bituminous mixtures - Test methods - Part 24: Resistance to fatigue *Indirect tensile test on cylindrical shaped specimens.* London, United Kingdom: British Standard and European Standard

ECHOLS, J. 1989. New mix method for fiber-reinforced asphalt. *Public Works,* 119.

EDGAR, R. 1998. Ten year performance of asphalt additive test sections: Lava butte road-fremont highway junction section.

EPPS, J. A. & MONISMITH, C. L. 1972. Fatigue of Asphalt Concrete Mixtures—Summary of Existing Information. *Fatigue of compacted bituminous aggregate mixtures.* ASTM International.

EPPS, J. A., MONISMITH, C. L., WARDEN, W., PELL, P., KALLAS, B., TERRELL, R., BUSCHING, H. & MCLEOD, N. Influence of mixture variables on the flexural fatigue properties of asphalt concrete. Association of Asphalt Paving Technologists Proc, 1969.

ERKENS, S., LIU, X., SCARPAS, A., MOLENAAR, A. & BLAAUWENDRAAD, J. Asphalt concrete response: experimental determination and finite element implementation. Proceeding of the 9th International Conference on Asphalt Pavements, Copenhagen, 2002.

FAHEEM, A. F. & BAHIA, H. U. 2010. Modelling of asphalt mastic in terms of filler-bitumen interaction. *Road Materials and Pavement Design,* 11**,** 281-303.

FAKHRI, M. & HOSSEINI, S. A. 2017. Laboratory evaluation of rutting and moisture damage resistance of glass fiber modified warm mix asphalt incorporating high RAP proportion. *Construction and Building Materials,* 134**,** 626-640.

FARIA, R., MOURA, P., DELGADO, J. & DE ALMEIDA, A. T. 2012. A sustainability assessment of electric vehicles as a personal mobility system. *Energy Conversion and Management,* 61**,** 19-30.

FERRY, J. D. 1980. *Viscoelastic properties of polymers*, John Wiley & Sons.

FREEMAN, R., BURATI, J. L., AMIRKHANIAN, S. N. & BRIDGES, W. Polyester fibers in asphalt paving mixtures. Association of Asphalt Paving Technologists Proc, 1989.

FU, S.-Y., LAUKE, B., MÄDER, E., YUE, C.-Y. & HU, X. 2000. Tensile properties of short-glass-fiber-and short-carbon-fiber-reinforced polypropylene composites. *Composites Part A: Applied Science and Manufacturing,* 31**,** 1117-1125.

GAJEWSKI, M., SYBILSKI, D. & BANKOWSKI, W. 2015. The influence of binder rheological properties on asphalt mixture permanent deformation. *The Baltic Journal of Road and Bridge Engineering, zaakceptowany do druku*.

GALINSKY, J. 1984. Performance of bituminous surface with fibers on I-65, final report. *Indiana Department of Highways, West Lafayette, Indiana*.

GOODRICH, J. L. Asphalt and polymer modified Asphalt properties related to the performance of Asphalt concrete mixes (with discussion). Association of Asphalt Paving Technologists Proc, 1988.

GOODRICH, J. L. 1991. Asphaltic binder rheology, asphalt concrete rheology and asphalt concrete mix properties (with discussion). *Journal of the Association of Asphalt Paving Technologists,* 60.

GOPALAKRISHNAN, K., CEYLAN, H. & INANC, F. 2007. Using X-ray computed tomography to study paving materials. *Construction Materials,* 160**,** 15.

GUAN, B., XIONG, R., HE, R., CHEN, S.-F. & DING, D.-H. 2014. Investigation of Usability of Brucite Fiber in Asphalt Mixture. *International Journal of Pavement Research and Technology,* 7**,** 193-202.

HAORAN, Z., JUN, Y., LING, C., JUAN, C. & JUN, W. Influence of polyester fibre on the performance of Asphalt mixes. Proceedings of the 26th Southern African Transport Conference (SATC 2007), 2007. 12.

HARVEY, J. T., DEACON, J. A., TAYBALI, A. A., LEAHY, R. B. & MONISMITH, C. L. A reliability-based mix design and analysis system for mitigating fatigue distress. Eighth International Conference on Asphalt PavementsFederal Highway Administration, 1997.

HASSAN, H. F. & AL-JABRI, K. S. 2005. Effect of organic fibers on open-graded friction course mixture properties. *International Journal of Pavement Engineering,* 6**,** 67-75.

HASSAN, N. A., AIREY, G. & COLLOP, A. 2012. *Microstructural characterisation of rubber modified asphalt mixtures.* University of Nottingham.

HEFER, A. W. 2005. *Adhesion in bitumen-aggregate systems and quantification of the effect of water on the adhesive bond.* Texas A&M University.

HEJAZI, S. 2007. *Mechanical reinforcement of hot mix asphalt using textile materials.* MSc. Thesis, Department of Textile Engineering, Isfahan University of Technology, Iran.

HERRAIZ, T. R., HERRAIZ, J. I. R., DOMINGO, L. M. & DOMINGO, F. C. 2016. Posidonia oceanica used as a new natural fibre to enhance the performance of asphalt mixtures. *Construction and Building Materials,* 102**,** 601-612.

HICKS, R. G. 1991. *Moisture damage in asphalt concrete*, Transportation Research Board.

HOFMAN, R., OOSTERBAAN, B., ERKENS, S. & VAN DER KOOIJ, J. Semi-circular bending test to assess the resistance against crack growth. 6th RILEM Symposium on performance testing and evaluation of bituminous materials, 2003. 257-263.

HONGU, T. & PHILIPS, G. 1990. New Fibers ellis hor wood series in polymercience and technology. *Fibers and Polymers,* 3**,** 1-7.

HOSSAIN, M. I. & TAREFDER, R. A. 2015. Behavior of asphalt mastic films under laboratory controlled humidity conditions. *Construction and Building Materials,* 78**,** 8-17.

HUANG, B., CHEN, X. & SHU, X. 2009. Effects of electrically conductive additives on laboratory-measured properties of asphalt mixtures. *Journal of Materials in Civil Engineering,* 21**,** 612-617.

HUANG, B., LI, G. & MOHAMMAD, L. N. 2003. Analytical modeling and experimental study of tensile strength of asphalt concrete composite at low temperatures. *Composites Part B: Engineering,* 34**,** 705-714.

HUANG, B., SHU, X. & ZUO, G. 2013. Using notched semi circular bending fatigue test to characterize fracture resistance of asphalt mixtures. *Engineering Fracture Mechanics,* 109**,** 78-88.

HUANG, H. & WHITE, T. 1996. Dynamic properties of fiber-modified overlay mixture. *Transportation Research Record: Journal of the Transportation Research Board***,** 98-104.

HUANG, X. 2009. Fabrication and properties of carbon fibers. *Materials,* 2**,** 2369-2403.

HUANG, Y. H. 2004. *Pavement analysis and design,* United States of America, Pearson Prentice Hall.

JAHROMI, S. G. & KHODAII, A. 2008. CARBON FIBER REINFORCED ASPHALT CONCRETE. *Arabian Journal for Science & Engineering (Springer Science & Business Media BV),* 33.

JENKS, W., JENCKS, F., HARRIGAN, E., ADCOCK, M., DELANEY, E. & FREER, H. 2011. NCHRP Report 673: A manual for design of hot mix asphalt with commentary. *Transportation Research Board, Washington, DC.*

JIMENEZ, R. A. & GALLAWAY, B. M. Behavior of asphaltic concrete diaphragms to repetitive loadings. International Conference on the Structural Design of Asphalt PavementsUniversity of Michigan, Ann Arbor, 1962.

JOHN C. GLENNON, D. E., P.E, 2015. Roadway Hydroplaning – Measuring Pavement Wheel Rut Depths to Determine Maximum Water Depths. January 2015 ed.: Motor-Vehicle Accident Investigation and Reconstruction Services

JTG E20 2011. Standard test methods of bitumen and bituminous mixtures for highway engineering. PR China, Beijing: Minsitry of Transport.

KALOUSH, K. E., BILIGIRI, K. P., ZEIADA, W. A., RODEZNO, M. C. & REED, J. X. 2010. Evaluation of fiber-reinforced asphalt mixtures using advanced material characterization tests. *Journal of Testing and Evaluation,* 38**,** 400-411.

KANITPONG, K. & BAHIA, H. U. Role of adhesion and thin film tackiness of asphalt binders in moisture damage of HMA. Association of Asphalt Paving Technologists Technical Sessions, 2003, Lexington, Kentucky, USA, 2003.

KIM, J. & KOH, C. 2012. Development of a predictive system for estimating fatigue life of asphalt mixtures using the indirect tensile test. *Journal of Transportation Engineering,* 138**,** 1530-1540.

KIM, K. W., DOH, Y. S. & LIM, S. 1999. Mode I reflection cracking resistance of strengthened asphalt concretes. *Construction and Building Materials,* 13**,** 243-251.

KIM, Y.-R., PARK, H. M., ARAGÃO, F. T. S. & LUTIF, J. E. S. 2009. Effects of aggregate structure on hot-mix asphalt rutting performance in low traffic volume local pavements. *Construction and Building materials,* 23**,** 2177-2182.

KIM, Y. & PARK, T.-S. 2013. Reinforcement of recycled foamed asphalt using short polypropylene fibers. *Advances in Materials Science and Engineering,* 2013.

KIM, Y. R. & WEN, H. 2002. Fracture energy from indirect tension testing. *Asphalt Paving Technology,* 71**,** 779-793.

KRANS, R., TOLMAN, F. & VAN DE VEN, M. Semi-circular bending test: a practical crack growth test using asphalt concrete cores. RILEM proceedings, 1996. Chapman & Hall, 123-132.

KROL, J. & MATRASZEK, K. 2012. Bitumen high temperature properties characterised by multiple stress creep recovery test (MSCR). *Drogownictwo,* 10**,** 321-324.

KUNA, K. 2015. *Mix design considerations and performance characteristics of foamed bitumen mixtures (FBMs).* University of Nottingham.

LABIB, M. & MAHER, A. 1999. Recycled plastic fibers for asphalt mixtures.

LAURINAVICIUS, A. & OGINSKAS, R. 2006. Experimental research on the development of rutting in asphalt concrete pavements reinforced with geosynthetic materials. *Journal of civil engineering and management,* 12**,** 311-317.

LEE, S. 2004. Long-term performance assessment of asphalt concrete pavements using the third scale model mobile loading simulator and fiber reinforced asphalt concrete.

LEE, S. J., RUST, J. P., HAMOUDA, H., KIM, Y. R. & BORDEN, R. H. 2005. Fatigue cracking resistance of fiber-reinforced asphalt concrete. *Textile Research Journal,* 75**,** 123-128.

LI, C. & LI, L. 2012. Criteria for controlling rutting of asphalt concrete materials in sloped pavement. *Construction and Building Materials,* 35**,** 330-339.

LI, X.-J. & MARASTEANU, M. 2010. Using semi circular bending test to evaluate low temperature fracture resistance for asphalt concrete. *Experimental mechanics,* 50**,** 867-876.

LIAO, M.-C. 2007. *Small and large strain rheological and fatigue characterisation of bitumen-filler mastics.* PhD thesis. University of Nottingham, UK.

LIM, I., JOHNSTON, I., CHOI, S. & BOLAND, J. Fracture testing of a soft rock with semi-circular specimens under three-point bending. Part 1—mode I. International journal of rock mechanics and mining sciences & geomechanics abstracts, 1994. Elsevier, 185-197.

LING, T., XIA, W., DONG, Q. & HE, D. 2008. Study on the Influence of the Fiber and Modified Asphalt upon the Performance of Asphalt Mixture. *Pavements and Materials: Characterization, Modeling, and Simulation.*

LITTLE, D. N. & BHASIN, A. 2006. Using surface energy measurements to select materials for asphalt pavement. NCHRP Project 9-37.

LIU, Q., SCHLANGEN, E., GARCÍA, Á. & VAN DE VEN, M. 2010. Induction heating of electrically conductive porous asphalt concrete. *Construction and Building Materials,* 24**,** 1207-1213.

LS-299 2001. Method of Test for The Determination of Asphalt Cement's Resistance to Ductile Failure Using Double Edge Notched Tension Test (DENT). USA: Ministry of Transportation of Ontario Laboratory Testing Manual.

LU, Q. & HARVEY, J. T. 2006. Evaluation of moisture sensitivity of hot mix asphalt by flexural beam fatigue test. *Asphalt Concrete: Simulation, Modeling, and Experimental Characterization.*

LU, X. & ISACSSON, U. 1997. Compatibility and storage stability of styrene-butadiene-styrene copolymer modified bitumens. *Materials and Structures,* 30**,** 618-626.

MAHREZ, A., KARIM, M. & KATMAN, H. 2003. Prospect of using glass fiber reinforced bituminous mixes. *Journal of the Eastern Asia Society for Transportation Studies,* 5**,** 794-807.

MAHREZ, A. & KARIM, M. R. Rutting characteristics of bituminous mixes reinforced with glass fiber. Proceedings of the Eastern Asia Society for Transportation Studies The 7th International Conference of Eastern Asia Society for Transportation Studies, 2007, 2007. Eastern Asia Society for Transportation Studies, 282-282.

MAHREZ, A. & KARIM, M. R. 2010. Fatigue characteristics of stone mastic asphalt mix reinforced with fiber glass. *International Journal of the Physical Sciences,* 5**,** 1840-1847.

MAHREZ, A., KARIM, M. R. & KATMAN, H. Y. B. 2005. Fatigue and deformation properties of glass fiber reinforced bituminous mixes. *Journal of the Eastern Asia Society for Transportation Studies,* 6**,** 997-1007.

MARASTEANU, M. 2007. Emerging methods in asphalt binder rheological characterization. *Road materials and pavement design,* 8**,** 257-284.

MASAD, E., JANDHYALA, V., DASGUPTA, N., SOMADEVAN, N. & SHASHIDHAR, N. 2002. Characterization of air void distribution in asphalt mixes using X-ray computed tomography. *Journal of materials in civil engineering,* 14**,** 122-129.

MASAD, E., MUHUNTHAN, B., SHASHIDHAR, N. & HARMAN, T. 1999. Internal structure characterization of asphalt concrete using image analysis. *Journal of computing in civil engineering,* 13**,** 88-95.

MASAD, E. A., ZOLLINGER, C., BULUT, R., LITTLE, D. N. & LYTTON, R. L. 2006. Characterization of HMA moisture damage using surface energy and fracture properties (with discussion). *Journal of the Association of Asphalt Paving Technologists,* 75.

MASSON, J. & LACASSE, M. 1999. A review of adhesion mechanisms at the crack sealant/asphalt concrete interface. *Durability of building and construction sealants***,** 259-274.

MATHEWS, F. & RAWLINGS, R. 1994. Polymer Matrix Composite. *Composite Materials: Engineering and sciences***,** 168-200.

MATTHEWS, F. L. & RAWLINGS, R. D. 1999. *Composite materials: engineering and science*, Elsevier.

MAURER, D. A. & MALASHESKIE, G. J. 1989. Field performance of fabrics and fibers to retard reflective cracking. *Geotextiles and Geomembranes,* 8**,** 239-267.

MCDANIEL, R., SOLEYMANI, H. & SHAH, A. 2002. Use of reclaimed asphalt pavement (RAP) under Superpave specifications: A regional pooled fund project.

MCDANIEL, R. S. 2015. *Fiber additives in asphalt mixtures*.

MEZGER, T. G. 2011. *The Rheology Handbook,* Hanover Gemany, Vincentz Network.

MITTAL. 2003. *Handbook of Adhesive Technology* United States of America, Taylor & Francis Group, LLC.

MO, L. 2010. *Damage development in the adhesive zone and mortar of porous asphalt concrete.* PhD thesis PhD Thesis, TU Delft, Delft University of Technology.

MO, L., HUURMAN, M., WU, S. & MOLENAAR, A. 2009. Ravelling investigation of porous asphalt concrete based on fatigue characteristics of bitumen–stone adhesion and mortar. *Materials & Design,* 30**,** 170-179.

MOHAMADZADEH, M., ABOLFAZL, ZIAEE, S. A., MOLASHAHI, H. F. & QAZIZADEH, M. J. 2014. Effects of waste fibers stabilizers on the draindown and moisture damage sensitivity properties of SMA mixtures. *International Journal of Transportation Engineering,* 2.

MOHAMMED, M., PARRY, T. & GRENFELL, J. 2017. Fibre behaviour and influence on the properties of asphalt mortar. *Bearing Capacity of Roads, Railways and Airfields*.

MOHAMMED, M., PARRY, T. & GRENFELL, J. 2018. Influence of fibres on rheological properties and toughness of bituminous binder. *Construction and Building Materials,* 163**,** 901-911.

MOLENAAR, A., SCARPAS, A., LIU, X. & ERKENS, S. 2002. Semi-circular bending test; simple but useful? *Journal of the Association of Asphalt Paving Technologists,* 71.

MONISMITH, C. & SALAM, Y. Distress characteristics of asphalt concrete mixes. Association of Asphalt Paving Technologists Proc, 1973.

MORAES, R., VELASQUEZ, R. & BAHIA, H. 2011. Measuring the effect of moisture on asphalt-aggregate bond with the bitumen bond strength test. *Transportation Research Record: Journal of the Transportation Research Board***,** 70-81.

MORAES, R., VELASQUEZ, R. & BAHIA, H. 2017. Using bond strength and surface energy to estimate moisture resistance of asphalt-aggregate systems. *Construction and Building Materials,* 130**,** 156-170.

MUNN, W. 1989. Fiber-reinforced hot mix promises improved stability. *Highways and Heavy Construction,* 132.

MYRE, J. 1990. Fatigue of asphalt pavements. *Third International Conference on Bearing Capacity of Roads and Airfields.* Norway:: SINTEF.

NA CHIANGMAI, C. 2010. *Fatigue-fracture relation on asphalt concrete mixtures.* Master, University of Illinois.

NAGABHUSHANA, M., TIWARI, D. & JAIN, P. 2013. Rutting in Flexible Pavement: An Approach of Evaluation with Accelerated Pavement Testing Facility. *Procedia-Social and Behavioral Sciences,* 104**,** 149-157.

NAJD, A., CHAO, Z. & YING, G. 2005. Experiments of fracture behavior of glass fiber reinforced asphalt concrete. *Journal of Chang'an University (Natural Science Edition),* 25.

NAVARRO, F., PARTAL, P., MARTıNEZ-BOZA, F. & GALLEGOS, C. 2004. Thermo-rheological behaviour and storage stability of ground tire rubber-modified bitumens. *Fuel,* 83**,** 2041-2049.

NEJAD, F. M., AFLAKI, E. & MOHAMMADI, M. 2010. Fatigue behavior of SMA and HMA mixtures. *Construction and Building Materials,* 24**,** 1158-1165.

ODA, S., FERNANDES JR, J. L. & ILDEFONSO, J. S. 2012. Analysis of use of natural fibers and asphalt rubber binder in discontinuous asphalt mixtures. *Construction and Building Materials,* 26**,** 13-20.

OLSSON, J., ZENG, L. F. & WIBERG, N.-E. Finite element analysis of road rutting. European Congress on Computational Methods in Applied Sciences and Engineering, ECCOMAS 2000, Barcelona, Spain, September 11-14, 2000, 2000.

OTTE, E. 1977. *A structural design procedure for cement-treated layers in pavements.* University of Pretoria.

OYEKUNLE, L. 2007. Influence of chemical composition on the physical characteristics of paving asphalts. *Petroleum Science and Technology,* 25**,** 1401-1414.

OZEN, H., AKSOY, A., TAYFUR, S. & CELIK, F. 2008. Laboratory performance comparison of the elastomer-modified asphalt mixtures. *Building and Environment,* 43**,** 1270-1277.

PARK, P. 2012. *Characteristics and Applications of High-Performance Fiber Reinforced Asphalt Concrete.* PhD, The University of Michigan.

PELL, P. Fatigue of asphalt pavement mixes. Intl Conf Struct Design Asphalt Pvmts, 1967.

PELL, P. & COOPER, K. 1975. The Fatigue of Testing and Mix Variables on The Fatigue Performance of Bituminous Materials. *Baltimore, Phoenix, Arizona: Association of Asphalt Paving Technologists,* 44.

PELL, P. & TAYLOR, I. Asphaltic road materials in fatigue. Association of Asphalt Paving Technologists Proc, 1969.

PELTONEN, P. 1991. Wear and deformation characteristics of fibre reinforced asphalt pavements. *Construction and building materials,* 5**,** 18-22.

PEREZ-JIMENEZ, F., BOTELLA, R., MOON, K.-H. & MARASTEANU, M. 2013. Effect of load application rate and temperature on the fracture energy of asphalt mixtures. Fénix and semi-circular bending tests. *Construction and Building Materials,* 48**,** 1067-1071.

PINK, H. S., MERZ, R. E. & BOSNIACK, D. Asphalt rheology: Experimental determination of dynamic moduli at low temperature. Association of Asphalt Paving Technologists Proceedings, 1980.

PONIKIEWSKI, T. & GOŁASZEWSKI, J. 2016. X-Ray investigation and strength measurement of steel fibre reinforced self-compacting concrete beams. *Transactions of the VŠB–Technical University of Ostrava, Civil Engineering Series.,* 16**,** 141-150.

POULIKAKOS, L. D. & PARTL, M. N. A comparison of Swiss and Japanese porous asphalt through various mechanical tests. STRC 4th Swiss Transport Research Conference, 2003 Swiss.

PSZCZOLA, M., JACZEWSKI, M., RYS, D., JASKULA, P. & SZYDLOWSKI, C. 2018. Evaluation of Asphalt Mixture Low-Temperature Performance in Bending Beam Creep Test. *Materials,* 11**,** 100.

PUTMAN, B. J. 2011. Effects of fiber finish on the performance of asphalt binders and mastics. *Advances in Civil Engineering,* 2011.

PUTMAN, B. J. & AMIRKHANIAN, S. N. 2004. Utilization of waste fibers in stone matrix asphalt mixtures. *Resources, conservation and recycling,* 42**,** 265-274.

QIAN, S., MA, H., FENG, J., YANG, R. & HUANG, X. 2014. Fiber reinforcing effect on asphalt binder under low temperature. *Construction and Building Materials,* 61**,** 120-124.

QIN, X., SHEN, A. & GUO, Y. 2016. Experimental study on road performance of basalt fiber reinforced Bitumen mastics. *Journal of Building Materials,* 19**,** 660-664.

QIU, H., TAN, X., SHI, S. & ZHANG, H. 2013. Influence of filler–bitumen ratio on performance of modified asphalt mortar by additive. *Journal of Modern Transportation,* 21**,** 40-46.

RAGAB, A., FARAG, R. K., KANDIL, U. F., EL-SHAFIE, M., SALEH, A. & EL-KAFRAWY, A. F. 2016. Thermo-mechanical properties improvement of asphalt binder by using methylmethacrylate/ethylene glycol dimethacrylate. *Egyptian Journal of Petroleum,* 25**,** 397-407.

RAITHBY, R. & RAMSHAW, J. 1972. Effects of secondary compaction on the fatigue performance of a hot-rolled asphalt.

RAZMI, A. & MIRSAYAR, M. 2017. On the mixed mode I/II fracture properties of jute fiber-reinforced concrete. *Construction and Building Materials,* 148**,** 512-520.

READ, J. & WHITEOAK, D. 2003. *The shell bitumen handbook*, Thomas Telford.

READ, J. M. 1996. *Fatigue cracking of bituminous paving mixtures.* University of Nottingham England.

READ, J. M. & COLLOP, A. C. 1997. Practical fatigue characterization of bituminous paving mixture. *Journal of the Association of Asphalt Paving Technologists,* 66.

REDDY, A. 2014. Carbon Fibre Manufacturing from PAN and its Adhesion to Vinyl Ester Matrices

REYNOLDS, P. & COSGROVE, T. 2005. Colloid Science-Principles, Methods, and Applications. Blackwell Publishing Ltd.

ROQUE, R., SANKAR, B. & TECHNOLOGISTS, A. P. 1999. Determination of Crack Growth Rate Parameters Of Asphalt Mixtures Using the Superpave lOT.

SAHA, G. & BILIGIRI, K. P. 2016. Fracture properties of asphalt mixtures using semi-circular bending test: a state-of-the-art review and future research. *Construction and Building Materials,* 105**,** 103-112.

SANTUCCI, L., SCHMIDT, R., MAJIDZADEH, K., PELL, P. & KRCHMA, L. The effect of asphalt properties on the fatigue resistance of asphalt paving mixtures. Association of Asphalt Paving Technologists Proc, 1969.

SEATTLIE WA PAVING. 2019. *Commercial asphalt paving and parking lot paving* [Online]. United States of America. [Accessed 11/06/2019 2019].

SEBAALY, P., BAZI, G., WEITZEL, D., COULSON, M. & BUSH, D. Long term performance of crumb rubber mixtures in Nevada. Proc., of the Asphalt Rubber 2003 Conf, 2003. 111-126.

SELIM, A. A., TAHA, R. & BAYOMY, F. Laboratory performance of quartzite based Stone Matrix Asphalt Mixtures (SMAM). Infrastructure: New Materials and Methods of Repair, 1994. ASCE, 635-642.

SERFASS, J. & SAMANOS, J. 1996. Fiber-modified asphalt concrete characteristics, applications and behavior (with discussion). *Journal of the Association of Asphalt Paving Technologists,* 65.

SERIN, S., MOROVA, N., SALTAN, M. & TERZI, S. 2012. Investigation of usability of steel fibers in asphalt concrete mixtures. *Construction and Building Materials,* 36**,** 238-244.

SILVA, H. M. R. D. D. Study on the use of bituminous mixtures modified with acrylic fibres in road pavement overlays. 1st Inter Conf on Transportation Infrastructure-ICTI, 2008. China Academy of Transportation Sciences (CATS).

SINGH, G., TIWARI, D., JAIN, P. & SWAMI, A. 2016. A Critical Review of Endurance Limits of Bituminous Mixes for Developing Countries. *Transportation Research Procedia,* 17**,** 438-444.

SOCAL DA SILVA, L., DE CAMARGO FORTE, M. M., DE ALENCASTRO VIGNOL, L. & CARDOZO, N. S. M. 2004. Study of rheological properties of pure and polymer-modified Brazilian asphalt binders. *Journal of materials science,* 39**,** 539-546.

SORENSEN, A. & WICHERT, B. 2009. Asphalt and Bitumen in Ullmann's Encyclopedia of Industrial Chemistry Wiley. VCH, Weinheim.

STUART, K. D. & MALMQUIST, P. 1994. Evaluation of using different stabilizers in the US route 15 (Maryland) stone matrix asphalt. *Transportation Research Record*.

SUCHISMITA, A. 2009. *A Study of Effects of Binder Quality and Natural Fiber on Stone Matrix Asphalt Mixtures.*

SUO, Z. & WONG, W. G. 2009. Analysis of fatigue crack growth behavior in asphalt concrete material in wearing course. *Construction and Building Materials,* 23**,** 462-468.

TABATABAEE, N. & TABATABAEE, H. 2010. Multiple stress creep and recovery and time sweep fatigue tests: Crumb rubber modified binder and mixture performance. *Transportation Research Record: Journal of the Transportation Research Board***,** 67-74.

TAPKIN, S. 2008. The effect of polypropylene fibers on asphalt performance. *Building and Environment,* 43**,** 1065-1071.

TAPKıN, S., CEVIK, A. & USAR, U. 2010. Prediction of Marshall test results for polypropylene modified dense bituminous mixtures using neural networks. *Expert Systems with Applications,* 37**,** 4660-4670.

TAPKIN, S., USAR, U., TUNCAN, A. & TUNCAN, M. 2009. Repeated creep behavior of polypropylene fiber-reinforced bituminous mixtures. *Journal of Transportation Engineering,* 135**,** 240-249.

TAREFDER. 2003. *Laboratory and model prediction of permanent deformation in asphalt concrete.* PhD thesis, PhD thesis,, PhD thesis, University of Oklahoma.

TAYFUR, S., OZEN, H. & AKSOY, A. 2007. Investigation of rutting performance of asphalt mixtures containing polymer modifiers. *Construction and Building Materials,* 21**,** 328-337.

THANH, D. V., FENG, C. P. & LONG, L. H. 2011. Analysis of high temperature stability and water stability of SMA mixture using orthogonal experiments. *International Journal of Civil & Structural Engineering,* 2**,** 635-647.

THOM, N. 2008. *Principles of pavement engineering*, Thomas Telford London.

TOPAL, A. & SENGOZ, B. 2005. Determination of fine aggregate angularity in relation with the resistance to rutting of hot-mix asphalt. *Construction and Building Materials,* 19**,** 155-163.

UHLMEYER, J., WILLOUGHBY, K., PIERCE, L. & MAHONEY, J. 2000. Top-down cracking in Washington state asphalt concrete wearing courses. *Transportation Research Record: Journal of the Transportation Research Board***,** 110-116.

VALE, A. C. D., CASAGRANDE, M. D. T. & SOARES, J. B. 2013. Behavior of natural fiber in stone matrix asphalt mixtures using two design methods. *Journal of Materials in Civil Engineering,* 26**,** 457-465.

VAN DE VEN, M., SMIT, A. D. F. & KRANS, R. L. Possibilities of a semi-circular bending test. Eighth International Conference on Asphalt PavementsFederal Highway Administration, 1997.

VAN OSS, C., CHAUDHURY, M. & GOOD, R. 1987. Monopolar surfaces. *Advances in colloid and interface science,* 28**,** 35-64.

VAN POEL, C. D. 1954. A general system describing the visco - elastic properties of bitumens and its relation to routine test data. *Journal of applied chemistry,* 4**,** 221-236.

WANG, Y. 1999. Utilization of recycled carpet waste fibers for reinforcement of concrete and soil. *Polymer-Plastics Technology and Engineering,* 38**,** 533-546.

WARDLE, L. 1977. A Computer Program for the Analysis of Multiple Complex Circular Loads on Layered Anisotropic Media.

WAY, G. The rubber pavements association, technical advisory board leading the way in asphalt rubber research. Proceedings of the asphalt rubber 2003 conference, Brasilia, Brazil, 2003. 17-33.

WEN, H. 2001. *Fatigue performance evaluation of WesTrack asphalt mixtures based on viscoelastic analysis of indirect tensile test.* North Carolina State University, US.

WILJANEN, B. R. 2003. *The pavement performance and life-cycle cost impacts of carbon fiber modified hot mix asphalt.* Michigan Technological University.

WU, M.-M., LI, R., ZHANG, Y.-Z., FAN, L., LV, Y.-C. & WEI, J.-M. 2015. Stabilizing and reinforcing effects of different fibers on asphalt mortar performance. *Petroleum Science,* 12**,** 189-196.

WU, M., LI, R., ZHANG, Y., WEI, J., LV, Y. & DING, X. 2014. Reinforcement effect of fiber and deoiled asphalt on high viscosity rubber/SBS modified asphalt mortar. *Petroleum Science,* 11**,** 454-459.

WU, S.-P., CHEN, Z., YE, Q.-S. & LIAO, W.-D. 2006. Effects of fibre additive on the high temperature property of asphalt binder. *Journal of Wuhan University of Technology-Materials Science Edition,* 21**,** 118-120.

WU, S., YE, Q., LI, N. & YUE, H. 2007. Effects of fibers on the dynamic properties of asphalt mixtures. *Journal of Wuhan University of Technology-Mater. Sci. Ed.,* 22**,** 733-736.

WU, Z., MOHAMMAD, L. N., WANG, L. & MULL, M. A. 2005. Fracture resistance characterization of superpave mixtures using the semi-circular bending test. *Journal of ASTM International,* 2**,** 1-15.

XIAO, F., AMIRKHANIAN, S. & JUANG, C. H. 2007. Rutting resistance of rubberized asphalt concrete pavements containing reclaimed asphalt pavement mixtures. *Journal of Materials in Civil Engineering,* 19**,** 475-483.

XIONG, R., FANG, J., XU, A., GUAN, B. & LIU, Z. 2015. Laboratory investigation on the brucite fiber reinforced asphalt binder and asphalt concrete. *Construction and Building Materials,* 83**,** 44-52.

XU, Q., CHEN, H. & PROZZI, J. A. 2010. Performance of fiber reinforced asphalt concrete under environmental temperature and water effects. *Construction and Building materials,* 24**,** 2003-2010.

YASREEN, S., MADZLAN, N. & IBRAHIM, K. 2011. The Effect of Fine Aggregate Properties on the Fatigue Behavior of the Conventional and Polymer Modified Bituminous Mixtures Using Two Types of Sand as Fine Aggregate. *World Academy of Science, Engineering and Technology,* 58.

YE, Q., WU, S., AND & LI, N. 2009. Investigation of the dynamic and fatigue properties of fibre-modified asphalt mixtures. *International Journal of Fatigue* 31**,** 1598-1602.

YI-QIU, T., LI, Z.-H., ZHANG, X.-Y. & DONG, Z.-J. 2010. Research on high-and low-temperature properties of asphalt-mineral filler mastic. *Journal of materials in civil engineering,* 22**,** 811-819.

YOO, P. J. & KIM, K.-H. 2014. Thermo-plastic fiber's reinforcing effect on hot-mix asphalt concrete mixture. *Construction and Building Materials,* 59**,** 136-143.

YU, X. & SUN, L. 2010. Anti-cracking ability of asphalt mixture added with polyester fiber. *Traffic and Transportation Studies 2010.*

ZACHARIAS, M. & EMERY, S. Application of the Brookfield viscometer test method in South African road grade bitumen specifications. PROCEEDINGS OF THE 6TH CONFERENCE ON ASPHALT PAVEMENTS FOR SOUTHERN AFRICA, CAPSA'94, HELD CAPE TOWN OCTOBER 1994. VOL 2, 1994.

ZEGEYE, E., LE, J.-L., TUROS, M. & MARASTEANU, M. 2012. Investigation of size effect in asphalt mixture fracture testing at low temperature. *Road Materials and Pavement Design,* 13**,** 88-101.

ZEIADA, W. 2012. *Endurance limit for HMA based on healing phenomenon using viscoelastic continuum damage analysis.* Arizona State University.

ZEIADA, W., KALOUSH, K., UNDERWOOD, B. & MAMLOUK, M. 2013. Effect of air voids and asphalt content on fatigue damage using the viscoelastic continuum damage analysis. *Airfield and Highway Pavement 2013: Sustainable and Efficient Pavements.*

ZHANG, J., AIREY, G. D., GRENFELL, J. & APEAGYEI, A. K. 2017. Moisture damage evaluation of aggregate–bitumen bonds with the respect of moisture absorption, tensile strength and failure surface. *Road Materials and Pavement Design,* 18**,** 833-848.

ZHANG, J., AIREY, G. D. & GRENFELL, J. R. 2015a. Experimental evaluation of cohesive and adhesive bond strength and fracture energy of bitumen-aggregate systems. *Materials and Structures***,** 1-15.

ZHANG, J., WALUBITA, L. F., FARUK, A. N., KARKI, P. & SIMATE, G. S. 2015b. Use of the MSCR test to characterize the asphalt binder properties relative to HMA rutting performance–A laboratory study. *Construction and Building Materials,* 94**,** 218-227.

ZHANG, Z., ROQUE, R., BIRGISSON, B. & SANGPETNGAM, B. 2001. Identification and verification of a suitable crack growth law (with discussion). *Journal of the Association of Asphalt Paving Technologists,* 70.

ZHOU, F., SCULLION, T. & SUN, L. 2004. Verification and modeling of three-stage permanent deformation behavior of asphalt mixes. *Journal of Transportation Engineering,* 130**,** 486-494.

ZHOU, L., LI, P. & ZHANG, Z. Investigation of high temperature properties of asphalt mixture containing fibers. Material Design, Construction, Maintenance, and Testing of Pavements: Selected Papers from the 2009 GeoHunan International Conference, 2009. 139-144.

ZHU, H., YANG, J., CONG, L., CUI, J. & WAN, J. 2007. Influence of polyester fibre on the performance of Asphalt mixes. *Southern African Transport Conference (SATC)*

ZOU, G.-L., ZHANG, X.-N. & HAN, C.-D. 2001. Utilization of DSR for evaluation of pavement performance. *Journal of Harbin University of Civil Engineering & Architecture,* 34**,** 112-115.

ZUBE, E. 1956. Wire mesh reinforcement in bituminous resurfacing.